STUDIES ON C-H FUNCTIONALIZATION OF CYCLIC 1,3-DIKETONES, QUINOXALIN-2(1*H*)-ONES AND α-ARYL ESTERS UNDER THERMAL, PHOTOCHEMICAL AND CONTINUOUS FLOW CONDITIONS

विद्या वाचस्पति की उपाधि की अपेक्षाओं की आंशिक पूर्ति में प्रस्तुत शोध प्रबंध

A thesis submitted in partial fulfillment of the requirements of the degree

Doctor of Philosophy

In Chemistry

द्वारा / By

शंखजीत मोंडल

Shankhajit Mondal

पंजीकरण सं. / Registration No.: 20192021

शोध प्रबंध पर्यवेक्षक / Thesis Supervisor:

डॉ.बूपथी ज्ञानप्रकाशम / Dr. Boopathy Gnanaprakasam



भारतीय विज्ञान शिक्षा एवं अनुसंधान संस्थान पुणे

INDIAN INSTITUTE OF SCIENCE EDUCATION AND RESEARCH

PUNE MAHARASHTRA, INDIA-411008

2025

This Thesis is Dedicated to My Beloved Parents, My Esteemed Chemistry Teacher, Avijit Basak Sir, and All My Friends for Their Unwavering Love and Support in Making All My Success Possible

Declaration by student

Name: Shankhajit Mondal

Reg. No.: 20192021

Thesis Supervisor: Dr. Boopathy Gnanaprakasam

Department: Chemistry

Date of joining programme: 1st August, 2019

Date of presynopsis: 28th May, 2025

Title of Thesis: Studies on C-H Functionalization of Cyclic-1,3-diketones, Quinoxalin-2(1H)-ones and α-aryl esters under Thermal, Photochemical and Continuous Flow Conditions

I declare that this written submission represents my idea in my own words and where others' ideas have been included; I have adequately cited and referenced the original sources. I declare that I have acknowledged collaborative work and discussions wherever such work has been included. I also declare that I have adhered to all principles of academic honesty and integrity and have not misrepresented or fabricated or falsified any idea/data/fact/source in my submission. I understand that violation of the above will be cause for disciplinary action by the Institute and can also evoke penal action from the sources which have thus not been properly cited or from whom proper permission has not been taken whenever needed.

The work reported in this thesis is the original work done by me under the guidance of

Dr. Boopathy Gnanaprakasam.

Date: 08/08/2025

Signature of the student



CERTIFICATE

It is certified that the work incorporated in the thesis entitled "Studies on C-H Functionalization of Cyclic-1,3-diketones, Quinoxalin-2(1*H*)-ones and α-aryl esters under Thermal, Photochemical and Continuous Flow Condition" Submitted by **Shankhajit Mondal** was carried out by the candidate, under my supervision. The work presented here or any part of it has not been included in any other thesis submitted previously for the award of any degree or diploma from any other University or institution.

Date: 08/08/2025

Supervisor

Dr. Boopathy Gnanaprakasam

(Associate professor)

ACKNOWLEDGEMENT

At the outset, I would like to express my deep and sincere gratitude to my thesis supervisor Dr. Boopathy Gnanaprakasam for giving me the opportunity to work with him. I thank him for his excellent guidance and constant support and encouragement throughout my Ph.D. I shall always cherish all that he has taught me during these past few years. I would like to thank my RAC members: Dr. Santosh Mhaske from NCL Pune and Prof. Ramakrishna G Bhat from IISER Pune for giving me positive appreciation, insightful comments, constructive criticism, and valuable suggestions during my Ph.D. I would like to express my sincere gratitude to our former director, Jayant B. Udgaonkar and present director Sunil Bhagwat for providing an exceptional research facility, funding, and multidisciplinary research atmosphere at IISER Pune.

The successful completion of my Ph.D. would not have been possible without the unwavering support of my beloved parents. I express my deepest gratitude to my father, Mr. Gopal Chandra Mondal whose constant care, encouragement, and guidance have been a source of strength throughout my life. I am equally thankful to my mother, Mrs. Sukla Mondal, for her support and care. I am grateful that they gave me the freedom to choose what I desired. I wholeheartedly thank my chemistry professors of KN college (SN sir, AKD sir, SKG sir, AD sir, and PM sir) for their excellent teaching and concept building capacity. It was their inspiring and captivating lectures in college that ignited my passion for pursuing higher studies in chemistry.

I would like to thank the administrative staff of IISER Pune, Mr. Mayuresh Kulkarni, Mr. Tushar Kurulkar, Mrs. Sayalee, Mr. Mahesh, Mr. Ganesh, Mr. Yathish, Ms. Megha, Mr. Sanjay. Also, I am grateful to the technical service staff IISER Pune, Mr. Parveen Nasa, Neeta Deo, Nisha Kurkure, Mr. Nitin Dalvi, Mr. Suresh, Mr. T. S. Yatish, Mrs. Hemlata, Mrs. Megha Paygude, Mr. Ganesh Dimbar, Dr. Sandeep Kanade, Mr. Ravinder.

I am thankful to my group members who have been my family away from home. I would like to thank my former labmates: Dr. Girish, Dr. Akanksha, Dr. Nirmala, Dr. Akash Ubale, Dr. Moseen Shaikh, Dr. Akash Jamdade, Dr. Suthar, Writam, and present labmates Gokul, Swami, Somanth, Padmavathy, Pramod, Abhijit, Bhakti, and Shital. I would like to say a big thank to my IISER friends Mr. Bhoj, Mr. Akshay, Ms. Simran, and Ms. Ritika who have always been there for me in every difficult situation. I am very much thankful to my 8th floor gang comprising of Dr. Parikshit, Mr. Rishu, Mr. Harsh, and Mr. Hooda for having a dynamic post lab fun, enjoyment and late-night coffee. I shall never forget the fun and the quality time I have spent with them during covid time in hostel. I am fortunate to have the cheerful friends like Koushik, Rajdeep, Ananya, Rittika, Bikram, Suman, Souvik etc. during my B.Sc. I shall always cherish those golden memories of college days specially along the bank of Ganga and at the square field. I am indebted to my chemistry teacher, Avijit Basak sir, whose captivating teaching style sparked my interest in chemistry, particularly organic chemistry.

Finally, I am thankful to all the faculty members of the chemistry department, IISER-Pune for their support. I gratefully acknowledge IISER Pune for financial support throughout the tenure.

Shankhajit Mondal

TABLE OF CONTENTS

Table of contents ……i-ii

Abbreviations …… iii-iv

Preface ……v-vii

Chapter 1: Introduction to C-H Functionalization using Different Approaches

1.1. Abstract……2
1.2. Introduction to C-H functionalization ……3-4
1.3. Brief historical account …… 4-6
1.4. Metal catalyzed C-H functionalization ……..6-9
1.5. Metal free C-H functionalization ……..9-12
1.6 Reactive sites on cyclic 1,3-diketones ……..12-13
1.7 Reactive sites on quinoxalin-2(1*H*)-ones ……..13-15
1.8 Reactive sites on α-aryl esters ……15-16
1.9 Rationale behind the thesis work…… 16
1.10 Objective of our projects……16-19
1.11 Reference ……19-21

Chapter 2: Continuous Flow Fe-zeolite Catalyzed C-H Functionalization of Cyclic 1,3-diketones via Meinwald Rearrangement

2.1 Abstract……23
2.2 Introduction 23-28
2.3 Rationale behind the present work ……..28
2.4 Results and Discussions ……...28-42
2.5 Conclusion ……..42
2.6 Experimental section 42-46
2.7. Analytical data of products 46-57
2.8. Appendix-I: Copies of NMR spectra, GC-MS, XRD data…….....57-69
2.9. Conclusion 69-71

Chapter 3: Visible Light Mediated Organophotoredox Catalyzed Synthesis of Tetraketones using Tertiary Amines as Alkyl Synthon

3.1. Abstract ……..73
3.2 Introduction ……..... 73-77
3.3. Results and discussions 77-86

3.4. Conclusion 86
3.5. Experimental section 87
3.6. Analytical data of products 88-97
3.7. Appendix II: Copies of NMR spectra, GC-MS and SCXRD data 98-109
3.8. Reference 110-111

Chapter 4: Visible Light Induced Sequential Nitrogen Insertion and C-H Benzotriazolation of Quinoxaline-2(1*H*)-ones

4.1 Abstract 113
4.2 Introduction 113-117
4.3 Results and discussions 117-122
4.4 Conclusions 122
4.5 Experimental section 122-123
4.6 Analytical data of products 123-136
4.7. Appendix-III: Copies of NMR spectra and XRD data 136-151
4.8. Reference.....151-153

Chapter 5A: Visible Light-Induced Sequential Nitrogen Insertion and Benzotriazolation of Diazo Esters

5.1A. Abstract 155
5.2A. Introduction 155-158
5.3A. Results and discussions 158-161
5.4A. Conclusions 161-162
5.5A. Experimental section 162-163
5.6A. Analytical data of products 163-165
5.7A. Appendix-IV: Copies of NMR spectra 165-169
5.8A. Reference.....170-171

Chapter 5B: NBS Promoted C-H benzotriazolation of α-aryl esters

5.1B. Abstract 173
5.2B. Introduction 173-176
5.3B. Rational behind present work 176
5.4B. Results and discussions 176-180
5.5B. Conclusions 180
5.6B. Experimental section 181
5.7B. Analytical data of products 181-188
5.8B. Appendix-V: Copies of NMR spectra, XRD structure 188-195
5.9A. Reference.....195-197
Publication Details 198-207

List of Abbreviation

Ac	Acetyl
[Acr Mes]$^+$	9-mesityl-10-methylacridinium
ACN	Acetonitrile
Ar	Aryl
Atm	Atmospheric
Aq	Aqueous
Bn	Benzyl
BHT	Butylated Hydroxytoluene
BPO	Benzoyl peroxide
Bs	Broad singlet
Bu	Butyl
BuLi	Butyllithium
Calcd.	Calculated
Cat.	Catalytic
CCDC	Cambridge crystallographic data centre
Conc.	Concentrated
^{o}C	Degree Celsius
δ	Chemical shift in ppm
d	Doublet in NMR
DBU	1,8-Diazabicyclo[5.4.0]undec-7-ene
dba	Dibenzylideneacetone
DCM	Dichloromethane
DCE	Dichloroethane
DEPT	Distortionless enhancement by polarization transfer
DMF	*N, N*-Dimethyl formamide
DMSO	Dimethyl sulfoxide
DMA	*N, N*-Dimethylacetamide
Dppf	1,1'-Bis(diphenylphosphino)ferrocene
ee	Enantiomeric excess
EI	Electron impact
EtOAc	Ethyl acetate
Eq.	Equivalent
ESI TOF	Electrospray ionization time-of-flight
FTIR	Fourier-transform infrared spectroscopy
g	Grams
GC-MS	Gas chromatography-mass spectrometry

h	hours
Hz	Hertz
HRMS	High-resolution mass spectroscopy
IR	Infra-red
J	Coupling constant in NMR
LDA	Lithium diisopropylamide
$LiAlH_4$	Lithium aluminium hydride
M	Molar (mol L^{-1})
m/z	Mass to charge ratio
Me	Methyl
m	Multiplet in NMR
mg	Milligram
min	Minutes
mL	Millilitre
mmol	Millimoles
MS	Mass spectroscopy
NBS	*N*-bromosuccinimide
NMR	Nuclear magnetic resonance
NHPI	N-Hydroxyphthalimide
Oct	Octyl
Pd/C	Palladium on carbon
p	Pentet in NMR
Pr	Propyl
ppm	Parts per million
PIFA	[Bis(trifluoroacetoxy)iodo] benzene
PS	Photosensitizer
rt	room temperature
RB	Rose Bengal
q	Quartet in NMR
s	Singlet in NMR
TMS	Tetramethylsilane
THF	Tetrahydrofuran
TPPT	Triphenylpyrylium tetrafluoroborate
Ts	*p*-toluenesulfonyl (tosyl)
UV	Ultraviolet-visible spectroscopy

SYNOPSIS

C–H functionalization represents a transformative strategy in organic synthesis, enabling the direct modification of carbon–hydrogen bonds into a wide range of functional groups. This approach eliminates the need for pre-activated substrates, thereby enhancing step economy, reducing waste, and improving overall synthetic efficiency. Its ability to achieve site-selective transformations has opened new avenues for the streamlined construction of structurally diverse and complex molecules. The present dissertation explores the strategic development of novel C–H functionalization methodologies for diverse organic scaffolds including cyclic 1,3-diketones, quinoxalinones, and α-aryl esters. Direct C–H bond transformation remains a powerful approach in organic synthesis, enabling atom- and step-economical access to complex molecules. This work emphasizes metal-free and photocatalytic protocols under mild conditions, aligning with the principles of green and sustainable chemistry. Cyclic 1,3-diketones, owing to their enolizable nature, serve as versatile nucleophilic partners for constructing functionalized heterocycles. Quinoxalinones, as privileged nitrogen heterocycles, were further modified via selective C–H functionalization to expand their chemical and biological utility and the same methodology has been applied to α-diazo esters. In parallel, α-aryl esters were investigated for site-selective functionalization, unlocking pathways for the formation of new C–N and C–C bonds.

Chapter 1: Introduction to C-H Functionalization

The thesis begins with an overview of C-H functionalization including history, advantages and applications in natural products, drugs synthesis. After that, various approaches of C-H functionalization reactions have been described with relevant examples. Several metal-catalyzed as well as metal free strategies under thermal and photochemical conditions for direct C-H functionalization reactions have been explored. Finally, aim and rationale for this thesis have been elucidated.

Chapter 2: Continuous Flow Fe-zeolite Catalyzed C-H Functionalization of Cyclic 1,3-diketones via Meinwald Rearrangement

In this chapter, we have presented heterogeneous Fe@zeolite catalyzed method for diverse bioactive tetraketone synthesis starting from epoxdes and cyclic 1,3-diketones. Initially, this chapter includes literature overview for zeolite catalyzed transformations, previous reports on tetraketone and xanthene synthesis. Subsequently, it describes rationale behind this work and

detailed optimization studies for tetraketone synthesis, broad substrate scope under batch and continuous flow conditions. Then, it elaborates the Fe@zeolite catalyzed cyclization of tetraketones to form bioactive xanthenes. Later, detailed mechanistic investigations and plausible mechanistic pathway have been delineated.

Chapter 3: Visible Light Mediated Organophotoredox Catalyzed C-H Functionalization of Cyclic 1,3-diketones using Tertiary Amines as Alkyl Synthon

This chapter describes an innovative, environmentally-benign photoredox Eosin-Y catalyzed strategy for C-H functionalization of cyclic 1,3-diketones using tertiary amines as unusual source of alkyl groups. In the beginning, we have discussed different functions of tertiary amines in photoredox catalysis with thorough literature precedents. Subsequently, we have described the rationale behind the thesis, the detailed optimization study, substrate scope and post-synthetic modification. Later, we have elaborately depicted the photophysical, electrochemical studies and control experiments to assess the mechanism. At the end, we have sketched the plausible mechanism.

Chapter 4: Visible Light Induced C-H Benzotriazolation of Quinoxaline-2(1*H*)-ones

This chapter presents an efficient method for C-H benzotriazolation of quinoxaline-2(1*H*)-ones under photochemical conditions via insitu generation of benzotriazoles from *o*-phenylenediamines and *tert*-butyl nitrite. Initially, the immense biological applications of quinoxalinone derivatives have been described. Then, a brief literature overview has been provided describing different photochemical reactions established for C-H functionalization reaction at C-3 position of qunoxalinones. Next, optimization studies and detailed substrate scope of the developed protocol has been discussed. Subsequently, synthetic application of products and large-scale synthesis have been demonstrated. Finally, Mechanistic investigation and plausible mechanism have been explained.

Chapter 5A: Visible Light-Induced Sequential Nitrogen Insertion and Benzotriazolation of Diazo Esters

In this chapter, photochemical N-H insertion reaction between insitu generated benzotriazole motif and α-diazo esters have been discussed. Initially, a brief literature overview shows some representative examples of reaction of α-diazo esters. Afterwards, optimization of reaction, substrate scope, mechanistic investigation and plausible mechanism have been described.

Chapter 5B: NBS Promoted C-H Benzotriazolation of α-aryl esters

This chapter details a direct one-pot C-H benzotriazolation reaction of α-aryl ester with insitu benzotiazoles under metal-free conditions using NBS as brominating agent and benzoyl

peroxide as radical initiator. At first, a brief literature overview has been presented focusing on direct C-N bond formation methods with α-aryl esters. After that, optimization studies and substrate scope have been elaborated. Later, mechanistic studies have been described and mechanism has been proposed.

Chapter 1

Introduction to C-H Functionalization using Different Approaches

Introduction to C-H Functionalization using Different Approaches

1.1. Abstract

C-H functionalization reaction is known to be a versatile approach for synthesis and diversification of complex molecules. In this type of reactions, a C-H bond is functionalized by appropriate functional group. By suitable choice of reaction conditions, a series of molecules could be functionalized. Cyclic 1,3-diketones have highly reactive sp^3 C-H bond at C-2 position and offer a site for sp^3 C-H functionalization reaction. On the other hand, quinoxalinones have C-H bond at C-3 position. This position being highly reactive, sp^2 C-H functionalization could be carried out preferably. On the other hand, α-aryl esters also contain C-H bond flanked by ester and aryl functionality and could be functionalized by means of careful selection of reaction conditions. This thesis describes new approaches for sp^3 C-H functionalization of cyclic 1,3-diketones and α-aryl esters and sp^2 C-H functionalization of quinoxaline-2(1*H*)-ones. In this brief introduction, at first, historical account of C-H functionalization has been depicted. Then, various chemical transformations aimed at C-H functionalization under metal catalyzed and metal free conditions have been exemplified. After having the detailed literature accounts on the C-H functionalization, the rationale and objective of the research work has been presented at the end of this chapter.



1.2. Introduction to C-H functionalization

C-H functionalization refers to a class of chemical transformations that involve the direct modification of C-H bonds by installing suitable functional groups.[1a] Therefore, C-H functionalization would give rise to value-added products.[1b-c] As C-H functionalization involves replacement of C-H bond, it is evident that the ease of C-H functionalization will depend of C-H bond dissociation energy.[2] By careful selection of reagents and reaction conditions, we can achieve diverse C-H functionalized product at different organic molecules. Just like other chemical reactions, C-H functionalizations can also be catalytic or non-catalytic. In classical organic chemistry, certain functional groups make nearby C-H bonds acidic and then an electrophile gets installed at that position forming the basis of classical C-H functionalization reaction. In contrast, catalytic C−H bond functionalization introduces functional groups at C−H bonds that lack the activating influence of existing functional groups.

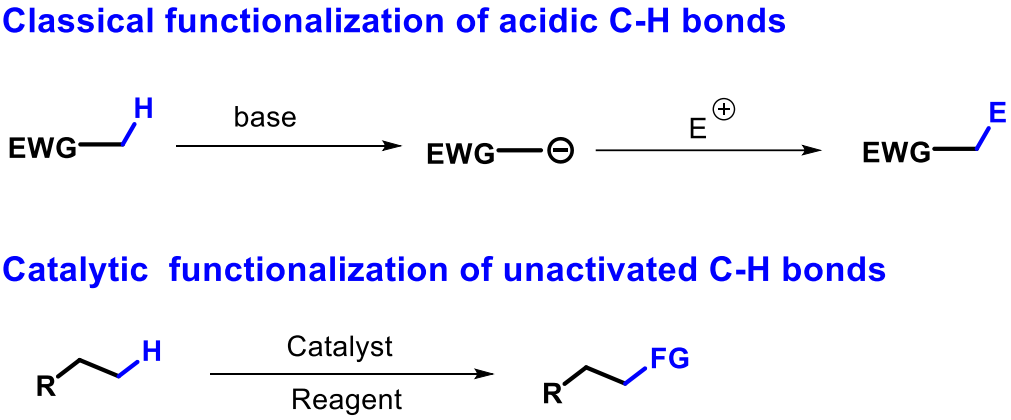


Figure 1.1: Classical and catalytic ways of C-H functionalization

C–H functionalization strategies offer numerous advantages which render them highly attractive for executing synthetically challenging organic transformations (Figure 1.2).[3] The advantages of C-H functionalization reactions include:

- The need for pre-functionalization is avoided as we can directly install functional group at C-H bond.
- As a result, we get high step economy and hence possibility of waste generation is minimized
- Employing C-H functionalization we can synthesize and diversify complex organic molecules
- C-H functionalization provides easy and convenient disconnections of complex molecules from simplest starting materials and improves the overall efficiency of a desired transformation.

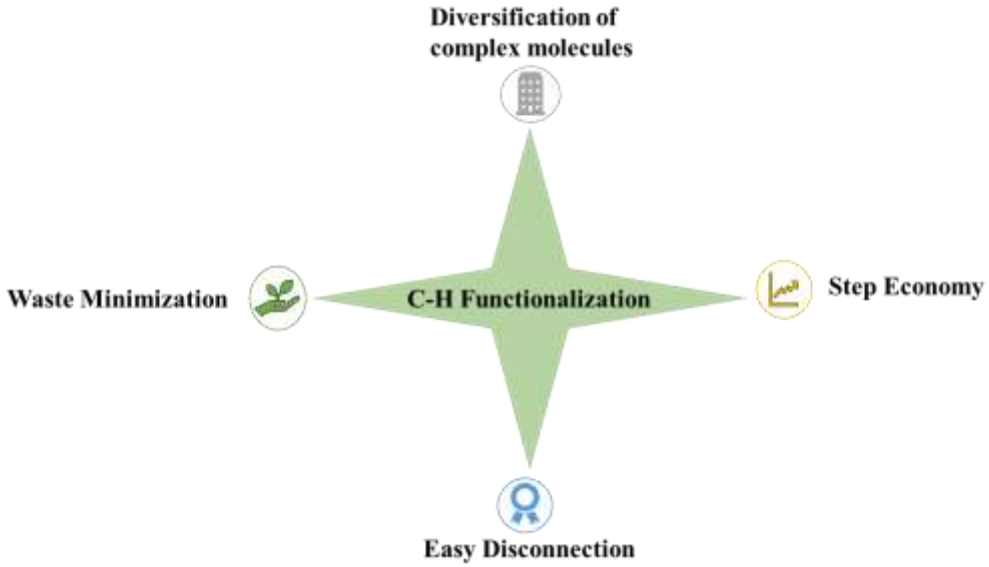
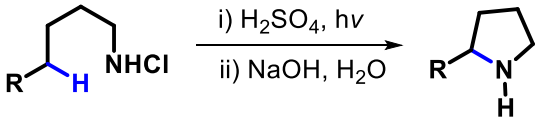


Figure 1.2: Advantages of C-H functional functionalization

Hence, a growing interest has been found among the organic chemists for developing new protocols of C-H functionalization.

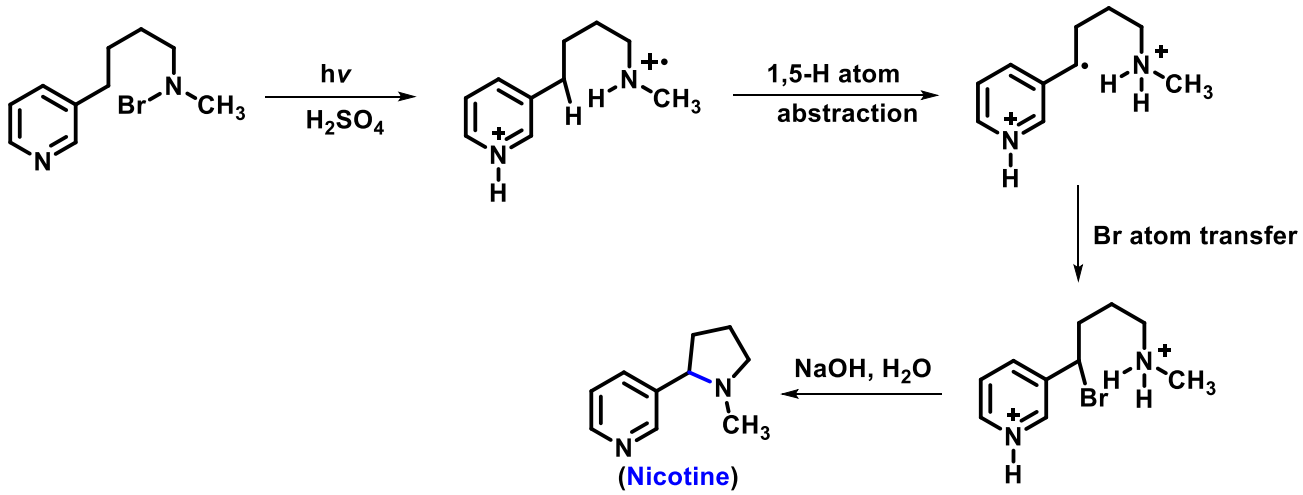
1.3. Brief historical account of C-H functionalization

Organic chemistry has started developing as a separate branch of chemistry after the groundbreaking discovery of urea production in 1828 by Friedrich Wöhler.[4] Historically, the first ever C-H functionalization reaction has been reported to be Hofmann–Löffler–Freytag reaction in 1883 where intramolecular C-H functionalization occurs (C-H amination) forming cyclic amines.[5]



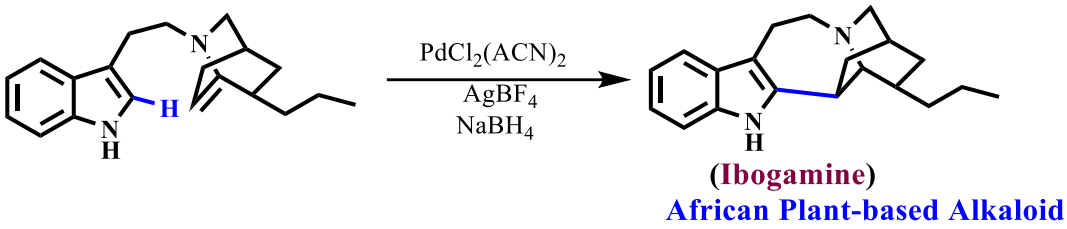
Scheme 1.1: First example of C-H functionalization reaction

This newly discovered C-H functionalization reaction has further been applied for first ever laboratory production of nicotine.[6] Such applications prove the powerfulness and practical utility of C-H functionalization. Soon after this, many such C-H functionalization reactions have been discovered that paved the path of successful synthesis of complex natural products, drugs etc.



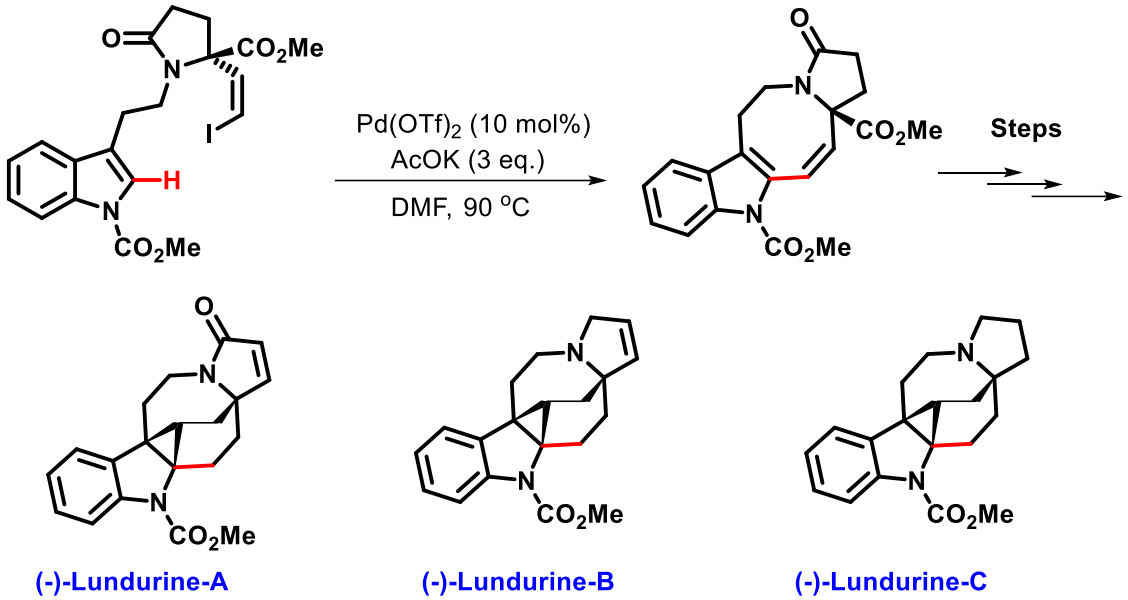
Scheme 1.2: Nicotine synthesis using C-H functionalization reaction

Currently, the direct C-H functionalization concept has reached the zenith of success in total synthesis of variety of natural products, drugs, pharmaceuticals, perfumeries etc.[7] Following example by Larsen *et al.* depicts its use in complex natural product synthesis (Scheme 1.3). In this example, intramolecular C-H functionalization occurs to afford the African plant based alkaloid Ibogamine.[8] The transformation proceeds via a conventional Heck-type reaction, wherein C–N bond formation occurs at the expense of a C–H bond, leading to the construction of the cyclic alkaloid framework.



Scheme 1.3: Synthesis of Ibogamine utilizing intramolecular C-H functionalization reaction

Later on, Zhai *et al.* have demonstrated an excellent strategy for the asymmetric total synthesis of plant based natural products (-)-Lundurin-A, (-)-Lundurin-B and (-)-Lundurin-C by intramolecular C-H functionalization reaction (Scheme 1.4).[9] The main reaction of this synthesis was the Pd (II)-catalyzed intramolecular C-H vinylation reaction that eventually forms the eight membered cyclic core structure in a Heck type reaction. Then after few steps, the three natural products of (-)-Lundurin series could be synthesized.



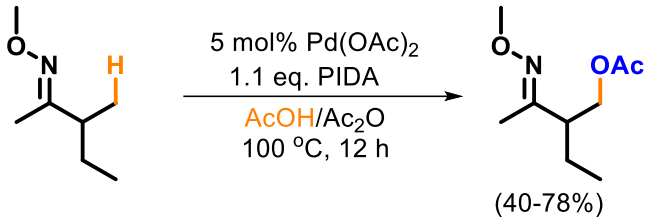
Scheme 1.4: Total synthesis of (-)-Lundurin-A to C by C-H vinylation reaction

Further, several examples of C-H functionalization have come till date. Most of C-H functionalization reactions are driven by catalytic influences. Categorically, catalytic C-H functionalization reactions could be classified into two parts: i) metal catalyzed and ii) metal free.

1.4. Metal catalyzed C-H functionalization

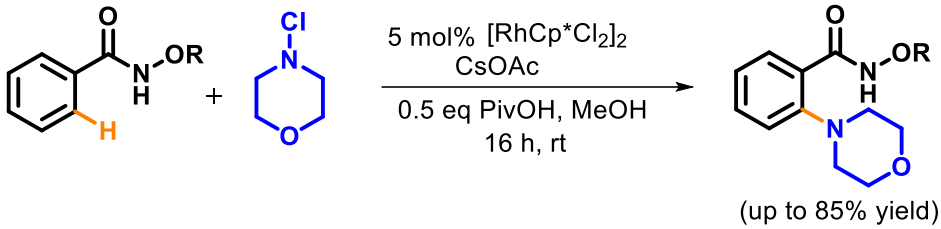
Metal catalyzed, mainly transition metal catalyzed C-H functionalization has emerged as a powerful tool for organic synthesis.[10] Manifold commercially available as well as specially designed transition metal-based catalyst systems have been employed for C-H functionalization reactions. The regioselective direct conversion of C–H bonds into C–C bonds by means of classical catalytic cross-coupling reactions between organohalides and organometallic compounds RM (M = Li, MgX, ZnX, BR_2, SnR_3, SiR_3, etc.) has brought significant revolution in the advancement of organic synthesis.[11] Transition metal catalysts mainly palladium, rhodium, ruthenium complexes have been widely documented for C-H functionalization reactions.[12] Few examples have been presented below:

In 2006, Sanford *et al*. have established a Pd (II) catalyzed acetoxylation reaction of oxime ether using oxone as the source of environmentally benign oxidant (Scheme 1.5).[13] In this reaction, acetic acid was used as a solvent.



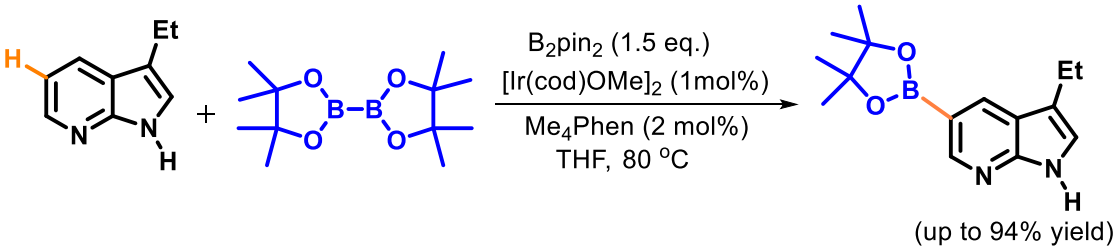
Scheme 1.5: Pd-catalyzed C-H acetoxylation reaction of oxime ether

In 2012, Glorius *et al.* have demonstrated Rh (III) catalyzed C-H amination of *N*-pivaloyloxyamides with *N*-chloroalkyl amines at room temperature (Scheme 1.6).[14]



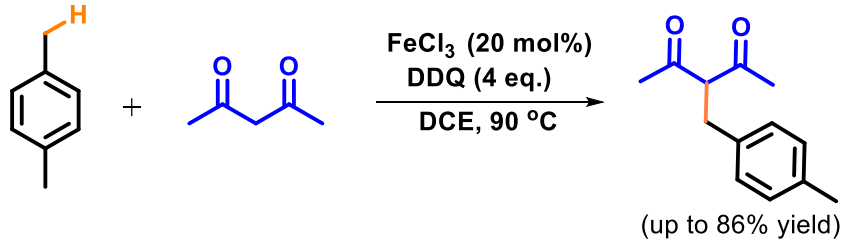
Scheme 1.6: Rh-catalyzed C-H amination of *N*-pivaloyloxyamines

In 2014, Hartwig *et al.* have developed an efficient Ir-catalyzed selective C-H borylation reaction of heteroarenes like pyrazoles, pyrimidines, benzoxazoles, benzothiazoles and azaindoles (Scheme 1.7).[15]



Scheme 1.7: Ir-catalyzed site-selective C-H borylation of heteroarenes

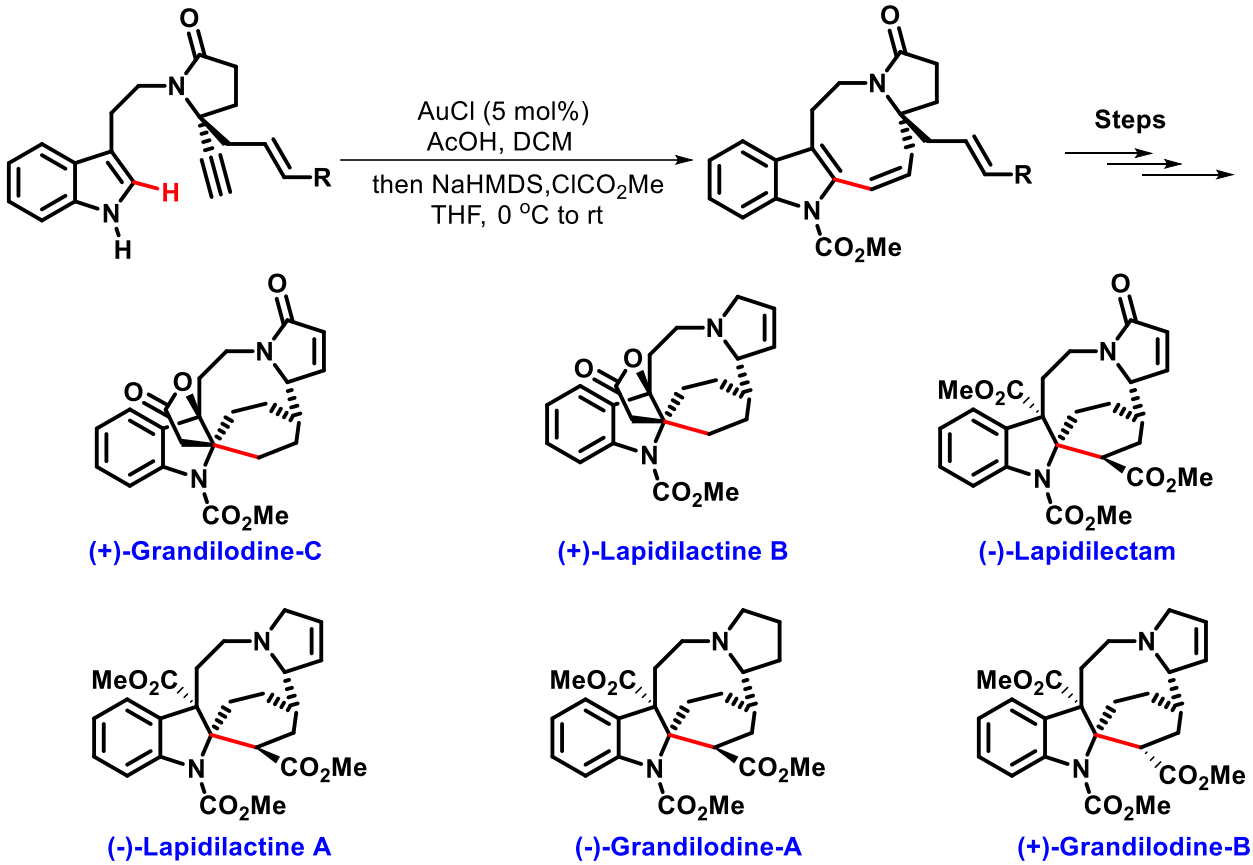
In 2015, Song *et al.* have described a mild strategy for Fe-catalyzed tandem cross-dehydrogenative coupling (CDC) of the methyl group in arylmethanes with 1,3-dicarbonyl compounds using DDQ as oxidant (Scheme 1.8).[16]



Scheme 1.8: Fe-catalyzed crossdehydrogenative coupling of 1,3-dicarbonyls and arylmethanes

Metal catalyzed C-H functionalization reactions have extensively been applied to access complex natural products, drugs, pharmaceuticals etc. To exemplify one, Echavarren *et al.* have reported Au-

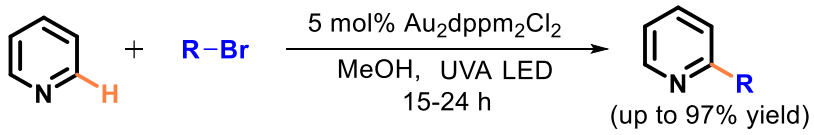
catalyzed C-H hydroarylation to access Lapidilectine and Grandilodine class of natural products (Scheme 1.9).[17]



Scheme 1.9: Au-catalyzed hydroarylation to access Lapidilectine and Grandilodine natural producs

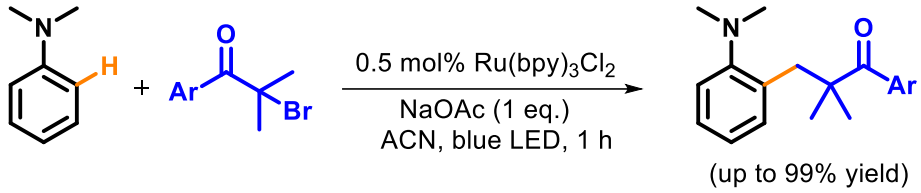
In last two decades, transition metal-based photocatalysts like polypyridyl complexes of ruthenium and iridium have found immense application in organic synthesis for undergoing such unqiue transformation that are not achievable under conventional routes.[18] As a result, transition metal photoredox catalyzed C-H functionalization has grown simultaneously. Few examples have been given below:

In 2016, Barriault *et al.* has shown photoredox gold catalyzed alkylation of heteroarenes where unactivated alkyl bromides have been used for generation of alkyl radicals.[19] The reaction eventually gives rise to formation of 2-alkylated pyridines (Scheme 1.10).



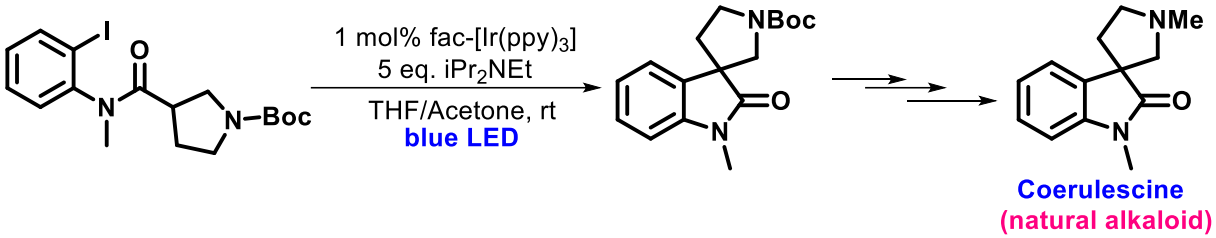
Scheme 1.10: Photoredox Au-catalyzed alkylation of heteroarenes

In the same year, Li *et al.* has displayed a photoredox Ru catalyzed method for direct intermolecular quaternary alkylation of aniline derivatives using bromoketones as source of alkyl group (Scheme 1.11).[20]



Scheme 1.11: Photoredox Ru-catalyzed alkylation of aniline derivatives

Transition metal based photoredox catalyzed transformations have also been extended to total synthesis of natural products.[21] Xu and co-workers recently utilised a [fac-Ir(ppy)$_3$]-mediated intramolecular 1,5-H atom transfer reaction to synthesize the natural alkaloids, coerulescine (Scheme 1.12).[22]

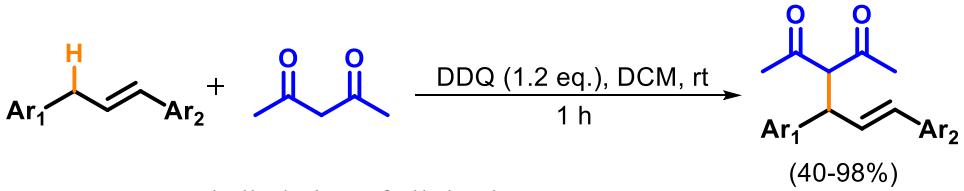


Scheme 1.12: Photoredox Ir-catalyzed synthesis of natural alkaloid Coerulescine

1.5. Metal free C-H functionalization

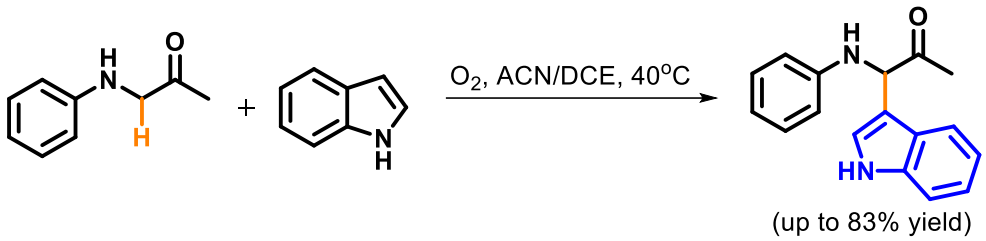
Although enormous catalytic C–H functionalization reactions employing transition metals have been developed and utilized for synthesis of pharmaceuticals, drugs, perfumeries etc. but considered environmentally less sustainable as metal-based waste is known to cause environmental impact. As a result, metal-free protocols have gained popularity for eco-friendly and sustainable organic transformation.[23-25] Much efforts have been put forward for metal-free C-H functionalization reactions. Some of the transformations have been enlisted below:

In 2008, Bao *et al.* has orchestrated metal free DDQ promoted coupling methodology between 1,3-dicarbonyls and allylic compounds for allyl alkylation (Scheme 1.13).[26]



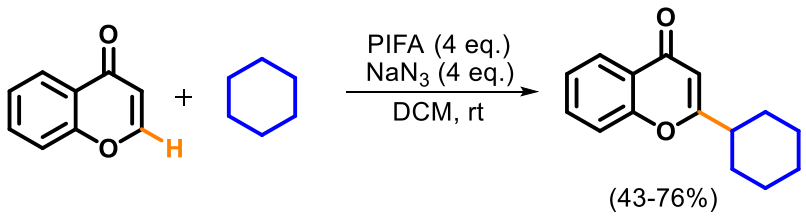
Scheme 1.13: DDQ promoted alkylation of allyl substrates

In 2014, Tang *et al.* have reported an unprecedented aerobic cross-coupling reaction between glycine derivatives and indoles. As this coupling reaction avoids the use of transition metals, additives, high temperatures and hazardous solvents, appears to be highly sustainable and green (Scheme 1.14).[27]



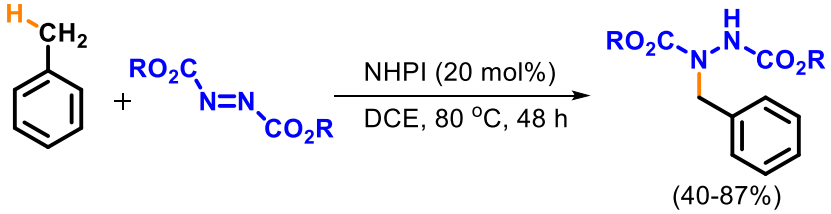
Scheme 1.14: Auto-oxidative cross-coupling between glycine derivatives and indoles

In the same year, Antonchick *et al.* have published a work describing the hypervalent iodine (PIFA) mediated direct oxidative C-H functionalization reaction between C-2 position of chromone or thiochromone with alkanes to access bio-active organic molecules (Scheme 1.15).[28]



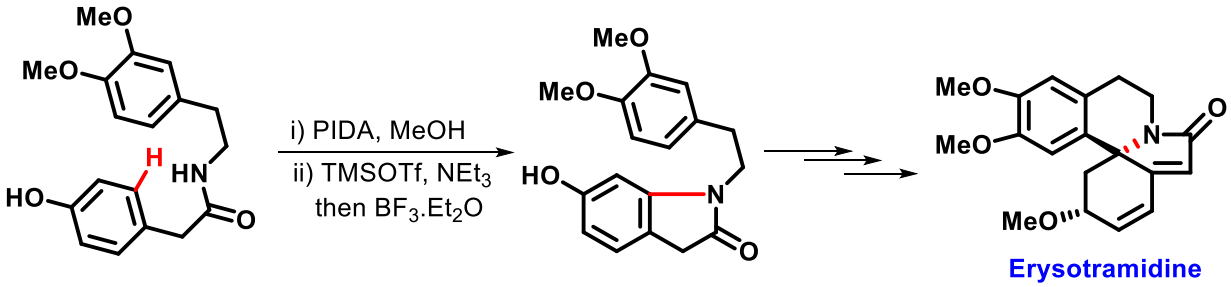
Scheme 1.15: Hypervalent iodine mediated C-H functionalization of chromones and thiochromones with alkanes

In 2012, Inoue *et al.* have illustrated a work showing *N*-hydroxyphthalimide mediated C-H amination reaction between benzylic and propargylic C-H and dialkyl azodicarboxylate which entails an indirect route for installation of -NH_2 group at C-H bond (Scheme 1.16).[29]



Scheme 1.16: NHPI mediated C-H amination at benzylic and propargylic positions

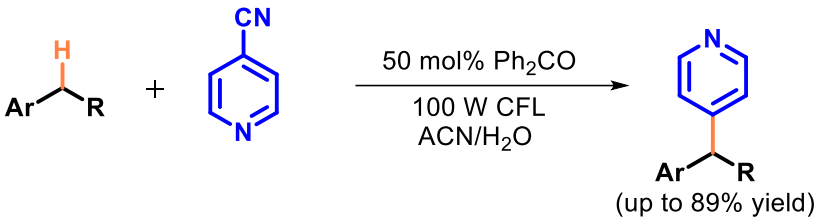
Environmental benignness and sustainibility has popularized metal free C-H functionalization as a tool for complex natural product synthesis.[30] To exemplify one, in 2014, total synthesis of erysotramidine has been performed by Canesi *et al.* where the key spiranic core was assembled by a metal-free hypervalent iodine PIDA mediated intramolecular C-H amination method (Scheme 1.17).[31] Further, a Pictet-Spengler cyclization gave the natural product Erysotramidine.



Scheme 1.17: NHPI mediated C-H amination at benzylic and propargylic positions

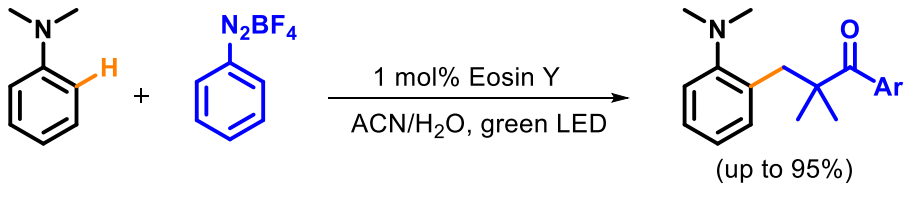
Like the thermal reactions, metal-free photoredox catalyzed reactions have also flourished organic synthesis because of its capability to undergo unusual organic transformations in extremely greener and sustainable approach.[32] Organophotoredox catalysts like Eosin Y, Rose Bengal, Rhodamine B, Acridinium salts, Benzophenone etc. have been widely used for development of new effective transfromations.[33] Few such examples have been given below:

In 2013, Inoue *et al.* have detailed a photochemically driven approach for C-H pyridination at benzylic position using CFL lamp and benzophenone as photosensitizer (Scheme 1.18).[34]



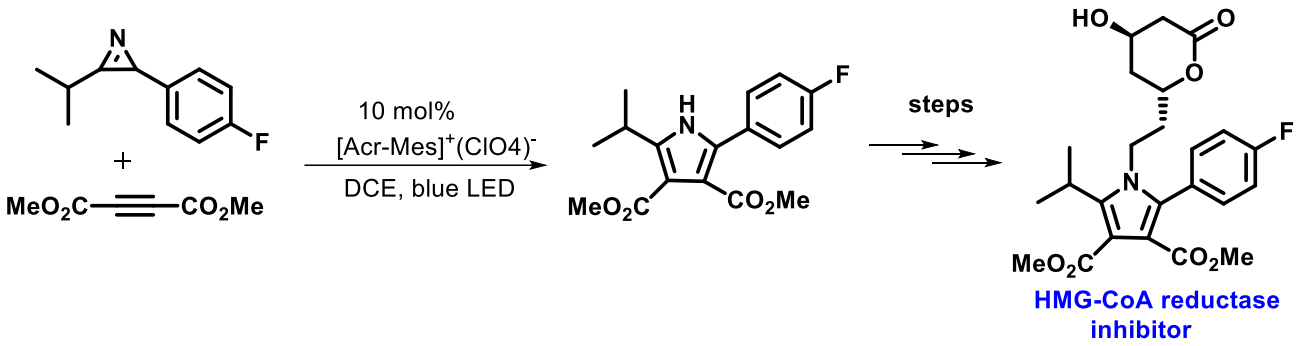
Scheme 1.18: Photo-induced C-H pyridination at benzylic position

In 2014, Yadav *et al*. has introduced a strategy for Eosin Y photoredox catalyzed C-H arylation of aniline derivatives utilizing aryldiazonium salts as the source of aryl group (Scheme 1.19).[35]



Scheme 1.19: Eosin Y catalyzed C-H arylation of aniline derivatives

The growing impact of metal-free organophotoredox catalyzed transformation in terms of sustainability has prompted researchers to carry out total synthesis of natural products.[36] For example, Xiao and co-workers have reported an interesting formal [3 +2] cycloaddition of 2*H*-azirines with Michael acceptors and used it in the formal synthesis of the HMG-CoA reductase inhibitor (Scheme 1.20).[37]



Scheme 1.20: Organo-photoredox catalyzed synthesis of HMG-CoA reductase inhibitor

1.6. Reactive sites on cyclic 1,3-diketones and its C-H functionalization

Cyclic 1,3-diketones presents a rigid, cyclic structure with two carbon groups that can exist in keto-enol tautomeric form. The main reactive sites in cyclic 1,3-diketones are C-2 carbon that is flanked by two carbonyl groups. The C-2 carbon provides acidic H and nucleophilic (Figure 1.3).

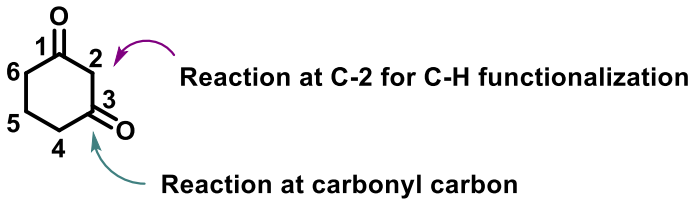
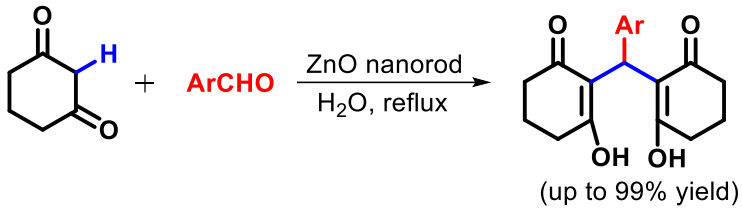


Figure 1.3: Reactive sites at Cyclic 1,3-diketone molecules

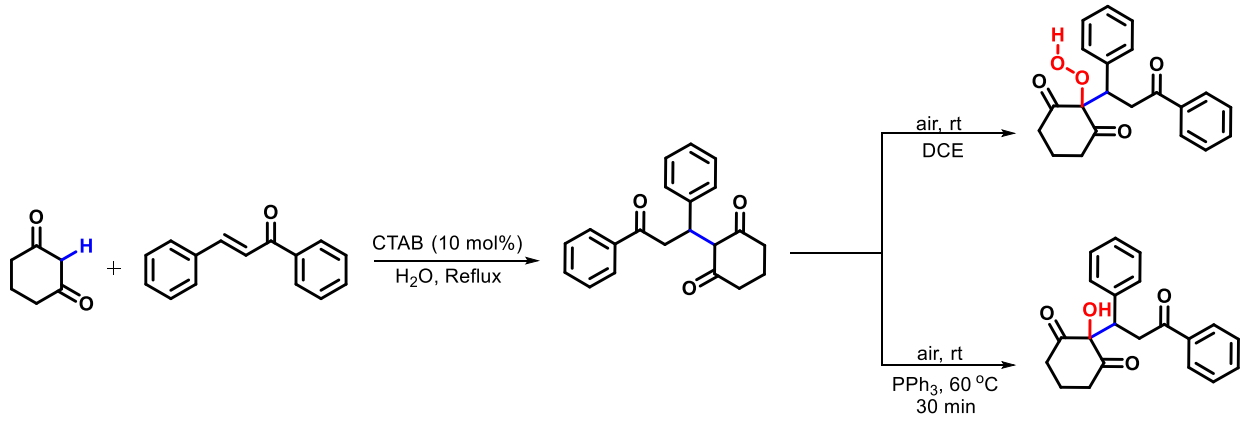
Therefore, a lot of reports have been published previously focusing on the C-H functionalization at C-2 carbon of cyclic-1,3-diketones.[38] Some of the results have been described below:

In 2017, Yaghoubi *et al.* have performed C-H functionalization reaction at C-2 position of cyclic-1,3-diketones by reacting with aldehyde under the catalytic influence of ZnO nanorod-decorated graphene oxide and obtained tetraketones (Scheme 1.21).[39]



Scheme 1.21: C-H functionalization of cyclic-1,3-diketones with aldehydes

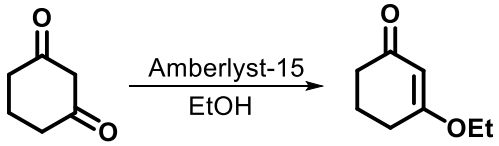
In 2011, Xia *et al.* have carried out CTAB catalyzed Michael addition reaction between cyclic 1,3-diketones and chalcones to obtain C-H functionalized product and the product has been further synthetically diversified to obtain oxygenated products (Scheme 1.22).[40]



Scheme 1.22: Michael addition of cyclic 1,3-diketones and auto-oxidation

Apart from the C-2 functionalization, several works have been done involving the carbonyl group of cyclic 1,3-diketones. For example, one of work from our group has been exemplified below:

In 2019, our group has reported reaction between alcohols and cyclic 1,3-diketones in presence of heterogeneous Amberlyst-15 catalyst (Scheme 1.23).[41]



Scheme 1.23: Synthesis of vinylogous ester with cyclic 1,3-dione

1.7. Reactive sites on quinoxalin-2(1*H*)-ones and its C-H functionalization

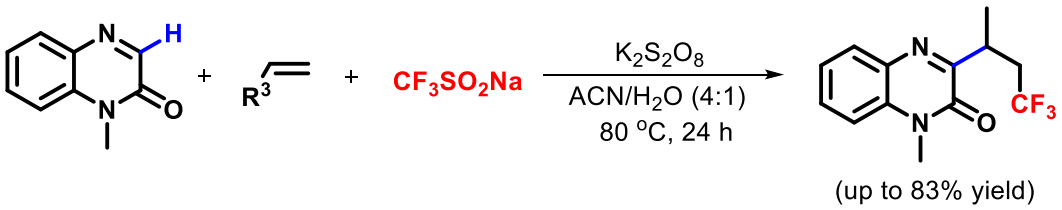
Quinoxalin-2(1*H*)-ones are 2 nitrogen containing bicyclic heterocycle. Both the rings have ununiform electronic distribution. The nitrogen containing ring is electron deficient and presents a scaffold for performing various kind of reactions. Particularly, the C-3 carbon is highly reactive and shows unique reactivity for carrying out sp^2 C-H functionalization (Figure 1.4).



Figure 1.4: Reactive centre for C-H functionalization in quinoxalinones

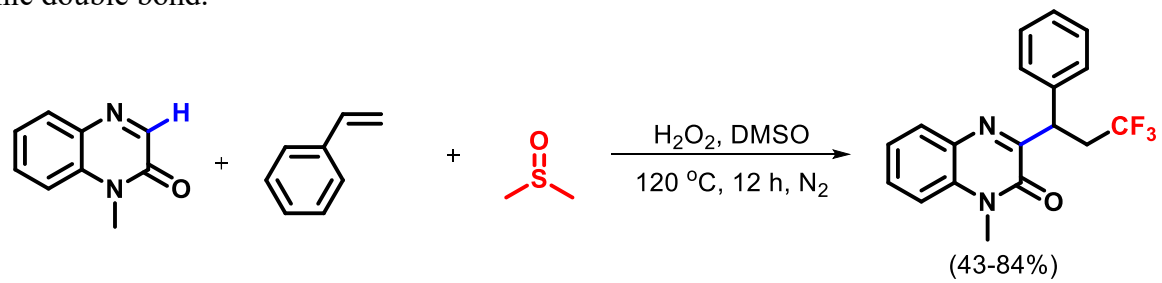
By introducing different group at C-3 position of quinoxalin-2(1*H*)-ones, it is possible to modulate the biological activity of the quinoxalinone derivative. Hence production of new derivatives of quinoxalinones is expected to expand the scope of further bio-medicinal assessment. Therefore, several attempts have been made to extensively functionalize the C-3 position of quinoxalinones.[42] Some of the reports have been given below:

In 2020, Wei *et al.* developed a three-component reaction for C-3 C-H functionalization of quinoxalinones using unactivated alkenes and Langlois' Reagent as source of trifluoromethyl (Scheme 1.24).[43]



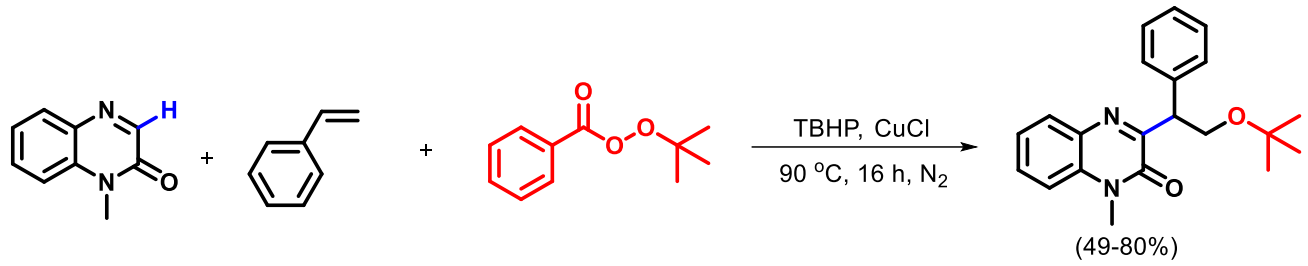
Scheme 1.24: Trifluoroalkylation of quinoxalinones with unactivated alkenes

In 2021, Xiong *et al.* have demonstrated a green, operationally simple and convenient three component hydrocarbylation reaction of quinoxalinones using hydrogen peroxide as the oxidant (Scheme 1.25).[44] In this reaction DMSO acts as the source of methyl group that adds across the olefinic double bond.



Scheme 1.25: H_2O_2 promoted alkylation of quinoxalinones with styrenes and dimethyl sulfoxide

In the next year, Lin *et al.* have executed a three-component tandem alkylation reaction at C-3 position of quinoxalinone *tert*-butyl peroxybenzoate as the source of alkyl group (Scheme 1.26).[45]



Scheme 1.26: TBHP promoted CuCl catalyzed three component alkylation of quinoxalinones

1.8. Reactive sites on α-aryl esters and its C-H functionalization

The esters of phenyl acetic acids are also uniquitous motif in organic synthesis. It has two possible reaction sites: i) reaction at methylene carbon flanked by aryl ring and ester group for C-H functionalization and ii) reaction at carbonyl carbon (Figure 1.5).

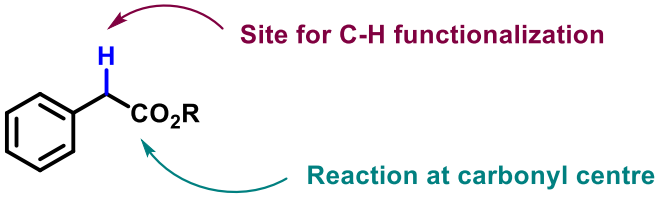
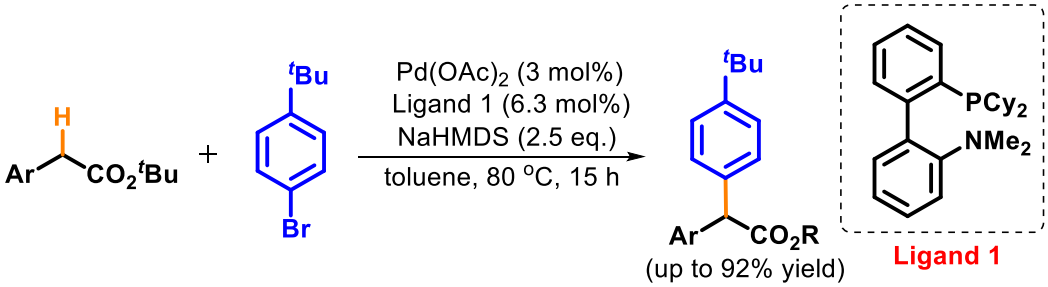


Figure 1.5: Reaction sites at α-aryl esters

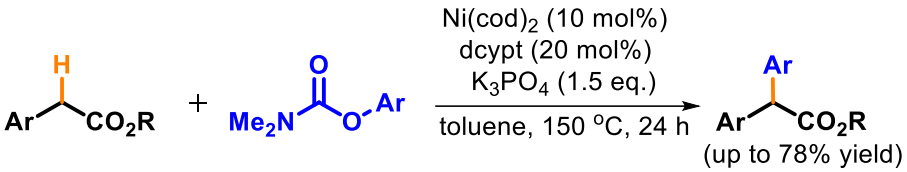
The C-H bond at α-position has been extensively functionalized. Few examples are shown below.

In 2001, Buchwald *et al.* have demonstrated an efficient method for C-H arylation of α-aryl esters using $Pd(OAc)_2$ and bulky electron-rich *o*-biphenyl phosphines (Scheme 1.26).[46]



Scheme 1.26: Pd-catalyzed C-H arylation of α-aryl esters

In 2015, Itami *et al.* have reported Ni-catalyzed arylation of α-aryl ester using *O*-arylpivalates or *O*-arylcarbamates as source of aryl group.[47]



Scheme 1.26: Ni-catalyzed C-H arylation of α-aryl esters

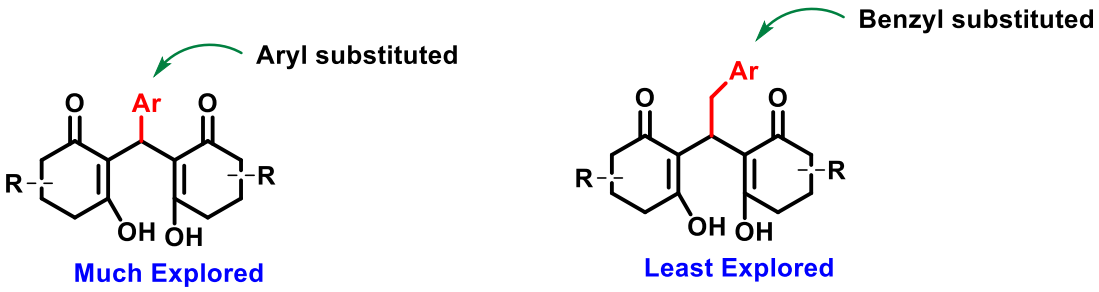
1.9. Rationale behind the thesis work

In the literature, various methodologies including metal catalyzed and metal-free conditions have been reported for the C-H functionalization reaction with cyclic 1,3-diketones, quinoxaline-2(1*H*)-ones and α-aryl esters under thermal and photochemical conditions. Alkyl, aryl, ether thioether, halide, amine etc functional groups have been installed at the expense of C-H bonds under suitable reaction condition. Derivatives of functionalized cyclic 1,3-diketones, quinoxaline-2(1*H*)-ones are widely documented for their various biomedical and therapeutic application. Therefore, further broadening the scopes of new series of functionalized cyclic 1,3-diketones, quinoxaline-2(1*H*)-ones and α-aryl esters will extend the platform for further biological assessments. Various well-established methods have been used for C-H functionalization of functionalized cyclic 1,3-diketones, quinoxaline-2(1*H*)-ones and α-aryl esters. However, many of those requires: i) the use of toxic reagents, ii) sensitive catalysts, iii) expensive metal catalysts iv) multi-step synthesis which limits their utilization in several organic transformations. In this context, our research group has focused on developing a simple, mild metal-assisted/metal-free and effective protocol for the C-H functionalization reaction, their scale up in flow and finding further synthetic application.

1.10. Objectives of our projects

A. Continuous flow Fe-zeolite catalyzed C-H functionalization of cyclic 1,3-diketones via Meinwald rearrangement

Tetraketones are therapeutically important and find usefulness as drug candidates, several kinds of inhibitor molecule. Conventionally, tetraketones have been prepared by the condensation of cyclic 1,3-diketones and aldehydes under the influence of acid catalyst. But most of the previous methods have synthesized direct aryl substituted tertektones whereas the benzyl derivative substituted tetreaketones are essentially left unexplored (scheme 1.21). The possible reason could be that the benzyl surrogate, i.e, phenyl acetaldehyde derivatives are relatively difficult to prepare.

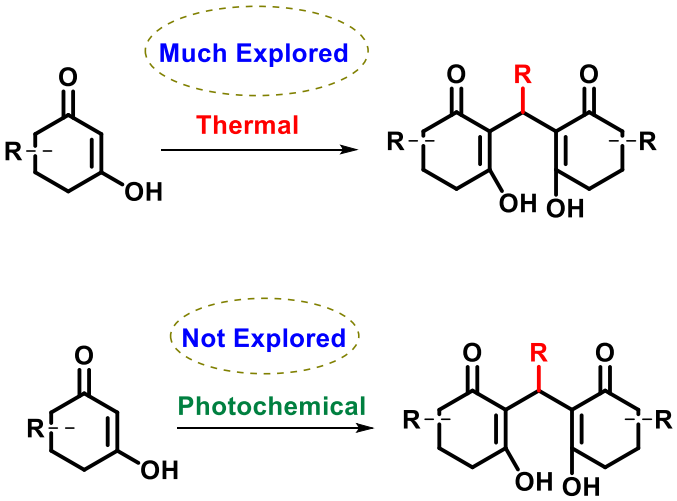


Scheme 1.27: Aryl and benzyl substituted tetraketones

So, generation of such new classes of tetraketones will undoubtedly expand the scope for further biomedical evaluation. Therefore, considering all the things stated above, our main objective for this chapter will be synthesis of benzyl substituted tetrakeotones and transfer the methodology under continuous flow and finding other synthetic applications of tetraketone molecules.

B. Organophotoredox catalyzed C-H functionalization of cyclic 1,3-diketones using tertiary amines as alkyl synthon

Although a large number of methods are available for the synthesis of tetraketones, most of the methods involve use of specially designed lewis acid catalysts, ionic liquids and most of these reactions are usually performed either under heating conditions or by reflux. In all these reactions, aldehydes have been used as the alkyl surrogates for tetraketones. Now-a-days, photoredox catalysis has emerged as green, sustainable and environmentally benign ways for organic transformations. To the best of our knowledge, so far, no reports are available for the tetraketone synthesis under photoredox catalysis conditions (Scheme 1.23). So, it is also needful to find an alternate alkyl surrogate other than aldehydes that will work under photoredox catalysis conditions.

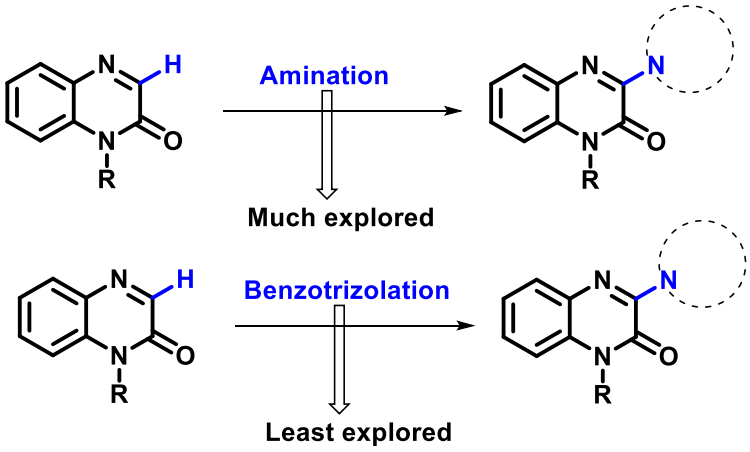


Scheme 1.28: State of art for tetraketone synthesis using different processes

Therefore, main objective of this chapter will be tetraketone synthesis utilizing eco-friendly photochemical conditions that avoids harsh conditions like high temperature and find a suitable alkyl surrogate that works under redox active photocatalysis conditions.

C. Photochemical sp^2 C-H benzotriazolation of quinoxalin-2(1*H*)-ones

Most of the derivatives of quinoxalin-2(1*H*)-one is endowed with momentous biological activities. So, expanding the scope of new functionalized quinoxaninones will definitely present the platform for further remarkable biological activites. As a result, attempts have been made to extensively functionalize the C-3 position of quinoxalin-2(1*H*)-one. Previously, several methods have been established for: (i) C-C bond formations like alkylation, arylation, trifluoromethylation; (ii) C-O bond formations like etherification, esterifications, hydroxylation; (iii) C-S bond formations like thioetherification, thioesterification; (iv) C-N bond formations like amination with different types of aliphatic, alicyclic and aromatic amines. From literature, it is known that benzotriazole type molecules show prominent agricultural applications. So, we hypothesized that if we can couple quinoxalinones with benzotriazole, the resulting benzotriazolated quinoxalinones could be potentially bioactive material. Although, quinoxalinone has been extensively studied for different C-H amination reaction but the benzotrizolation reaction has not been explored much (Scheme 1.29).



Scheme 1.29: State of art for C-N bond formation with quinoxalinones

Therefore, objective of this project will be to develop a simple, mild and efficient protocol for the synthesis of benzotriazolated quinoxalinones.

D. Benzotriazolation of α-aryl esters

α-amino substituted carbonyls show promising pharmaceutical activities. So, installation of amine functionality with α-aryl esters is highly desirable. We have envisioned to introduce benzotrazole moiety at α position of α-arylester. Our objective is to benzotriazolate the α-position of α-aryl ester.



Scheme 1.30: Benzotriazolation of α-aryl ester

1.11. References:

(1) (a) Hartwig, J. F.; Larsen, M. A. *ACS Cent. Sci.* **2016**, *2*, 281-292. (b) Davies, H. M. L.; Morton, D. *J. Org. Chem.* **2016**, *81*, 343-350. (c) Yamaguchi, J.; Yamaguchi, A. D.; Itami, *Angew.Chem., Int. Ed*. **2012**, *51*, 8960−9009.

(2) Xue, X. S.; Ji, P.; Zhou, B.; Cheng, J. P. *Chem. Rev.* **2017**, *117*, 8622−8648.

(3) Dalton, T.; Faber, T.; Glorius, F. C−H Activation:Toward Sustainability and Applications. *ACS Central. Sci.* **2021**, *7*, 245−261.

(4) Friedrich Wöhler (1828). "Ueber künstliche Bildung des Harnstoffs". Annalen der Physik und Chemie. 88 (2): 253–256.

(5) Hofmann, A. W. Berichte der deutschen chemischen Gesellschaft, Ueber die Einwirkung des Broms in alkalischer Lösung auf die Amine. Chem. Ges. **1883**, *16*, 558−560.

(6) Loffler, K.; Kober, S. *Chemische Berichte*, **1909**, *42*, 3431-3438.

(7) Wang, X.; Liu, Y.; Li, Y.; Zhang, H.; Zhang, X**.** *Chem. Eur. J.* **2022**, *28*, e202104278.

(8) Hartwig, J. F.; Larsen, M. A. *ACS Cent. Sci.* **2016**, *2*, 281-292.

(9) W. Xu, J. Zhao, C. Tao, H. Wang, Y. Li, B. Cheng, H. Zhai. *Org. Lett.* **2018**, *20*, 1509–1512.

(10) Wan, J. P.; Gan, L.; Liu, Y. *Org. Biomol. Chem.* **2017**, *15*,9031−9043.

(11) (a) Biffis, A.; Centomo, P.; Del Zotto, A.; Zecca, M. *Chem. Rev.* **2018**, *118*, 2249−2295. (b) Kambe, N.; Iwasaki,T.; Terao, J. *Chem. Soc. Rev*. **2011**, *40*, 4937−4947.

(12) (a) Liu, X. W.; Shi, J. L.; Yan, J. X.; Wei, J. B.; Peng, K.; Dai, L.; Li, C.G.; Wang, B. Q.; Shi, Z. J. *Org. Lett.* **2013**, *15*, 5774−5777. (b) Qi, X.; Li, Y.; Bai, R.; Lan, Y. *Acc. Chem. Res*. **2017**, *50*, 2799−2808. (c) Liu, C. X.; Yin, S. Y.; Zhao, F. N.; Yang, H.; Feng, Z. L. J.; Gu, Q.;You, S. L. *Chem. Rev*. **2023**, *123*, 10079-10134.

(13) Desai, L. V.; Malik, H. A.; Sanford, M. S. *Org. Lett*. **2006**, *8*, 1141-1144.

(14) Grohmann, C.; Wang, H.; Glorius, F. *Org. Lett*. **2012**, *14*, 656– 659.

(15) Larsen, M. A.; Hartwig, J. F. *J. Am. Chem. Soc.* **2014**, *136*, 4287-4299.

(16) Yang, K.; Song, Q. *Org. Lett*. **2015**, *17*, 548-551.

(17) F. M. Miloserdov, M. S. Kirillova, M. E. Muratore, A. M. Echavarren. *J. Am.Chem. Soc.* **2018**, *140*, 5393–5400.

(18) (a) Zhang, J., Rueping, M. *Nat. Catal.* **2024**, *7*, 963–976. (b) Prier, C. K.; Rankic, D. A.; MacMillan, D. W. C. *Chem. Rev.* **2013**, *113*, 7, 5322−5363.

(19) McCallum, T.; Barriault, L. *Chem. Sci*. **2016**, *7*, 4754−4758.

(20) Cheng, J.; Deng, X.; Wang, G.; Li, Y.; Cheng, X.; Li, G. *Org. Lett*. **2016**, *18*,4538−4541.

(21) Nicholls, T. P.; Leonori, D.; Bissember, A. C. *Nat. Prod. Rep.* **2016**, *33* (11), 1248–1254.

(22) Chen, J.-Q.; Wei, Y.-L.; Xu, G.-Q.; Liang, Y.-M.; Xu, P.-F. *Chem. Commun*. **2016**, *52*, 6455–6458.

(23) Hayler, J. D.; Leahy, D. K.; Simmons, E. M. *Organometallics*. **2019**, *38*, 1, 36−46.

(24) Anastas, P. T.; Kirchhoff, M. M. *Acc. Chem. Res*. **2002**, *35* (9), 686–692.

(25) Li, J.; Albrecht, J.; Borovika, A.; Eastgate, M. D. *ACS Sustainable Chem. Eng*. **2018**, *6* (1), 1121–1132.

(26) Cheng, D.; Bao, W. *Adv. Synth. Catal*., **2008**, *350*, 1263–1266.

(27) Huo, C.; Yuan, Y.; Wu, M.; Jia, X.; Wang, X.; Chen, F.; Tang, J. *Angew. Chem., Int. Ed*., **2014**, *53*, 13544–13547.

(28) Narayan, R.; Antonchick, A. P. *Chem. Eur. J*., **2014**, *20*, 4568–4572.

(29) Amaoka, Y.; Kamijo, S.; Hoshikawa, T.; Inoue, M. *J. Org. Chem*., **2012**, *87*(22), 9959–9969.

(30) Roy, S.; Panja, S.; Sahoo, S. R.; Chatterjee, S.; Maiti, D. *Chem. Soc. Rev.* **2023**, *52*, 2391–2479.

(31) L'Homme, C.; Menard, M. A.; Canesi, S. *J. Org. Chem*. **2014**, *79* (17), 8481–8490.

(32) (a) Kumar Hota, S.; Jinan, D.; Prakash Panda, S.; Pan, R.; Sahoo, B.; Murarka, S. *Asian J. Org. Chem*. **2021**, *10*, 1848−1860. (b) Crisenza, G. E. M.; Melchiorre, P. *Nat. Commun*. **2020**, *11*, 803. (c) Gupta, S.; Kundu,A.; Ghosh, S.; Chakraborty, A.; Hajra, A. *Green Chem*. **2023**, *25* (25), 8459−8493.

(33) (a) Singla, D.; Luxami, V.; Paul, K. *Organic Chemistry Frontiers* **2022**, *10* (1), 237−266. (b) Singh, P. P.; Singh, J.; Srivastava, V. *RSC Adv.* **2023**, *13*, 10958−10986.

(34) Hoshikawa, T.; Inoue, M. *Chem. Sci.* **2013**, *4*, 3118−3123.

(35) Kapoor, R.; Chawla, R.; Yadav, L. D. S. *Tetrahedron Lett.,* **2019**, *60*, 805-809.

(36) Nicewicz, D. A.; Nguyen, T. M. *Chem. Rev.* **2016**, *116* (17), 10075–10166

(37) Xuan, J.; Xia, X.-D.; Zeng, T.-T.; Feng, Z.-J.; Chen, J.-R.; Lu, L.-Q.; Xiao, W.-J. *Angew. Chem., Int. Ed.* **2014**, *53* (22), 5653–5656.

(38) (a) Bityukov, O. V.; Serdyuchenko, P. Y.; Vil', V. A.; Nikishin, G. I.; He, L.-N.; Terent'ev, *Eur. J. Org. Chem*. **2024**, *27*, e202400078. (b) Kumar, R.; Raghuvanshi, K.;Verma, R. K.; Singh, M. S. *Tetrahedron Lett*. **2010**, *51*, 5933-5936. (c) Chowdhury, S.; Nandi, G. C.; Samai, S.; Singh, M. S. *Org. Lett.* **2011**, *13*, 3762−3765. (d) Chung, T. W.; Narhe, B. D.; Lin, C.-C.; Sun, C. M. *Org. Lett*. **2015**, *17*, 5368-5371.

(39) Hasanzadeh Banakar, S.; Dekamin, M. G.; Yaghoubi, A. *New J. Chem.* **2018**, *42*, 14246−14262

(40) Wang, G.-W.; Lu, Q.-Q.; Xia, J.-J. *Eur. J. Org. Chem*. **2011**, *2011*, 4429-4438.

(41) Mohanta, N.; Chaudhari, M. B.; Digrawal, N. K.; Gnanaprakasam, B. *Org. Process Res. Dev*. **2019**, *23*, 1034−1045.

(42) Yang, Q.; Wang, B.; Wu, M.; Lei, Y. Z. *Molecules*. **2023**, *28* (6), 2513.

(43) Meng, N.; Wang, L.; Liu, Q.; Li, Q.; Lv, Y.; Yue, H.; Wang, X.;Wei, W. *J. Org. Chem.* **2020**, *85* (11), 6888−6896.

(44) Lin,S.; Yao, H.; Zhong, X.; Wang, B.; Yan, Z.; Xiong,F. *Synlett* **2021**, *32*,1213-1218.

(45) Zhong, X.; Li, X.; Yao, H.; Yan, Z.; Guo, H.; Min, L.; Lin. S. *Synlett* **2022**, *33*, 998–1002.

(46) Moradi, W. A.; Buchwald, S. L. *J. Am. Chem. Soc*. **2001**, *123* (33), 7996–8002.

(47) Koch, E.; Takise, R.; Studer, A.; Yamaguchi, J.; Itami, K. *Chem. Commun.* **2015**, *51*, 855–857.

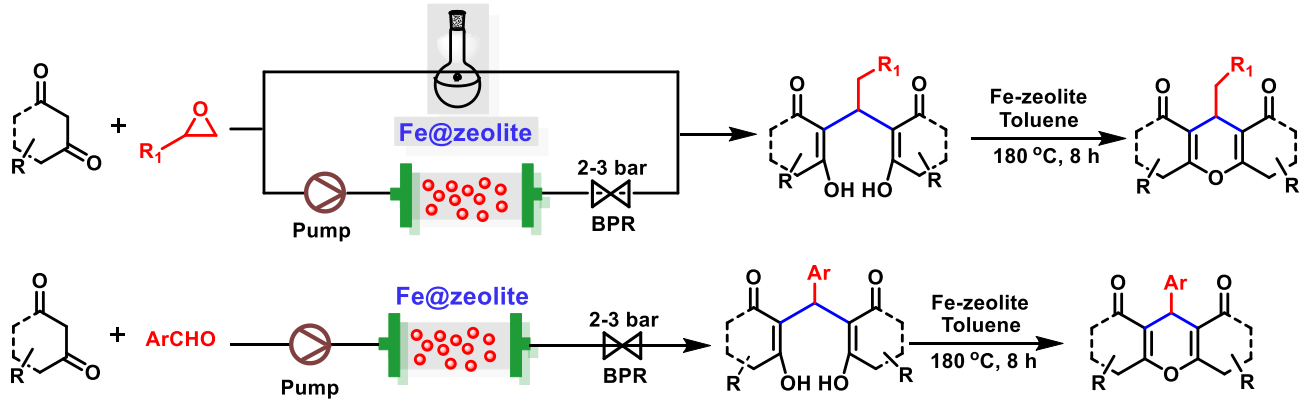
Chapter 2

Continuous Flow Fe-zeolite Catalyzed C-H Functionalization of Cyclic 1,3-diketones via Meinwald Rearrangement

Continuous Flow Fe-zeolite Catalyzed C-H Functionalization of Cyclic 1,3-diketones via Meinwald Rearrangement

2.1. Abstract

In this chapter, an eco-friendly approach for the biologically relevant tetraketones using epoxides and cyclic-1,3-diketones in the presence of Fe-zeolite as a catalyst via Meinwald rearrangement has been discussed under batch and continuous flow module. When the temperature is raised to 180 °C, these tetraketones undergo cyclization reaction in the presence of Fe@zeolite to afford xanthene derivatives. Moreover, the scope of Fe@zeolite catalyst has also been expanded for the direct reaction of aldehyde and cyclic 1,3-diketones affording the corresponding tetraketones in high yield. Advantageously, the protocol offers gram scale synthesis in batch as well as in continuous flow. This method for tetraketone synthesis is sustainable which does not produce any waste. The Fe@zeolite used in this process is easy to synthesize in multigram-scale, cost-effective, and recyclable.



2.2. Introduction

Tetraketones represent a distinct class of highly functionalized carbonyl compounds featuring four ketone groups, typically arranged in a 1,3,5,7-tetraoxo or related linear or cyclic fashion.[1] These compounds are of considerable interest in synthetic and medicinal chemistry owing to their high electrophilicity and potential for enolate formation at multiple centers. Tetraketones are widely used as tyrosinase inhibitor, laser dye, efficient ligand in electron transfer kinetics, lipoxygenase inhibitor, anticancer agent, antioxidant agent and amastigote growth inhibitiors (Figure 2.1).[2-5]

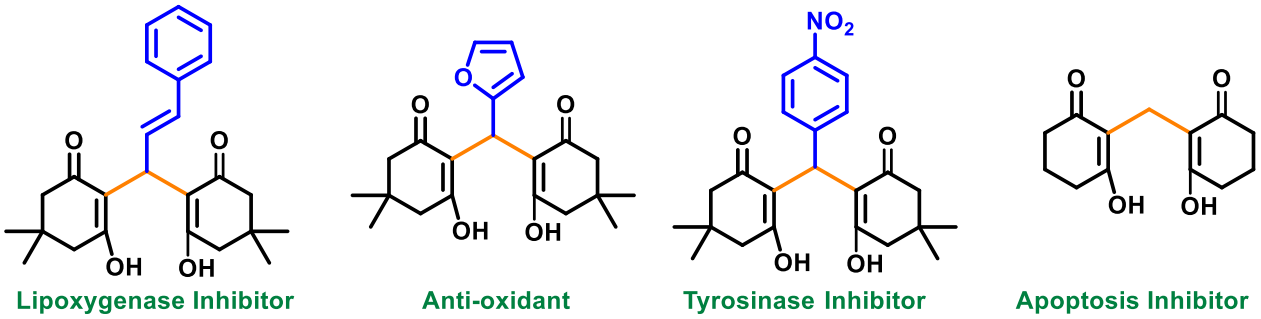


Figure 2.1: Representative examples of biologically active tetraketones

Furthermore, tetraketones are useful intermediates for the synthesis of biologically important xanthenes via cyclisation reactions in the presence of acid catalyst. In general, xanthene possesses different biological activity that includes antibacterial, antifungal, antimalarial, leishmanicidal, and anti-inflammatory effects, potential anti-cancer agent, selective positive allosteric modulator of the d-opiod receptors and selective oestrogen receptor modulator respectively (Figure 2.2).[6-11]

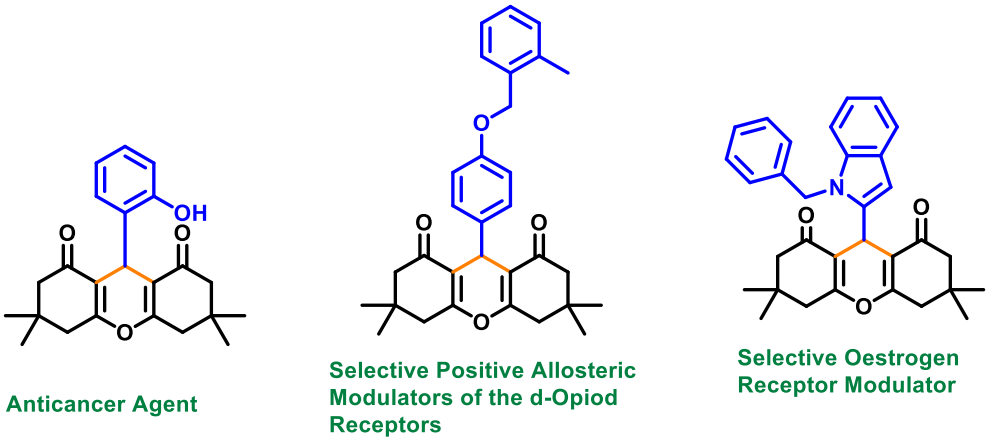
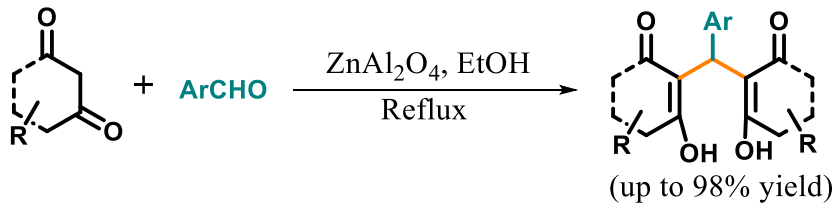


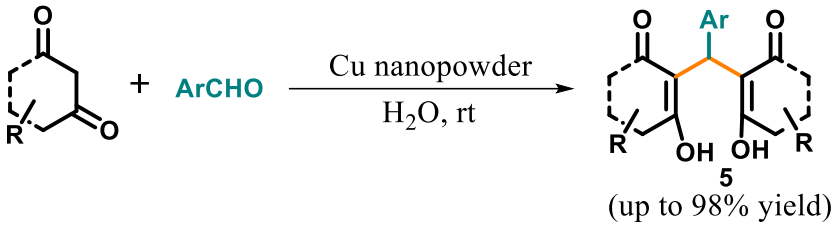
Figure 2.2: Representative examples of biologically active xanthenes

Previously, several works have been reported for tetraketone synthesis. Most of the tetraketones have been accessed by the lewis acid catalysed reaction of aldehyde as the source of electrophile and cyclic 1,3-diketone as a nucleophile. For example, previously Sathiyanarayanan *et al.* have explored nano $ZnAl_2O_4$ catalyzed condensation aldehyde and cyclic 1,3-diketone to produce tetraketones (Scheme 2.1).[12]



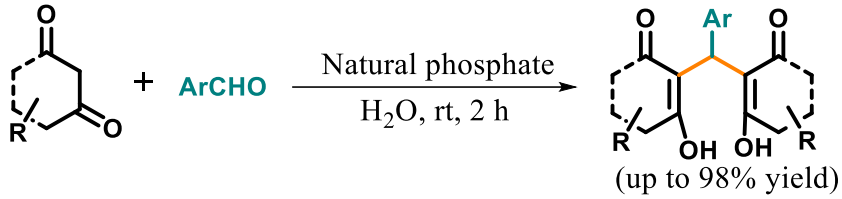
Scheme 2.1: Nano $ZnAl_2O_4$ catalyzed synthesis of tetraketones

Stark *et al.* have reported dendridic Cu nanopowder catalyzed tetraketone synthesis exhibiting compatibility with a wide range of substrates (Scheme 2.2).[13]



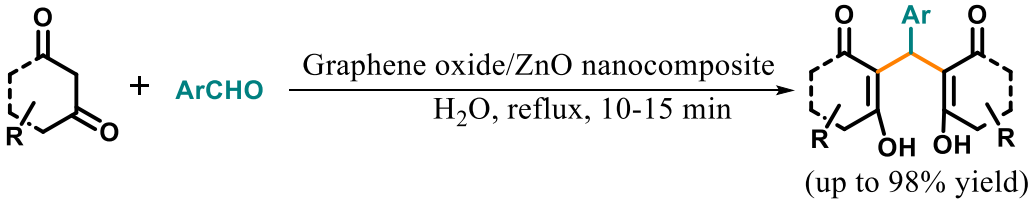
Scheme 2.2: Cu nanopowder catalyzed synthesis of tetraketones

In another notable contribution, Bekhradnia *et al*. have developed a green synthesis method of tetraketones using natural phosphate as catalyst in water under ambient conditions (Scheme 2.3).[14]



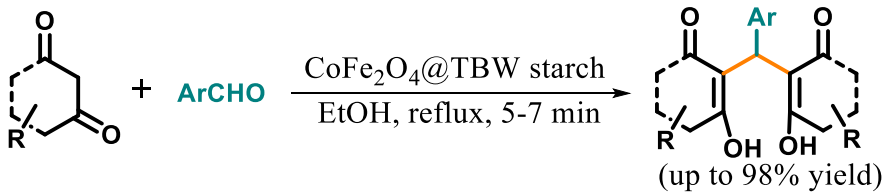
Scheme 2.3: Natural phosphate catalyzed synthesis of tetraketones

Building upon nanocomposite catalysis, Yaghoubi *et al.* utilized a graphene oxide/ZnO system in water under reflux to achieve efficient tetraketone formation (Scheme 2.4).[15]



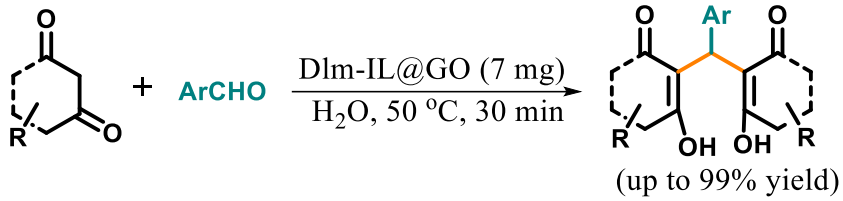
Scheme 2.4: Graphene oxide/ZnO nanocomposite catalyzed synthesis of tetraketones

Adding to the range of eco-friendly approaches, Danishfar *et al.* have reported bread-waste $CoFe_2O_4$@TBW bio-catalyzed tetraketone synthesis (Scheme 2.5).[16]



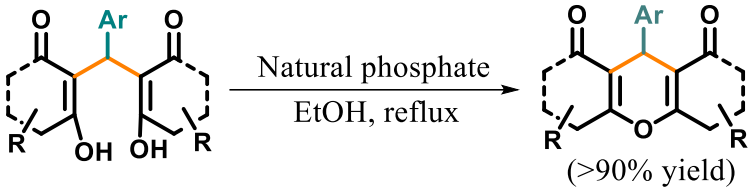
Scheme 2.5: $CoFe_2O_4$@TBW starch bio-catalyzed synthesis of tetraketones

Recently, Mozumdar *et al*. have demonstrated a biscationic imidazolium ionic liquid catalyzed method for tetraketone preparation (Scheme 2.6).[17]



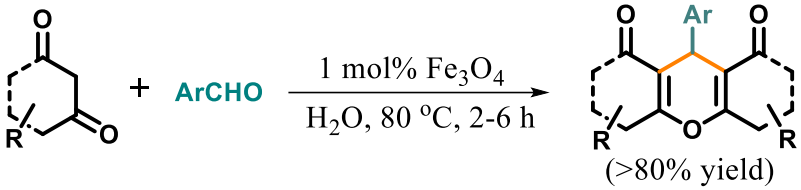
Scheme 2.6: Ionic liquid catalyzed synthesis of tetraketones

Several reports have explicitly shown the synthesis methods for xanthene either starting from tetraketones or directly from cyclic 1,3-diketones and aldehydes. In 2017, Bekhradnia *et al*. have shown that tetraketones, when isolated, can undergo cyclization with natural phosphate catalyst in ethanol under reflux, yielding xanthenes (Scheme 2.7).[18]



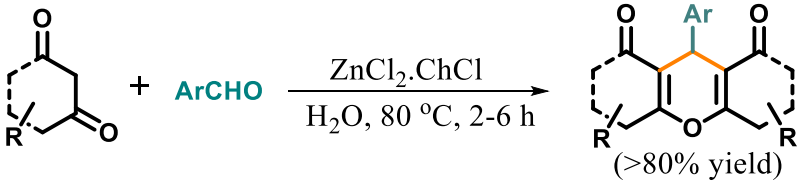
Scheme 2.7: Natural phosphate catalyzed xanthenedione synthesis

In a complementary study, Nasrabadi *et al*. have demonstrated a process for direct synthesis of xanthenes star ting from aldehydes and cyclic 1,3-diketones (Scheme 2.8).[19]



Scheme 2.8: Fe_3O_4 magnetic nanoparticle catalyzed synthesis of tetraketone

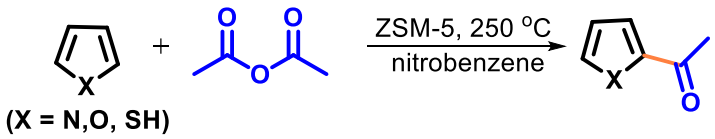
Furthermore, Hashemi *et al*. have established a protocol for choline chloride based deep eutectic solvent catalyzed tandem reactions forming xanthene (Scheme 2.9).[20]



Scheme 2.9: Choline chloride catalyzed tetraketone synthesis

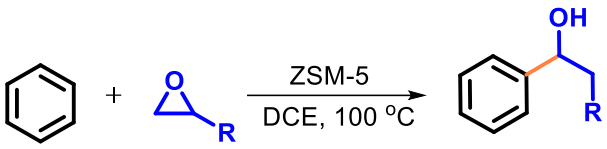
Concerning environmental benignness, sustainable chemistry plays crucial role for the syntheses of complex and high value-added molecules.[21-24] A chemical reaction towards the synthesis of several drugs and active pharmaceutical intermediate could be a sustainable chemical process only when it provides the better atom economy, waste minimization and recyclable properties.[25] Moreover, heterogeneous catalysis plays pivotal role in industrial processes because of the excellent capabilities of accelerating the rate of reactions with low cost, high conversion, and product selectivity. The recyclability nature of heterogeneous catalysts enables green and sustainable manufacturing and avoids the secondary pollution problem.[26] To date, heterogeneous catalysts play an important part in manufacturing approximately 80-90% of all chemicals in the world.[27] Among the heterogeneous catalysts, zeolite has long been a choice of many for its versatile lewis acidic nature.[28] Zeolite is widely used in oil industries for isomerization of hydrocarbons.[29] Besides industrial utility, zeolite has also been utilized for carrying out several fundamental organic transformations.

Among early advancements in zeolite catalysis, Holderich and coworkers have established ZSM-5 catalyzed Friedel Crafts acylation reaction of 5 membered heterocycles using acetic anhydride as acylating reagent.[30] The reaction efficiently works at higher temperature (Scheme 2.10).



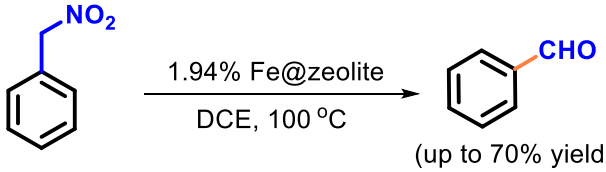
Scheme 2.10: ZSM-5 catalyzed Friedel-Crafts Acylation reaction

In a related study, Sheldon and coworkers have demonstrated a protocol for zeolite catalyzed direct ring opening of epoxide with benzene at 100 °C (Scheme 2.11).[31]



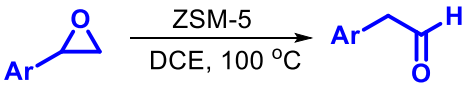
Scheme 2.11: ZSM-5 catalyzed direct ring opening of epoxide with benzene

In continuation of efforts to develop robust heterogeneous systems, our lab has prepared Fe@zeolite catalyst with iron support. Fe@zeolite catalyst has been successfully utilized for efficient conversion of nitro compounds to form carbonyls (Scheme 2.12).[32]



Scheme 2.12: Fe@zeolite catalyzed Nef oxidation of nitro compounds to aldehyde

Besides direct ring opening, zeolite catalyst has been used for intramolecular ring opening of epoxides called Meinwald rearrangement and the reaction has further been utilized for multicomponent reaction (Scheme 2.13).[33]



Scheme 2.13: ZSM-5 catalyzed Meinwald rearrangement

Being inspired by all the above results, we have drawn our interest primarily in heterogeneous catalyzed epoxide ring opening reactions with cyclic 1,3-diketones. Being highly strained molecules, epoxides are susceptible to ring opening by nucleophiles to get rid of angle strain.[34] Previously, regiodivergent hydroborative ring-opening of epoxides with selective C-O bond activation, nickel catalyzed regiodivergent opening of epoxides with aryl halides, zirconocene and photoredox catalyzed ring opening of epoxides have been reported.[35-38] Its important to mention that the modern catalytic/non-catalytic reactions are constrained with the chemical process safety, space and energy efficiency, selectivity and reproducibility when the application is focused towards the industry as well as academia. In this regard, applications of continuous flow chemistry have attracted significant interest as a way to implement and improve chemical processes in order to satisfy the growing demand for chemical sustainability.[39-42] Moreover, continuous flow chemistry satisfies many of the green chemistry principles, including waste minimization, energy efficiency, and process safety.[43-44]. In continuous flow fixed bed reactors, catalytic reactions take place inside heterogeneous catalyst bed in a continuous manner in shorter reaction time. Therefore, we also intended to extend our results in continuous flow reactors.

2.3. Rationale behind the present work

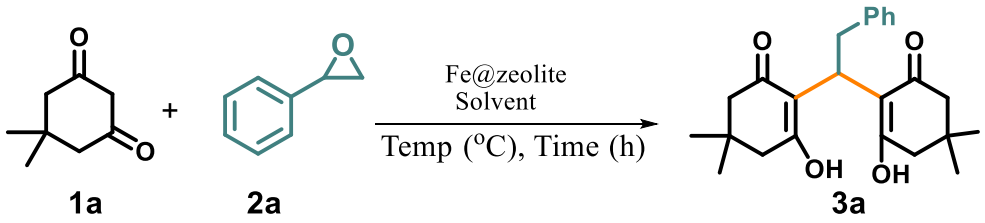
Tetraketones show immense medicinal importance. So, synthesis of tetraketones beyond the conventional types, will naturally expand the scope of its further biomedical assessment. Previously, a large number of reports have been published for tetraketone synthesis. All these tetraketones have aryl group flanked by two diketone moieties but tetraketones with benzyl group flanked by diketone molecules have been left unexplored. In this chapter, we have reported the synthesis of new classes of tetraketone molecules in batch and continuous flow protocol.

2.4. Results and discussion

In this chapter, an iron zeolite heterogeneous catalyzed straightforward and efficient method for the synthesis of new classes of tetraketones have been developed by in situ generation of aldehydes from epoxides. Fe@zeolite catalyst was prepared according to literature procedure.[9] ICP analysis of the fresh Fe@zeolite catalyst was carried out and it was observed that 2.63% Fe is present in the form of iron oxide. In addition, the protocol has been transformed in continuous flow for scale up process. The tetraketones have been cyclized further to get xanthenes. Initially we have extensively carried out optimization studies and generalised the protocols with library of substrates. The results have been described below.

2.4.1. Optimization studies

The optimization for the formation of tetraketones was started by taking dimedone and styrene oxide as model substrates (Scheme 2.14). At first, model reaction was performed under the influence of several catalysts in 1,4-dioxane solvent.



Scheme 2.14: Model reaction between dimedone and styrene for opimization

Using β-H zeolite, 30% yield of product tetraketone was found. Then when Fe@zeolite catalyst was used as catalyst, the yield of the product was 40%. Further, changing the catalyst to Ni@zeolite, 34% yield of the isolated product was observed (Figure 2.3). Therefore, Fe@zeolite appeared to be superior catalyst with respect to the model reaction. Next, we checked the reaction using $FeCl_3.6H_2O$ as catalyst and there was drastic reduction in yield compared to Fe@zeolite. Therefore, Fe@zeolite is the best suitable catalyst for the model reaction.

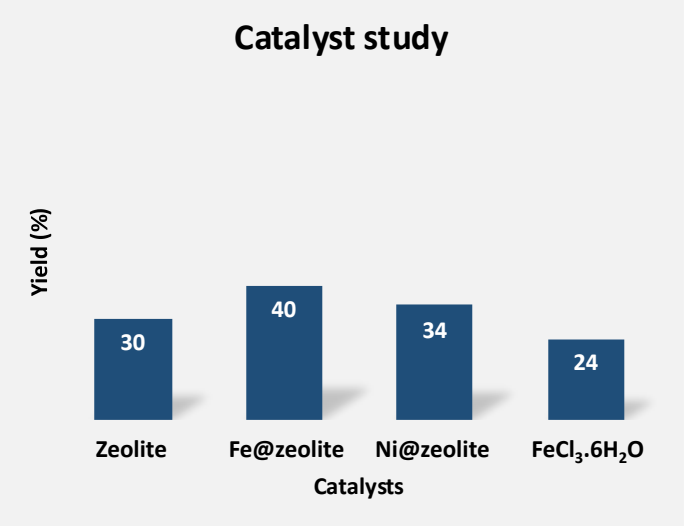


Figure 2.3: Effect of different catalyst screening on yield of **3a**

After that, we moved towards temperature optimization with the model reaction taking Fe@zeolite as catalyst and 1,4-dioxane as solvent. We observed that the temperature shows a direct proportionality relationship with yield (Figure 2.4). With increase of temperature, yield of the product sharply increased. At room temperature, we obtained 28% yield of product. Then with rise of temperature, yield of the product started increasing.

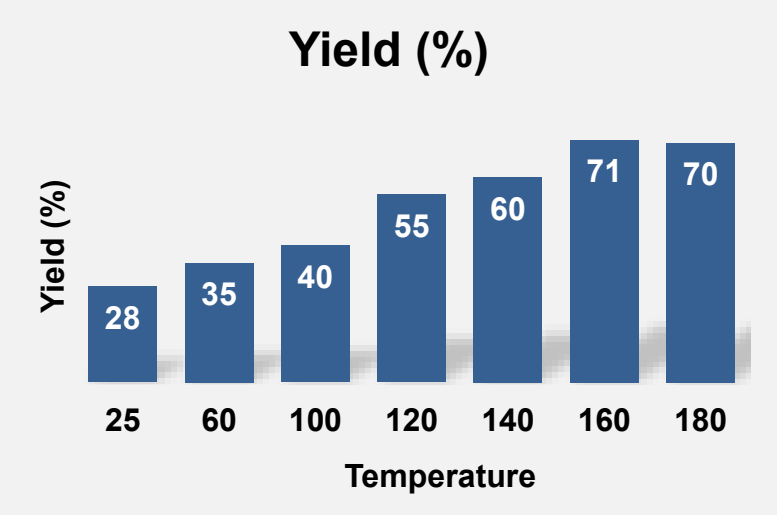


Figure 2.4: Effect of temperature on yield of product **3a**

The highest yield of product (71%) was observed at 160 °C temperature (Figure 2.4). So, 160 °C was the optimum temperature for the reaction. Then to further improve the yield of the product, the effect of solvent was investigated by varying different polar as well as non-polar solvents (Figure 2.5). Interestingly, it was observed that in polar solvents like THF, MeOH, DMF product yield was very less. In DMSO, no desired product was achieved. Probably, lone pair of these

solvents coordinate to active sites of Fe@zeolite catalyst thereby reducing the active sites available for reactant molecules. But switching to non-polar solvents, appreciable increase in yield of product was obtained. Toluene and DCE delivered the best yield of the product. DCE being halogenated solvent, toluene was choosen to be the best optimum solvent for the reaction.

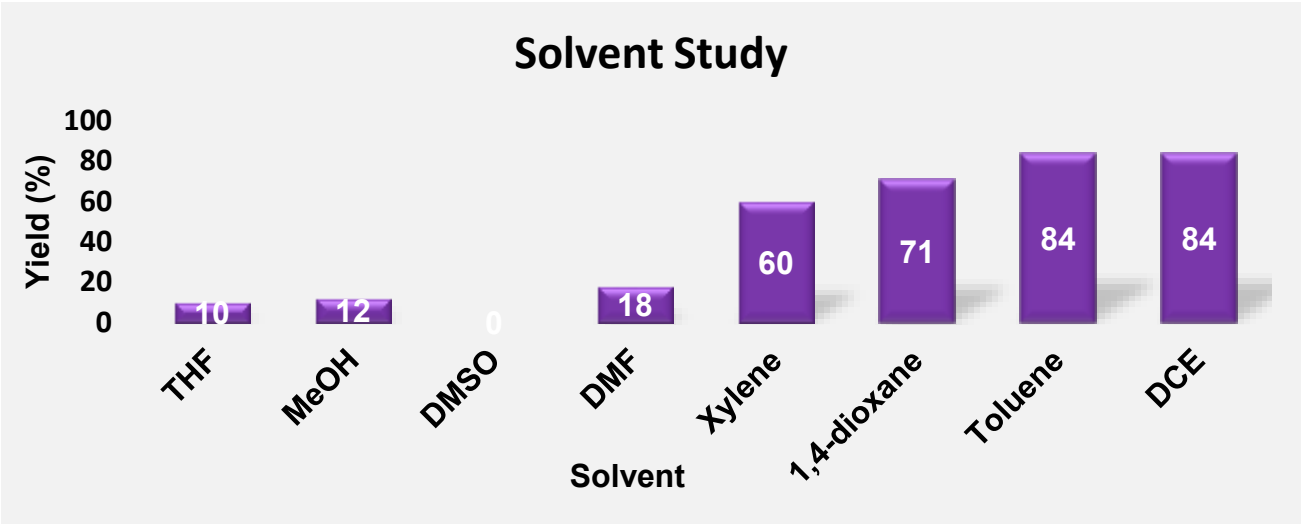


Figure 2.5: Effect of different solvents on the yield of **3a**

Then the reaction was performed at different time in toluene solvent at 160 °C temperature taking the same model substrates (Figure 2.6). It was found that the reaction gave best yield in 8 h.

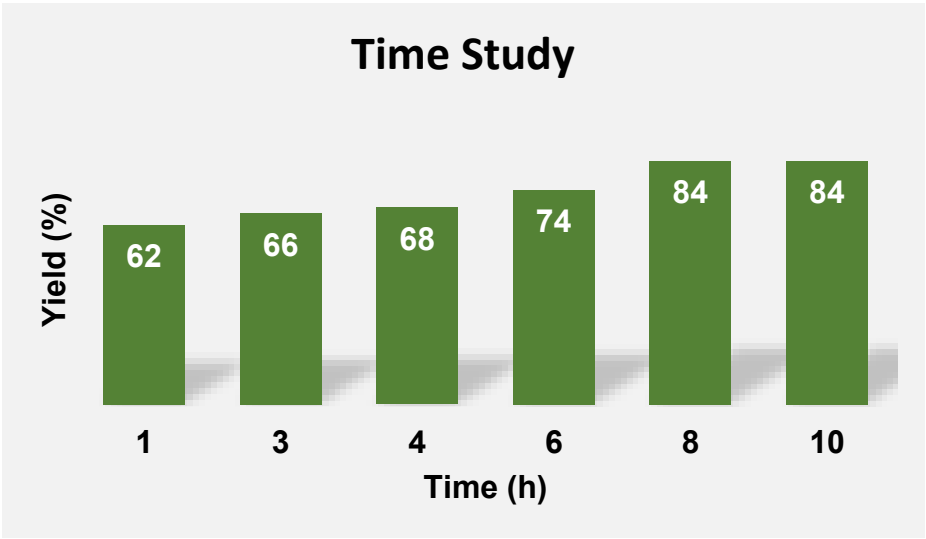
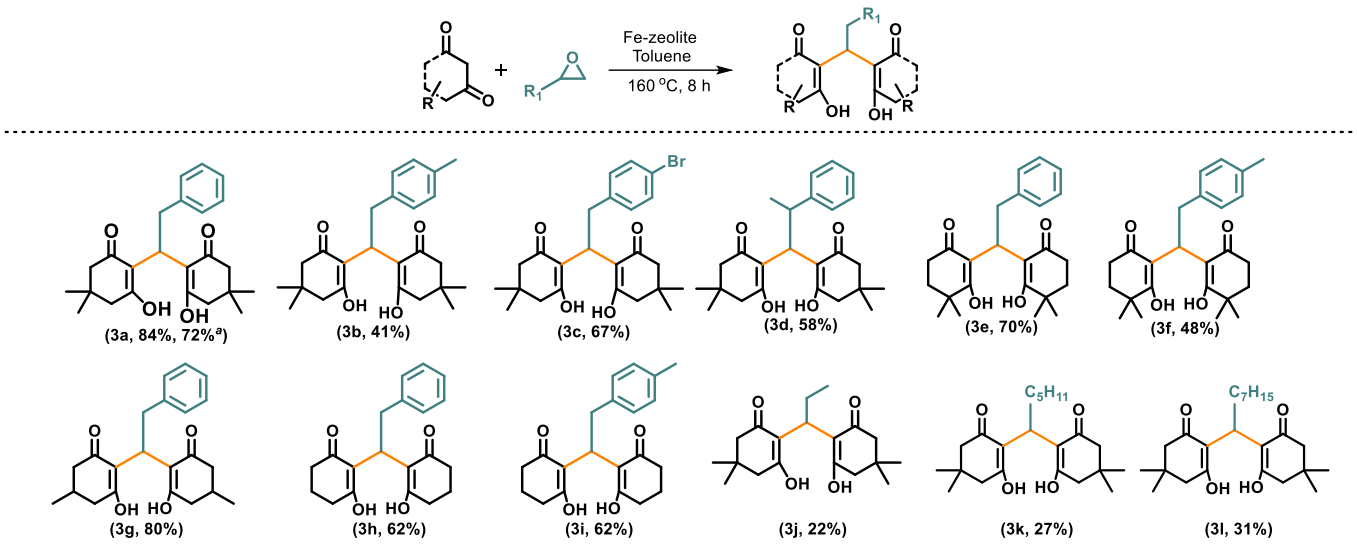


Figure 2.6: Yield of **3a** at different reaction time

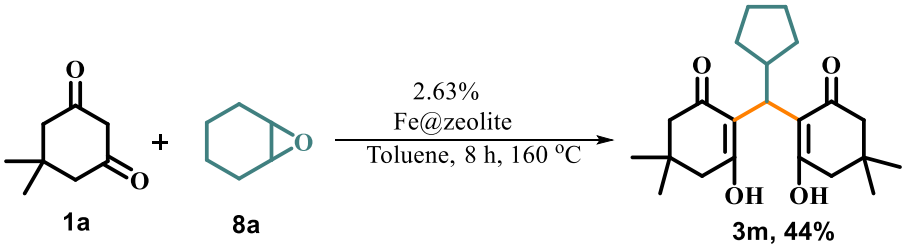
Therefore, the best optimum condition for the reaction is toluene as reaction solvent, 160 °C as reaction temperature in 8 h. With these optimized conditions in hand, we investigated the scope of this strategy with other cyclic 1,3-diketones and epoxides (Scheme 2.15).



Scheme 2.15: Substrate scope of tetraketone synthesis

Reaction conditions: **1** (2 eq.), **2** (1 eq.) contained in a sealed tube were heated at 160 °C in toluene for 8 h. [a]Reaction with 1 g scale of styrene epoxide.

Thus, the reaction of 5,5-dimethylcyclohexane-1,3-dione with 4-methyl styrene oxide, 4-bromo styrene oxide and alfa-methyl styrene oxide afforded the tetraketones **3b**, **3c** and **3d** in 41%, 67%, and 58% yields respectively. The reaction of 4,4-dimethyl cyclohexane-1,3-dione with styrene oxide and 4-methyl styrene oxide led to the formation of product **3e** and **3f** in 70% and 58% yields. Moreover, the reaction of 5-methylcyclohexane-1,3-dione with styrene oxide results **3g** in 80% yield. The unsubstituted cyclohexane 1,3-dione upon reaction with styrene oxide and 4-methyl styrene oxide forms the teraketone **3h** and **3i** in 62% and 62% yields respectively. Next, this reaction was performed with aliphatic epoxides to validate the generality of this methodology. The reaction of 5,5-dimethylcyclohexane-1,3-dione upon reaction with propylene oxide, 1,2-epoxyhexane and 1,2-epoxyoctane afforded the corresponding tetraketones **3j**, **3k**, and **3l** in 22%, 27% and 31% yields respectively. In case of aliphatic epoxides, most of the starting materials were unreacted in the reaction mixture. The bond connectivity of the tetraketone shows that two diketone moieties are joined at the same carbon which indicates that the reaction is not simple ring opening of epoxide rather it is possible only when the diketone reacts with aldehyde.

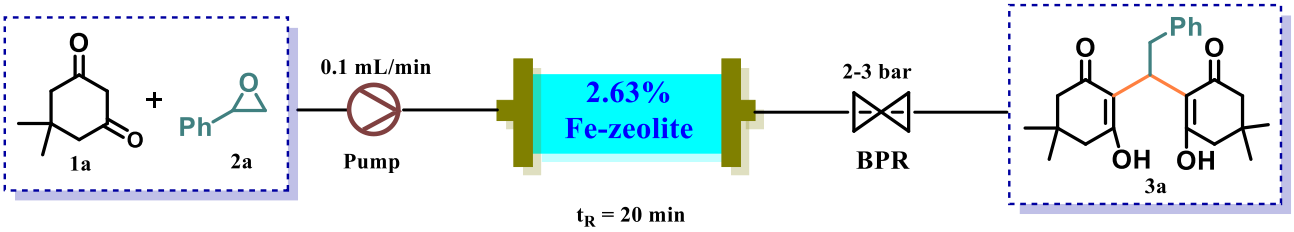


Scheme 2.16: Ring contraction of epoxycyclohexane with dimedone

Interestingly, when the reaction of dimedone was carried out with epoxycyclohexane, cyclopentyl substituted tetraketone **3m** has been formed in 44% yield (Scheme 2.16). The product **3m** was obtained by the initial ring contraction of epoxycyclohexane via Meinwald rearrangement reaction to form the transient cyclopentane carbaldehyde, which upon reaction with the two molecules of dimedone resulted the product **3m**.

As batch reaction requires high temperature reaction condition for the formation of tetraketone **3**, this put forward to the safety hazard in the large-scale reaction. Moreover, the heterogeneous catalyst was stirred with the magnetic bead, resulting in the change of the surface activity and also difficult in recyclability. Considering these aspects, next we performed tetraketone synthesis under continuous flow. To execute the continuous flow synthesis, the reaction condition was initially optimized under continuous flow. For the initial optimization, dimedone and styrene oxide was choosen as model substrates (Table 2.1).

Table 2.1: Optimization of tetraketone synthesis in continuous flow

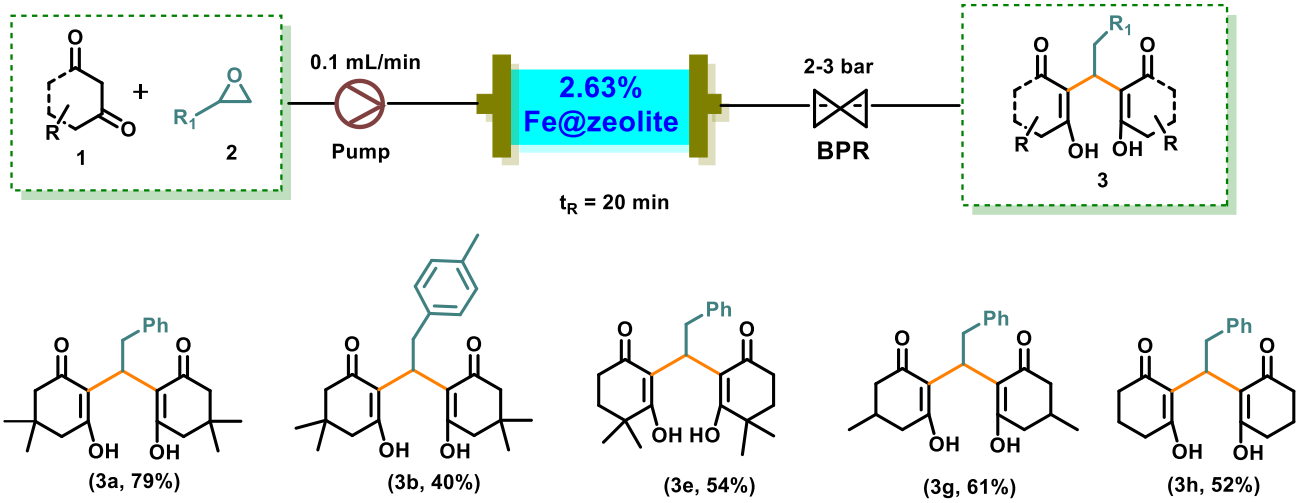


Entry	Catalyst bed (cm)	Catalyst	Flow rate (mL/min)	Temp (°C)	Solvent	% Yield (3a)
1	2	2.63% Fe-Zeolite	0.1	100	1,4-dioxane	30
2	2	2.63% Fe-Zeolite	0.1	130	1,4-dioxane	36
3	3	2.63% Fe-Zeolite	0.1	130	1,4-dioxane	40
4	5	2.63% Fe-Zeolite	0.1	130	1,4-dioxane	53
5	6	2.63% Fe-Zeolite	0.1	130	1,4-dioxane	60
6	6	2.63% Fe-Zeolite	0.1	140	1,4-dioxane	79
7	6	2.63% Fe-Zeolite	0.2	140	1,4-dioxane	60

8	6	2.63% Fe-Zeolite	0.3	140	1,4-dioxane	49
9	6	2.63% Fe-Zeolite	0.5	140	1,4-dioxane	20

Reaction condition: 0.1 M solution of epoxides **2** and 0.2 M solution of cyclic 1,3-diketone **1** in 1,4-dioxane were mixed and flown through the 6.6 × 150 mm Omnifit packed bed reactor (1g of Fe-zeolite, 6 cm bed height) (Vapourtec R-series) with 0.1 mL/min flow rate at 140 ºC; The mentioned yields are isolated yields.

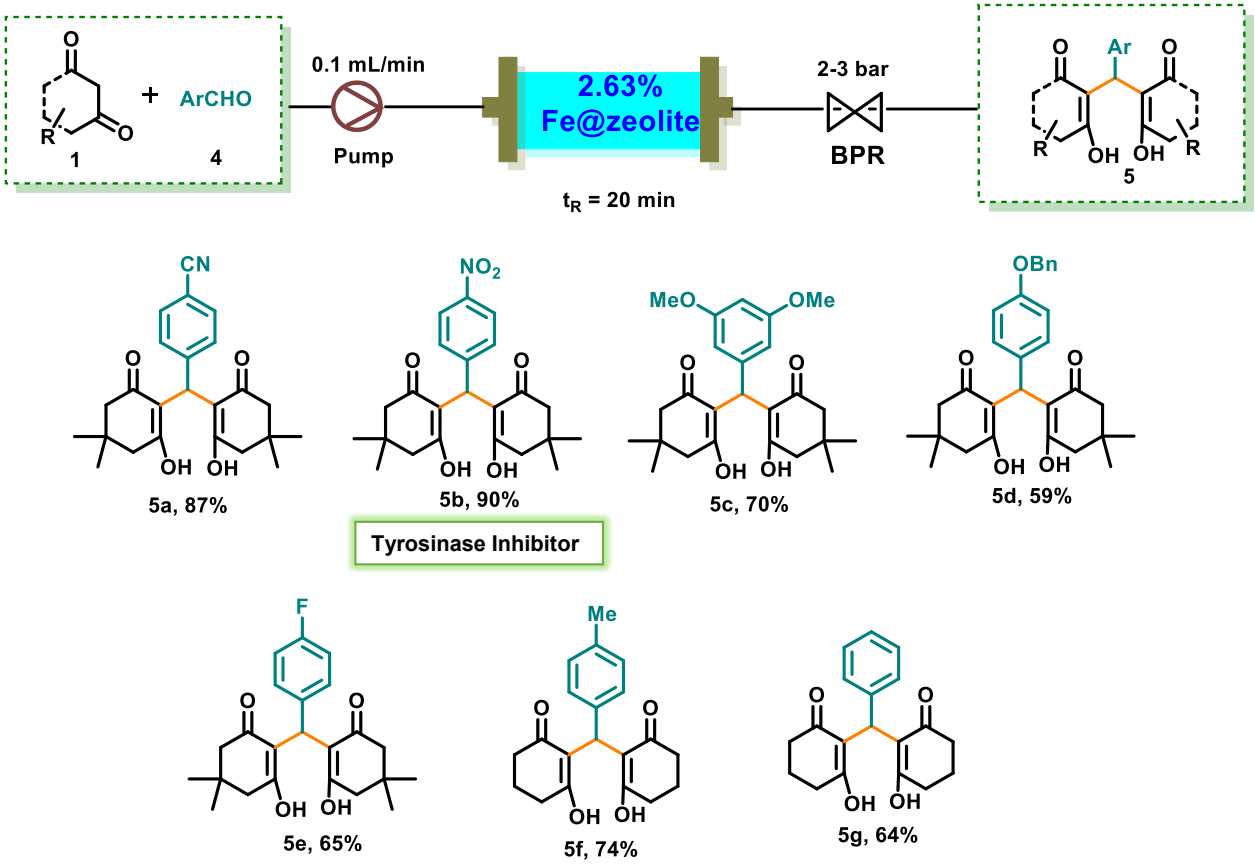
As diketones **3** were found to be insoluble in toluene, we performed all the reaction in 1,4-dioxane as a solvent. Fe@zeolite catalyst was filled in the Omnifit packed bed reactor and the temperatures were varied during the course of optimization study. To check the effect of solvent, flow rate, and concentration various experiments were performed, and results are summarized in (Table 2.1, entries 1-6). For instance, with 2 cm bed height of Fe@zeolite at 100 ºC temperature by flowing 0.2 M:0.1 M solution of **1a**:**2a** in 1,4-dioxane solvent at 0.1 mL/ min flow rate, the product **3a** was obtained in 30% yield (Table 2.1, entry 1). Later, at the same bed height when temperature was increased to 130 ºC, product yield was found to increase to 36% (Table 2.1, entry 2). Then, keeping the temperature fixed at 130 ºC, when the bed height was increased to 3 cm, the product yield was found to increase to 40%. Next at the same bed height when temperature was increased to 130 ºC, product yield was found to increase to 36% (Table 2.1, entry 2). Then keeping the temperature fixed at 130 ºC, when the bed height was increased to 3 cm, the product yield was found to increase to 40%. At 5 cm and 6 cm bed height, yield of the product **3a** was 53% and 60% respectively (Table 2.1, entries 3-5). Finally at 140 ºC temperature and 6 cm bed height, 79% yield of the product **3a** was obtained (Table 2.1, entry 6).



Scheme 2.17: Substrate scope of tetraketone synthesis in continuous flow

Reaction condition: **1** (10 mL, 0.2 M), **2** (10 mL, 0.1 M) were flown through Omnifit® (6.6 x 150 mm) bed reactor packed with 6 cm Fe@zeolite (1 g) bed at 0.1 mL/min flow rate in 1,4-dioxane solvent through vapourtec continuous flow

Further, this optimized continuous flow condition was subjected with other substrates (Scheme 2.17). Various combination of epoxide and cyclic-1,3-diketone afforded the respective xanthenes **3b**, **3e**, **3g** and **3h** in 40%, 54%, 61% and 52% yields, respectively. Interestingly, all the products were obtained by using one-time packed Fe@zeolite packed bed reactor.

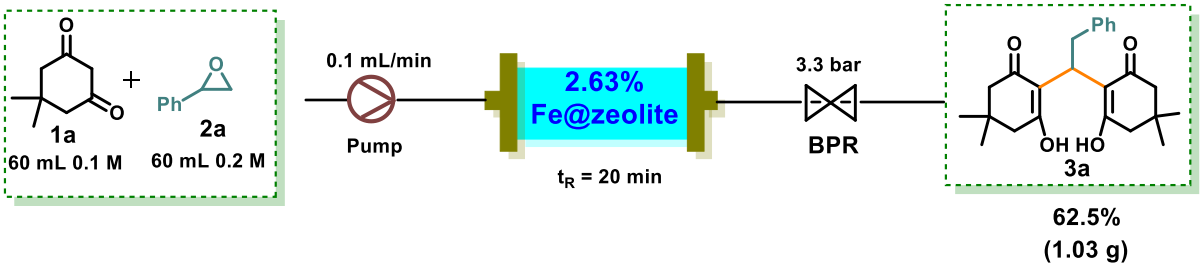


Scheme 2.18: Substrate scope of tetraketone synthesis in continuous flow

Reaction condition: **1** (5 mL, 0.2 M), **5** (5 mL, 0.1 M) were flown through Omnifit® (6.6 x 150 mm) bed reactor packed with 6 cm Fe@zeolite (1 g) bed at 0.1 mL/min flow rate in 1,4-dioxane solvent through vapourtec continuous flow

---

Having these results, we extended the scope of the Fe@zeolite catalysis in continuous flow by taking aldehyde directly as a electrophile and cyclic-1,3-diketone as a nucleophile under same reaction condition as previously described with epoxide (Scheme 2.18). We found that the tetraketone has formed as a sole product in the reaction. Thus, the reaction of 5,5-dimethyl-cyclohexane-1,3-dione reacts with 4-cyanobenzaledhyde, 4-nitrobenzaldehyde, 3,5-dimethoxybenzaldehyde, 4-benzyloxybenzaldehyde and 4-fluorobenzaldehyde under continuous flow to afford **5a** to **5e** in 87%, 90%, 70%, 59% and 65% yields, respectively (Scheme 2.18). Similarly, the reaction of cyclohexane-1,3-dione with 4-methylbenzaldehyde and benzaldehyde afforded the respective tetraketones **5f** and **5g** in 74% and 64% yields



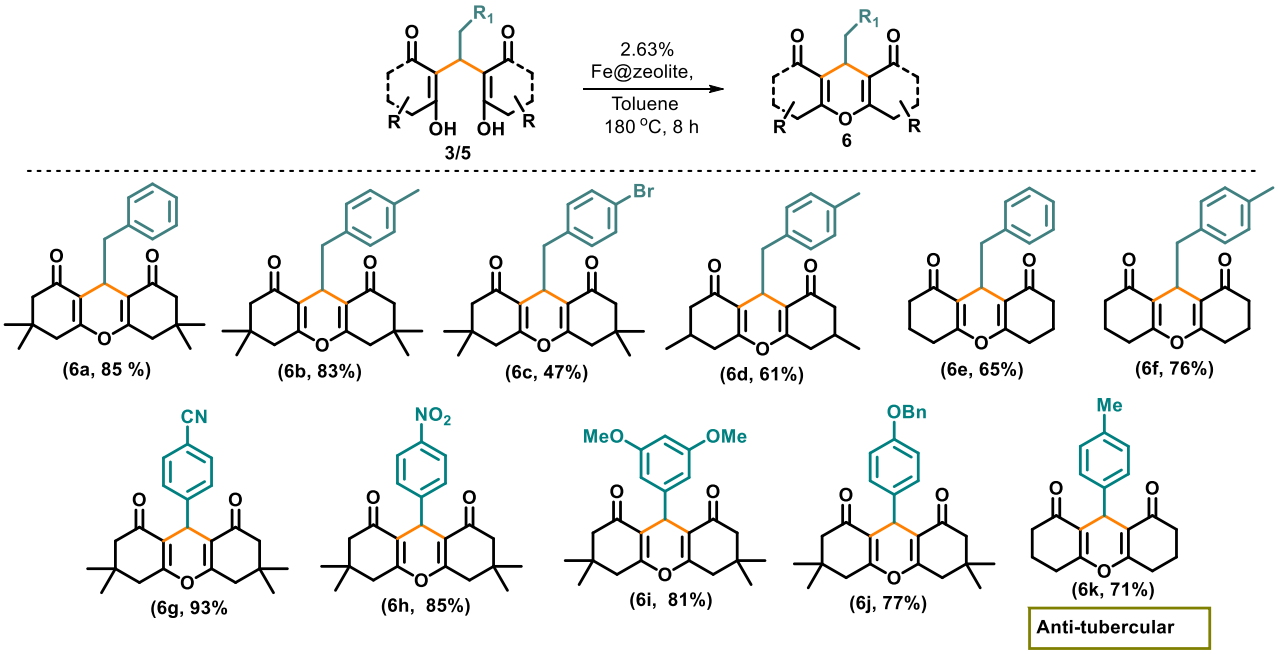
Scheme 2.19: Gram scale synthesis of tetraketone **3a** in continuous flow condition

Similarly, a gram scale synthesis of the tetraketone **3a** was performed in continuous flow (Scheme 2.19). For the gram scale synthesis, the reaction of dimedone and styrene oxide was carried out by using 1,4-dioxane as a solvent. The solution of 6 mmol styrene oxide and 12 mmol dimedone were flown with 0.1 mL/min flow rate at 140 °C with 6 cm bed height of Fe@zeolite catalyst for 10 hrs which led to 1.03 g of corresponding tetraketone **3a** in 62.5 % yield. Furthermore, this Fe@zeolite catalyst bed is still active to produce the product **3a**.

2.4.8. Cyclization reaction

When the non-cyclic product **3a** was heated in presence of Fe@zeolite at 160 °C, the starting material was recovered with very little conversion. Subsequently, the compound **3a** was subjected for high temperature condition at 180 °C, we found that the complete conversion of starting material to form the xanthene **6a** in 85% yield. This reaction failed to form the xanthene **6a** in the absence of Fe-zeolite catalyst at 180 °C. Therefore, optimal condition for cyclization requires both

the catalyst and high temperature condition. Next, we attempted cyclization of other tetraketones using Fe-zeolite catalyst at 180 °C in toluene solvent (Scheme 2.20).



Scheme 2.20: Substrate scope for tetraketone synthesis in continuous flow condition

Reaction condition: 1 (25 mL, 0.1 M) 6b was flown through Omnifit® (6.6 x 150 mm) bed reactor packed with 6 cm Fe@zeolite (1 g) bed at 0.1 mL/min flow rate in toluene solvent

This annulation reaction with **3b** afforded the product **6b** in 83% yield. Similarly, cyclization reaction with **3c** and **3g** gave products **6c** and **6d** in 47% and 61% yield, respectively. Similar reaction with **3h** and **3i** produced products **6e** and **6f** in 65% and 76% yield respectively. Next cyclization of **5** was performed using Fe-zeolite under high temperature condition (Scheme 2.20). Thus, the reaction of **5a** under the experimental condition produced **6g** in 93% yield. Similarly, **5b**, **5c**, **5d** and **5f** afforded **6h**, **6i**, **6j**, **6k** in 85%, 81%, 77% and 71% yields respectively (Scheme 2.21).

2.4.8. Recyclability test

Next, the recyclability of this robust heterogeneous Fe-zeolite catalyst was checked.

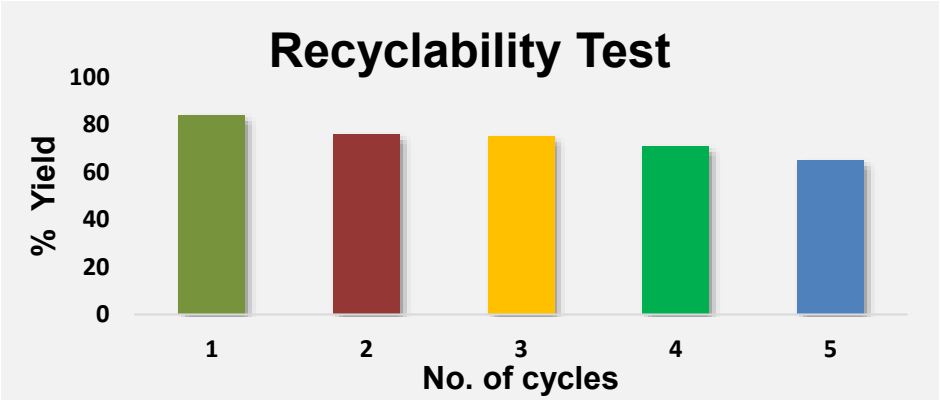
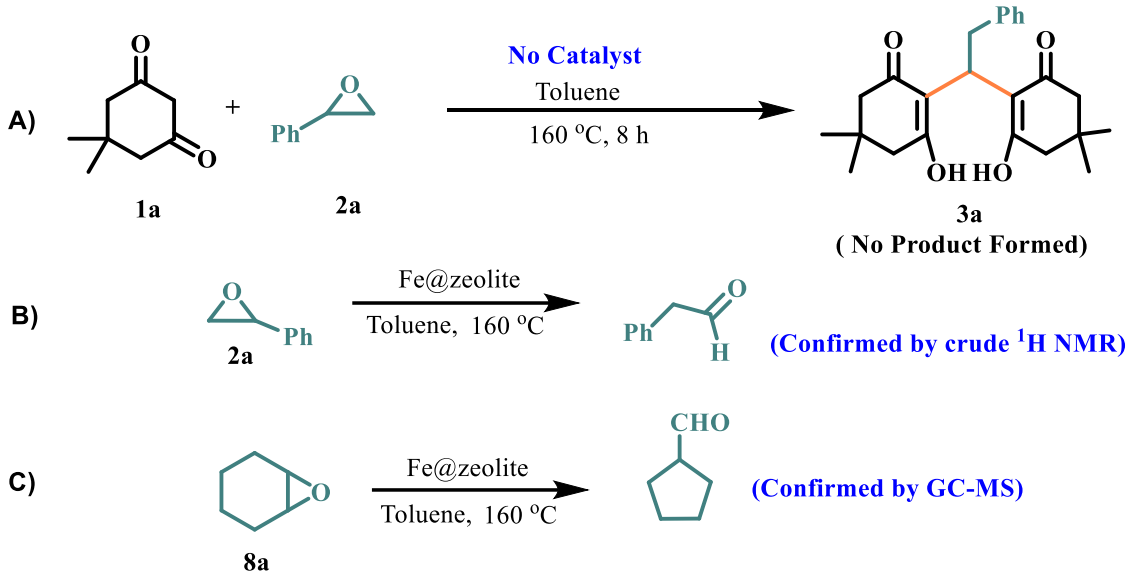


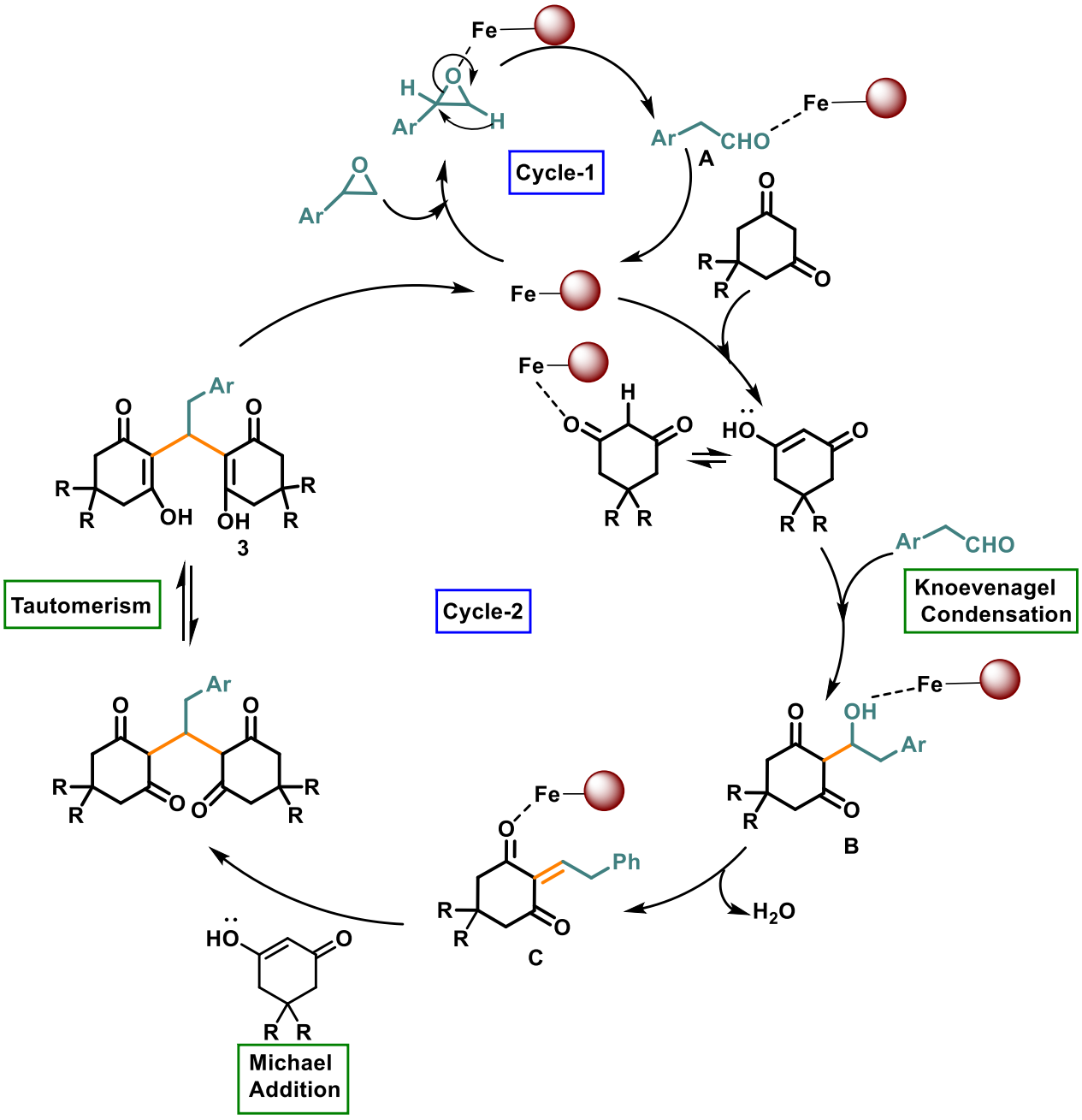
Figure 2.7: Recyclability test of Fe-zeolite catalyst

tetraketone **3a** (Figure 2.7). After completion of each cycle, the catalyst was separated with the help of filter paper, washed with toluene, dried at 100 °C for 2 hrs and then the catalyst was used directly for the next cycle. This procedure is repeated for another three more cycles. In this way the catalytic cycle was continued upto 5 cycles with slight decrease in yield of **3a**.



Scheme 2.22: Control experiments to assess the mechanism

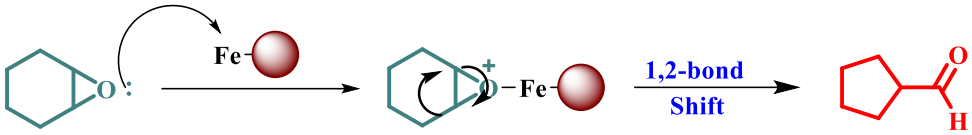
In order to confirm the role of the catalyst, a series of control experiments was carried out in absence of the Fe-zeolite catalyst (Scheme 2.22). It was observed that the product **3a** is not formed under the optimized reaction condition. Therefore, it is clear evidence that Fe-zeolite has significant role for the reaction. Another reaction was carried out in absence of dimedone. Then, the reaction mixture was filtered to get a clear solution, which was analyzed by ^{1}H NMR. The crude ^{1}H NMR of the reaction mixture shows aldehyde peak at 9.6 ppm. The presence of aldehyde peak further confirmed that the reaction proceeds through transient aldehyde formed in-situ via Meinwald rearrangement. In order to confirm the ring contraction product, an experiment was performed by taking the 1,2-epoxycyclohexane and heating it in presence of Fe-zeolite at 160 °C temperature in toluene solvent. The filtered solution of the reaction mixture was subjected to GC-MS and indicates the formation of cyclopentane carbaldehyde .



Scheme 2.23: Proposed mechanism for Fe-zeolite catalyzed tetraketone formation

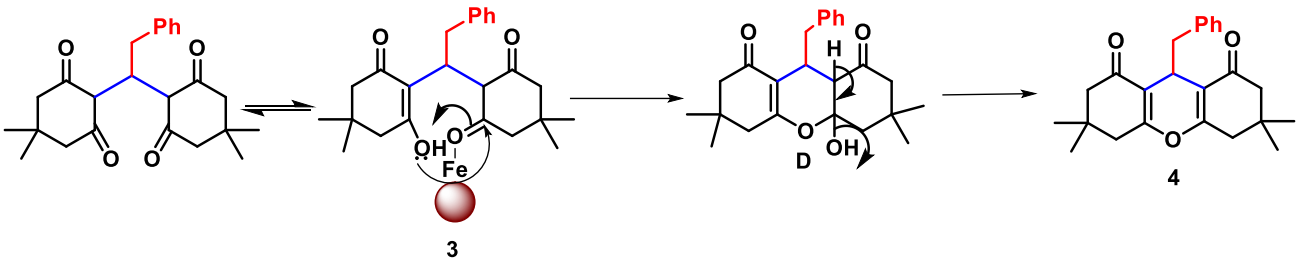
Based on above experimental evidences, we have proposed plausible mechanism for the Fe@zeolite catalyzed formation of tetraketone **3**. The mechanism has been depicted in two cycles (Scheme 2.23). In the first cycle aldehyde is generated from epoxide under the catalytic influence of Fe-zeolite. First epoxide oxygen lone pair coordinates with Fe-zeolite. This facilitates 1,2-hydride shift (Meinwald Rearrangement) giving rise to the formation of aldehyde **A**. Then, the cycle-2 initiates the Knoevenagel condensation with the cyclohexane-1,3-dione and the transient aldehyde to form hydroxy compound B, which subsequently eliminates the water to form

conjugated ketone **C**. Next, the intermediate **C** undergoes Michael addition with another equivalent of cyclohexane 1,3-dione to give the tetraketone **3**.



Scheme 2.24: Mechanism of ring contraction of epoxy cyclohexane

In case of cyclic six membered epoxide, first the oxygen lone pair coordinates with iron and then undergoes 1,2-bond migration to give cyclopentyl carbaldehyde (Scheme 2.24).



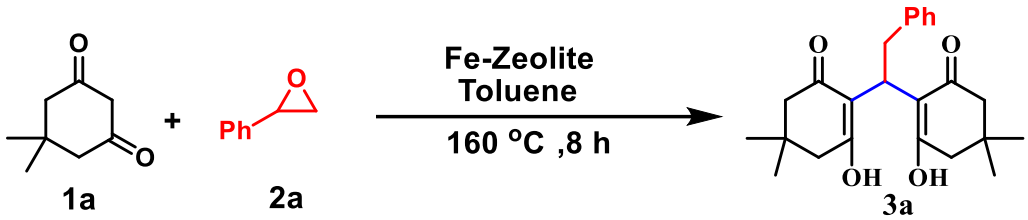
Scheme 2.25: Proposed mechanism of intramolecular cyclisation to form xanthenedienone

Next we have proposed the mechanism for the Fe@zeolite catalyzed xanthene formation from the tetraketone **3** and **5** (Scheme 2.25). The tetraketones **3** and **5** can exist in keto-enol tautomeric form. Initially, coordination of Fe-zeolite with the carbonyl of the tetraketone **3** or **5** and followed by intramolecular nucleophilic attack by enolic -OH affords the hemiacetal moiety **D**. Subsequently, the intermediate **D** undergoes elimination of H_2O under high heating to furnish the xanthene derivative **4**.

Table 2.2: Green chemistry metrics for the model reaction and comparison with previous work

Green Chemistry Matrix	E-factor	Process Mass Intensity (PMI)	Reaction Mass Efficiency (RME)	Carbon Efficiency (CE)
Jin et. al	0.60	1.61	62.13%	65%
Our work	0.25	1.25	80.12%	83.6%

To validate the sustainability of this process, the green chemistry metrics have been calculated for the model reaction to form 3a based on the literature (Table 3).[32] Besides high recoverability of the catalyst up to 5 cycle, this present approach was found to be associated with the better green chemistry metrics such as low E-factor (0.25), low PMI (1.25), high RME (80.12%), and high CE (83.6%). We have calculated the green chemistry matrix for model reaction with the help of literature report.[45]



MW	140.18	120.15	382.5
mmol	0.832	0.416	0.347
amount	116	50	133

E-factor:

The ideal value of E-factor is zero.

E-factor = [total mass of raw materials - the total mass of product]/ mass of product.

E-factor of **3a** = [(116 + 50)-133]/133

= 0.25

Process mass intensity (PMI):

PMI= ∑ (mass of stoichiometric reactants)/[mass of product]

= (116+50)/ 133

= 1.25

Reaction mass efficiency (RME):

RME = [mass of product /∑ (mass of stoichiometric reactants)] × 100

= [133 / (116+50)] × 100

= 80.12%

Carbon efficiency (CE):

CE denotes the percentage of carbon in the reactants that remains in the product.

CE= [Amount of carbon in product/ Total carbon present in reactants] x 100

= [no. of moles of product x no. of carbons in product / (moles of 1a x carbons in 1a + moles of 2a x carbons in 2)] x 100

= [0.347 x 24 / (0.416 x 8 + 0.832 x 8)] x 100

= [8.345 / (3.328 + 6.656)] x 100

= 83.6%

2.5. Conclusion

In conclusion, we have demonstrated batch/continuous-flow synthesis of biologically active tetraketones from epoxide and cyclic-1,3-diketone using Fe-zeolite heterogeneous catalyst through in-situ formation of aldehyde (Meinwald rearrangement) at 160 ºC. This reaction was demonstrated with good substrate scope in high yield. Moreover, this tetraketones generated the xanthene derivatives when heated in toluene solvent in the presence of Fe@zeolite at 180 ºC and was supported with good number of examples. Moreover, the Fe@zeolite was also useful catalyst for the reaction of aldehyde and the 1,3-diketones to form tetraketones and xanthenes under continuous-flow module. Furthermore, a gram scale application was demonstrated for the tetraketone formation under batch/continuous-flow process. Advantageously, this catalyst is inexpensive, easily synthesizable and recyclable. A single catalytic system performed the multiple reaction applications and avoided the hazardous byproduct formation. Moreover, this continuous flow temperature directed Fe-catalyzed reaction is highly sustainable to minimize the safety hazard of the high temperature reaction.

2.6. Experimental section and characterization data

2.6.1. General information and data collection

All the chemicals were purchased from Sigma-Aldrich and Thermofischer Scientific and used without further modification. All solvents were purchased from Rankem and Finar Chemicals. Deuterated solvents were used as received. Column chromatographic separations were performed over 100−200 mesh silica-gel. Visualization was accomplished with UV light. The ^{1}H and $^{13}C\{1H\}$ NMR spectra were recorded on 400 and 100 MHz, respectively, using Bruker or JEOL spectrometers. Abbreviations used in the NMR follow-up experiments: b, broad; s, singlet; d, doublet; t, triplet; q, quartet. HRMS spectra were obtained with Waters-synapt G2 using electrospray ionization (ESI-TOF). Infrared (ATIR) spectra were obtained with a Bruker Alpha-E infrared spectrometer. Single-crystal diffraction analysis data were collected at 100K with a BRUKER KAPPA APEX III CCD Duo diffractometer (operated at 1500 W power: 50 kV, 30 mA) using graphite monochromatic Mo-Kα radiation and Cu-Kα radiation.

2.6.2. Preparation of the Fe@zeolite catalyst[9]: 5 g of zeolite was suspended in 20 mL of deionized water. A 10% $FeCl_3.6H_2O$ solution was prepared in deionized water. This suspension was stirred for 6 h in rotary evaporator for uniform dispersion. Water was removed under vacuum, and the metal loaded samples were dried at 120 °C for 2 h. The dried samples were calcined at 500 °C for 8 h. The % of Fe on zeolite support was analysed by Microwave Plasma Atomic Emission Spectroscopy (MP-AES) analysis which showed that catalyst contains 2.63% of Fe.

2.6.3. Experimental procedure:

A. **Procedure for starting material preparation**: Substrates (2-(p-tolyl)oxirane and 2-methyl-2-phenyloxirane) prepared according to reported literature procedure.[46, 47]

B. **Experimental procedure for the synthesis of tetraketone (3) from epoxide and cyclic-1,3-dione in batch**: Cyclic 1,3-diketone **1** (2 equivalent), epoxide **2** (1 equivalent), and 30 mg of 2.63% Fe-zeolite were mixed in an oven dried sealed tube and 2 mL toluene was added. Then the reactor was placed in a preheated oil bath and heated at 160 ºC for 8 h. After completion of the reaction, the solvent was evaporated in rotary evaporator and the crude reaction mixture was directly purified by 100-200 mesh silica-gel column chromatography (EtOAc: pet ether = 5:95 to 10:90) to afford the tetraketone **3**.

C. General procedure for synthesis of tetraketone from epoxide and cyclic-1,3-diketone under continuous-flow: In a typical procedure, the 10 mL 0.1M solution of epoxide and 10 mL 0.2 M cyclic-1,3-diketone in 1,4-dioxane were premixed and flown through Omnifit® (6.6 x 150 mm) packed bed column packed with 2.63% Fe-Zeolite up to 6 cm (1.0 g) at 2-3 bar pressure at 140 ºC with 0.1 mL/min flow rate and residence time t_R = 20 min. After reaction completion, the catalyst bed was washed with 1,4-dioxane. The solvent was evaporated under vacuum. The residue was further purified by 100-200 mesh silica gel chromatography (EtOAc : pet ether = 5:95 to 10:90) to afford the pure product **3**.

D. General procedure for synthesis of tetraketone from aldehyde and cyclic-1,3-diketone in continuous-flow: In a typical procedure, the 5 mL 0.1M solution of aldehyde and 5 mL 0.2 M cyclic-1,3-diketone in 1,4-dioxane were premixed and flown through Omnifit® (6.6 x 150 mm) packed bed column packed with 2.63% Fe-Zeolite up to 6 cm (1.0 g) of bed at room temperature at 2-3 bar pressure at 140 ºC with 0.1 mL/min flow rate and residence time t_R = 20 min. After reaction completion, the catalyst bed was washed with 1,4-dioxane. The solvent was evaporated using a rotary evaporator. The residue was directly purified by silica gel chromatography (EtOAc : pet ether = 5:95 to 20:80).

E. General procedure for the synthesis of xanthene 6 via cyclisation reaction of tetraketones: To an oven dried 10 mL sealed tube 50 mg tetraketone **3/5** and 30 mg of 2.63% Fe-zeolite were added and then 2 mL toluene was added. Next the reactor was placed in a preheated oil bath and heated at 180 ^{o}C in Carousel hot plate for 8 h. After completion of the reaction, the solvent was removed using rotary evaporator and the crude reaction mixture was directly purified by 100-200 mesh silica-gel column chromatography (EtOAc: pet ether = 10:90 to 20:80) to afford the xanthene **6**.

F. Experimental procedure for the gram scale synthesis of tetraketone (3a) from styrene oxide and 5,5-dimethyl cyclohexane-1,3-dione in batch: 5,5-dimethylcyclohexane-1,3-dione **1a** (2.3 gm, 16.66 mmol), styrene oxide **2a** (1 gm, 8.33 mmol), and 600 mg of 2.63% Fe-zeolite were mixed in an oven dried sealed tube and 2 mL toluene was added. Then the reaction mixture was heated at 160 ^{o}C for 8 h. After completion of the reaction, the solvent was evaporated in rotary evaporator and the crude reaction mixture was directly purified by 100-200 mesh silica-gel column chromatography (EtOAc: pet ether = 5:95) to afford 2,2'-(2-phenylethane-1,1-diyl) bis (3-hydroxy-5,5-dimethylcyclohex-2-en-1-one) **3a** (2.31 g, 72.39 %) as white crystal.

G. Experimental procedure for the gram scale synthesis of tetraketone (3a) from styrene oxide and 5,5-dimethylcyclohexane-1,3-dione in flow: 60 mL 0.1M solution of styrene oxide (720 mg, 6 mmol) and 60 mL 0.2 M 5,5-dimethylcyclohexane-1,3-diketone (1680 mg, 12 mmol) in 1,4-dioxane were premixed and flown through Omnifit® (6.6 x 150 mm) packed bed column packed with 2.63% Fe-Zeolite up to 6 cm (1g) at 2-3 bar pressure at 140 ^{o}C with 0.1 mL/min flow rate and residence time t_R = 20 min. After reaction completion, the catalyst bed was washed with 1,4-dioxane. The solvent was evaporated under vacuum. The residue was further purified by 100-200 mesh silica gel chromatography (EtOAc : pet ether = 5:95) to afford 2,2'-(2-phenylethane-1,1-diyl)bis(3-hydroxy-5,5-dimethylcyclohex-2-en-1-one) **3a** (1.03 g mg, 62.5% yield) as the pure product.

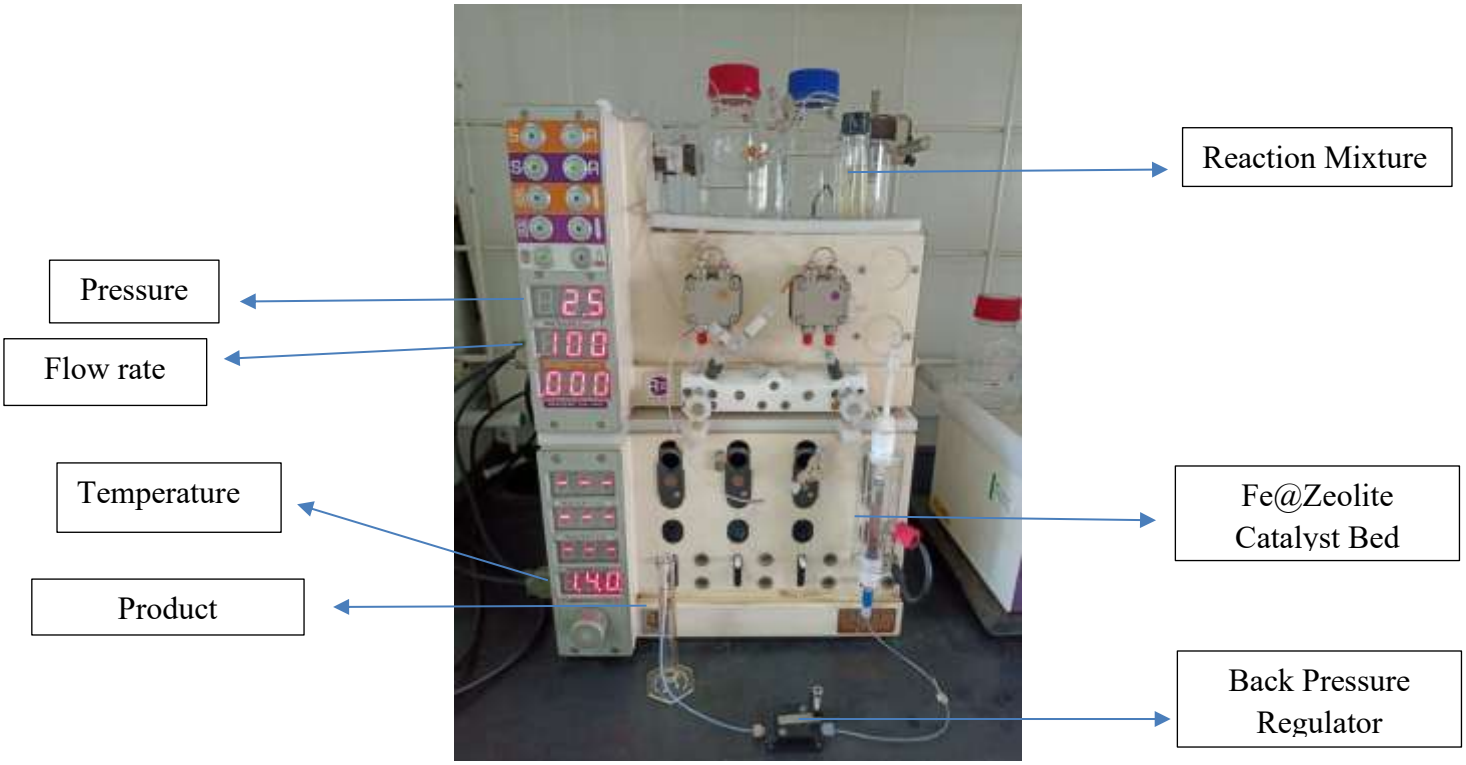


Figure 2.8: Set up for reaction in continuous flow

2.6.4. Experimental procedure for recyclability:

(a) First run of the catalyst: 5,5-dimethylcyclohexane-1,3-dione **1a** (350 mg, 2.5 mmol), styrene oxide **2a** (150 mg, 1.25 mmol), and 90 mg of Fe-zeolite were introduced in an oven dried sealed tube and 2 mL toluene was added. Then the reactor was placed in a preheated oil bath and the reaction was conducted for 8h under vigorous stirring. The catalyst was separated by filtration and the catalyst thus separated was washed twice with toluene and subjected to drying in oven for 2 h. The solvent of the filtrate solution was evaporated under rotary evaporator and directly by 100-200 mesh silica gel column chromatography to afford **3a** (397mg, 84%). The weight of the dried catalyst was 72 mg after cooling.

(b) Second run of the catalyst: 5,5-dimethylcyclohexane-1,3-dione **1a** (279 mg, 1.99 mmol), styrene oxide **2a** (119 mg, 0.99 mmol), and 72 mg of Fe-zeolite were introduced in an oven dried sealed tube and 2 mL toluene was added. Then the reactor was placed in a preheated oil bath and the reaction was conducted for 8h under vigorous stirring. The catalyst was separated by filtration and the catalyst thus separated was washed twice with toluene and subjected to drying in oven for 2 h. The solvent of the filtrate solution was evaporated under rotary evaporator and directly by 100-200 mesh silica gel

column chromatography to afford **3a** (285 mg, 76%). The weight of the dried catalyst was 72 mg after cooling.

(c) Third run of the catalyst: 5,5-dimethylcyclohexane-1,3-dione **1a** (232 mg, 1.99 mmol), styrene oxide 2a (100 mg, 0.83 mmol), and 60 mg of Fe-zeolite were introduced in an oven dried sealed tube and 2 mL toluene was added. Then the reactor was placed in a preheated oil bath and the reaction was conducted for 8h under vigorous stirring. The catalyst was separated by filtration and the catalyst thus separated was washed twice with toluene and subjected to drying in oven for 2 h. The solvent of the filtrate solution was evaporated under rotary evaporator and directly by 100-200 mesh silica gel column chromatography to afford **3a** (238 mg, 75%). The weight of the dried catalyst was 46 mg after cooling.

(d) Fourth run of the catalyst: 5,5-dimethylcyclohexane-1,3-dione **1a** (178 mg, 1.276 mmol), styrene oxide **2a** (76 mg, 0.638 mmol), and 46 mg of Fe-zeolite were introduced in an oven dried sealed tube and 2 mL toluene was added. Then the tube was placed in a preheated oil bath and the reaction was conducted for 8 h under vigorous stirring. The catalyst was separated by filtration and the catalyst thus separated was washed twice with toluene and subjected to drying in oven for 2 h. The solvent of the filtrate solution was evaporated under rotary evaporator and directly by 100-200 mesh silica gel column chromatography to afford **3a** (173mg, 75%). The weight of the dried catalyst was 28 mg after cooling.

(e) Fifth run of the catalyst: 5,5-dimethylcyclohexane-1,3-dione **1a** (106 mg, 0.75 mmol), styrene oxide **2a** (46 mg, 0.38 mmol), and 28 mg of Fe-zeolite were introduced in an oven dried sealed tube and 2 mL toluene was added. Then the reactor was placed in a preheated oil bath and the reaction was conducted for 8 h under vigorous stirring. The catalyst was separated by filtration and the catalyst thus separated was washed twice with toluene and subjected to drying in oven for 2 h. The solvent of the filtrate solution was evaporated under rotary evaporator and directly by 100-200 mesh silica gel column chromatography to afford **3a** (94 mg, 65%). The weight of the dried catalyst was 11 mg.

2.7. Analytical data for the product:

2,2'-(2-phenylethane-1,1-diyl)bis(3-hydroxy-5,5-dimethylcyclohex-2-en-1-one) (3a): Batch condition: Synthesized according to general procedure **B**, using styrene oxide (50 mg, 0.416 mmol) and 5,5-dimethylcyclohexane-1,3-dione (116 mg, 0.816 mmol) to 2,2'-(2-phenylethane-1,1-diyl) bis (3-hydroxy-5,5-dimethylcyclohex-2-en-1-one) **1a** (133 mg, 84%) as a White Crystal.

Flow condition: Synthesized according to general procedure **C**, a solution of 0.2 M 5,5-dimethylcyclohexane-1,3-dione (280 mg, 2 mmol) and 0.1 M styrene oxide (120 mg, 1 mmol) in 20 mL dioxane were flown through the packed bed of Fe-Zeolite (bed height 6.0 cm) with 2.2 bar at 0.1 mL/min to afford 2,2'-(2-phenylethane-1,1-diyl)bis(3-hydroxy-5,5-dimethylcyclohex-2-en-1-one) **3a** (173 mg, 79% yield). Melting point: 158-160 ºC. ^{1}H NMR (400 MHz, $CDCl_3$) δ [ppm] = 12.79 (s, 1H), 7.19 (m, 4H), 7.11 (m, 1H), 4.37 (t, *J* = 8 Hz, 1H), 3.32 (d, *J* = 8 Hz, 2H), 2.23 (s, 4H), 2.18 (s, 2H), 2.17 (s, 2H), 1.00 (s, 6H), 0.69 (s, 6H). ^{13}C{^{1}H} NMR (100 MHz, $CDCl_3$) δ [ppm] = 190.3, 190.0, 140.0, 128.8, 128.5, 126.3, 116.1, 46.9, 46.1, 34.7, 31.3, 30.9, 30.1, 25.9. IR (neat): 3003.95, 2919.80, 2896.15, 1709.95 cm^{-1}. HRMS (ESI-TOF) m/z: $[M + H]^+$ calcd for $C_{24}H_{30}O_4$: 383.2222; found: 383.2215. **Crystal preparation:** The crystal is grown by simple recrystallization method. The pure compound isolated after column chromatography is dissolved in dichloromethane and layered with hexane and kept at room temperature for 2 days to get pure crystal. **Crystal Data**: Compound 3a ($C_{24}H_{30}O_4$, M = 382.5 g mol^{-1}) crystallized as white needle-shaped crystals in the monoclinic crystal system with space group $P2_1/c$. The unit cell parameters are: a = 8.702(3) Å, b = 20.224(7) Å, c = 11.877(4) Å, with α = 90°, β = 98.716(9)°, and γ = 90°. The calculated unit cell volume is 2066.2(12) $Å^3$ with Z = 4 and a calculated density ($D_{al}c_ed$) of 1.230 g cm^{-3}. Data were collected at 296(2) K using Mo Kα radiation (λ = 0.71073 Å). A total of 1903 reflections were measured, of which 1729 were observed with $I > 2\sigma(I)$. The structure was refined to $R_1 = 0.1078$, $wR_2 = 0.2679$ for observed data and $R_1 = 0.1147$, $wR_2 = 0.2744$ for all data, with a goodness of fit (GoF) of 1.006. The absorption coefficient (μ) was 0.082 mm^{-1}, and F(000) = 824. The data completeness extended to a theta value of 19.924°.

2,2'-(2-(p-tolyl)ethane-1,1-diyl)bis(3-hydroxy-5,5-dimethylcyclohex-2-en-1-one) (3b): Batch condition: Synthesized according to general procedure **B**, using 5,5-dimethylcyclohexane-1,3-dione (104 mg, 0.74 mmol) and 2-(p-tolyl)oxirane (50 mg, 0.373 mmol) to afford 2,2'-(2-(p-tolyl)ethane-1,1-diyl)bis(3-hydroxy-5,5-dimethylcyclohex-2-en-1-one) **3b** (60 mg, 41%) as a yellow solid.

Flow condition: Synthesized according to general procedure **C**, a solution of 0.1 M 5,5-dimethylcyclohexane-1,3-dione (140 mg, 1 mmol) and 0.05 M 2-(p-tolyl)oxirane (67 mg, 0.5 mmol) in 20 mL 1,4-dioxane were flown through the packed bed of Fe-zeolite (bed height 6.0 cm) with 2-3 bar at 0.1 mL/min to afford 2,2'-(2-(p-tolyl)ethane-1,1-diyl)bis(3-hydroxy-5,5-dimethylcyclohex-2-en-1-one) **3b** (118 mg, 40% yield). Melting point: 165-167 ºC. ^{1}H NMR (400 MHz, $CDCl_3$) δ 12.77 (s, 1H), 7.05 (d, *J* = 4 Hz, 2H), 7.00 (d, *J* = 8Hz, 2H), 4.33 (t, *J* = 8 Hz, 1H), 3.27 (d, *J* = 8 Hz, 2H), 2.24 (d, *J* = 4 Hz, 8H), 2.19 (s, 3H), 1.00 (s, 6H), 0.71 (s, 6H). ^{13}C{^{1}H} NMR (100 MHz, $CDCl_3$) δ [ppm] = δ 190.2, 189.9, 137.1, 135.7, 129.0, 128.6, 116.1, 46.9, 46.1, 34.2, 31.3, 30.9, 29.9, 25.9, 20.9.

IR (neat): 3361.80, 3020.77, 2980.16, 1589.02 cm^{-1}. HRMS (ESI-TOF) m/z: $[M + H]^+$ calcd. for $C_{25}H_{32}O_4$ 397.2379; found 397.2374.

2,2'-(2-(4-bromophenyl)ethane-1,1-diyl)bis(3-hydroxy-5,5-dimethylcyclohex-2-en-1-one) (3c): Synthesized according to general procedure **B**, using 5,5-dimethylcyclohexane-1,3-dione (70 mg, 0.50 mmol) and 2-(4-bromophenyl)oxirane (50 mg, 0.25 mmol) to afford 2,2'-(2-(4-bromophenyl)ethane-1,1-diyl)bis(3-hydroxy-5,5-dimethylcyclohex-2-en-1-one) **3c** (80 mg, 67 %) as white solid. Melting point: 131-133 ºC. ^{1}H NMR (400 MHz, $CDCl_3$) δ 11.59 (s, 1H), 7.33 (d, *J* = 8 Hz, 2H), 7.05 (d, *J* = 8 Hz, 2H), 4.31 (t, *J* = 8 Hz, 1H), 3.27 (d, *J* = 8 Hz, 2H), 2.23 (s, 4H), 2.20 (s, 4H), 1.00 (s, 6H), 0.73 (s, 6H).^{13}C{^{1}H} NMR (100 MHz, $CDCl_3$) δ [ppm] = 190.4, 190.03, 139.1, 131.5, 130.6, 120.1, 115.8, 46.9, 46.1, 34.11, 31.2, 30.9, 30.0, 25.9. IR (neat): 3407.52, 3005.15, 2980.45, 1712.64 cm^{-1}. HRMS (ESI-TOF) m/z: $[M + H]^+$ calcd for $C_{24}H_{29}BrO_4$: 461.1327; found 461.1325.

2,2'-(2-phenylpropane-1,1-diyl)bis(3-hydroxy-5,5-dimethylcyclohex-2-en-1-one)) (3d): Synthesized according to general procedure **B**, using 5,5-dimethylcyclohexane-1,3-dione (104 mg, 0.74 mmol) and 2-methyl-2-phenyloxirane (50 mg, 0.373 mmol) to afford 2,2'-(2-phenylpropane-1,1-diyl)bis(3-hydroxy-5,5-dimethylcyclohex-2-en-1-one) **3d** (81 mg, 58%) as a yellow solid. Melting point: 156-158 ºC. ^{1}H NMR (400 MHz, $CDCl_3$) δ 12.71 (s, 1H), 7.18 (m, 1H), 7.08 (m, 1H), 4.16 (d, *J* = 12 Hz, 1H), 4.10 (m, 1H), 2.36 (m, 4H),1.99 (m, 4H), 1.15 (m, 12H), 0.87 (s, 3H). ^{13}C{^{1}H} NMR (100 MHz, $CDCl_3$) δ [ppm] = 190.6, 189.4, 128.6, 126.9, 126.4, 116.6, 115.6, 47.2, 45.9, 37.4, 31.1, 30.3, 30.2, 26.8, 24.9, 22.4. IR (neat): 3402.44, 2975.26, 2910.17, 1708.26 cm^{-1}. HRMS (ESI-TOF) m/z: $[M + H]^+$ calcd for $C_{24}H_{30}O_4$: 397.2379; found: 397.2377.

2,2'-(2-phenylethane-1,1-diyl)bis(3-hydroxy-4,4-dimethylcyclohex-2-en-1-one) (3e): Batch condition: Synthesized according to general procedure **B**, using styrene oxide (50 mg, 0.416 mmol) and 4,4-dimethylcyclohexane-1,3-dione (116 mg, 0.832 mmol) to afford 2,2'-(2-phenylethane-1,1-diyl)bis(3-hydroxy-4,4-dimethylcyclohex-2-en-1-one) **3e** (110 mg, 70%) as a white solid.

Flow condition: Synthesized according to general procedure **C**, a solution of 0.2 M 4,4-dimethylcyclohexane-1,3-dione (280 mg, 2 mmol) and 0.1 M styrene oxide (120 mg, 1 mmol) in 20 mL dioxane was flown through the packed bed of Fe-zeolite (bed height 6.0 cm) with 2.2 bar pressure at 0.1 mL/min to afford 2,2'-(2-phenylethane-1,1-diyl)bis(3-hydroxy-4,4-dimethylcyclohex-2-en-1-one) **3e** (143 mg, 54% yield). Melting point: 138-140 ºC. ^{1}H NMR (400 MHz, $CDCl_3$) δ 13.19 (s, 1H), 7.15 (m, 5H), 4.20 (t, *J* = 32 Hz, 1H), 3.21 (d, *J* = 8 Hz, 2H), 2.37 (m, 4H), 1.56 (m, 4H), 1.05 (m, 12H). ^{13}C{^{1}H} NMR (100 MHz, $CDCl_3$) δ [ppm] = 204.1, 203.7, 182.9, 182.2, 140.6, 129.2, 128.5,

126.3, 115.6, 39.7, 34.9, 34.2, 32.1, 28.4, 27.8. IR (neat): 2927.69, 2900.02, 2879.40, 1718.61 cm^{-1}. HRMS (ESI-TOF) m/z: $[M + H]^+$ calcd for for $C_{24}H_{30}O_4$: 383.2222; found 383.2221.

2'-(2-(p-tolyl)ethane-1,1-diyl)bis(3-hydroxy-4,4-dimethylcyclohex-2-en-1-one) (3f): Synthesized according to general procedure **B**, using 2-(p-tolyl)oxirane (50 mg, 0.373 mmol) and 4,4-dimethylcyclohexane-1,3-dione (104.44 mg, 0.746 mmol) to afford 2'-(2-(p-tolyl)ethane-1,1-diyl)bis(3-hydroxy-4,4-dimethylcyclohex-2-en-1-one) **3f** (70 mg, 48%) as a white solid. Melting point: 142-144 ºC. ^1H NMR (400 MHz, $CDCl_3$) δ 12.05 (s, 1H), 6.98 (m, 4H), 4.15 (t, *J* = 8 Hz, 1H), 3.19 (d, *J* = 8Hz, 2H), 2.41 (m, 4H), 2.27 (s, 3H), 1.6 (m, 4H), 1.08 (s,3H), 1.06 (s, 3H), 1.05 (s, 3H), 0.96 (s, 3H). $^{13}C\{^1H\}$ NMR (100 MHz, $CDCl_3$) δ [ppm] = 204.1, 203.8, 182.9, 182.1, 137.3, 135.5, 128.8,128.7, 115.4, 39.7, 38.9, 34.6, 34.2, 28.4, 26.2, 26.0, 24.3. IR (neat): 3434.52, 3001.13, 2990.39, 1741.20 cm^{-1}. HRMS (ESI-TOF) m/z: $[M + H]^+$ calcd for $C_{25}H_{32}O_4$:396.2379; found 396.2369.

2,2'-(2-phenylethane-1,1-diyl)bis(3-hydroxy-5-methylcyclohex-2-en-1-one) (3g):

Batch condition: Synthesized according to general procedure **B**, using styrene oxide (50 mg, 0.416 mmol) and 5-methylcyclohexane-1,3-dione (128mg, 0.832 mmol) to afford 2,2'-(2-phenylethane-1,1-diyl)bis(3-hydroxy-5-methylcyclohex-2-en-1-one) **3g** (117 mg, 80%) as a White solid.

Flow condition: Synthesized according to general procedure **C**, a solution of 0.2 M 5-methylcyclohexane-1,3-dione (256 mg, 2 mmol) and 0.1 M styrene oxide (120mg, 1 mmol) in 20 mL dioxane was flown through the packed bed of Fe-zeolite (bed height 6.0 cm) with 2.2 bar at 0.1 mL/min to afford 2,2'-(2-phenylethane-1,1-diyl)bis(3-hydroxy-5,5-dimethylcyclohex-2-en-1-one) **3g** (148 mg, 61% yield). Melting point: 142-144 ºC. ^1H NMR (400 MHz, $CDCl_3$) δ [ppm] = 13.13 (s, 1H), 7.13 (m, 5H), 4.18 (t, *J* = 8 Hz, 1H), 3.38 (dd, *J* = 13.7, 9.2 Hz, 1H), 3.27 (d, *J* = 8 Hz, 2H), 3.18 (dd, *J* = 13.7, 7.9 Hz, 1H), 2.42 (m, 8H), 1.00 (d, *J* = 4 Hz, 6H). $^{13}C\{^1H\}$ NMR (100 MHz, $CDCl_3$) δ [ppm] = 191.6, 191.1, 128.6, 128.3, 128.1, 126.1, 116.8, 41.7, 40.9, 34.8, 32.1, 27.4, 20.5. IR (neat): 2954.52, 2900.23, 2868.55, 1726.03 cm^{-1}. HRMS (ESI-TOF) m/z: $[M + H]^+$ calcd for $C_{22}H_{26}O_4$: 355.1909; found: 355.1918.

2'-(2-phenylethane-1,1-diyl)bis(3-hydroxycyclohex-2-en-1-one) (3h):

Batch condition: Synthesized according to general procedure **B**, using styrene oxide (50 mg, 0.416 mmol) and cyclohexane-1,3-dione (112mg, 0.832 mmol) to afford 2'-(2-phenylethane-1,1-diyl)bis(3-hydroxycyclohex-2-en-1-one) **3h** (84 mg, 62%) as a yellow solid.

Flow condition: Synthesized according to general procedure **C**, a solution of 0.2 M cyclohexane-1,3-dione (224 mg, 2 mmol) and 0.1 M styrene oxide (120 mg, 1 mmol) in 20 mL dioxane was flown through the packed bed of Fe-zeolite (bed height 6.0 cm) with 2.2 bar at 0.1 mL/min to afford 2'-(2-phenylethane-1,1-diyl)bis(3-hydroxycyclohex-2-en-1-one) **3h** (110 mg, 52% yield). Melting point: 121-123 °C. ^{1}H NMR (400 MHz, $CDCl_3$) δ [ppm] = 13.11 (s, 1H), 7.07 (m, 5H), 4.12 (t, *J* = 8 Hz, 1H), 3.19 (d, *J* = 8 Hz, 2H), 2.23 (m, 12 H). ^{13}C{^{1}H} NMR (100 MHz, $CDCl_3$) δ [ppm] = 191.8, 191.4, 140.5, 128.7, 128.2, 126.2, 117.4, 34.9, 33.5, 32.7, 32.2, 19.9. IR (neat): 2945.35, 2870.35, 2850.28, 1716.09 cm^{-1}. HRMS (ESI-TOF) m/z: $[M + H]^+$ calcd for $C_{20}H_{22}O_4$: 327.1596; found: 327.1599.

2,2'-(2-(p-tolyl)ethane-1,1-diyl)bis(3-hydroxycyclohex-2-en-1-one) (3i): Synthesized according to general procedure **B**, using 2-(p-tolyl)oxirane (50 mg, 0.373 mmol) and cyclohexane-1,3-dione (84 mg, 0.746 mmol) to afford 2,2'-(2-(p-tolyl)ethane-1,1-diyl)bis(3-hydroxycyclohex-2-en-1-one) **3i** (79 mg, 62%) as a yellow solid. Melting point: 96-98 °C. ^{1}H NMR (400 MHz, $CDCl_3$) δ 13.17 (s, 1H), 7.00 (m, 4H), 4.17 (t, *J* = 8 Hz, 1H), 3.23 (d, *J* = 8 Hz, 2H), 2.44 (m, 3H), 2.33 (m, 4H), 2.28 (s, 3H), 2.25 (m, 1H), 1.84 (m, 2H), 1.61 (m, 2H). ^{13}C{^{1}H} NMR (100 MHz, $CDCl_3$) δ [ppm] = 191.7, 191.2, 137.1, 135.3, 129.0, 125.5, 117.1, 34.5, 33.5, 32.7, 32.2, 21.0, 19.8. IR (neat): 2938.32, 2920.85, 2895.82, 1730.94 cm^{-1}. HRMS (ESI-TOF) m/z: $[M + H]^+$ calcd for $C_{21}H_{24}O_4$: 341.1753; found 341.1749.

2,2'-(propane-1,1-diyl)bis(3-hydroxy-5,5-dimethylcyclohex-2-en-1-one) (3j): Synthesized according to general procedure **B**, using 2-methyloxirane (50 mg, 0.86 mmol) and 5,5-dimethylcyclohexane-1,3-dione (240 mg, 1.72 mmol) to afford 2,2'-(propane-1,1-diyl)bis(3-hydroxy-5,5-dimethylcyclohex-2-en-1-one) **3j** (60 mg, 22%) as a white solid. Melting point: 62-64 °C. ^{1}H NMR (400 MHz, $CDCl_3$) δ 12.47 (s, 1H), 3.81 (t, *J* = 8 Hz, 1H), 2.28 (m, 8H), 2.05 (m, 2H), 1.07 (s, 6H), 1.05 (s, 6H), 0.83 (t, *J* = 8 Hz, 3H). ^{13}C{^{1}H} NMR (100 MHz, $CDCl_3$) δ [ppm] = 190.2, 189.6, 116.5, 47.1, 46.3, 31.7, 31.2, 29.9, 26.6, 22.4, 13.6. IR (neat): 2961.01, 2953.61, 2899.17, 1724.58cm^{-1}. HRMS (ESI-TOF) m/z: $[M + H]^+$ calcd for $C_{19}H_{28}O_4$: 321.2066; found 321.2065.

2,2'-(hexane-1,1-diyl)bis(3-hydroxy-5,5-dimethylcyclohex-2-en-1-one) (3k): Synthesized according to general procedure **B**, using 2-butyloxirane (50 mg, 0.499 mmol) and 5,5-dimethylcyclohexane-1,3-dione (139 mg, 0.998 mmol) to afford 2,2'-(hexane-1,1-diyl)bis(3-hydroxy-5,5-dimethylcyclohex-2-en-1-one **3k** (49 mg, 27%) as a white solid. Melting point: 76-78 °C. ^{1}H NMR (400 MHz, $CDCl_3$) δ 12.49 (s, 1H), 3.91(t, *J* = 8 Hz, 1H), 2.28 (m, 8H), 1.24 (m, 6 H), 1.06 (s, 6H), 1.06 (s, 6H), 0.88 (m, 5H). ^{13}C{^{1}H} NMR (100 MHz, $CDCl_3$) δ [ppm] = 190.0, 189.7, 116.7, 47.1, 46.3, 31.8, 31.2, 29.9, 29.7, 29.7, 29.5, 29.3, 29.3, 29.2, 29.1, 26.6, 22.7, 14.2. IR (neat): 2948.87,

2867.05, 2860.17, 2854.13, 1717.51 cm^{-1}. HRMS (ESI-TOF) m/z: $[M + H]^+$ calcd for $C_{22}H_{34}O_4$: 363.2535; found 363.2542.

2,2'-(octane-1,1-diyl)bis(3-hydroxy-5,5-dimethylcyclohex-2-en-1-one) (3l): Synthesized according to general procedure **B**, using 2-hexyloxirane (50 mg, 0.390 mmol) and 5,5-dimethylcyclohexane-1,3-dione (109 mg, 0.780 mmol) to afford 2,2'-(octane-1,1-diyl)bis(3-hydroxy-5,5-dimethylcyclohex-2-en-1-one) **3l** (47 mg, 31%) as a white solid. Melting point: 88-90 ºC. ^1H NMR (400 MHz, $CDCl_3$) δ 12.49 (s, 1H), 3.90 (t, *J* = 8 Hz, 1H), 2.27 (m, 8H), 1.45 (m, 12 H), 1.06 (s, 6H), 1.05 (s, 6H), 0.85 (m, 3H). $^{13}C\{^1H\}$ NMR (100 MHz, $CDCl_3$) δ [ppm] = 190.0, 189.7, 116.7, 47.1, 46.3, 31.8, 31.2, 29.9, 29.6, 29.3, 29.3, 29.2, 29.1, 26.6, 22.7, 14.2. IR (neat): 2927.29, 2864.80, 2858.48, 1723.02 cm^{-1}. HRMS (ESI-TOF) m/z: $[M + H]^+$ calcd for $C_{24}H_{38}O_4$: 391.2848; found 391.2860.

2,2'-(cyclopentylmethylene)bis(3-hydroxy-5,5-dimethylcyclohex-2-en-1-one) (3m): Synthesized according to general procedure **B**, using 7-oxabicyclo[4.1.0]heptane (50 mg, 0.51 mmol) and 5,5-dimethylcyclohexane-1,3-dione (142 mg, 1.018 mmol) at 160 ºC in toluene to afford 2,2'-(cyclopentylmethylene)bis(3-hydroxy-5,5-dimethylcyclohex-2-en-1-one) **3m** (80 mg, 44%) as a white solid. Melting point: 148-150 ºC.^1H NMR (400 MHz, $CDCl_3$) δ 11.56 (s, 1H), 3.58 (d, *J* = 24 Hz, 1H), 3.15 (m, 1H), 2.28 (m, 4H), 2.27 (m, 4H), 1.60 (m, 8H), 1.07 (s, 6H), 1.06 (s, 6H). $^{13}C\{^1H\}$ NMR (100 MHz, $CDCl_3$) δ [ppm] = 190.2, 189.6, 117.0, 47.0, 46.2, 38.3, 36.6, 32.9, 31.1, 30.2, 26.5, 25.4. IR (neat): 2952.45, 2868.85, 2847.37, 1717.38 cm^{-1}. HRMS (ESI-TOF) m/z: $[M + H]^+$ calcd for $C_{22}H_{32}O_4$: 361.2379; found 361.2374.

4-(bis(2-hydroxy-4,4-dimethyl-6-oxocyclohex-1-en-1-yl)methyl)benzonitrile (5a): Synthesized according to general procedure **D**, a solution of 0.1 M 4-formylbenzonitrile (65 mg, 0.50 mmol) in 5 mL 1,4-dioxane and 5,5-dimethylcyclohexane-1,3-dione (140 mg, 1 mmol) in 5 mL 1,4-dioxane were flown through a packed bed of Fe-zeolite (bed height 6.0 cm) with 2-3 bar pressure at 0.1 mL/min to afford 4-(bis(2-hydroxy-4,4-dimethyl-6-oxocyclohex-1-en-1-yl)methyl)benzonitrile **5a** (119 mg, 87% from 7 mL collected reaction mixture) as white solid. Melting point: 165-167 ºC.^1H NMR (400 MHz, $CDCl_3$) δ [ppm] = 11.79 (s, 1H), 7.56 (d, *J* = 8 Hz, 2H), 7.19 (d, *J* = 8 Hz, 2H), 5.51 (s, 1H), 2.45 (m, 4H), 2.35 (m, 4H), 1.22 (s, 6H), 1.11 (s, 6 H). $^{13}C\{^1H\}$ NMR (100 MHz, $CDCl_3$) δ [ppm] = 190.9, 189.5, 144.3, 132.1, 127.6, 118.9, 114.8, 109.8, 47.0, 46.4, 33.3, 31.5, 29.6, 27.5. IR (neat): 2952.72, 2940.47, 2910.23, 2256.01, 1717.00 cm^{-1}. HRMS (ESI-TOF) m/z: $[M + H]^+$ calcd for $C_{24}H_{27}NO_4$: 394.2018; found: 394.2014.

2,2'-((4-nitrophenyl)methylene)bis(3-hydroxy-5,5-dimethylcyclohex-2-en-1-one) (5b): Synthesized according to general procedure **D**, a solution of 0.1 M 4-nitrobenzaldehyde (75 mg, 0.5

mmol) in 5 mL 1,4-dioxane and 0.2 M dimedone (140 mg, 1 mmol) in 5 mL 1,4-dioxane were flown through a packed bed of Fe-zeolite (bed height 6.0 cm) with 4.8 bar pressure at 0.1 mL/min to afford 2,2'-((4-nitrophenyl)methylene)bis(3-hydroxy-5,5-dimethylcyclohex-2-en-1-one) **5b** (127mg, 90% from 6.9 mL collected reaction mixture) as white solid. Melting point: 187-189 ºC. ^{1}H NMR (400 MHz, $CDCl_3$) δ [ppm] = 11.80 (s, 1H), 8.15 (m, 1H), 8.13 (m, 1H), 7.25 (m, 1H), 7.23 (m, 1H), 5.55 (s, 1H), 2.46 (m, 4H), 2.36 (m, 4H), 1.24 (s, 6H), 1.11 (s, 6H). ^{13}C{^{1}H} NMR (100 MHz, $CDCl_3$) δ [ppm] = 190.9, 189.6, 146.5, 146.2, 127.7, 123.5, 114.9, 47.0, 46.4, 33.3, 31.5, 29.5, 27.5. IR (neat): 3362.31, 3020.18, 2995.95, 1710.20 cm^{-1}. HRMS (ESI-TOF) m/z: $[M + H]^+$ calcd for $C_{23}H_{27}NO_6$: 414.1916; found: 414.1919.

2,2'-((3,5-dimethoxyphenyl)methylene)bis(3-hydroxy-5,5-dimethylcyclohex-2-en-1-one)(5c): Synthesized according to general procedure **D**, a solution of 0.1 M 3,5-dimethoxybenzaldehyde (83 mg, 0.5 mmol) in 5 mL 1,4-dioxane and 0.2 M 5,5-dimethylcyclohexane-1,3-dione (140 mg, 1 mmol) in 5 mL 1,4-dioxane were flown through a packed bed of Fe-zeolite (bed height 6.0 cm) with 2-3 bar pressure at 0.1 mL/min to afford 2,2'-((3,5-dimethoxyphenyl)methylene)bis(3-hydroxy-5,5-dimethylcyclohex-2-en-1-one) **5c** (108 mg, 70% from 7 mL collected reaction mixture) as white solid. Melting point: 184-186 ºC. ^{1}H NMR (400 MHz, $CDCl_3$) δ [ppm] = 11.97 (s, 1H), 6.78 (d, *J* = 8 Hz, 1H), 6.62 (m, 2H), 5.51 (s, 1H), 3.84 (s, 1H), 3.77 (s, 3H), 2.43 (m, 4H), 2.33 (m, 4H), 1.24 (s, 6H), 1.11 (s, 6H). ^{13}C{^{1}H} NMR (100 MHz, $CDCl_3$) δ [ppm] = 190.4, 189.4, 148.7, 147.0, 130.4, 118.9, 115.8, 110.5, 55.8, 55.7, 47.1, 46.4, 32.3, 31.2, 29.9, 27.1. IR (neat): 2954.05, 2930.13, 2909.19, 1710.09 cm^{-1}. HRMS (ESI-TOF) m/z: $[M + H]^+$ calcd for $C_{25}H_{32}O_6$: 429.2277; found: 429.2280.

2,2'-((4-(benzyloxy)phenyl)methylene)bis(3-hydroxy-5,5-dimethylcyclohex-2-en-1-one) (5d): Synthesized according to general procedure **D**, a solution of 0.1 M 4-(benzyloxy)benzaldehyde (106 mg, 0.5 mmol) in 5 mL 1,4-dioxane and 0.2 M dimedone (140 mg, 1 mmol) in 5 mL 1,4-dioxane were flown through a packed bed of Fe-zeolite (bed height 6.0 cm) with 2-3 bar pressure at 0.1 mL/min to afford 2,2'-((4-(benzyloxy)phenyl)methylene)bis(3-hydroxy-5,5-dimethylcyclohex-2-en-1-one) **5d** (66 mg, 59% from 5 mL collected reaction mixture) as yellow solid. Melting point: 222-224 ºC. ^{1}H NMR (400 MHz, $CDCl_3$) δ [ppm] = 11.91 (s, 1H), 7.40 (m, 4H), 7.32 (m, 1H), 7.00 (m, 2H), 6.88 (m, 2H), 5.48 (s, 1H), 5.03 (s, 2H), 2.43 (m, 4H), 2.33 (m, 4H), 1.22 (s, 6H), 1.10 (s, 6H). ^{13}C{^{1}H} NMR (100 MHz, $CDCl_3$) δ [ppm] = 190.4, 189.4, 156.9, 137.2, 130.2, 128.6, 127.9, 127.8, 127.5, 115.8, 114.6, 70.0, 47.1, 46.5, 32.1, 31.4, 29.7, 27.4. IR (neat): 2924.16, 2911.01, 2899.90, 1739.85 cm^{-1}. HRMS (ESI-TOF) m/z: $[M + H]^+$ calcd for $C_{30}H_{34}O_5$: 475.2484; found: 475.2482.

2,2'-((4-fluorophenyl)methylene)bis(3-hydroxy-5,5-dimethylcyclohex-2-en-1-one) (5e): Synthesized according to general procedure **D**, a solution of 0.1 M 4-fluorobenzaldehyde (62 mg, 0.5 mmol) in 5 mL 1,4-dioxane and 0.2 M dimedone (140 mg, 1 mmol) in 5 mL 1,4-dioxane were flown through a packed bed of Fe-zeolite (bed height 6.0 cm) with 2-3 bar pressure at 0.1 mL/min to afford 2,2'-((4-fluorophenyl)methylene)bis(3-hydroxy-5,5-dimethylcyclohex-2-en-1-one) **5e** (63 mg, 65% from 5 mL collected reaction mixture) as white solid. Melting point: 140-142 ºC. ^{1}H NMR (400 MHz, $CDCl_3$) δ [ppm] = 11.88 (s, 1H), 7.03 (m, 2H), 6.95 (m, 2H), 5.48 (s. 1H), 2.39 (m, 8H), 1.22 (s, 6H), 1.10 (s, 6H).^{13}C{^{1}H} NMR (100 MHz, $CDCl_3$) δ [ppm] = 190.6, 189.4, 128.3, 128.2, 115.6, 115.1, 114.9, 47.0, 46.4, 32.2, 31., 29.6, 27.41. IR (neat): 2956.78, 2946.46, 2830.22, 1716.37 cm^{-1}. HRMS (ESI-TOF) m/z: $[M + H]^+$ calcd for $C_{23}H_{27}FO_4$: 387.1970; found: 387.1970.

2,2'-(p-tolylmethylene)bis(3-hydroxycyclohex-2-en-1-one) (5f): Synthesized according to general procedure **D**, a solution of 0.1 M 4-methylbenzaldehyde (60 mg, 0.5 mmol) in 5 mL 1,4-dioxane and 0.2 M cyclohexa-1,3-dione (112 mg, 1 mmol) in 5 mL 1,4-dioxane were flown through a packed bed of Fe-zeolite (bed height 6.0 cm) with 2-3 bar pressure at 0.1 mL/min to afford 2,2'-(p-tolylmethylene)bis(3-hydroxycyclohex-2-en-1-one) **5f** (84 mg, 74% from 7 mL collected reaction mixture) as white solid. Melting point: 190-192 ºC.^{1}H NMR (400 MHz, $CDCl_3$) δ [ppm] = 12.35 (s, 1H), 7.06 (d, J = 8 Hz, 2H), 6.98 (d, *J* = 8 Hz, 2H), 5.43 (s, 1H), 2.60 (m, 4H), 2.41 (m, 4H), 2.30 (s, 3H), 2.03 (m, 4H). ^{13}C{^{1}H} NMR (100 MHz, $CDCl_3$) δ [ppm] = 192.0, 190.9, 135.3, 134.7, 128.9, 126.4, 116.6, 33.5, 33.0, 32.6, 20.9, 20.1. IR (neat): 3449.94, 3003.01, 2980.77, 1740.84 cm^{-1}. HRMS (ESI-TOF) m/z: $[M + H]^+$ calcd for $C_{20}H_{22}O_4$: 327.1596; found: 327.1595.

2,2'-(phenylmethylene)bis(3-hydroxycyclohex-2-en-1-one) (5g): Synthesized according to general procedure **D**, a solution of 0.1 M benzaldehyde (53 mg, 0.5 mmol) in 5 mL 1,4-dioxane and 0.2 M 1,3-cyclohexadione (112 mg, 1 mmol) in 5 mL 1,4-dioxane were flown through a packed bed of Fe-zeolite (bed height 6.0 cm) with 2-3 bar pressure at 0.1 mL/min to afford **5g** 2,2'-(phenylmethylene)bis(3-hydroxycyclohex-2-en-1-one) (119 mg, 64% from 6 mL collected reaction mixture) as white solid. Melting point: 216-218 ºC. ^{1}H NMR (400 MHz, $CDCl_3$) δ [ppm] = 12.35 (s, 1H), 7.28 (m, 1H), 7.24 (m, 1H), 7.16 (m, 2H), 5.47 (s, 1H), 2.61 (m, 4H), 2.44 (m, 4H), 2.03 (m, 4H). ^{13}C{1H} NMR (100 MHz, $CDCl_3$) δ [ppm] = 192.1, 190.9, 137.9, 128.2, 126.5, 125.9, 116.4, 33.5, 32.9, 20.1, 18.9. IR (neat): 3494.32, 3000.19, 2990.87, 1708.46 cm^{-1}. HRMS (ESI-TOF) m/z: $[M + H]^+$ calcd for $C_{19}H_{20}O_4$: 313.1440; found: 313.1446.

9-benzyl-3,3,6,6-tetramethyl-3,4,5,6,7,9-hexahydro-1*H*-xanthene-1,8(2*H*)-dione (6a): Synthesized according to general procedure **E**, using 2,2'-(2-phenylethane-1,1-diyl)bis(3-hydroxy-5,5-

dimethylcyclohex-2-en-1-one) **3a** (50 mg, 0.131 mmol) at 180 ºC in toluene to afford 9-benzyl-3,3,6,6-tetramethyl-3,4,5,6,7,9-hexahydro-1*H*-xanthene-1,8(2*H*)-dione **6a** (40 mg, 85%) as a yellow solid. Melting point: 120-122 ºC. ^{1}H NMR (400 MHz, $CDCl_3$) δ 7.16 (m, 3H), 6.86 (m, 2H), 4.06 (t, *J* = 4 Hz, 1H), 2.91 (d, *J* = 4 Hz, 2H), 2.28 (s, 4H), 2.14 (m, 4H), 1.05 (s, 6H), 1.04 (s, 6H).^{13}C{^{1}H} NMR (100 MHz, $CDCl_3$) δ [ppm] = 197.3, 164.2, 138.9, 130.1, 127.7, 126.2, 113.9, 51.2, 40.8, 38.2, 32.1, 28.6, 27.5. IR (neat): 3006.09, 2979.18, 1660.90 cm^{-1}. HRMS (ESI-TOF) m/z: $[M + H]^+$ calcd for $C_{24}H_{28}O_3$ 365.2116; found 365.2115.

3,3,6,6-tetramethyl-9-(4-methylbenzyl)-3,4,5,6,7,9-hexahydro-1*H*-xanthene-1,8(2*H*)-dione (6b): Synthesized according to general procedure **E**, using 2,2'-(2-(p-tolyl)ethane-1,1-diyl)bis(3-hydroxy-5,5-dimethylcyclohex-2-en-1-one) **3b** (50 mg, 0.133 mmol) in toluene at 180 ºC to afford 3,3,6,6-tetramethyl-9-(4-methylbenzyl)-3,4,5,6,7,9-hexahydro-1*H*-xanthene-1,8(2*H*)-dione **6b** (39 mg, 83%) as a light yellow solid . Melting point: 126-128 ºC.^{1}H NMR (400 MHz, $CDCl_3$) δ 6.97 (d, *J* = 4Hz, 2H), 6.74 (d, *J* = 4 Hz, 2H), 4.03 (t, *J* = 4 Hz, 1H), 2.88 (d, *J* = 4Hz, 2H), 2.28 (s, 4H), 2.27 (s, 4H), 2.17 (d, *J* = 8 Hz, 3H), 1.06 (s, 6H), 1.05 (s, 6H).^{13}C{^{1}H} NMR (100 MHz, $CDCl_3$) δ [ppm] = 197.2, 135.6, 135.5, 129.9, 128.4, 113.9, 51.1, 40.8, 37.7, 32.0, 28.6, 28.5, 27.5, 21.1. IR (neat): 2970.17, 2880.90, 1665.87 cm^{-1}. HRMS (ESI-TOF) m/z: $[M + H]^+$ calcd for $C_{25}H_{30}O_3$: 379.2273; found 379.2264.

9-(4-bromobenzyl)-3,3,6,6-tetramethyl-3,4,5,6,7,9-hexahydro-1*H*-xanthene-1,8(2*H*)-dione (6c): Synthesized according to general procedure **E**, using 2,2'-(2-(4-bromophenyl)ethane-1,1-diyl)bis(3-hydroxy-5,5-dimethylcyclohex-2-en-1-one) **3c** (40 mg, 0.087 mmol) in toluene at 180 ºC to afford 9-(4-bromobenzyl)-3,3,6,6-tetramethyl-3,4,5,6,7,9-hexahydro-1*H*-xanthene-1,8(2*H*)-dione **6c** (18 mg, 47%) as yellow solid. Melting point: 122-124 ºC.^{1}H NMR (400 MHz, $CDCl_3$) δ 7.30 (d, *J* = 8 Hz, 2H), 6.75 (d, *J* = 8 Hz, 2H), 4.04 (t, *J* = 4 Hz, 1H), 2.90 (d, *J* = 4 Hz, 2H), 2.28 (s, 4H), 2.21 (d, *J* = 4 Hz, 4H), 1.55 (s, 6H), 1.06 (s, 6H). ^{13}C{^{1}H} NMR (100 MHz, $CDCl_3$) δ [ppm] = 207.1, 197.2, 164.3, 138.0, 131.6, 120.1, 113.5, 51.1, 40.8, 37.6, 32.0, 31.0, 28.6. IR (neat): 2950.36, 2910.11, 1742.09 cm^{-1}. HRMS (ESI-TOF) m/z: $[M + H]^+$ calcd for $C_{24}H_{27}BrO_3$: 443.1222; found 443.1219.

9-benzyl-3,6-dimethyl-3,4,5,6,7,9-hexahydro-1*H*-xanthene-1,8(2*H*)-dione (6d): Synthesized according to general procedure **E**, using 2,2'-(2-(p-tolyl)ethane-1,1-diyl)bis(3-hydroxycyclohex-2-en-1-one) **3g** in toluene at 180 ºC to afford 9-(4-methylbenzyl)-3,4,5,6,7,9-hexahydro-1*H*-xanthene-1,8(2*H*)-dione **6d** (29 mg, 61%) as yellow solid. Melting point: 118-120 ºC.^{1}H NMR (400 MHz, $CDCl_3$) δ 7.17 (m, 3H), 6.77 (m, 2H), 4.06 (t, *J* = 4 Hz, 1H), 2.82 (m, 2H), 2.53 (d, *J* = 12 Hz, 2H), 2.21 (m, 4H), 2.04 (m, 4H), 1.08 (d, *J* = 4 Hz, 3H), 1.06 (d, *J* = 2.76 Hz, 3H). ^{13}C{^{1}H} NMR (100

MHz, $CDCl_3$) δ [ppm] = 197.2, 165.2, 138.4, 130.3, 127.7, 126.7, 113.3, 45.5, 37.8, 35.1, 28.7, 28.0, 21.0. IR (neat): 2885.66, 2849.88, 1721.38 cm^{-1}. HRMS (ESI-TOF) m/z: $[M + H]^+$ calcd for $C_{22}H_{24}O_3$: 337.1803; found 337.1804

9-benzyl-3,4,5,6,7,9-hexahydro-1*H*-xanthene-1,8(2*H*)-dione (6e): Synthesized according to general procedure **E**, using 2,2'-(2-phenylethane-1,1-diyl)bis(3-hydroxycyclohex-2-en-1-one) **3h** (50 mg, 0.153 mmol) in toluene at 180 ºC to afford 9-benzyl-3,4,5,6,7,9-hexahydro-1*H*-xanthene-1,8(2*H*)-dione **6e** (31 mg, 65%) as a light yellow solid. Melting point: 124-126 ºC .^{1}H NMR (400 MHz, $CDCl_3$) δ 7.17 (m, 3H), 6.81 (m, 2H), 4.09 (t, *J* = 4Hz, 1H), 2.82 (d, *J* =4 Hz, 2H), 2.49 (m, 2H), 2.38 (m, 2H), 2.23 (m, 4H), 1.98 (m, 4H).^{13}C{^{1}H} NMR (100 MHz, $CDCl_3$) δ [ppm] = 197.3, 165.8, 138.5, 130.2, 127.4, 126.2, 114.6, 38.2, 37.2, 27.1, 26.9, 20.5. IR (neat): 3000.57, 2990.28, 1718.07 cm^{-1}. HRMS (ESI-TOF) m/z: $[M + H]^+$ calcd for $C_{20}H_{20}O_3$: 309.1490; found 309.1489.

9-(4-methylbenzyl)-3,4,5,6,7,9-hexahydro-1*H*-xanthene-1,8(2*H*)-dione (6f): Synthesized according to general procedure **E**, using 2,2'-(2-(p-tolyl)ethane-1,1-diyl)bis(3-hydroxycyclohex-2-en-1-one) **3i** in toluene at 180 ºC to afford 9-(4-methylbenzyl)-3,4,5,6,7,9-hexahydro-1*H*-xanthene-1,8(2*H*)-dione **6f** (36.0 mg, 76%) as yellow solid. Melting point: 130-132 ºC. ^{1}H NMR (400 MHz, $CDCl_3$) δ 6.98 (d, *J* = 8 Hz, 2H), 6.69 (d, *J* = 8 Hz, 2H), 4.07 (t, *J* = 4 Hz, 1H), 2.78 (d, *J* = 4 Hz, 2H), 2.49 (m, 2H), 2.38 (m, 2H), 2.29 (s, 3H), 2.22 (m, 4H), 1.98 (m, 4H).^{13}C{^{1}H} NMR (100 MHz, $CDCl_3$) δ [ppm] = 197.3, 165.7, 135.6, 135.3, 130.1, 128.1, 114.7, 37.7, 37.2, 27.1, 26.9, 21.2, 20.5. IR (neat): 2967.14, 2925.16, 1739.94 cm^{-1}. HRMS (ESI-TOF) m/z: $[M + H]^+$ calcd for $C_{21}H_{22}O_3$: 323.1647; found: 323.1645.

4-(3,3,6,6-tetramethyl-1,8-dioxo-2,3,4,5,6,7,8,9-octahydro-1*H*-xanthen-9-yl)benzonitrile (6g): Synthesized according to general procedure **E**, using 4-(bis(2-hydroxy-4,4-dimethyl-6-oxocyclohex-1-en-1-yl)methyl)benzonitrile **5a** (50 mg, 0.127 mmol in toluene at 180 ºC for to afford 4-(3,3,6,6-tetramethyl-1,8-dioxo-2,3,4,5,6,7,8,9-octahydro-1*H*-xanthen-9-yl)benzonitrile **6g** (44 mg, 93%) as white solid. Melting point: 220-222 ºC.^{1}H NMR (400 MHz, $CDCl_3$) δ [ppm] = 7.52 (d, *J* = 8 Hz, 2H), 7.41 (d, *J* = 8 Hz, 2H), 4.76 (s, 1H), 2.48 (s, 4H), 2.20 (m, 4H), 1.11 (s, 6H), 0.98 (s, 6H). ^{13}C{^{1}H} NMR (100 MHz, $CDCl_3$) δ [ppm] = 196.3, 162.9, 149.4, 132.0, 129.3, 119.0, 114.6, 110.2, 67.1, 50.6, 40.8, 32.2, 29.2, 27.3. IR (neat): 2946.17, 2920.15, 1740.33 cm-1. HRMS (ESI-TOF) m/z: $[M + H]^+$ calcd for $C_{24}H_{25}NO_3$: 376.1916; found: 376.1912.

3,3,6,6-tetramethyl-9-(4-nitrophenyl)-3,4,5,6,7,9-hexahydro-1*H*-xanthene-1,8(2*H*)-dione (6h): Synthesized according to general procedure **E**, using 2,2'-((4-nitrophenyl)methylene)bis(3-hydroxy-5,5-dimethylcyclohex-2-en-1-one **5b** (30 mg, 0.0726 mmol) in at 180 ºC to afford 3,3,6,6-tetramethyl-

9-(4-nitrophenyl)-3,4,5,6,7,9-hexahydro-1*H*-xanthene-1,8(2*H*)-dione **6h** (24 mg, 85%) as white solid. Melting point: 222-224 ºC. ^{1}H NMR (400 MHz, $CDCl_3$) δ [ppm] = 8.09 (d, *J* = 8 Hz, 2H), 7.47 (d, *J* = 8 Hz, 2H), 4.62 (s, 1H), 2.4 (s, 4H), 2.21 (m, 4H), 1.11 (s, 6H), 0.99 (s, 6H). ^{13}C{^{1}H} NMR (100 MHz, $CDCl_3$) δ [ppm] = 196.3, 162.9, 151.5, 146.5, 129.4, 123.5, 114.6, 50.6, 40.9, 32.7, 32.2, 29.3, 27.3. IR (neat): 2917.10, 2900.13, 1710.29 cm^{-1}. HRMS (ESI-TOF) m/z: $[M + H]^+$ calcd for $C_{23}H_{25}NO_5$: 396.1811; found: 396.1811.

9-(3,5-dimethoxyphenyl)-3,3,6,6-tetramethyl-3,4,5,6,7,9-hexahydro-1*H*-xanthene-1,8(2*H*)-dione (6i): Synthesized according to general procedure **E**, using 2,2'-((3,5-dimethoxyphenyl)methylene)bis(3-hydroxy-5,5-dimethylcyclohex-2-en-1-one) **5c** (50 mg, 0.117 mmol), in toluene at 180 ºC to afford 9-(3,5-dimethoxyphenyl)-3,3,6,6-tetramethyl-3,4,5,6,7,9-hexahydro-1*H*-xanthene-1,8(2*H*)-dione **6i** (38 mg, 81%) as white solid. Melting point: 180-182 ºC. ^{1}H NMR (400 MHz, $CDCl_3$) δ [ppm] = 6.90 (d, *J* = 4 Hz, 1H), 6.74 (m, 2H), 4.70 (s, 1H), 3.85 (s, 3H), 3.79 (s, 3H), 2.45 (s, 4H), 2.21 (m, 4H), 1.10 (s, 6H), 1.00 (s, 6H). ^{13}C{^{1}H} NMR (100 MHz, $CDCl_3$) δ [ppm] = 196.5, 162.1, 148.5, 147.5, 136.9, 120.1, 115.8, 112.3, 110.9, 55.9, 55.8, 50.8, 40.9, 32.2, 31.2, 29.3, 27.3. IR (neat): 2940.53, 2909.18, 1710.12 cm^{-1}. HRMS (ESI-TOF) m/z: $[M + H]^+$ calcd for $C_{25}H_{30}O_5$: 410.2093; found: 410.2090.

9-(4-(benzyloxy)phenyl)-3,3,6,6-tetramethyl-3,4,5,6,7,9-hexahydro-1*H*-xanthene-1,8(2*H*)-dione (6j): Synthesized according to general procedure **E**, using 2,2'-((4-(benzyloxy)phenyl)methylene)bis(3-hydroxy-5,5-dimethylcyclohex-2-en-1-one) **5d** (30 mg, 0.063 mmol) in toluene at 180 ºC to afford 9-(4-(benzyloxy)phenyl)-3,3,6,6-tetramethyl-3,4,5,6,7,9-hexahydro-1*H*-xanthene-1,8(2*H*)-dione **6j** (22 mg, 77%) as white solid. Melting point: 162-164 ºC. ^{1}H NMR (400 MHz, $CDCl_3$) δ [ppm] = 7.38 (m, 4H), 7.30 (m,1H), 7.21 (s, 1H), 7.19 (s, 1H), 6.84 (s, 1H), 6.82 (s, 1H), 4.97 (s, 2H), 4.70 (s, 1H), 2.45 (s, 4H), 2.19 (m, 4H), 1.11 (s, 6H), 0.99 (s, 6H). 13C{1H} NMR (100 MHz, $CDCl_3$) δ [ppm] = 196.5, 162.1, 157.4, 137.2, 136.8, 129.4, 128.5, 127.6, 115.8, 114.4, 69.9, 50.78, 40.9, 32.2, 30.9, 29.3, 27.4. IR (neat): 2956.47, 2933.47, 1709.26 cm^{-1}. HRMS (ESI-TOF) m/z: $[M + H]^+$ calcd for $C_{30}H_{32}O_4$: 457.2379; found: 457.2380.

9-(p-tolyl)-3,4,5,6,7,9-hexahydro-1H-xanthene-1,8(2H)-dione (6k): Synthesized according to general procedure **E**, using 2,2'-(p-tolylmethylene)bis(3-hydroxycyclohex-2-en-1-one) **5f** (30 mg, 0.0919 mmol) in toluene at 180 ºC to afford 9-(p-tolyl)-3,4,5,6,7,9-hexahydro-1H-xanthene-1,8(2H)-dione **6k** (20 mg, 71%) as white solid. Melting point: 216-218 ºC. ^{1}H NMR (400 MHz, $CDCl_3$) δ [ppm] = 7.18 (d, *J* = 8 Hz, 2H), 7.02 (d, *J* = 8 Hz, 2H), 4.77 (s, 1H), 2.61 (m, 4H), 2.33 (m, 4H), 2.25 (s, 3H), 2.00 (m, 4H).^{13}C{^{1}H} NMR (100 MHz, $CDCl_3$) δ [ppm] = 196.6, 163.8, 141.5, 135.9, 128.9, 128.3,

117.0, 36.9, 31.2, 27.2, 21.1, 20.3. IR (neat): 2997.17, 2932.32, 1741.35 cm^{-1}. HRMS (ESI-TOF) m/z: $[M + Na]^+$ calcd for $C_{20}H_{20}O_3$: 331.1309; found: 331.1309.

2.8. Appendix I: Copies of ^1H and ^{13}C NMR spectra of representative compounds of NMR spectra

Entry	Figure No.	Data	Page No.
3a	2.9-2.10	^1H and ^{13}C	58
3b	2.11-2.12	^1H and ^{13}C	59
3c	2.13-2.14	^1H and ^{13}C	60
3d	2.15-2.16	^1H and ^{13}C	61
3e	2.17-2.18	^1H and ^{13}C	62
3f	2.19-2.20	^1H and ^{13}C	63
3m	2.21-2.22	^1H and ^{13}C	64
5a	2.23-2.24	^1H and ^{13}C	65
6a	2.25-2.26	^1H and ^{13}C	66
6i	2.27-2.28	^1H and ^{13}C	67

2.9.1 Representative examples of NMR spectra

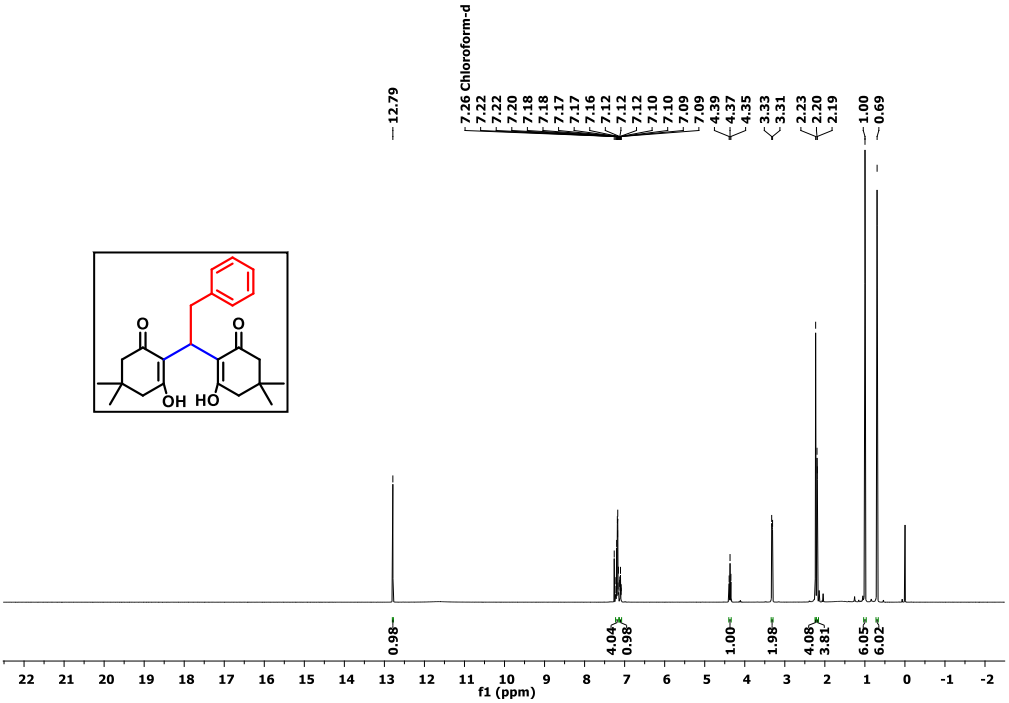


Figure 2.9: ^{1}H NMR of **3a**, 400 MHz, $CDCl_3$

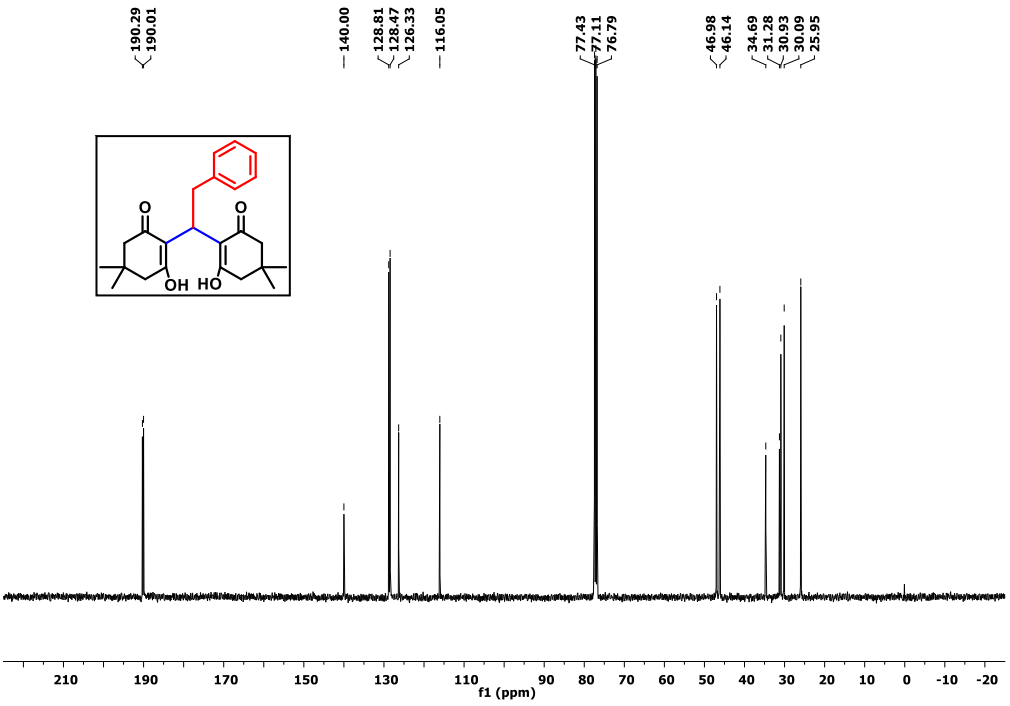


Figure 2.10: ^{13}C {^{1}H} NMR of **3a**, 100 MHz, $CDCl_3$

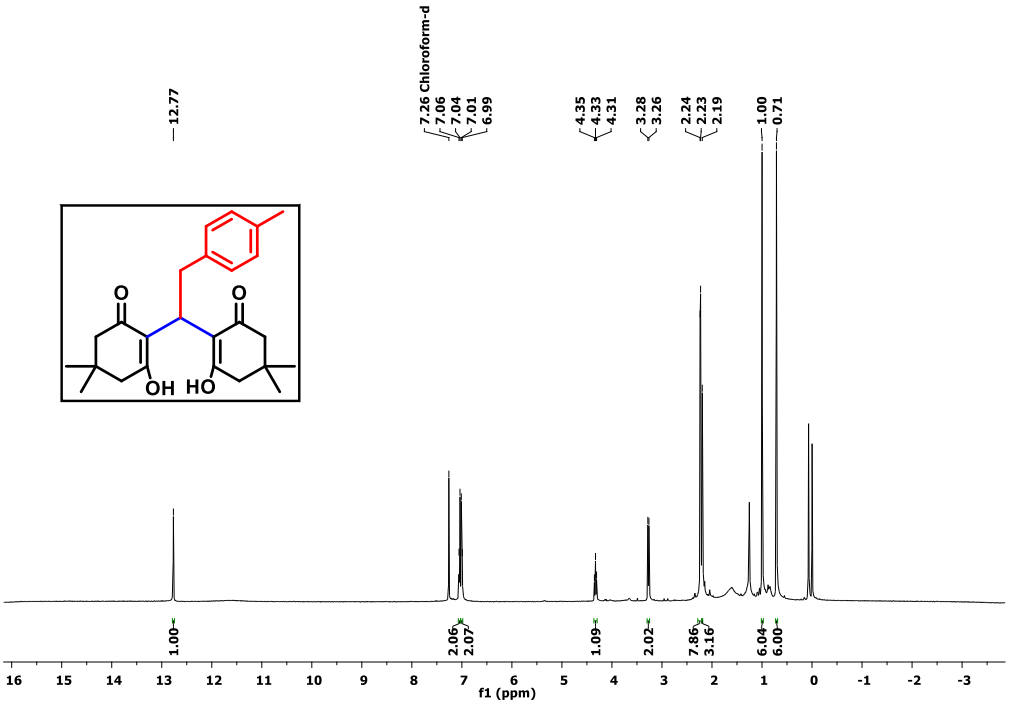


Figure 2.11: ^{1}H NMR of **3b**, 400 MHz, $CDCl_3$

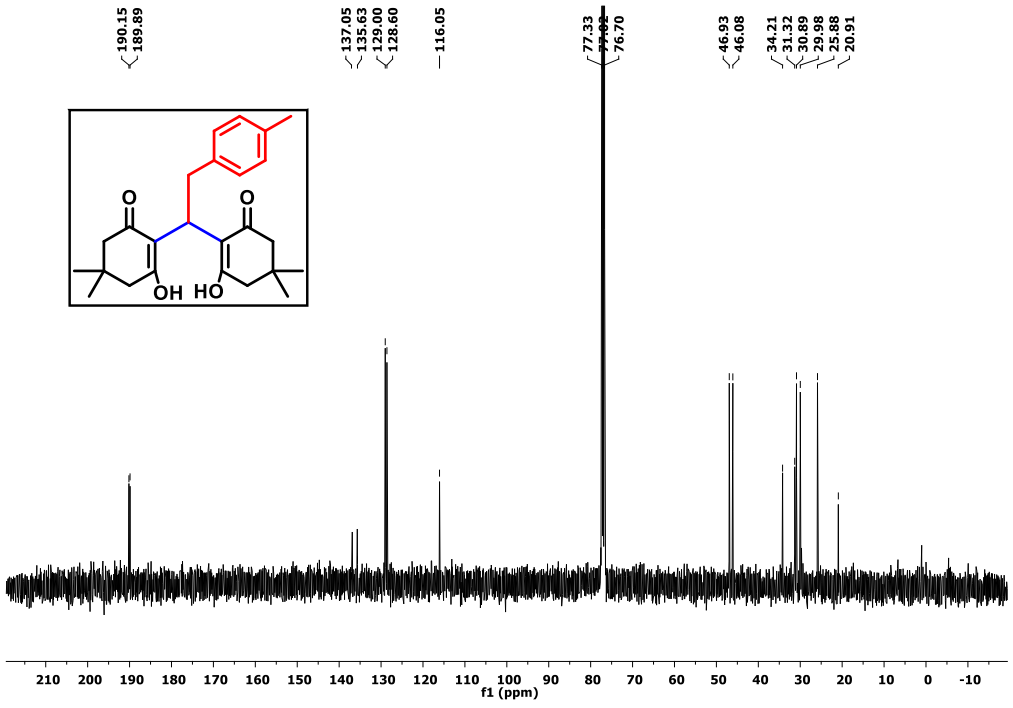


Figure 2.12: ^{13}C $\{^{1}H\}$ NMR of **3b**, 100 MHz, $CDCl_3$

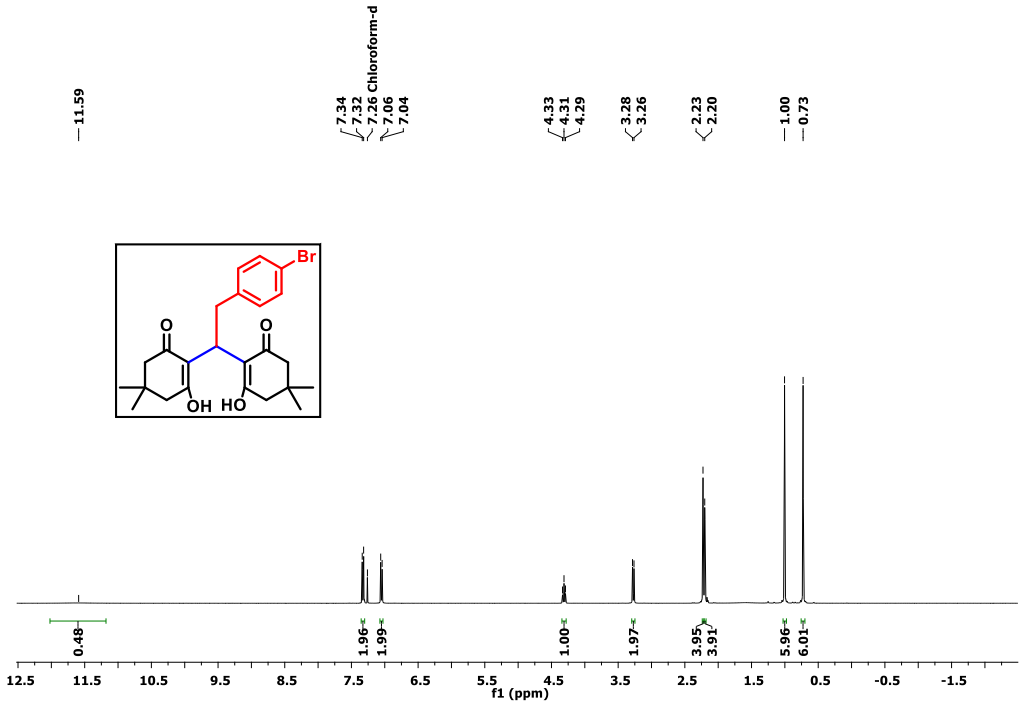


Figure 2.13: ^{1}H NMR of **3c**, 400 MHz, $CDCl_3$

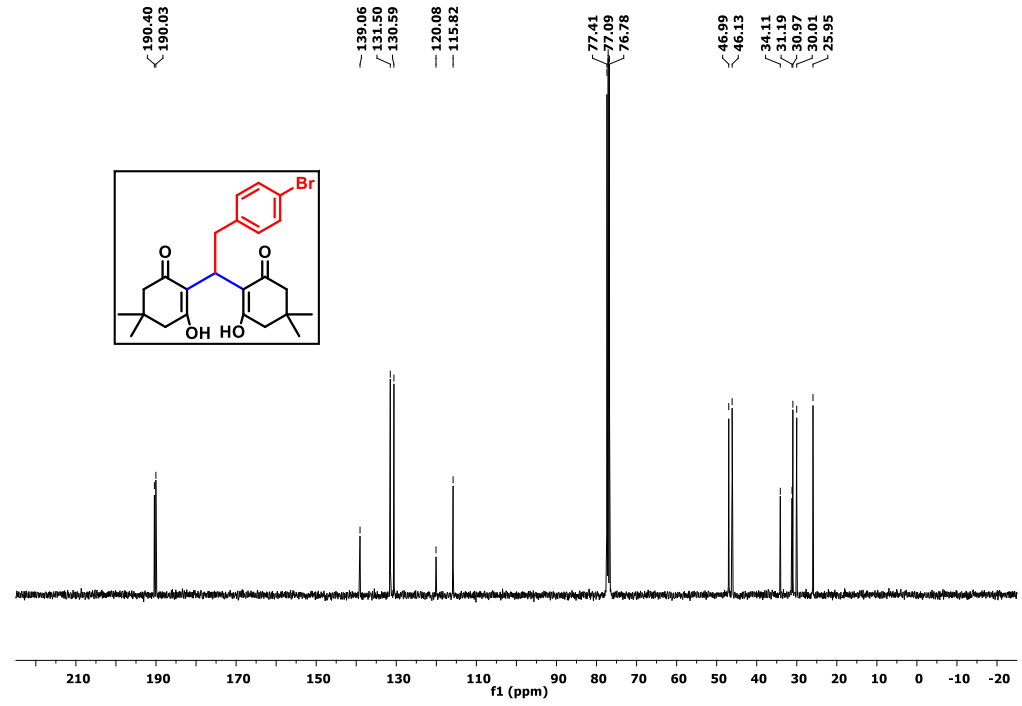
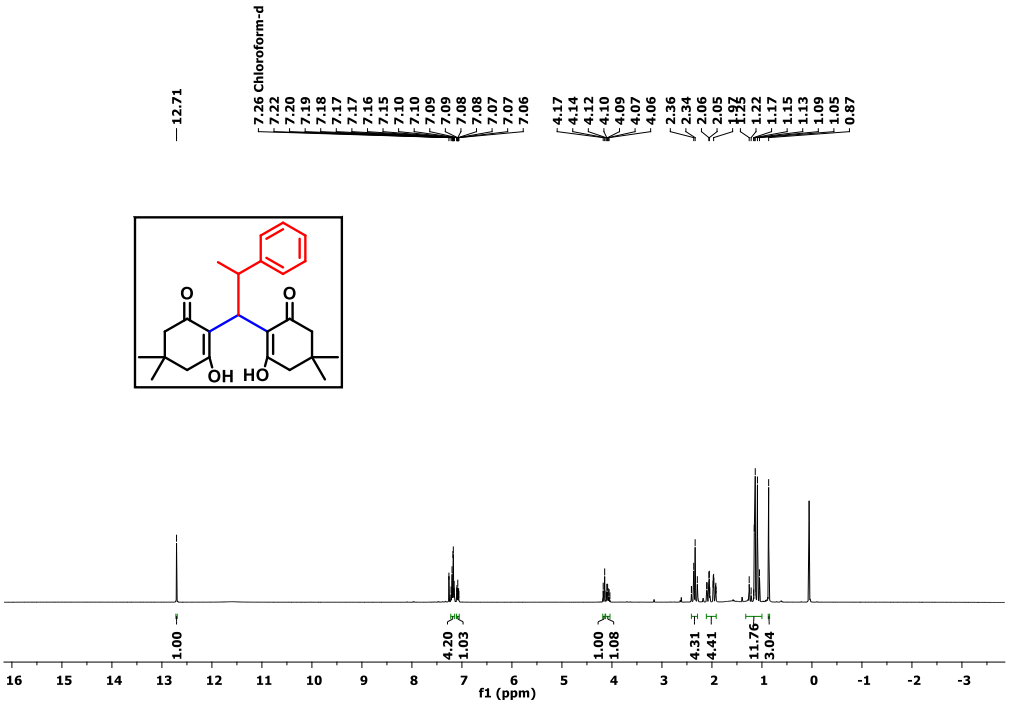


Figure 2.14: ^{13}C $\{^{1}H\}$ NMR of **3c**, 100 MHz, $CDCl_3$



Figuren 2.15: ^{1}H NMR of **3d**, 400 MHz, $CDCl_3$

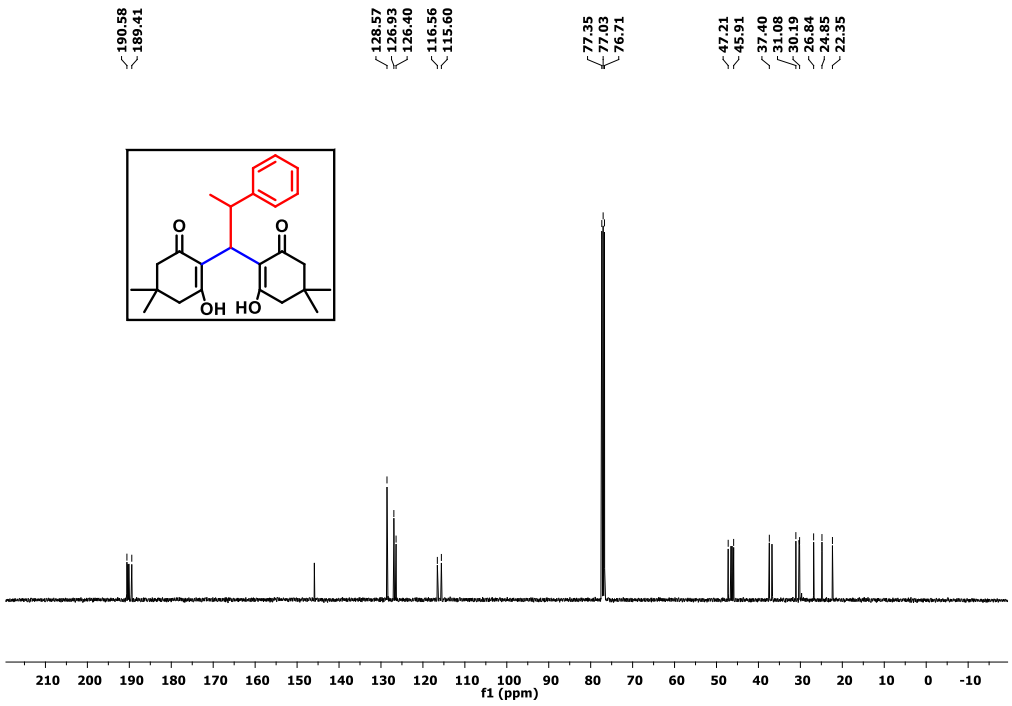


Figure 2.16: ^{13}C {^{1}H} NMR of **3d**, 100 MHz, $CDCl_3$

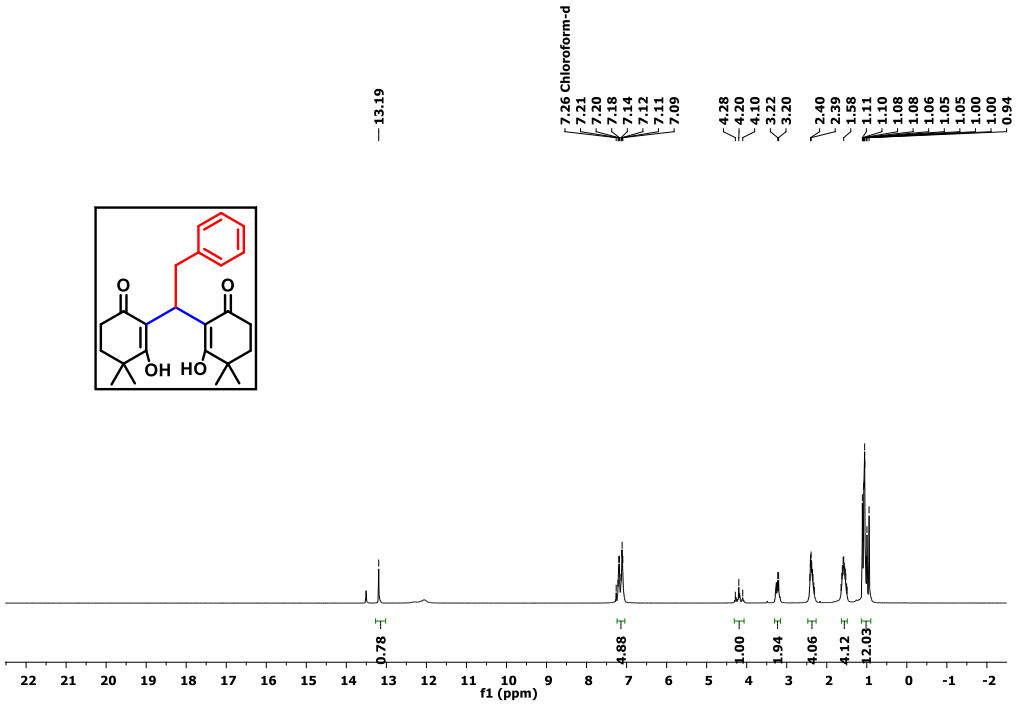


Figure 2.17: ^{1}H NMR of **3e**, 400 MHz, $CDCl_3$

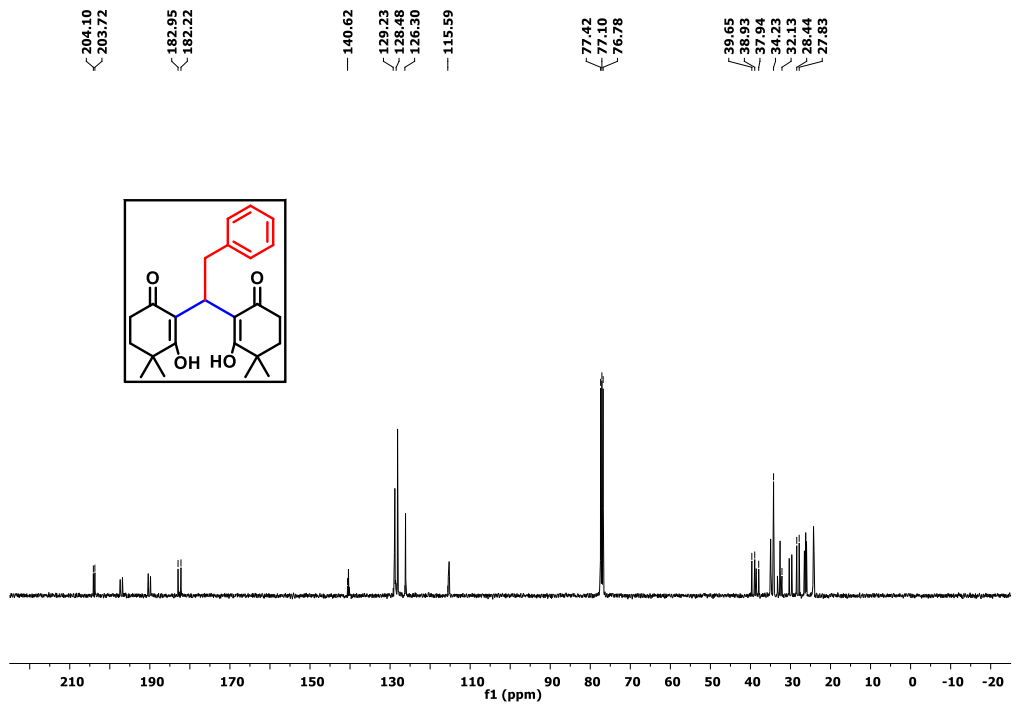


Figure 2.18: ^{13}C $\{^{1}H\}$ NMR of **3e**, 100 MHz, $CDCl_3$

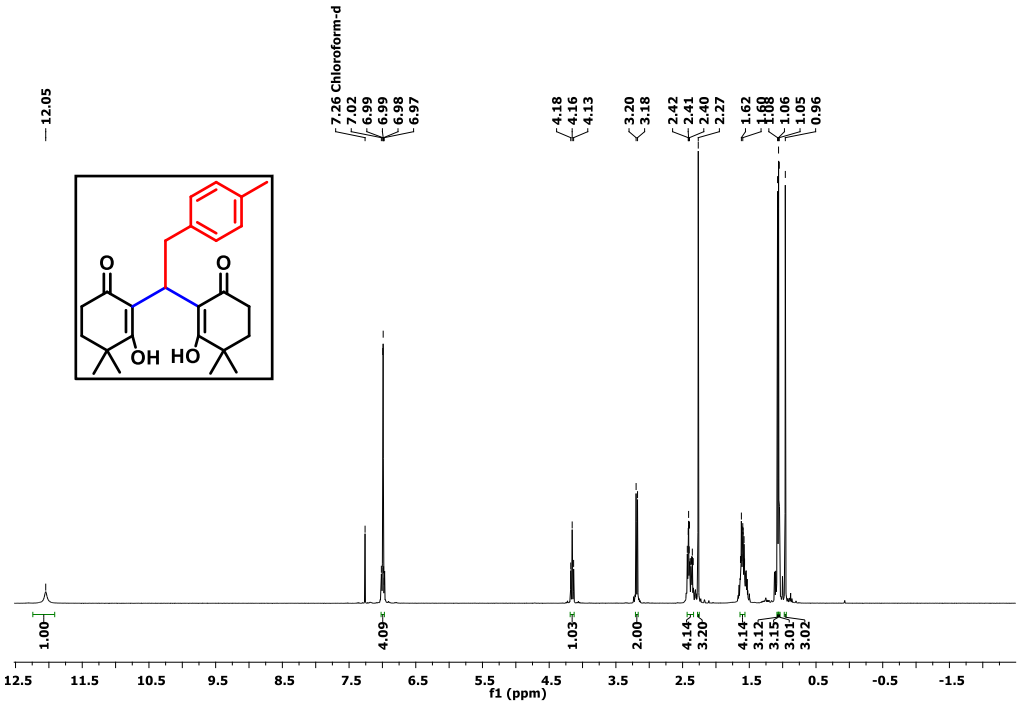


Figure 2.19: ^{1}H NMR of **3f**, 400 MHz, $CDCl_3$

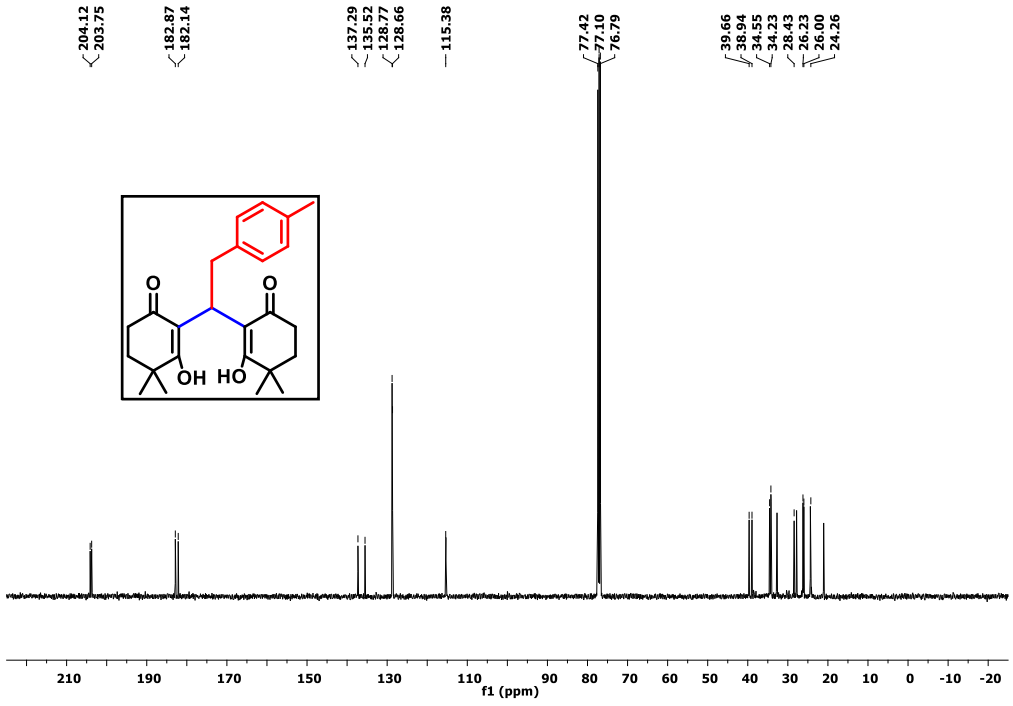


Figure 2.20: ^{13}C $\{^{1}H\}$ NMR of **3f**, 100 MHz, $CDCl_3$

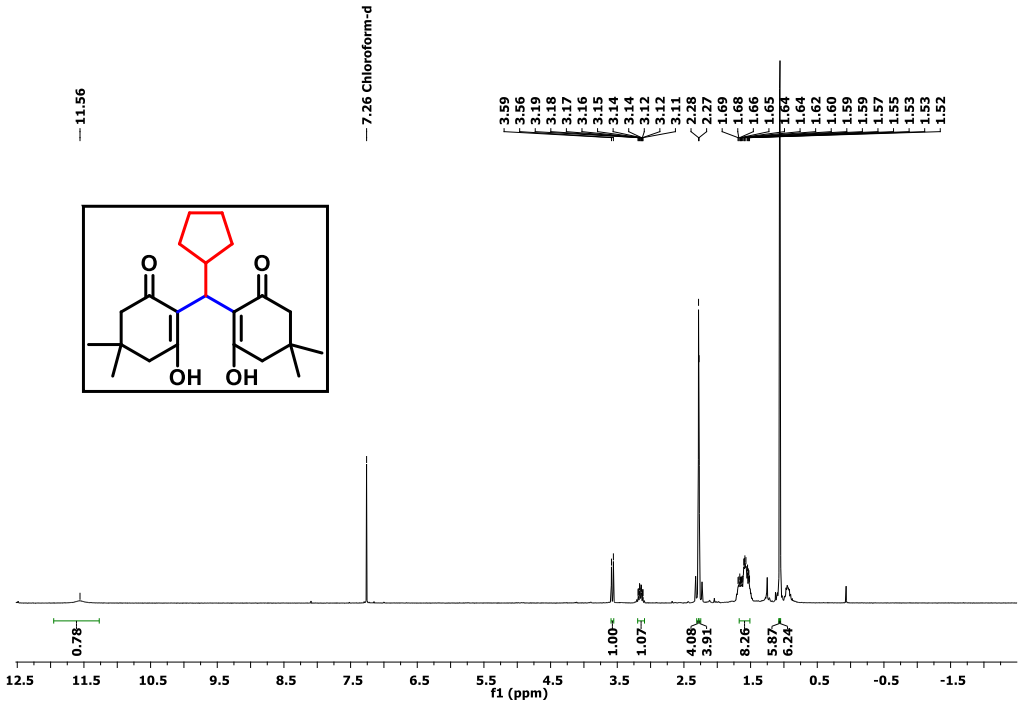


Figure 2.21: ^{1}H NMR of **3m**, 400 MHz, $CDCl_3$

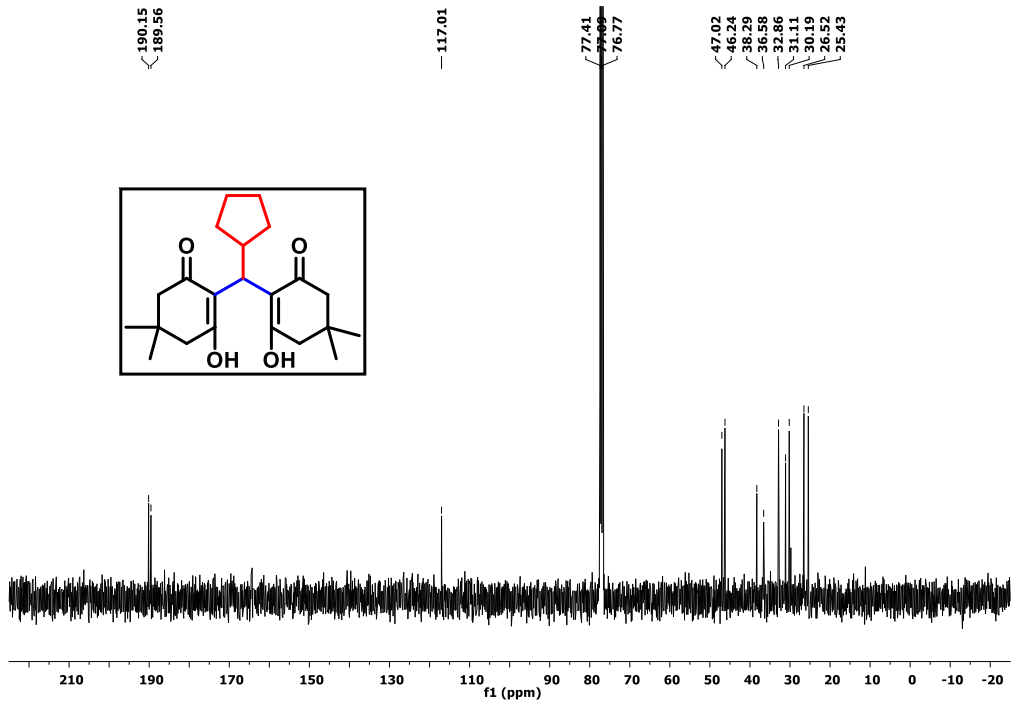


Figure 2.22: ^{13}C $\{^{1}H\}$ NMR of **3m**, 100 MHz, $CDCl_3$

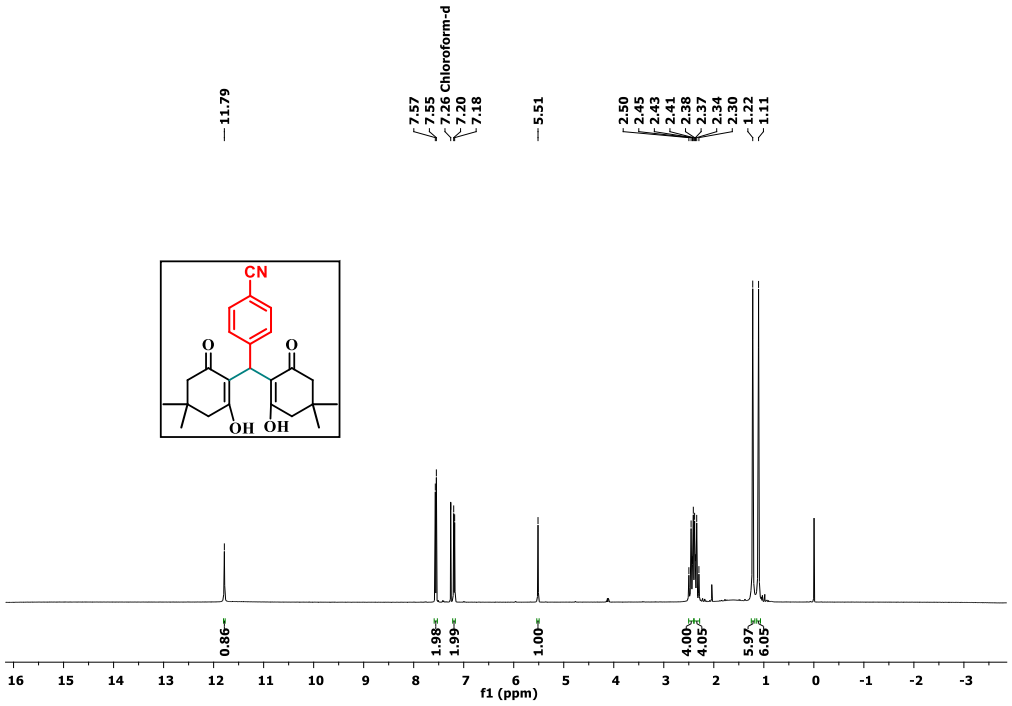


Figure 2.23: ^{1}H NMR of **5a**, 400 MHz, $CDCl_3$

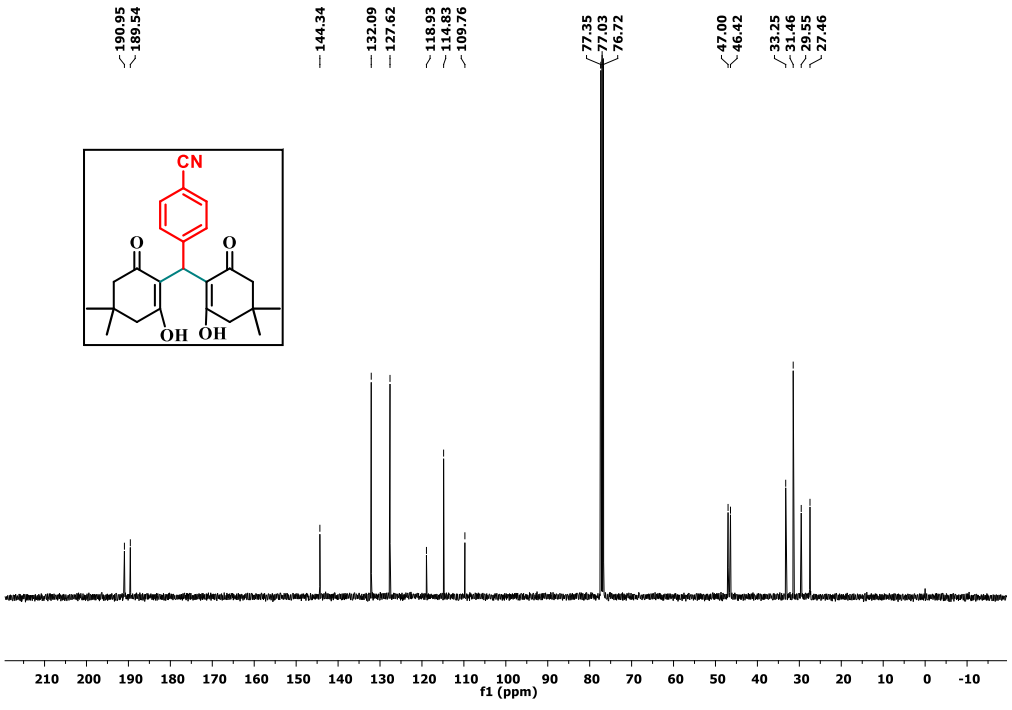


Figure 2.24: ^{13}C {^{1}H} NMR of **5a**, 100 MHz, $CDCl_3$

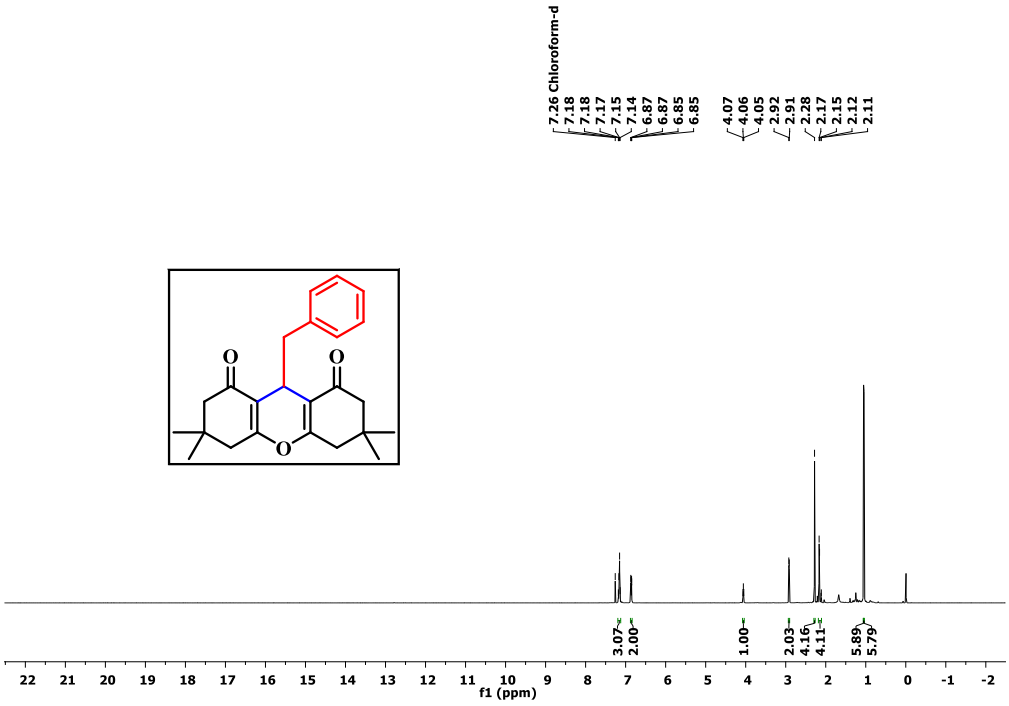


Figure 2.25: ^{1}H NMR of **6a**, 400 MHz, $CDCl_3$

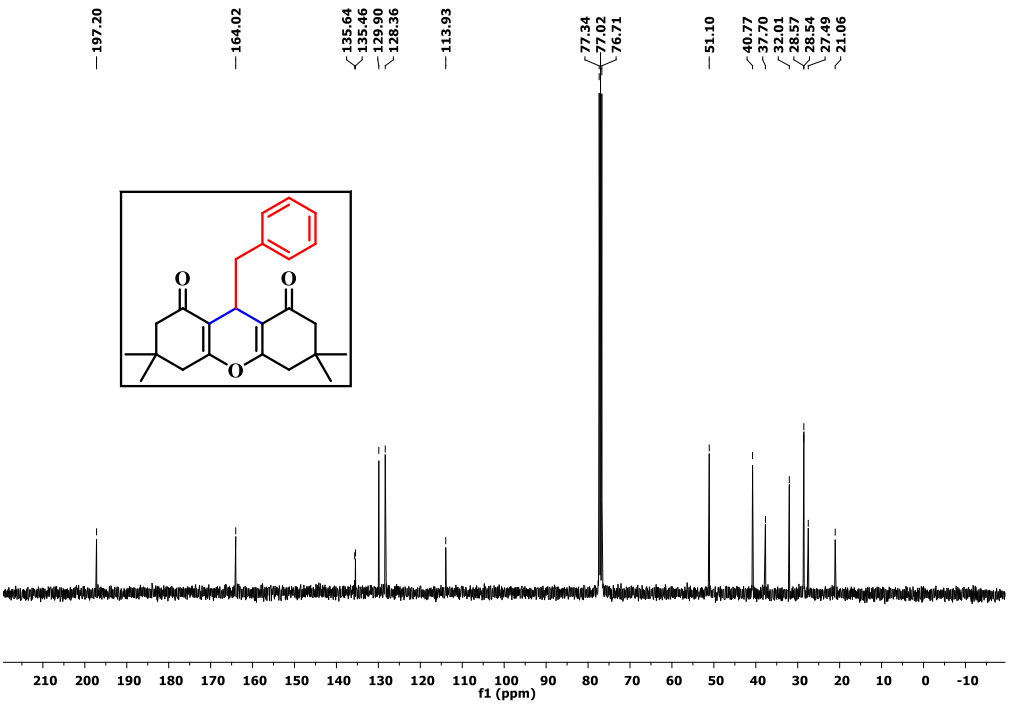


Figure 2.26: ^{13}C $\{^{1}H\}$ NMR of **6a**, 100 MHz, $CDCl_3$

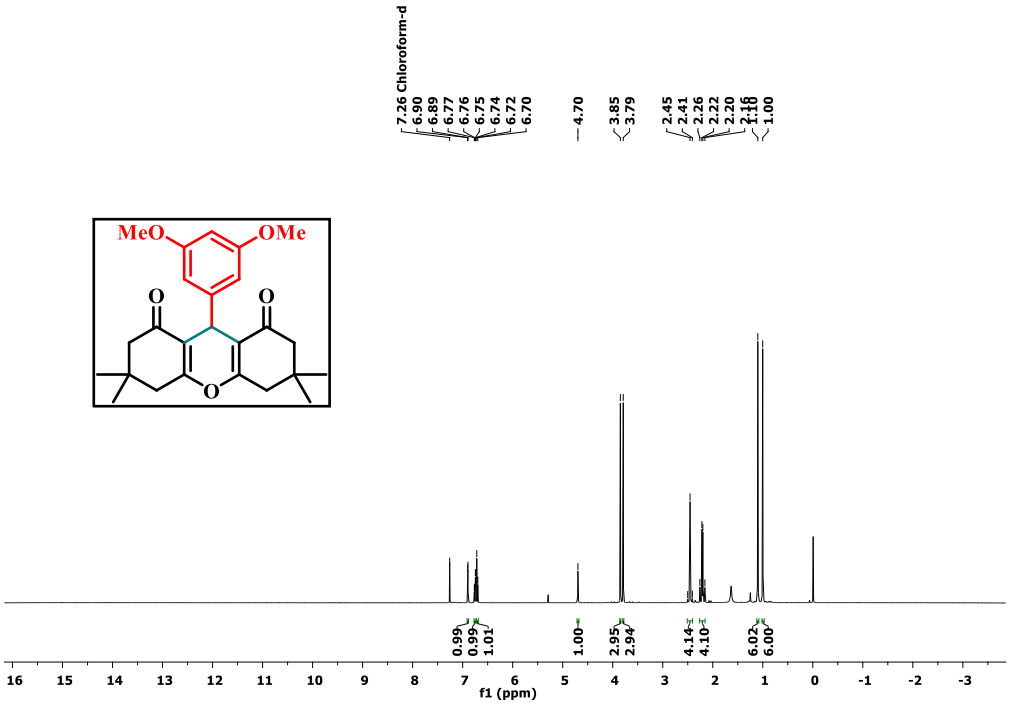


Figure 2.27: ^{1}H NMR of **6i**, 400 MHz, $CDCl_3$

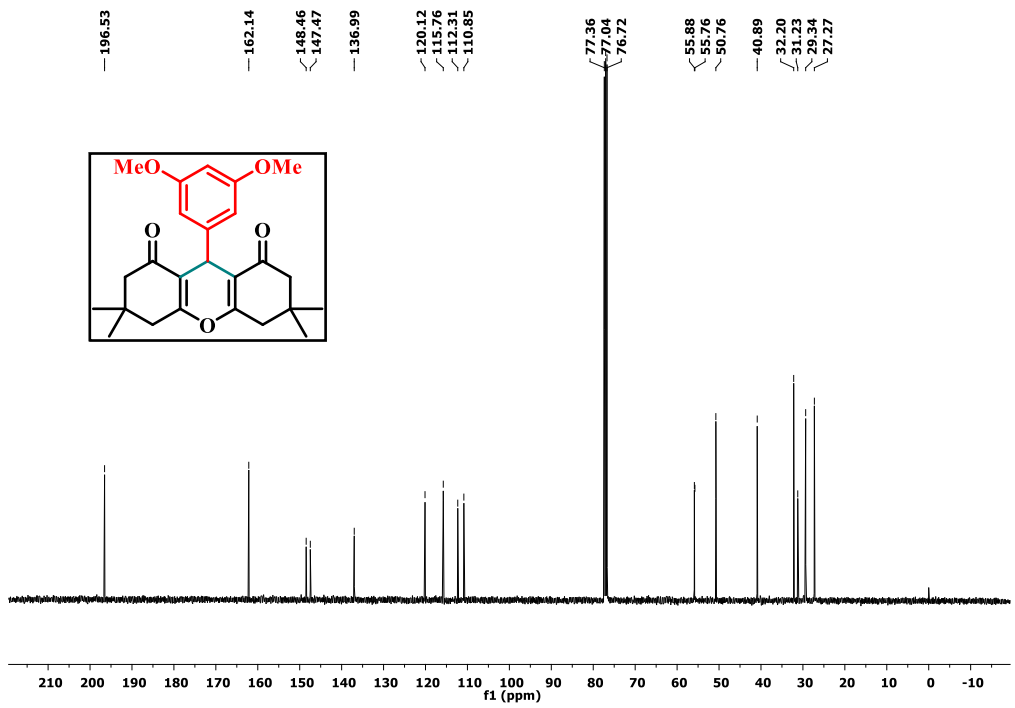


Figure 2.28: ^{13}C $\{^{1}H\}$ NMR of **6i**, 100 MHz, $CDCl_3$

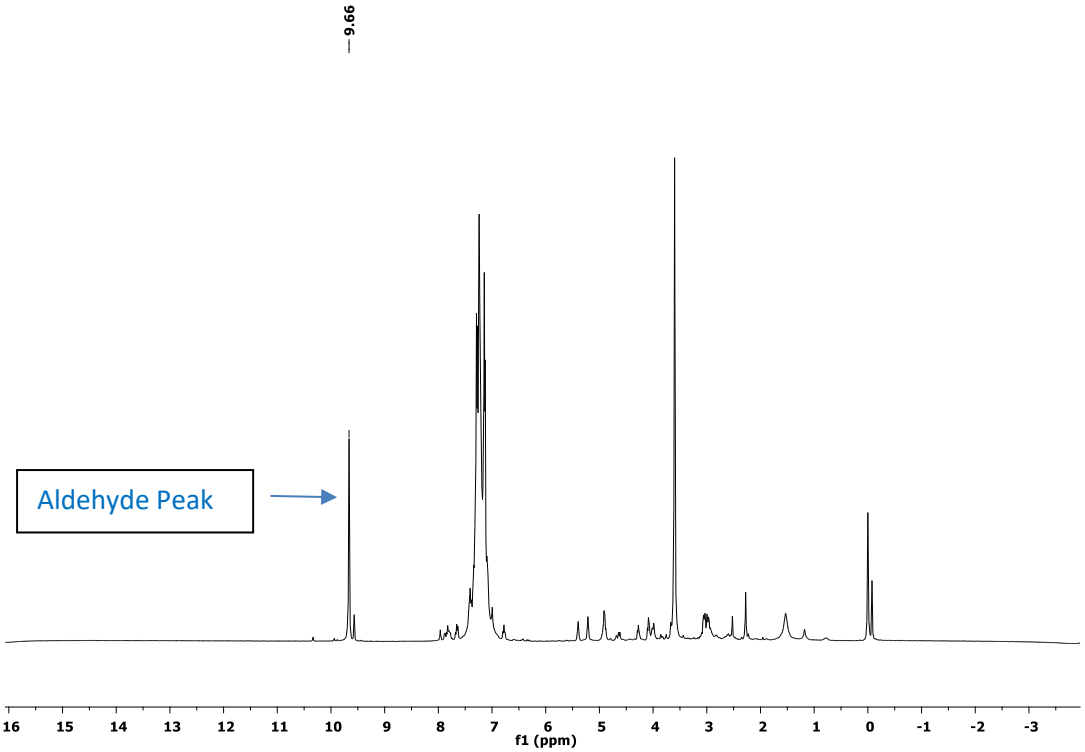


Fig 2.29: ^{1}H NMR of crude reaction mixture of styrene oxide in toluene heated in a sealed tube at 160 ^{o}C

2.8.2. GC-MS data:

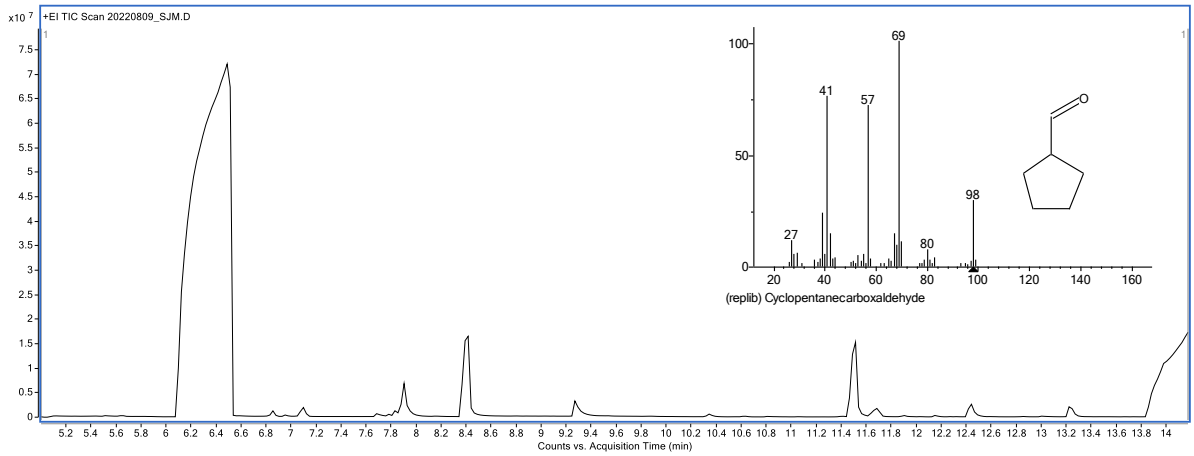


Figure 2.30: GCMS spectrum for the reaction of epoxy cyclohexane with Fe-zeolite

2.8.2. SCXRD data:

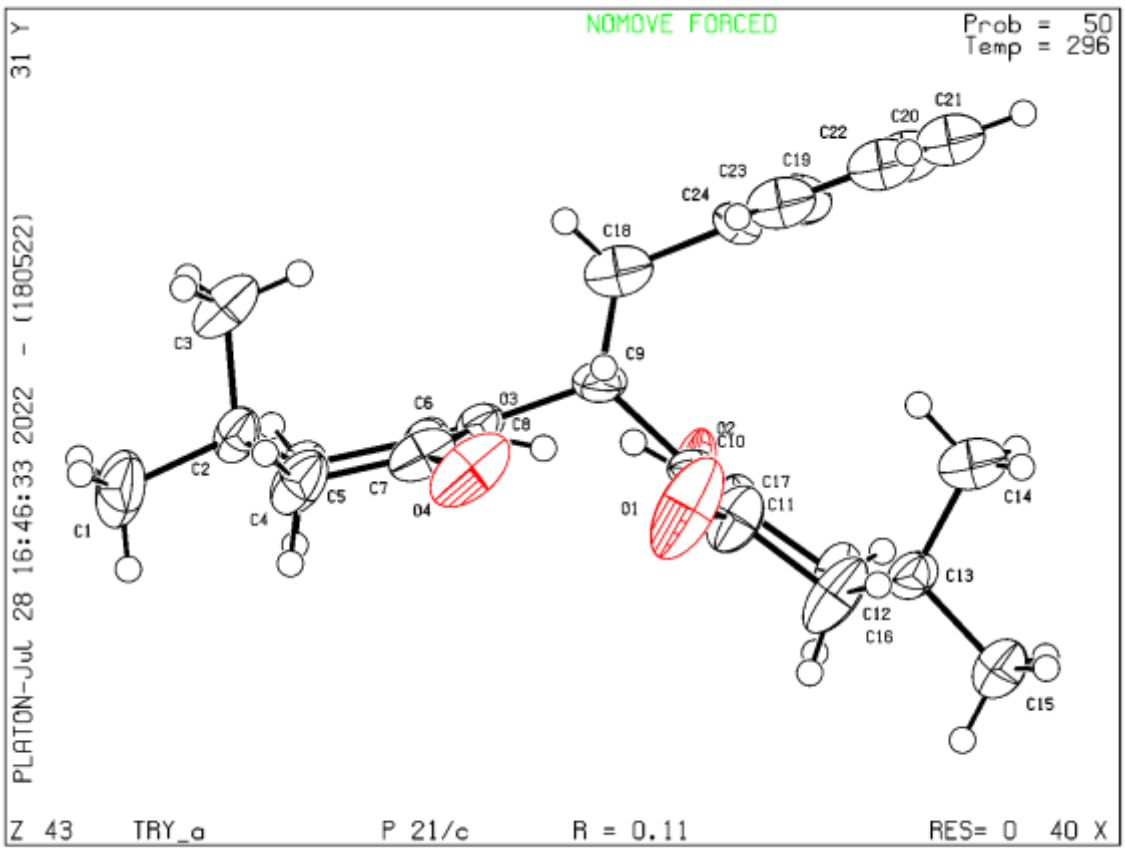


Figure 2.31: ORTEP drawing of **3a** showing thermal ellipsoids at the 50% probability level

2.9. References:

(1) J. Yu, L.-M. Wang, J.-Q. Liu, F.-L. Guo, Y. Liu, N. Jiao, *Green Chem.* **2010**, *12*, 216–219.

(2) Khan, K. M.; Maharvi, G. M.; Khan, M .T. H.; Shaikh, A. J.; Perveen, S.; Begum, S.; Choudhary, M. I. *Bioorg. Med. Chem*., **2006**, *14*, 344-351.

(3) Maharvi, G. M.; Ali, S.; Riaz, N.; Afza, N.; Malik, A.; Ashraf, M.; Iqbal, L.; Lateef, M. *J Enzyme Inhib Med Chem*., **2008**, *23*, 62-69.

(4) Menezesa, A. P. J.; Silvab, M. L.; Pereirab, W. L.; Costaa, G. P.; Hortaa, A. L.; Mendonçac, A. A. S.; Carneiroa, A. C. A.; Souzaa, Novaesc, R. D.; Teixeirab, R. R.; Talvani, A. *J Glob Antimicrob Resist*., **2020**, *22*, 466-476.

(5) Yamamura, T.; Shirasaki, K.; Sato, H.; Nakamura, Y.; Tomiyasu, H.; Satoh, I.; Shiokawa, Y. *J. Phys. Chem. C* **2007**, *111* (50), 18812–18820.

(6) Murthy, Y. L. N.; Mahesh, P.; Devi, B. R.; Durgeswarai, L. K. *Asian J. Chem.* **2014**, *26* (15), 4594–4598.

(7) Rahimifard, M.; Ziarani, G. M.; Badiei, A.; Asadi, S.; Soorki, A. A. *Res. Chem. Intermed.* **2016**, *42*, 3847–3861.

Winter, R. W.; Ignatushchenko, M.; Ogundahunsi, O. A. T.; Cornell, K. A.; Oduola, A. M. J.; Hinrichs, D. J.; Riscoe, M. K. *Antimicrob. Agents Chemother.* **1997**, *41* (7), 1449–1454.

(9) Nisar, M.; Ali, I.; Shah, M. R.; Badshah, A.; Qayum, M.; Khan, H.; Khand, I.; Ali, S. *RSC Adv.* **2013**, *3*, 21753–21758.

(10) Cidade, H.; Rocha, V.; Palmeira, A.; Marques, C.; Tiritan, M. E.; Ferreira, H.; Lobo, J. S.; Almeida, I. F.; Sousa, M. E.; Pinto, M. *Arab. J. Chem*. **2020**, *13*, 17–26.

(11) Kaya, M.; Basar, E.; Colak, F. *Med. Chem. Res.* **2011**, *20*, 1214–1219.

(12) Mandlimath, T. R.; Umamahesh, B; Sathiyanarayanan, K. *J. Mol. Catal. A: Chem*., **2014**, *391*, 198-207.

(13) Schneider, E. M.; Zeltner, M.; Kra¨nzlin, N.; Grassa, R. N.; Stark, W. J. *Chem. Commun*., **2015**, *51*, 10695-10698.

(14) Fallah, A.; Tajbakhsh, M.; Vahedi, H.; Bekhradnia, A. *Res Chem Intermed.,* **2017**, *43*, 29–43.

(15) Hasanzadeh Banakar, S.; Dekamin, M. G.; Yaghoubi, A. *New J. Chem.* **2018**, *42*, 14246–14262.

(16) Matloubi Moghaddam, F.; Aghili, S.; Daneshfar, M.; Moghimi, H.; Daneshfar, Z. *Res. Chem. Intermed.* **2023**, *49* (4), 1507–1543.

(17) Gupta, P.; Singh, B.; Dhama, M.; Pani, B.; Mozumdar, S. *New J. Chem.* **2024**, *48* (4), 1200–1212.

(18) Khodaei, M. M.; Khosropour, A. R.; Moghannian, H. *Chem. Pap.* **2008**, *62* (6), 583–589.

(19) Chibale, K.; Visser, M.; Schalkwyk, D. V.; Smith, P. J.; Saravanamuthu, A. H. *Catal. Sci. Technol.* **2012**, *2*, 2300–2305.

(20) Azizi, N.; Khodaei, M. M.; Esmailpour, S. C. R. *Chimie* **2013**, *16* (11), 997–1001.

(21) Horváth, I. T. *Chem. Rev.* **2018**, *118*, 2, 369–371.

(22) Anastas, P. T.; Eghbali, N. *Chem. Soc. Rev. 2010*, 39 (1), 301–312.

(23) Li, C.-J.; Trost, B. M. *Proc. Natl. Acad. Sci. U.S.A*. **2008**, *105* (36), 13197–13202.

(24) Sheldon, R. A. *Green Chem*. **2016**, 18, 3180–3183.

(25) Cioc, R. C.; Ruijter, E.; Orru, R. V.A. *Green Chem*., **2014**, *16*, 2958−2975.

(26) Friend, C. M.; Xu, B. *Acc. Chem. Res.,* **2017**, *50*, 3, 517–521.

(27) Hülsey, M. J.; Lim, C. W.; Yan, N. *Chem. Sci*., **2020**, *11*, 1456-1468.

(28) Moliner, M. *Dalton Trans.,* **2014**, *43*, 4197-4208.

(29) Primo, A.; Garcia, H. *Chem. Soc. Rev*., **2014**,*43*, 7548-7561.

(30) Hölderich, W.; Hesse, M.; Na¨umann, F. *Angew. Chem., Int. Ed*.**1988**, *27*, 226-246.

(31) Sheldon, R. A.; Elings, J. A.; Downing, R. S. *J. Mol. Catal. A*., **1998**, *134*, 129-135.

(32) Agalave, S. G.; Chaudhari, M. B.; Bisht, G. S.; Gnanaprakasam, B. *ACS Sustainable Chem. Eng*., **2018**, *6*, 12845−12854.

(33) Tiddens, M. R.; Gebbink, R. J. M. K.; Otte, M. *Org. Lett*., **2016**, *18*, 15, 3714–3717.

(34) Zhang, Y.; Hu, B.; Chen, Y.; Wang, Z. *Chem.-Eur. J*. **2024**, *30* ,59, No. e202402469 .

(35) Aziridines and Epoxides in Organic Synthesis; A. K. Yudin, Ed.;Wiley-VCH: Weinheim, 2006.

(36) Magre, M.; Paffenholz, E.; Cavallo, L.; Rueping, M. *J. Am. Chem. Soc*., **2020**, *142*, 33, 14286–14294.

(37) Zhao, Y.; Weix, D. J. *J. Am. Chem. Soc*., **2014**, *136*, 48−51.

(38) Aida, K.; Hirao, M.; Funabashi, A.; Sugimura, N.; Ota, E.; Yamaguchi, J. *Chem*., **2022**, *8*, 1762–1774.

(39) Wiles, C.; Watts, P. *Green Chem*., **2012**, *14*, 38-54.

(40) Plutschack, M. B.; Pieber, B.; Gilmore, K.; Seeberger, P. H. *Chem. Rev*. **2017**, *117* (18), 11796–11893.

(41) Webb, D.; Jamison, T. F. *Chem. Sci.* **2010**, *1*, 675–680.

(42) Ley, S. V.; Fitzpatrick, D. E.; Ingham, R. J.; Myers, R. M. *Angew. Chem., Int. Ed.* **2015**, *54* (11), 3449–3464.

(43) López, S.; Cortés-Borda, D.; Alcázar, J. *Green Chem*. **2021**, *23* (18), 6697–6713.

(44) Mo, Y.; Jensen, K. F. *React. Chem. Eng*. **2016**, *1*, 55–67.

(45) Rawat, M.; Rawat, D.S. *ACS Sustainable Chem. Eng*. **2022**, *10*, 30, 10014-10023.

(46) Capriati, V.; Florio, S.; Perna, F. M.; Salomone, A.; Abbotto, A.; Amedjkouh, M.; Nilsson Lill, S. O. *Chem. Eur. J*. **2009**, *15*, 7958–7979

(47) Tian, Y.; Jürgens, E.; Kunz, D. *Chem. Commun*. **2018**, *54*, 11340–11343.

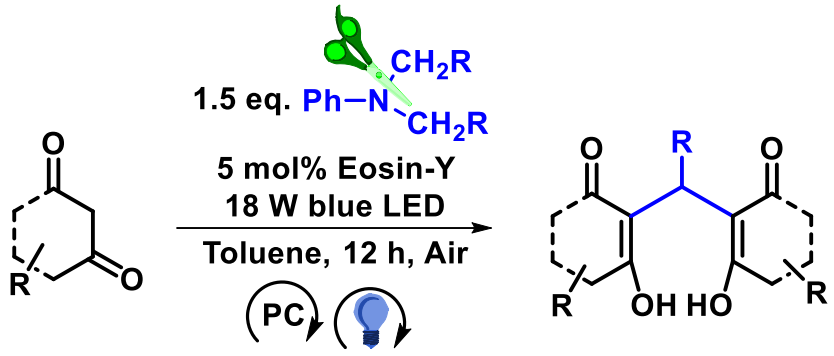
Chapter 3

Visible Light Mediated Organophotoredox Catalyzed Synthesis of Tetraketones using Tertiary Amines as Alkyl Synthon

Visible Light Mediated Organophotoredox Catalyzed Synthesis of Tetraketones using Tertiary Amines as Alkyl Synthon

3.1. Abstract

In this chapter, a mild and efficient method for the synthesis of bioactive tetraketones has been described using Eosin-Y as a photocatalyst under 18W blue LED irradiation. The reaction employs cyclic 1,3-diketones and tertiary amines as alkyl synthons, using air as a green oxidant and avoiding previously harsh conditions such as high temperatures. In this process, diverse tertiary amines undergo reductive quenching of the excited Eosin-Y catalyst to generate iminium ions, which are subsequently attacked by cyclic 1,3-diketones to afford tetraketones. The method demonstrates broad substrate scope, with 31 examples yielding up to 76%. Notably, the reaction also proceeds efficiently under solar light in the presence of Eosin-Y, as demonstrated by several representative examples.



3.2. Introduction

Light offers a non-hazardous and environmentally friendly energy source for driving chemical reactions, as it eliminates the need for high temperatures or harsh conditions typically required in thermal processes.[1-2] Through the use of redox-active, light-absorbing species, photocatalysis enables a wide range of challenging transformations, particularly in medicinal chemistry and natural product synthesis.[3-5] In addition to its broad synthetic utility, photoredox catalysis aligns well with several key principles of green chemistry.[6]

Tetraketones derived from cyclic 1,3-diketones have garnered considerable interest among synthetic chemists due to their broad pharmaceutical potential (Figure 3.1). As polyoxygenated compounds, tetraketones exhibit promising tyrosinase inhibitory activity.[7] Lipoxygenase products in mammalian cells are implicated in various disorders, including inflammation, tumor angiogenesis, and

bronchial asthma.[8-10] Notably, tetraketones have demonstrated significant lipoxygenase inhibitory properties.[11]

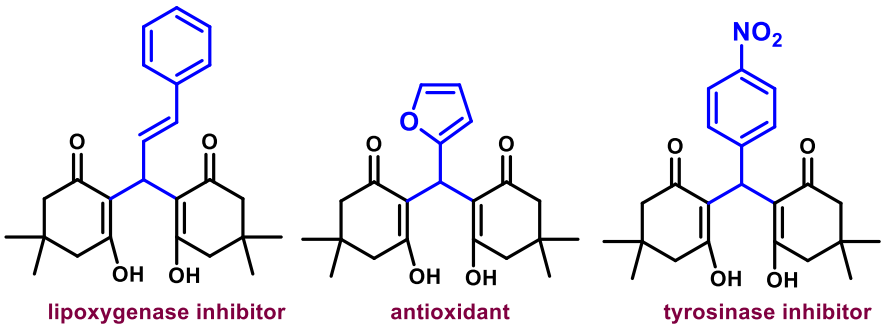


Figure 3.1: Representative examples of bioactive tetraketones.

Additionally, the pronounced antioxidant activity of tetraketones makes them effective therapeutic agents.[11] Owing to their significant biological relevance, tetraketones have attracted widespread interest from chemists and pharmacologists in both academia and industry. Numerous reports are available for the synthesis of tetraketones via the direct condensation of aldehydes with cyclic 1,3-diketones, employing a variety of homogeneous and heterogeneous catalysts. Catalytic systems such as meglumine, PPA-SiO_2, Pd nanoparticles, $Na_2CaP_2O_7$, and biofabricated ZnO nanoparticles have been explored for this purpose.[12-16] However, many of these methods require harsh reaction conditions, including high temperatures, toxic metal-based catalysts, and costly or specially engineered catalytic systems.[17-19] Consequently, there is a pressing need for the development of milder and more sustainable approaches for tetraketone synthesis.

Tertiary amines are most frequently used as base in organic synthesis.[20] But in photoredox catalysis tertiary amines serve for multiple purposes including as electron donor, for α-C-H functionalization, as alkyl synthon and as a source of dialkyl amine group (Figure 3.2). The examples of all types have been provided.

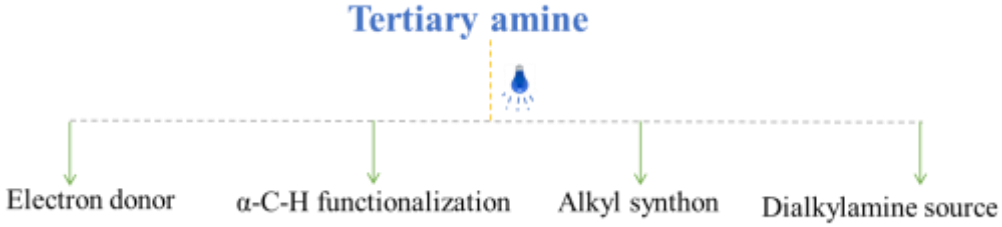
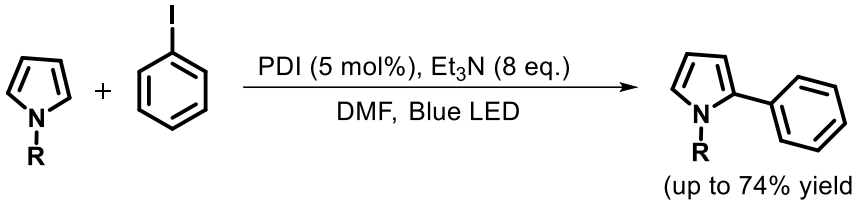


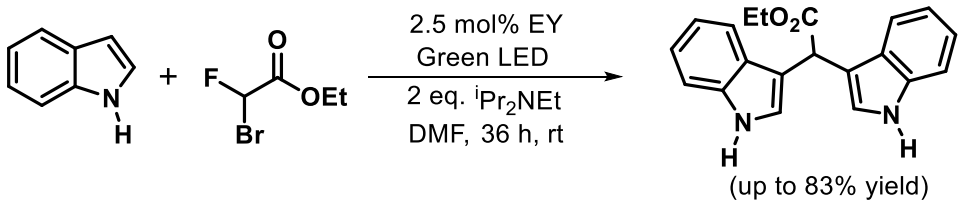
Figure 3.2: Representative examples of bioactive tetraketones.

Koneig *et al.* demonstrated the use of triethyl amine as sacrificial electron donor for initiating reductive quenching cycle of PDI photocatalyst for cross-coupling reaction (Scheme 3.1).[21]



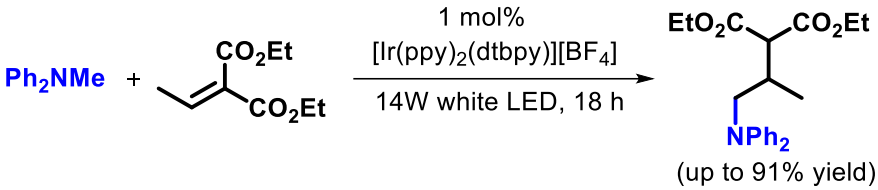
Scheme 3.1: Et_3N as sacrificial electron donor in photoredox catalysis

Singh *et al.* later employed DIPEA as an effective electron donor to initiate photoredox catalyst cycle of Eosin Y under green LED irradiation (Scheme 3.2).[22]



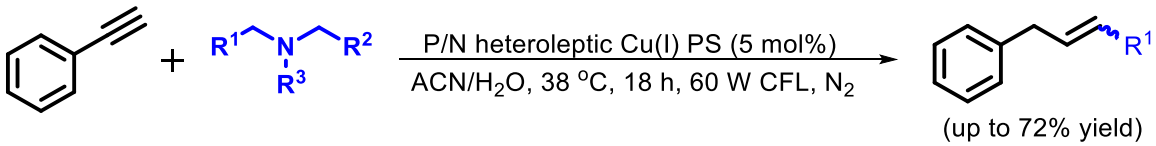
Scheme 3.2: DIPEA as sacrificial electron donor in Eosin Y catalyst cycle

A mechanistically distinct approach was introduced by Nishibayashi *et al.* through an iridium-based photocatalytic strategy for α-C–H bond functionalization of tertiary amines, leveraging single-electron transfer (SET) processes to activate the α-position. (Scheme 3.3).[23]



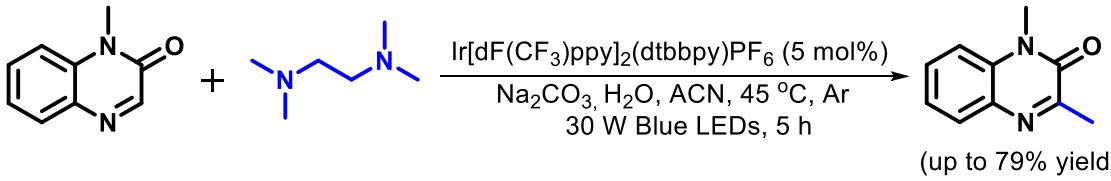
Scheme 3.3: Ir photoredox catalyzed α C-H functionalization of tertiary amine

In earlier investigations, Liu *et al.* utilized tertiary amines as alkyl radical progenitors for the hydroalkylation of alkynes under photoredox conditions, highlighting their utility as latent alkylating agents. (Scheme 3.4).[24]



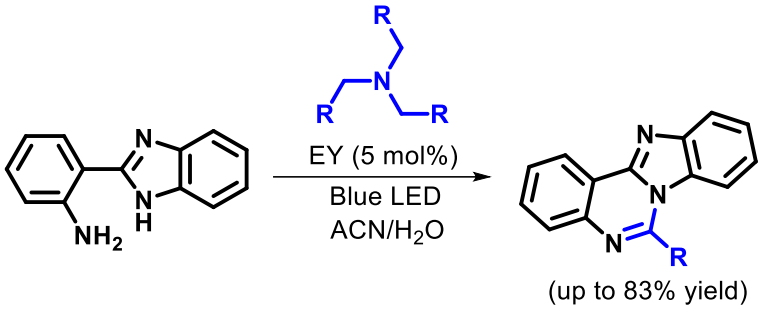
Scheme 3.4: Cu(I) photosensitized reaction of tertiary amines as alkyl source

More recently, Yang *et al.* demonstrated the use of tetramethylethylenediamine (TMEDA) as a methyl surrogate for the direct C–H methylation of heterocycles via iridium-catalyzed photoredox pathways under inert atmosphere, showcasing selective C(sp^2)–H functionalization (Scheme 3.5).[25]



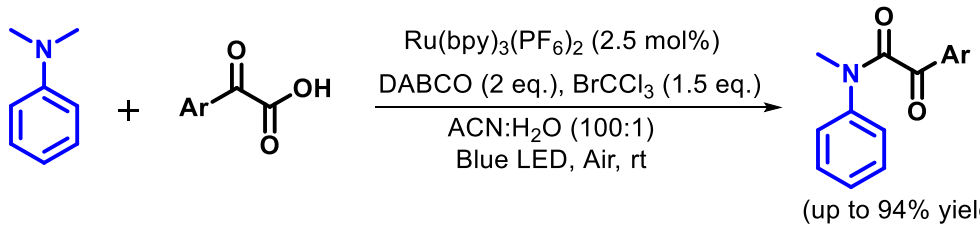
Scheme 3.5: Ir-photocatalyzed reaction of TMEDA as alkyl synthon

Parallel to these advances, P/N-ligated heteroleptic copper(I) complexes have been exploited as photosensitizers in C–H bond functionalization reactions by Senadi *et al*., offering an earth-abundant alternative to noble metal-based systems (Scheme 3.6).[26]



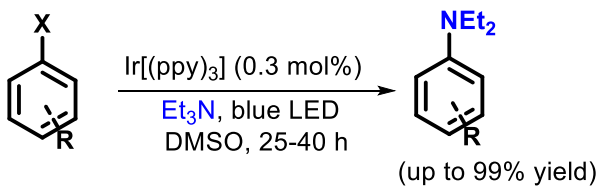
Scheme 3.6 Eosin Y catalyzed reaction of trialkyl amines as alkyl synthon

Jana *et al*. have described a divergent reactivity wherein tertiary amines undergo photoredox-mediated bond scission to generate dialkylamine moieties, expanding the chemical space accessible via amine feedstocks (Scheme 3.7).[27]



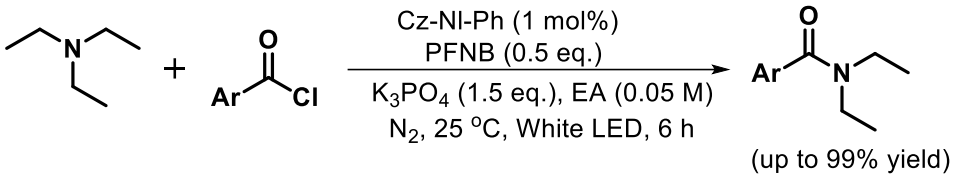
Scheme 3.7: Ru-photocatalyzed reaction of tertiary amines as the dialkyl amine source

Dilman *et al.* introduced a photocatalytic ipso-substitution protocol wherein haloarenes are converted to dialkylarylamines using iridium catalysis, thus achieving C–N bond formation via radical–polar crossover mechanisms (Scheme 3.8).[28]



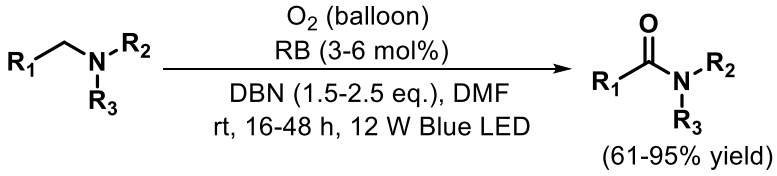
Scheme 3.8: Ir-photocatalyzed reaction of triethyl amine as source of dialkyl amine

In a mechanistically analogous transformation, Xo *et al.* exploited tertiary amines as precursors to dialkylamines through photocatalytic C–N bond cleavage under visible-light irradiation (Scheme 3.9).[29]



Scheme 3.9: Organophotoredox catalyzed generation of dialkyl amine from tertiary amine

Complementing these studies, Das *et al.* disclosed an aerobic photoredox methodology for α-oxygenation of tertiary amines, proceeding under molecular oxygen and light-driven conditions, thereby providing access to functionalized α-amino carbonyl scaffolds. (Scheme 3.10).[30]



Scheme 3.10: Rose Bengal photocatalyzed α oxygenation of tertiary amine

Being inspired by all these reports and other literature precedents, we hypothesized to employ tertiary amines as alkyl synthon under photoredox catalysis.[31-34] Herein, we report a photoredox-catalyzed strategy employing both aromatic and aliphatic tertiary amines as alkyl group donors for the synthesis of bioactive tetraketones. The existing methods use specially designed catalyst, harsh conditions to achieve tetraketones and also the direct use of aldehyde facilitates competitive aldol condensation reaction. Our method offers several notable advantages: it utilizes an inexpensive, metal-free organophotoredox catalyst; employs atmospheric oxygen as a green oxidant; and proceeds under visible light, eliminating the need for elevated temperatures. Collectively, these features render the protocol environmentally benign, cost-effective and sustainable.[35-37]

3.3. Results and discussion

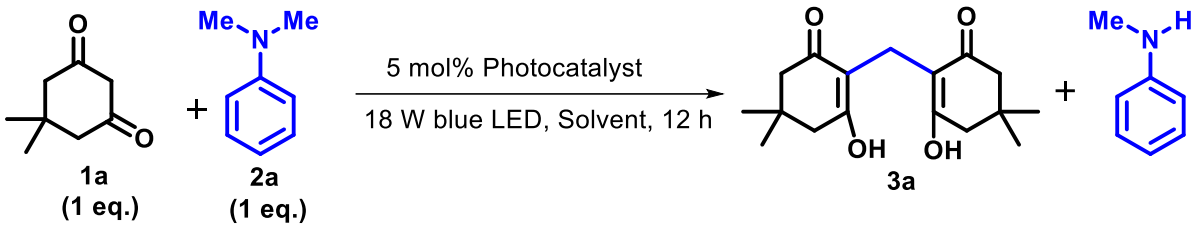
In this chapter, we have developed Eosin Y photoredox catalyzed method for the synthesis of tetraketones using tertiary amines as the source of alkyl motif. The protocol appears to be an eco-

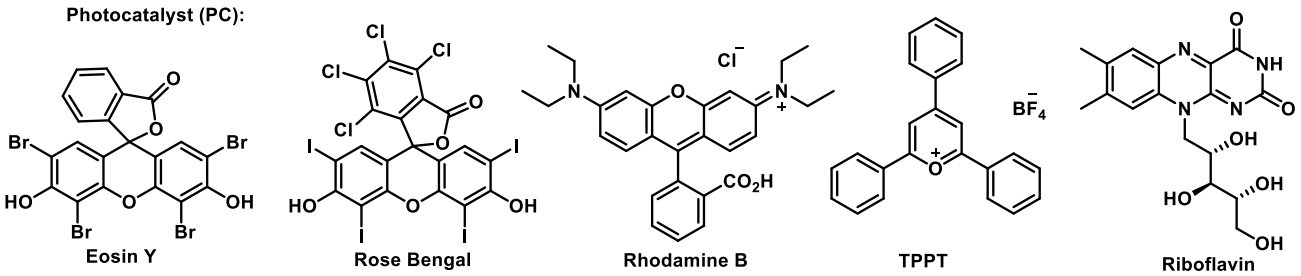
friendly alternative method to conventional condensation reaction between diketones and aldehydes and avoids use of high temperature and light promotes the reaction.

3.3.1. Optimization studies

We began our optimization studies using dimedone and *N*, *N*-dimethylaniline as model substrates. Initially, various organophotoredox catalysts were screened in acetonitrile (Table 3.1, Entries 1–5), among which Eosin Y delivered the highest yield of product **3a**.

[a]Table 3.1: Optimization table

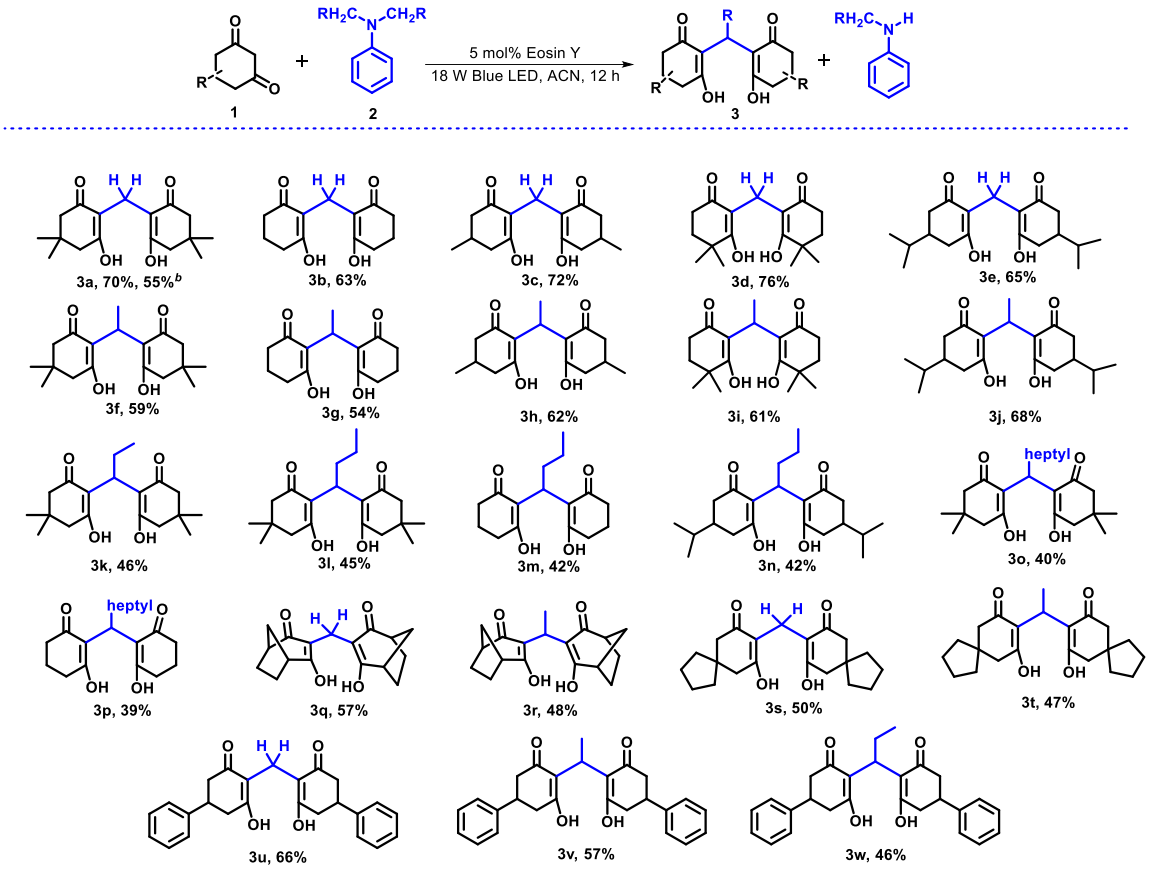




Entry	Photocatalyst (5 mol%)	Time (h)	Solvent (h)	Yield (%)
1	Rhodamine B	12	ACN	11
2	Rose Bengal	12	ACN	10
3	Riboflavin	12	ACN	25
4	TPPT	12	ACN	26
5	Eosin Y	12	ACN	41
6	Eosin Y	12	MeOH	37
7	Eosin Y	12	Water	23
8	Eosin Y	12	DMF	38
9	Eosin Y	12	1,4-dioxane	57
10	Eosin Y	12	Toluene	61
11	Eosin Y	12	^{t}BuOH	22
12	Eosin Y	12	DMC	28
13[b]	Eosin Y	12	Toluene	70
14[c]	Eosin Y	12	Toluene	70

[a]**Reaction conditions**: **1a** (1 equiv.), **2a** (1 equiv.) and 5 mol% photocatalyst were stirred in 2 mL solvents in open air under 18 W blue LED irradiation. [b]**2a** (1.5 equiv.) was used. [c]**2a** (2 equiv.) was used. All the yields mentioned are isolated yields.

(41%). Subsequently, different solvents were investigated (Table 3.1, Entries 6–13), and toluene was identified as the optimal solvent, providing the highest yield (Table 3.1, Entry 9). Using 1.5 equivalents of the tertiary amine further improved the yield to 70%. Neither increasing the amine loading nor extending the reaction time led to any significant improvement. Based on these studies, the optimized reaction conditions were determined to be: 1.0 equivalent of dimedone, 1.5 equivalents of *N*, *N*-dimethylaniline, 5 mol% Eosin Y under 18 W blue LED irradiation for 12 h in open air.



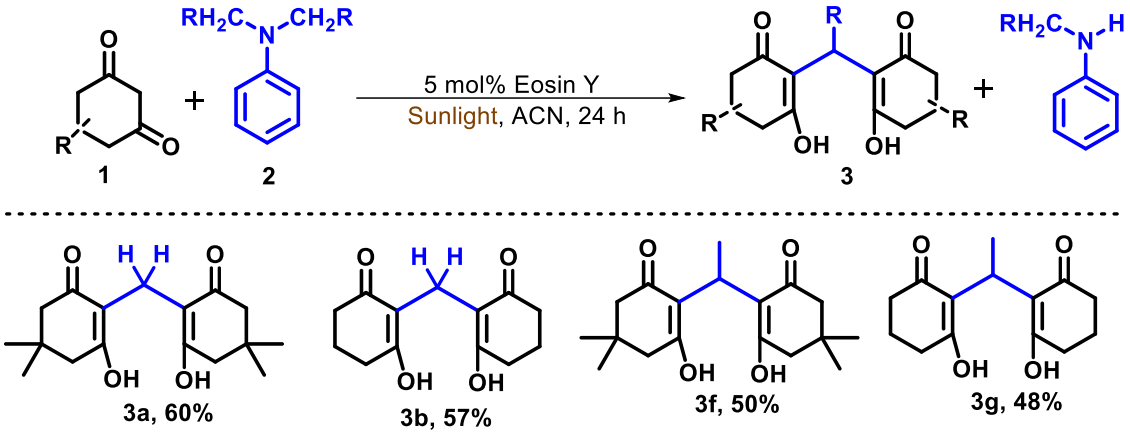
Scheme 3.11: Substrate scope for photochemical tetraketone synthesis

[a]**Reaction conditions**: Cyclic 1,3-diketone (1 equiv.), amine (1.5 equiv.), Eosin-Y (5 mol%), toluene (2 mL), 18 W blue LED, 32-35 °C, open air, 12 h. Yields refer to isolated yields.[b]Yield with 5 mmol scale.

Employing the optimized conditions, we explored the substrate scope of the reaction using various diketones and *N*,*N*-dialkylanilines (Scheme 3.11). Series of alkyl substituted cyclic 1,3-diketones

were subjected to react with *N*,*N*-dimethyaniline giving good to excellent yield of products **3a**-**3e**. Thus, the reaction of *N*,*N*-dimethylaniline with cyclohexane-1,3-dione, 5-methylcyclohexane-1,3-dione, 4,4- dimethylcyclohexane-1,3-dione, 5-isopropylcyclohexane-1,3-dione afforded tetraketones **3b**, **3c**, **3d** and **3e** in 63%, 72%, 76%, and 65% yields, respectively.

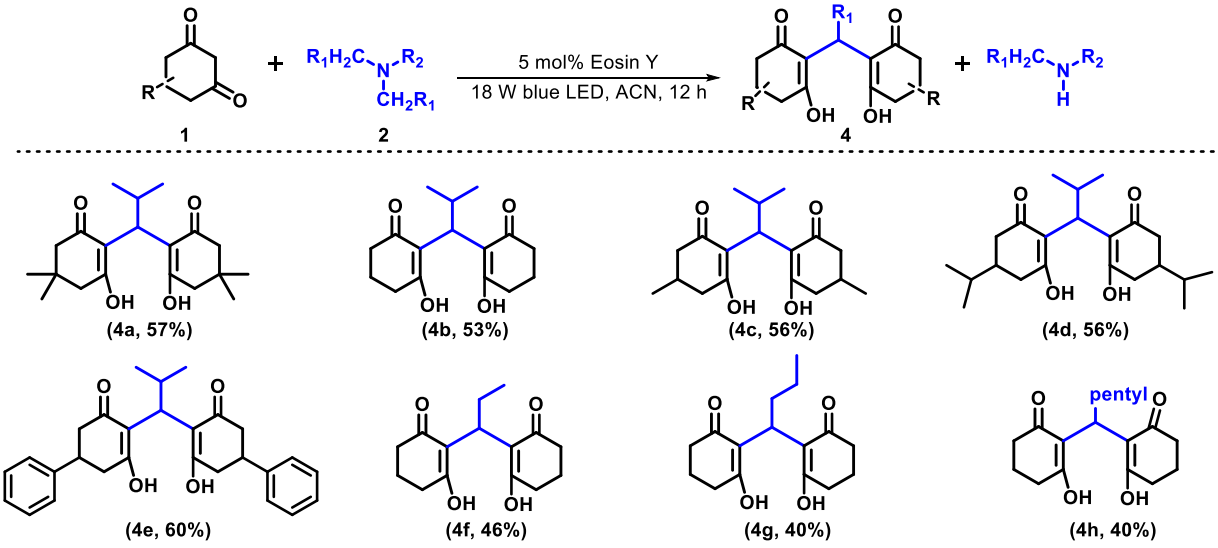
In all these reactions, *N*-methylaniline was observed as a side product, confirming that the bridged methylene group in the tetraketones originates from *N*,*N*-dimethylaniline during the photoredox reaction. This indicates that *N*-methylaniline forms via photoredox-catalyzed C–N bond cleavage. Furthermore, *N*,*N*-diethylaniline reacted with 5,5-dimethylcyclohexane-1,3-dione to yield compound **3f** in 59% yield. Reactions with other cyclic 1,3-diketones gave products **3g**–**3j** in 54%, 62%, 61%, and 68% yields, respectively. The use of *N*,*N*-dipropylaniline with 5,5-dimethylcyclohexane-1,3-dione furnished **3k** in 46% yield. Expanding the scope, *N*,*N*-dibutylaniline and *N*,*N*-dioctylaniline were also employed. Notably, *N*,*N*-dibutylaniline reacted with 5,5-dimethylcyclohexane-1,3-dione, cyclohexane-1,3-dione and 5-isopropylcyclohexane-1,3-dione, producing compounds **3l**–**3n** in 45%, 42%, and 42% yields, respectively. Likewise, reactions of *N*,*N*-dioctylaniline with 5,5-dimethylcyclohexane-1,3-dione and cyclohexane-1,3-dione afforded **3o** and **3p** in 40% and 39% yields. Gratifyingly, the methodology also tolerated spiro and bicyclic 1,3-diketones. Remarkably, bicyclo[3,2,1]octane-2,4-dione underwent reaction with *N*,*N*-dimethyl and diethylaniline to generate **3q** and **3r** in 57% and 48% yield respectively. Moreover, when the reaction was carried out with spiro[4,5]decane-7,9-dione, the desired tetraketones **3s** and **3t** were obtained in 50% and 47% yields respectively. Gratifyingly, 5-phenylcyclohexane-1,3-dione reacted with *N*,*N*-dimethylaniline, *N*,*N*-diethylaniline, and *N*,*N*-dipropylaniline, yielding **3u**, **3v**, and **3w** in 66%, 57%, and 46% yields, respectively. In addition, a reaction of **1a** with **2a** was demonstrated in 5 mmol scale to furnish the product **3a** in 55% yield. Cyclohexanone and cyclopentanone were unreactive in this reaction probably due to less nucleophilicity. This reaction with acyclic diketones like acetyl acetone and ethyl acetoacetate could not afford any product formation under the standard condition. These broad substrate scope inevitably proves the efficacy of the developed photocatalytic transformation.



Scheme 3.12: Eosin-Y catalyzed sunlight mediated synthesis of tetraketone using *N*,*N*-dialkylaniline

Reaction conditions: cyclic-1,3-diketone (1 equiv.), amine (1.5 equiv.), Eosin-Y (5 mol%), toluene (2 mL), Sunlight, open air, 12 h. Yields refer to isolated yields.

Interestingly, the reaction also worked well when the reaction mixture was exposed to sunlight in the presence of catalytic Eosin Y for 24 h (Scheme 3.12). Compounds **3a**, **3b**, **3f** and **3g** were obtained in 60%, 57%, 50% and 48% yields respectively under sunlight.



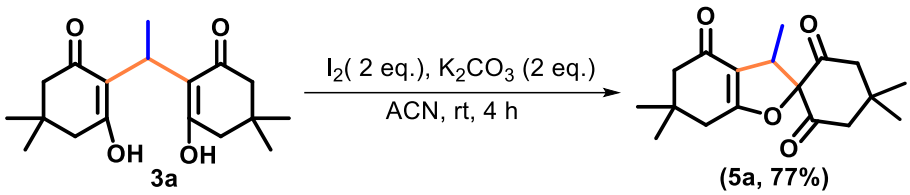
Scheme 3.13: Substrate scope for tetraketone synthesis with aliphatic tertiary amine

Reaction conditions: Cyclic 1,3-diketone (1 equiv.), amine (1.5 equiv.), Eosin-Y (5 mol%), toluene (2 mL), 18 W blue LED, 32-35 °C, open air, 12 h. Yields refer to isolated yields.

Having explored the scope of the reaction with *N*,*N*-dialkylanilines, we extended the applicability of the reaction with aliphatic tertiary amines (Scheme 3.13). It was found that aliphatic tertiary

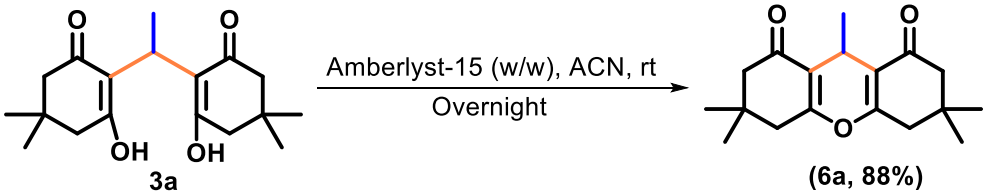
amines are well tolerated under the reaction condition affording moderate to good yield of the desired products. To our delight, triisobutylamine reacted with 5,5-dimethylcyclohexane-1,3-dione, cyclohexane-1,3-dione, 5-methylcyclohexane-1,3-dione and 5-isopropylcyclohexane-1,3-dione to provide **4a**, **4b**, **4c**, **4d** and **4e** in 57%, 53%, 56%, 56% and 60% yields respectively (Scheme 3.13). On the other hand, cyclohexane-1,3-dione reacted with tripropylamine, tributyl-amine and trihexylamine to afford **4f**, **4g** and **4h** in 46%, 40%, 40% yield respectively (Scheme 3.13).

Further, to demonstrate synthetic utility of tetraketones, we have carried out post-modification of tetraketones. At first, we have performed two diverse cyclisation reactions with tetra-ketones. In presence of I_2 and K_2CO_3, tricyclic spiro compound **5a** was obtained in 77% yield (Scheme 3.14).



Scheme 3.14: Post modification of tetraketones under basic condition

But the heterogeneous acid catalyst Amberlyst-15 caused normal ring-closure with expulsion of water to afford xanthene derivative **6a** in 88% yield (Scheme 3.15).



Scheme 3.15: Post modification of tetraketones under acidic condition

To gain insight into the role of Eosin Y in this reaction, a series of spectroscopic studies were conducted. Fluorescence titration revealed that the gradual addition of *N*,*N*-dimethylaniline led to a significant decrease in the fluorescence intensity of Eosin Y (Figure 3.3 a). This observation indicates static quenching, providing clear evidence that the excited state of the photocatalyst is being quenched by the amine.

Further support for this quenching process comes from Stern–Volmer analysis, which showed a linear relationship, strongly suggesting dynamic quenching of Eosin Y by the amine (Figure 3.3 b).

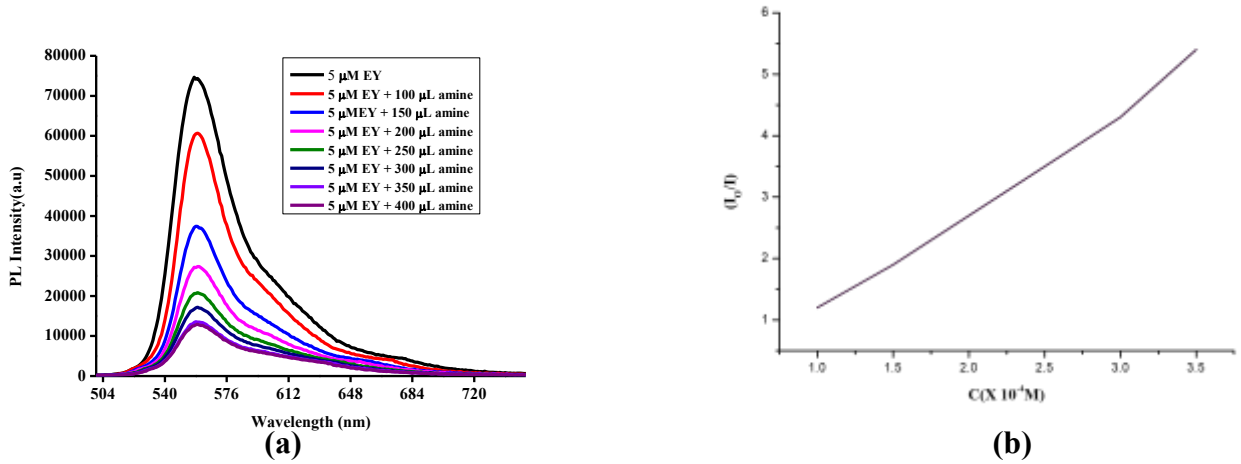


Figure 3.3: (a) Fluorescence quenching experiment of Eosin Y in presence of *N*,*N*-dimethylaniline **2a**; (b) Stern-Volmar quenching plot of Eosin-Y upon addition of **2a**

To understand the thermodynamic feasibility of this quenching step and direction of electron transfer, cyclic voltammetry (CV) was performed. Literature reports the half-wave potential ($E_{1/2}$) of Eosin Y as 0.83 V vs SCE, and that of *N*, *N*-dimethylaniline as 0.74 V vs SCE. This redox difference confirms that photoexcited Eosin Y can undergo reductive quenching via single-electron transfer from the amine. Additionally, we determined the $E_{1/2}$ values of N,N-diethylaniline and N,N-dibutylaniline through CV, which were found to be 0.73 V and 0.69 V vs SCE, respectively (Figure 3.4), further supporting the feasibility of reductive quenching by these amines.

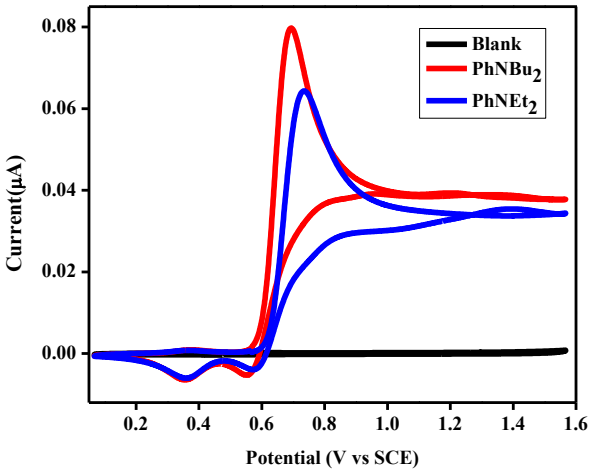


Fig 3.4: Cyclic voltammetry plot of *N*,*N*-diethylaniline and *N*, *N*-dibutylaniline

Afterwards, we carried out fluorescence lifetime measurements taking photocatalyst Eosin Y and the sacrificial electron donor *N*,*N*-dimethylaniline. The lifetime data also reinforce this mechanism: upon addition of 50 µL of compound **2a**, the average lifetime of Eosin Y decreased from 1.2 ns to 0.3 ns. This inevitably indicates that an excited-state charge transfer process is occurring in the reaction (Figure 3.5).

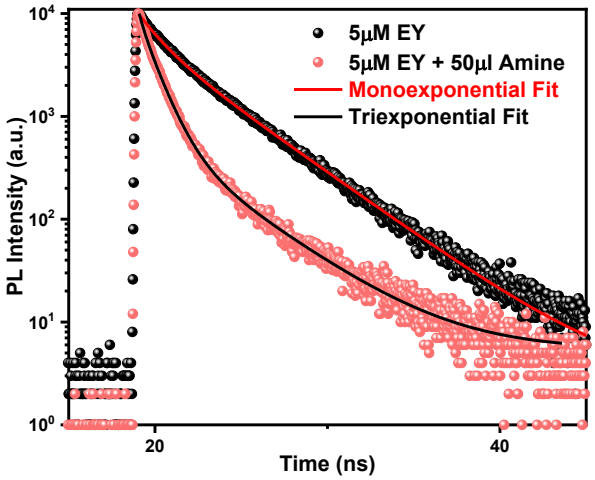
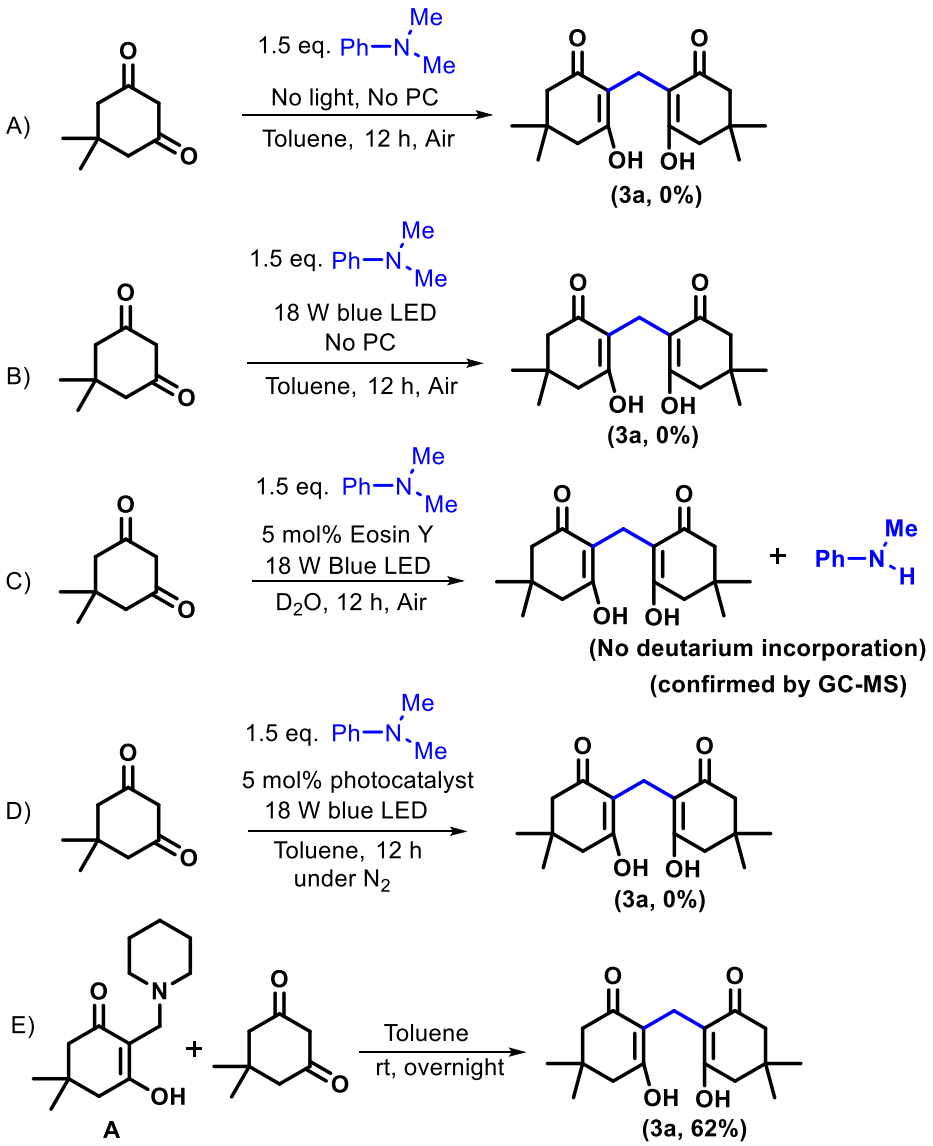


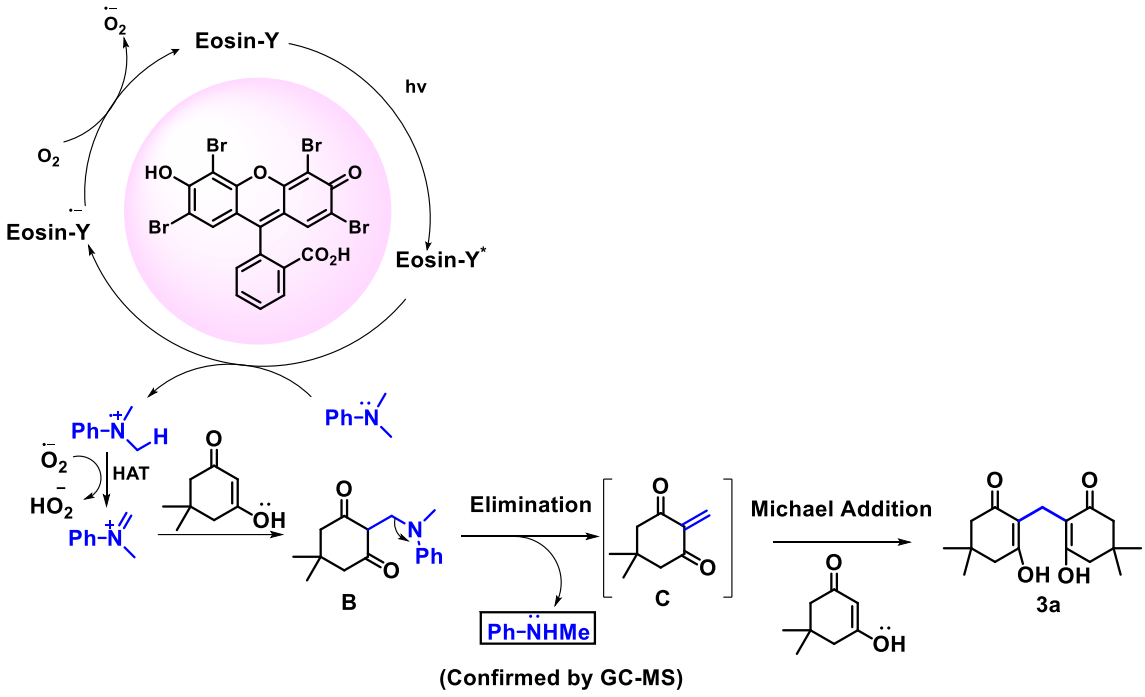
Figure 3.5: Fluorescence lifetime decay analysis

Further, we have carried out several experiments to understand the reaction pathway (Scheme 3.16). In absence of light and photocatalyst no product formation was observed. When reaction mixture was irradiated without addition of photocatalyst, only trace amount of product was found to form (entry A and B, Scheme 3.16). Therefore, both light and photocatalyst are essential for the reaction to occur. When the reaction was performed in D_2O solvent, no deuterium incorporation took place in any of the product (entry C, Scheme 3.16). This indicates that the adventitious water present in organic solvent has no role in the reaction.[38] Also, the reaction gives no product formation under inert atmosphere (entry D, Scheme 3.16).



Scheme 3.16: Experiments to support the mechanism

Based on all these spectroscopic experiments, control experiments and previous literature reports, we have proposed the plausible mechanism for the reaction (Scheme 3.17).[39-43] At first, upon blue LED irradiation Eosin Y moves to excited state. In excited state, the dye gets reductively quenched by single electron donation from the amine forming Eosin Y radical anion and *N*, *N*-dimethylamine radical cation.



Scheme 3.17: Plausible mechanism of photocatalyzed tetraketone synthesis

The oxygen radical anion abstracts hydrogen atom from amine radical cation forming iminium ion. Then cyclic-1,3-diketone attacks the iminium ion to form the intermediate B. As intermediate B could not be isolated under our experimental conditions, we have synthesized stable analogous compound A from previously reported procedure from our group which structurally resemble B (Scheme 3.17).[44] Then, B undergoes elimination reaction to form intermediate C. Subsequently, the intermediate C reacts with 5,5-dimethylcyclohexane-1,3-dione via Michael addition, to afford the product **3a**.

3.4. Conclusion

In conclusion, a novel approach for the alkylation of cyclic-1,3-diketones has been introduced, enabling the synthesis of tetraketones using tertiary amines in the presence of Eosin-Y as a photocatalyst. The reaction is conducted under mild conditions, with blue LED light at room temperature, offering several advantages, The use of Eosin-Y as a photocatalyst eliminates the need for expensive metal-based catalysts.The method avoids the use of toxic halogenated alkylating agents, which are common in traditional alkylation reactions. The reaction bypasses the need for multistep synthesis, providing a more efficient route to tetraketones. The generality of the reaction has been demonstrated with a wide variety of substrates. Detailed mechanistic studies have been carried out using photophysical and electrochemical techniques. The reaction has been shown to be compatible with solar light, making it a potentially more sustainable and scalable process.

3.5. Experimental section and characterization data

3.5.1 General information and data collection

All the chemicals were purchased from Sigma-Aldrich and Thermofischer Scientific and used without further modification. All solvents were purchased from Rankem and Finar Chemicals. Deuterated solvents were used as received. Column chromatographic separations were performed over 100−200 mesh silica-gel. Visualization was accomplished with UV light. The ^{1}H and $^{13}C\{^{1}H\}$ NMR spectra were recorded on 400 and 100 MHz, respectively, using Bruker or JEOL spectrometers. Abbreviations used in the NMR follow-up experiments: b, broad; s, singlet; d, doublet; t, triplet; q, quartet. HRMS spectra were obtained with Waters-synapt G2 using electrospray ionization (ESI-TOF). Infrared (ATIR) spectra were obtained with a Bruker Alpha-E infrared spectrometer. Single-crystal diffraction analysis data were collected at 100K with a BRUKER KAPPA APEX III CCD Duo diffractometer (operated at 1500 W power: 50 kV, 30 mA) using graphite monochromatic Mo Kα radiation and Cu-Kα radiation. The reaction was performed in 15 mL borosilicate test tube. The light source used was 18 W Lords blue LED. The wavelength of the LED was measured with Ocean Optics USB 400 instrument that detects 200-1100 nm wavelength and the spectra was recorded in SpectraSuit software. The wavelength of the radiation is 445 nm with FWHM = 18.96 nm. Cyclic Voltametry was performed in Bio-Logic VMP300 Potentiostat. Fluorescence quenching experiment was carried out in SHIMAZDU spectro fluorophotometer. The lifetime decay analysis was done in HORIBA DeltaFlex Time-Correlated Single Photon Counting system.

3.5 .2. Experimental Section

A. Experimental procedure: Substrates *N*, *N*-dipropylaniline, *N*, *N*-dibutylaniline and *N*, *N*-dioctylaniline were prepared according to reported literature procedure.[45]

B. General procedure for tetraketones synthesis: Cyclic-1,3-diketones (1 equiv.), *N*, *N*-dialkylaniline or trialkyl amine (1.5 equiv.) and Eosin-Y (5 mol%) were stirred in 2 mL toluene solvent in testube under 2 x 9 W blue LED irradiation for 12 h at room temperature. The test tube was kept at a distance of 2.5 cm from each LED. The temperature of the system was measured to be 30-35 oC using IR thermometer. The crude reaction mixture was purified directly by 100-200 mesh silica-gel column chromatography (EtOAc: pet ether = 5:95 to 10:90) to afford the product tetraketones.

3.7. Analytical data of products

2,2'-methylenebis(3-hydroxy-5,5-dimethylcyclohex-2-en-1-one) (3a) Prepared according to General Procedure **B**, using 5,5-dimethylcyclohexane-1,3-dione (0.357 mmol, 50 mg), *N*, *N*-dimethylaniline (0.5355 mmol, 65 mg) and Eosin-Y (0.01785 mmol, 12 mg). The crude reaction mixture was purified by silica gel column chromatography (pet ether/EtOAc = 95:5) to afford product **3a** (36.5 mg, 70%). Melting point: 187-189 ºC. ^{1}H NMR (400 MHz, $CDCl_3$) δ [ppm] 11.55 (s, 2H), 3.15 (s, 2H), 2.28 (s, 4H), 2.27 (s, 4H), 1.04 (s, 12H); $^{13}C\{^{1}H\}$ NMR (100 MHz, $CDCl_3$) δ 189.6, 113.5, 46.0, 31.8, 29.5, 27.1, 15.9. IR (neat): 2955, 2943, 2937, 1610 cm-1. HRMS (ESI-TOF) calculated for $C_{17}H_{24}O_4$ $[M+H]^+$ m/z 293.1753, found 293.1747.

Large scale synthesis of 3a: 5,5-dimethylcyclohexane-1,3-diketones (0.7 g, 5 mmol, 1 equiv.), *N*,*N*-dimethylaniline (908 mg, 7.5 mmol, 1.5 equiv.) and Eosin-Y (5 mol%, 162 mg) were stirred in 6 mL toluene solvent in a 25 mL Schlenk tube under 2 x 9 W blue LED irradiation kept at a distance of 2.5 cm from each lamp for 12 h under room temperature condition. The temperature of the system was measured to be 30-35 ºC using IR thermometer. The crude reaction mixture was purified directly by 100-200 mesh silica-gel column chromatography (EtOAc: pet ether= 5:95) to afford **3a** (0.4 g, 55%) as white solid.

2,2'-methylenebis(3-hydroxycyclohex-2-en-1-one) (3b) Prepared according to General Procedure **B**, using cyclohexane-1,3-dione (0.45 mmol, 50 mg), *N*, *N*-dimethylaniline (0.67 mmol, 81 mg) and Eosin-Y (0.02 mmol, 13 mg). The crude reaction mixture was purified by silica gel column chromatography (pet ether/EtOAc = 90:10) to afford product **3b** (33 mg, 63%) as white solid. Melting point: 120-122 ºC. ^{1}H NMR (400 MHz, $CDCl_3$) δ [ppm] 11.96 (s, 2H), 3.13 (s, 2H), 2.50 – 2.46 (m, 4H), 2.38 – 2.30 (m, 4H), 1.96 – 1.87 (m, 4H); $^{13}C\{^{1}H\}$ NMR (100 MHz, $CDCl_3$) δ 191.1, 114.7, 32.3, 20.3, 16.5. IR (neat): 2924, 2925, 2890, 1605 cm^{-1}. HRMS (ESI-TOF) calculated for $C_{13}H_{16}O_4$ $[M+H]^+$ m/z 237.1127, found 237.1124.

2,2'-methylenebis(3-hydroxy-5-methylcyclohex-2-en-1-one) (3c) Prepared according to General Procedure **B**, using 5-methylcyclohexane-1,3-dione (0.4 mmol, 50 mg), *N*, *N*-dimethylaniline (0.6 mmol, 73 mg) and Eosin-Y (0.02 mmol, 13 mg). The crude reaction mixture was purified by silica gel column chromatography (pet ether/EtOAc = 90:10) to afford product **3c** (37 mg, 72%) as white solid. Melting point: 143-145 ºC. ^{1}H NMR (400 MHz, $CDCl_3$) δ [ppm] 11.98 (s, 1H), 11.69 (s, 1H), 3.12 (s, 2H), 2.51 – 2.46 (m, 4H), 2.25 – 2.18 (m, 2H), 2.10 to 2.00 (m, 4H), 1.06 – 1.05 (m, 6H); $^{13}C\{^{1}H\}$ NMR (100 MHz, $CDCl_3$) δ 190.9, 114.4, 40.7, 40.1, 28.0, 20.8, 16.4. IR (neat): 2955, 2934, 2920, 1607 cm^{-1}. HRMS (ESI-TOF) calculated for $C_{15}H_{20}O_4$ $[M+H]^+$ m/z 265.1440, found 265.1440.

2,2'-methylenebis(3-hydroxy-4,4-dimethylcyclohex-2-en-1-one) (3d) Prepared according to General Procedure **B**, using 4,4-dimethylcyclohexane-1,3-dione (0.357 mmol, 50 mg), *N*, *N*-dimethylaniline (0.54 mmol, 65 mg) and Eosin-Y (0.02 mmol, 12 mg). The crude reaction mixture was purified by silica gel column chromatography (pet ether/EtOAc = 95:5) to afford product **3d** (39.5 mg, 76%) as colourless liquid. ^{1}H NMR (400 MHz, $CDCl_3$) δ [ppm] 12.01 (s, 1H), 11.98 (s, 1H), 3.08 (s, 2H), 2.47 – 2.46 (m, 4H), 1.78 – 1.74 (m, 4H), 1.20 (s, 3H), 1.17 (s, 3H), 1.12 (s, 3H), 1.10 (s, 3H); ^{13}C{^{1}H} NMR (100 MHz, $CDCl_3$) δ 203.4, 196.6, 189.7, 182.0, 113.0, 112.8, 38.8, 37.7, 34.7, 34.6, 29.5, 27.5, 25.9, 25.6, 24.6, 24.5, 17.6. IR (neat): 2927, 2911, 2889, 1598 cm^{-1}. HRMS (ESI-TOF) calculated for $C_{17}H_{24}O_4$ $[M+H]^+$ m/z 293.1753, found 293.1747.

2,2'-methylenebis(3-hydroxy-5-isopropylcyclohex-2-en-1-one) (3e) Prepared according to General Procedure **B**, using 5-isopropylcyclohexane-1,3-dione (0.33 mmol, 50 mg), *N*, *N*-dimethylaniline (0.5 mmol, 60 mg) and Eosin-Y (0.017 mmol, 11 mg). The crude reaction mixture was purified by silica gel column chromatography (pet ether/EtOAc = 95:5) to afford product **3e** (34 mg, 65%) as white solid. Melting point: 168-170 ºC. ^{1}H NMR (400 MHz, $CDCl_3$) δ [ppm] 12.01 (s, 1H), 11.63 (s, 1H), 3.12 (d, *J* = 5.8 Hz, 2H), 2.54 – 2.42 (m, 4H), 2.32 – 2.03 (m, 4H), 1.83 – 1.73 (m, 2H), 1.61 – 1.52 (m, 2H), 0.92 (d, *J* = 6.7 Hz, 12H); ^{13}C{^{1}H} NMR (100 MHz, $CDCl_3$) δ 191.4, 191.2, 118.6, 38.5, 37.5, 36.7, 24.1, 19.6, 16.0. IR (neat): 2924, 2904, 2885, 1607 cm^{-1}. HRMS (ESI-TOF) calculated for $C_{19}H_{28}O_4$ $[M+H]^+$ m/z 321.2066, found 321.2061.

2,2'-(ethane-1,1-diyl)bis(3-hydroxy-5,5-dimethylcyclohex-2-en-1-one) (3f) Prepared according to General Procedure **B**, using 5,5-dimethylcyclohexane-1,3-dione (0.357 mmol, 50 mg), *N*, *N*-diethylaniline (0.54 mmol, 80 mg) and Eosin-Y (0.01785 mmol, 12 mg). The crude reaction mixture was purified by silica gel column chromatography (pet ether/EtOAc = 95:5) to afford product **3f** (32 mg, 59%) as white solid. Melting point: 130-132 ºC. ^{1}H NMR (400 MHz, $CDCl_3$) δ [ppm] 12.51 (s, 1H), 11.58 (s, 1H), 4.14 (q, *J* = 7.4 Hz, 1H), 2.35 – 2.21 (m, 8H), 1.49 (d, *J* = 7.5 Hz, 3H), 1.05 (s, 12H); ^{13}C{^{1}H} NMR (100 MHz, $CDCl_3$) δ 189.6, 189.5, 117.7, 47.0, 46.2, 31.2, 29.7, 26.5, 23.6, 15.7. IR (neat): 2963, 2944, 2928, 1577 cm^{-1}. HRMS (ESI-TOF) calculated for $C_{18}H_{26}O_4$ $[M+H]^+$ m/z 307.1909, found 307.1901.

2,2'-(ethane-1,1-diyl)bis(3-hydroxycyclohex-2-en-1-one) (3g) Prepared according to General Procedure **B**, using cyclohexane-1,3-dione (0.45 mmol, 50 mg), *N*, *N*-diethylaniline (0.67 mmol, 100 mg) and Eosin-Y (0.02 mmol, 13 mg). The crude reaction mixture was purified by silica gel column chromatography (pet ether/EtOAc = 90:10) to afford product **3g** (30 mg, 54%) as white solid. Melting point: 149-151 ºC. ^{1}H NMR (400 MHz, $CDCl_3$) δ [ppm] 12.91 (s, 1H), 12.10 (s, 1H), 4.11 (q, *J* = 7.5

Hz, 1H), 2.53 – 2.45 (m, 4H), 2.35 – 2.25 (m, 4H), 1.94 – 1.78 (m, 4H), 1.47 (d, *J* = 7.5 Hz, 3H); $^{13}C\{^{1}H\}$ NMR (100 MHz, $CDCl_3$) δ 191.2, 191.1, 119.0, 33.5, 32.7, 24.0, 20.0, 16.0. IR (neat): 2955, 2947, 2930, 1586 cm^{-1}. HRMS (ESI-TOF) calculated for $C_{14}H_{18}O_4$ $[M+H]^+$ m/z 251.1283, found 251.1280.

2,2'-(ethane-1,1-diyl)bis(3-hydroxy-5-methylcyclohex-2-en-1-one) (3h) Prepared according to General Procedure **B**, using 5-methylcyclohexane-1,3-dione (0.4 mmol, 50 mg), *N*, *N*-diethylaniline (0.6 mmol, 89 mg) and Eosin-Y (0.02 mmol, 13 mg). The crude reaction mixture was purified by silica gel column chromatography (pet ether/EtOAc = 90:10) to afford product **3h** (34 mg, 62%) as white solid. Melting point: 60-62 ºC. ^{1}H NMR (400 MHz, $CDCl_3$) δ [ppm] 12.86 (s, 1H),12.06 (s, 1H), 4.13 – 4.06 (m, 1H), 2.51 – 2.45 (m, 4H), 2.28 – 2.23 (m, 2H), 2.08 – 1.96 (m, 4H), 1.45 (dd, *J* = 7.5, 2.4 Hz, 3H), 1.04 (d, *J* = 6.1 Hz, 6H); $^{13}C\{^{1}H\}$ NMR (100 MHz, $CDCl_3$) δ 191.0, 190.9, 118.7, 41.8, 41.0, 27.5, 24.0, 20.6, 15.9. IR (neat): 2957, 2942, 2930, 1591 cm^{-1}. HRMS (ESI-TOF) calculated for $C_{16}H_{22}O_4$ $[M+H]^+$ m/z 279.1596, found 279.1593.

2,2'-(ethane-1,1-diyl)bis(3-hydroxy-4,4-dimethylcyclohex-2-en-1-one) (3i) Prepared according to General Procedure **B**, using 4,4-dimethylcyclohexane-1,3-dione (0.357 mmol, 50 mg), *N*, *N*-diethylaniline (0.54 mmol, 80 mg) and Eosin-Y (0.02 mmol, 12 mg). The crude reaction mixture was purified by silica gel column chromatography (pet ether/EtOAc = 95:5) to afford product **3i** (33.5 mg, 61%) as colourless liquid. ^{1}H NMR (400 MHz, $CDCl_3$) δ [ppm] 12.97 (s, 1H), 12.05 (s, 1H), 4.13 – 3.97 (m, 1H), 2.45 (dt, *J* = 10.0, 5.1 Hz, 4H), 1.84 – 1.62 (m, 4H), 1.41 (d, *J* = 7.4 Hz, 3H), 1.18 (d, *J* = 12.0 Hz, 6H), 1.10 (dd, *J* = 7.4, 4.6 Hz, 6H); $^{13}C\{^{1}H\}$ NMR (100 MHz, $CDCl_3$) δ 203.5, 196.6, 189.7, 182.1, 113.0, 112.9, 38.9, 37.8, 34.7, 34.6, 29.5, 27.6, 25.9, 25.7, 24.7, 24.6, 17.7, 17.6. IR (neat): 2924, 2901, 2880, 1591 cm^{-1}. HRMS (ESI-TOF) calculated for $C_{18}H_{26}O_4$ $[M+H]^+$ m/z 307.1909, found 307.1904.

2,2'-(ethane-1,1-diyl)bis(3-hydroxy-5-isopropylcyclohex-2-en-1-one) (3j) Prepared according to General Procedure **B**, using 5-isopropylcyclohexane-1,3-dione (0.33 mol, 50 mg), *N*, *N*-diethylaniline (0.5 mmol, 73 mg) and Eosin-Y (0.017 mmol, 11 mg). The crude reaction mixture was purified by silica gel column chromatography (pet ether/EtOAc = 95:5) to afford product **3j** (37 mg, 68%) as white solid. Melting point: 124-126 ºC. ^{1}H NMR (400 MHz, $CDCl_3$) δ [ppm] 12.90 (s, 1H), 12.11 (s, 1H), 4.10-4.05 (m, 1H), 2.55 – 2.49 (m, 4H), 2.08 – 1.96 (m, 4H), 1.79 – 1.69 (m, 2H), 1.57 – 1.52 (m, 2H), 1.49 – 1.44 (m, 3H), 0.92 (d, *J* = 6.7 Hz, 12H); $^{13}C\{^{1}H\}$ NMR (100 MHz, $CDCl_3$) δ 191.3, 191.1, 118.6, 38.5, 37.5, 36.6, 31.7, 24.0, 19.8, 19.6, 15.9, 15.6. IR (neat): 2963, 2960, 2933, 1596 cm^{-1}. HRMS (ESI-TOF) calculated for $C_{20}H_{30}O_4$ $[M+H]^+$ m/z 335.2222, found 335.2215.

2,2'-(propane-1,1-diyl)bis(3-hydroxy-5,5-dimethylcyclohex-2-en-1-one) (3k) Prepared according to General Procedure **B**, using 5,5-dimethylcyclohexane-1,3-dione (0.357 mmol, 50 mg), *N*, *N*-propylaniline (0.54 mmol, 95 mg) and Eosin-Y (0.01785 mmol, 12 mg). The crude reaction mixture was purified by silica gel column chromatography (pet ether/EtOAc = 95:5) to afford product **3k** (26 mg, 46%) as white solid. Melting point: 145-147 ºC. ^{1}H NMR (400 MHz, $CDCl_3$) δ [ppm] 12.47 (s, 1H), 11.58 (s, 1H), 3.81 (t, *J* = 8.0 Hz, 1H), 2.29 – 2.26 (m, 8H), 2.04 (p, *J* = 7.4 Hz, 2H), 1.06 (d, *J* = 5.0 Hz, 12H), 0.83 (t, *J* = 7.3 Hz, 3H); ^{13}C{^{1}H} NMR (100 MHz, $CDCl_3$) δ 190.1, 189.6, 116.5, 47.0, 46.2, 31.7, 31.1, 30.0, 26.6, 22.3, 13.6. IR (neat): 2960, 2949, 2919, 1583 cm^{-1}. HRMS (ESI-TOF) calculated for $C_{19}H_{28}O_4$ $[M+H]^+$ m/z 321.2066, found 321.2067.

2,2'-(butane-1,1-diyl)bis(3-hydroxy-5,5-dimethylcyclohex-2-en-1-one) (3l) Prepared according to General Procedure **B**, using 5,5-dimethylcyclohexane-1,3-dione (0.357 mmol, 50 mg), *N*, *N*-dibutylaniline (0.54 mmol, 110 mg) and Eosin-Y (0.01785 mmol, 12 mg). The crude reaction mixture was purified by silica gel column chromatography (pet ether/EtOAc = 95:5) to afford product **3l** (27 mg, 45%) as white solid. Melting point: 116-118 ºC. ^{1}H NMR (400 MHz, $CDCl_3$) δ [ppm] 12.49 (s, 1H), 11.56 (s, 1H), 3.93 (t, *J* = 8.0 Hz, 1H), 2.29 – 2.26 (m, 8H), 2.01 – 1.95 (m, 2H), 1.23 – 1.17 (m, 2H), 1.05 (d, *J* = 2.9 Hz, 12H), 0.86 (t, *J* = 7.3 Hz, 3H); ^{13}C{^{1}H} NMR (100 MHz, $CDCl_3$) δ 190.1, 189.7, 116.7, 47.1, 46.3, 31.3, 31,2, 30.0, 29.4, 26.6, 22.1, 13.9. IR (neat): 2966, 2939, 2906, 1582 cm^{-1}. HRMS (ESI-TOF) calculated for $C_{20}H_{30}O_4$ $[M+H]^+$ m/z 335.2222, found 335.2222.

2,2'-(butane-1,1-diyl)bis(3-hydroxycyclohex-2-en-1-one) (3m) Prepared according to General Procedure **B**, using cyclohexane-1,3-dione (0.45 mmol, 50 mg), *N*, *N*-dibutylaniline (0.67 mmol, 100 mg) and Eosin-Y (0.02 mmol, 13 mg). The crude reaction mixture was purified by silica gel column chromatography (pet ether/EtOAc = 90:10) to afford product **3m** (26 mg, 42%) as white solid. Melting point: 88-90 ºC. ^{1}H NMR (400 MHz, $CDCl_3$) δ [ppm] 12.88 (s, 1H), 11.99 (s, 1H), 3.87 (q, *J* = 8 Hz, 1H), 2.52 – 2.46 (m, 4H), 2.34 – 2.26 (m, 4H), 1.95 – 1.91 (m, 4H), 1.91 – 1.83 (m, 2H), 0.87 – 0.83 (m, 2H); ^{13}C{^{1}H} NMR (100 MHz, $CDCl_3$) δ 191.6, 191.0, 117.8, 33.5, 32.7, 31.7, 29.8, 22.0, 20.0, 13.8. IR (neat): 2955, 2941, 2924, 1583 cm^{-1}. HRMS (ESI-TOF) calculated for $C_{16}H_{22}O_4$ $[M+H]^+$ m/z 279.1596, found 279.1591.

2,2'-(butane-1,1-diyl)bis(3-hydroxy-5-isopropylcyclohex-2-en-1-one) (3n) Prepared according to General Procedure **B**, using 5-isopropylcyclohexane-1,3-dione (0.33 mol, 50 mg), *N*, *N*-diethylaniline (0.5 mmol, 73 mg) and Eosin-Y (0.017 mmol, 11 mg). The crude reaction mixture was purified by silica gel column chromatography (pet ether/EtOAc = 95:5) to afford product **3n** (24.5 mg, 42%) as yellow liquid. ^{1}H NMR (400 MHz, $CDCl_3$) δ [ppm] 12.87 (s, 1H), 12.08 (s, 1H), 3.89 – 3.82 (m, 1H),

2.55 – 2.49 (m, 4H), 2.04 – 2.00 (m, 4H), 1.98 – 1.92 (m, 2H), 1.77 – 1.69 (m, 2H), 1.57 – 1.52 (m, 2H), 1.19 – 1.2 (m, 2H), 0.92 (d, *J* = 6.7 Hz, 12H), 0.87 – 0.84 (m, 3H); $^{13}C\{^{1}H\}$ NMR (100 MHz, $CDCl_3$) δ 191.7, 191.1, 117.4, 38.6, 37.4, 36.7, 31.7, 31.3, 29.8, 22.0, 19.6, 13.8. IR (neat): 2963, 2945, 2929, 1589 cm^{-1}. HRMS (ESI-TOF) calculated for $C_{22}H_{34}O_4$ $[M+H]^+$ m/z 363.2535, found 363.2533.

2,2'-(octane-1,1-diyl)bis(3-hydroxy-5,5-dimethylcyclohex-2-en-1-one) (3o) Prepared according to General Procedure **B**, using 5,5-dimethylcyclohexane-1,3-dione (0.357 mmol, 50 mg), *N*, *N*-dioctylaniline (0.54 mmol, 151 mg) and Eosin-Y (0.01785 mmol, 12 mg). The crude reaction mixture was purified by silica gel column chromatography (pet ether/EtOAc = 95:5) to afford product **3o** (28 mg, 40%) as yellow liquid. ^{1}H NMR (400 MHz, $CDCl_3$) δ [ppm] 12.48 (s, 1H), 3.90 (t, *J* = 8.0 Hz, 1H), 2.31 – 2.22 (m, 8H), 1.99 (dd, *J* = 15.1, 7.9 Hz, 2H), 1.22 (m, 8H), 1.06 (d, *J* = 4.0 Hz, 12H), 0.87 – 0.82 (m, 5H) ; $^{13}C\{^{1}H\}$ NMR (100 MHz, $CDCl_3$) δ 190.0, 189.6, 116.6, 47.0, 46.2, 31.8, 31.1, 29.9, 29.6, 29.2, 29.2, 29.1, 29.0, 26.5, 22.6, 14.1. IR (neat): 2963, 2944, 2918, 1610 cm^{-1}. HRMS (ESI-TOF) calculated for $C_{24}H_{38}O_4$ $[M+H]^+$ m/z 391.2848, found 391.2845.

2,2'-(octane-1,1-diyl)bis(3-hydroxycyclohex-2-en-1-one) (3p) Prepared according to General Procedure **B**, using cyclohexane-1,3-dione (0.45 mmol, 50 mg), *N*, *N*-dioctylaniline (0.67 mmol, 188 mg) and Eosin-Y (0.02 mmol, 14 mg). The crude reaction mixture was purified by silica gel column chromatography (pet ether/EtOAc = 95:5) to afford product **3p** (29 mg, 39%) as yellow liquid. ^{1}H NMR (400 MHz, $CDCl_3$) δ [ppm] 12.88 (s, 1H), 12.03 (s, 1H), 3.85 (t, *J* = 7.9 Hz, 1H), 2.53 – 2.46 (m, 4H), 2.36 – 2.25 (m, 4H), 1.99 – 1.89 (m, 4H), 1.87– 1.76 (m, 2H), 1.27 – 1.13 (m, 10H), 0.86 (t, *J* = 6.9 Hz, 3H); $^{13}C\{^{1}H\}$ NMR (100 MHz, $CDCl_3$) δ 191 .6, 191.0, 117.8, 33.5, 32.7, 31.8, 30.1, 29.2, 29.2, 29.2, 28.9, 22.6, 20.0, 14.1. IR (neat): 2958, 2938, 2929, 1588 cm^{-1}. HRMS (ESI-TOF) calculated for $C_{20}H_{30}O_4$ $[M+H]^+$ m/z 335.2222, found 335.2227.

4-hydroxy-3-(((1R,5S)-2-hydroxy-4-oxobicyclo[3.2.1]oct-2-en-3-yl)methyl)bicyclo[3.2.1]oct-3-en-2-one (3q) Prepared according to General Procedure **B**, using bicyclo[3.2.1]octane-2,4-dione (0.18 mmol, 25 mg), *N*, *N*-dimethylaniline (0.27 mmol, 33 mg) and Eosin-Y (0.009 mmol, 6 mg). The crude reaction mixture was purified by silica gel column chromatography (pet ether/EtOAc = 95:5) to afford product **3t** (15 mg, 57%) as white solid. Melting point: 171-173 ºC. ^{1}H NMR (400 MHz, $CDCl_3$) δ [ppm] 11.64 (s, 2H), 2.98 (s, 2H), 2.92 (m, 4H), 2.07 – 2.03 (m, 8H), 1.44 – 1.41(m, 4H); $^{13}C\{^{1}H\}$ NMR (100 MHz, $CDCl_3$) δ 195.2, 110.8, 45.2, 37.1, 28.0, 27.7, 15.4, 14.9. IR (neat): 2974, 2956, 2938, 1617 cm^{-1}. HRMS (ESI-TOF) calculated for $C_{17}H_{20}O_4$ $[M+H]^+$ m/z 289.1440, found 289.1436.

4-hydroxy-3-(1-((1R,5S)-2-hydroxy-4-oxobicyclo[3.2.1]oct-2-en-3-yl)ethyl)bicyclo[3.2.1]oct-3-en-2-one (3r) Prepared according to General Procedure **B**, using bicyclo[3.2.1]octane-2,4-dione (0.18

mmol, 25 mg), *N*, *N*-diethylaniline (0.27 mmol, 40 mg) and Eosin-Y (0.009 mmol, 6 mg). The crude reaction mixture was purified by silica gel column chromatography (pet ether/EtOAc = 95:5) to afford product **3r** (13 mg, 48%) as brown solid. Melting point: 146-148 ºC. ^{1}H NMR (400 MHz, $CDCl_3$) δ [ppm] 12.53 (s, 2H), 3.90 (q, *J* = 7.5 Hz, 1H), 2.91– 2.90 (m, 4H), 2.06 – 2.01 (m, 4H), 1.84 (d, *J* = 11.2 Hz, 2H), 1.47 – 1.37 (m, 8H); ^{13}C{^{1}H} NMR (100 MHz, $CDCl_3$) δ 195.3, 195.0, 115.2, 46.3, 45.3, 36.5, 28.2, 27.9, 22.9, 15.7. IR (neat): 2966, 2952, 2932, 1704 cm^{-1}. HRMS (ESI-TOF) calculated for $C_{18}H_{22}O_4$ $[M+H]^+$ m/z 303.1596, found 303.1597.

8,8'-methylenebis(9-hydroxyspiro[4.5]dec-8-en-7-one) (3s) Prepared according to General Procedure **B**, using spiro[4.5]decane-7,9-dione (0.15 mmol, 25 mg), *N*, *N*-dimethylaniline (0.23 mmol, 27 mg) and Eosin-Y (0.008 mmol, 5 mg). The crude reaction mixture was purified by silica gel column chromatography (pet ether/EtOAc = 95:5) to afford product **3s** (13 mg, 50%) as white solid. Melting point: 102-104 ºC. ^{1}H NMR (400 MHz, $CDCl_3$) δ [ppm] δ 11.66 (s, 2H), 3.13 (s, 2H), 2.42 – 2.34 (m, 8H), 1.68 – 1.64 (m, 8H), 1.51–1.46 (m, 8H); ^{13}C{^{1}H} NMR (100 MHz, $CDCl_3$) δ 190.2, 114.2, 44.7, 43.1, 42.6, 39.8, 39.3, 31.6, 24.3, 16.2. IR (neat): 2957, 2947, 2904, 1613 cm^{-1}. HRMS (ESI-TOF) calculated for $C_{21}H_{28}O_4$ $[M+H]^+$ m/z 345.2066, found 345.2062.

8,8'-(ethane-1,1-diyl)bis(9-hydroxyspiro[4.5]dec-8-en-7-one) (3t) Prepared according to General Procedure **B**, using spiro[4.5]decane-7,9-dione (0.15 mmol, 25 mg), *N*, *N*-diethylaniline (0.23 mmol, 34 mg) and Eosin-Y (0.008 mmol, 5 mg). The crude reaction mixture was purified by silica gel column chromatography (pet ether/EtOAc = 95:5) to afford product **3t** (12.5 mg, 47%) as white solid. Melting point: 123-125 ºC. ^{1}H NMR (400 MHz, $CDCl_3$) δ [ppm] δ12.62 (s, 1H), 11.67 (s, 1H), 4.11 (q, *J* = 7.5 Hz, 1H), 2.44 – 2.29 (m, 8H), 1.67 – 1.63 (m, 8H), 1.61 – 1.49 (m, 8H), 1.47 (d, *J* = 8 Hz, 3H); ^{13}C{^{1}H} NMR (100 MHz, $CDCl_3$) δ 190.2, 190.2, 118.4, 45.7, 44.9, 41.9,39.3, 36.7, 24.3, 23.8, 15.8. IR (neat): 2949, 2939, 2928, 1594 cm^{-1}. HRMS (ESI-TOF) calculated for $C_{22}H_{30}O_4$ $[M+H]^+$ m/z 359.2222, found 359.2218.

4,4''-methylenebis(5-hydroxy-1,6-dihydro-[1,1'-biphenyl]-3(2H)-one) (3u) Prepared according to General Procedure **B**, using 5-phenylcyclohexane-1,3-dione (0.26 mol, 50 mg), *N*, *N*-methylaniline (0.4 mmol, 49 mg) and Eosin-Y (0.013 mmol, 9 mg). The crude reaction mixture was purified by silica gel column chromatography (pet ether/EtOAc = 90:10) to afford product **3u** (34 mg, 66%) as yelow solid. Melting point: 213-215 ºC. ^{1}H NMR (400 MHz, $CDCl_3$) δ [ppm] 12.11 (s, 1H), 11.76 (s, 1H), 7.38 – 7.34 (m, 5H), 7.25 – 7.23 (m, 5H), 3.26 (s, 2H), 2.79 – 2.73 (m, 8H), 2.60 – 2.59 (m, 2H); ^{13}C{^{1}H} NMR (100 MHz, $CDCl_3$) δ 190.2, 189.8, 142.3, 128.9, 127.2, 126.7, 114.5, 39.8, 39.3, 38.5,

16.5. IR (neat): 3029, 2930, 2887, 1599 cm^{-1}. HRMS (ESI-TOF) calculated for $C_{25}H_{24}O_4$ $[M+H]^+$ m/z 389.1753.2222, found 389.1755.

4,4''-(ethane-1,1-diyl)bis(5-hydroxy-1,6-dihydro-[1,1'-biphenyl]-3(2H)-one) (3v) Prepared according to General Procedure **B**, using 5-phenylcyclohexane-1,3-dione (0.26 mol, 50 mg), *N*, *N*-diethylaniline (0.4 mmol, 49 mg) and Eosin-Y (0.013 mmol, 9 mg). The crude reaction mixture was purified by silica gel column chromatography (petroleum ether/EtOAc = 90:10) to afford product **3v** (30 mg, 57%) as yelow solid. Melting point: 175-177 ºC. ^{1}H NMR (400 MHz, $CDCl_3$) δ [ppm] 12.99 (s, 1H), 12.23 (s, 1H), 7.38 – 7.29 (m, 5H), 7.25 – 7.20 (m, 5H), 4.24 – 4.16 (m, 1H), 3.31– 3.22 (m, 2H), 2.83 – 2.68 (m, 4H), 2.60– 2.52 (m, 4H), 1.58 (d, *J* = 7.5 Hz, 3H); ^{13}C{^{1}H} NMR (100 MHz, $CDCl_3$) δ 190.5, 190.3, 142.2, 128.9, 128.8, 127.2, 126.8, 118.8,40.9, 40.0, 38.1, 24.2, 16.1, 15.6. IR (neat): 2925, 2899, 2875, 1585 cm^{-1}. HRMS (ESI-TOF) calculated for $C_{26}H_{26}O_4$ $[M+H]^+$ m/z 403.1909, found 403.1909.

4,4''-(propane-1,1-diyl)bis(5-hydroxy-1,6-dihydro-[1,1'-biphenyl]-3(2H)-one) (3w) Prepared according to General Procedure **B**, using 5-phenylcyclohexane-1,3-dione (0.26 mol, 50 mg), *N*, *N*-dipropylaniline (0.4 mmol, 71 mg) and Eosin-Y (0.013 mmol, 9 mg). The crude reaction mixture was purified by silica gel column chromatography (pet ether/EtOAc = 90:10) to afford product **3s** (26 mg, 47%) as yelow solid. Melting point: 148-150 ºC. ^{1}H NMR (400 MHz, $CDCl_3$) δ [ppm] 12.94 (s, 1H), 12.14 (s, 1H), 7.38 – 7.33 (m, 5H), 7.26 – 7.22 (m, 5H), 3.86 (t, *J* = 7.9 Hz, 1H), 3.30 – 3.22 (m, 2H), 2.80 – 2.74 (m, 4H), 2.61 – 2.53 (m, 4H), 2.15 – 2.06 (m, 2H), 0.90 (t, *J* = 7.3 Hz, 3H); ^{13}C{^{1}H} NMR (100 MHz, $CDCl_3$) δ 190.9, 190.1, 142.2, 128.9, 128.7, 127.1, 126.8, 126.7, 117.3, 40.8, 40.1, 38.1, 32.2, 22.3, 13.5. IR (neat): 3407, 2960, 2945, 1703 cm^{-1}. HRMS (ESI-TOF) calculated for $C_{27}H_{28}O_4$ $[M+H]^+$ m/z 417.2066, found 417.2059.

2,2'-(2-methylpropane-1,1-diyl)bis(3-hydroxy-5,5-dimethylcyclohex-2-en-1-one) (4a) Prepared according to General Procedure **B**, using 5,5-dimethylcyclohexane-1,3-dione (0.357 mmol, 50 mg), triisobutylamine (0.54 mmol, 99 mg) and Eosin-Y (0.02 mmol, 12 mg). The crude reaction mixture was purified by silica gel column chromatography (pet ether/EtOAc = 95:5) to afford product **4a** (34 mg, 57%) as white solid Melting point: 147-149 ºC. ^{1}HNMR (400 MHz, $CDCl_3$) δ [ppm] 12.43 (s, 1H), 11.49 (s, 1H), 3.45 (d, *J* = 11.2 Hz, 1H), 2.99 – 2.88 (m, 1H), 2.35 – 2.23 (m, 8H), 1.06 (d, *J* = 9.0 Hz, 12H), 0.84 (d, *J* = 6.4 Hz, 6H); ^{13}C{^{1}H} NMR (100 MHz, $CDCl_3$) δ 190.4, 189.5, 116.5, 47.0, 46.3, 38.1, 31.1, 30.0, 26.8, 25.7, 22.3. IR (neat): 2963, 2930, 2921, 1585 cm^{-1}. HRMS (ESI-TOF) calculated for $C_{20}H_{30}O_4$ $[M+H]^+$ m/z 335.2222, found 335.2221.

2,2'-(2-methylpropane-1,1-diyl)bis(3-hydroxycyclohex-2-en-1-one) (4b) Prepared according to General Procedure **B**, using cyclohexane-1,3-dione (0.45 mmol, 50 mg), triisobutylamine (0.67 mmol, 124 mg) and Eosin-Y (0.02 mmol, 14 mg). The crude reaction mixture was purified by silica gel column chromatography (pet ether/EtOAc = 90:10) to afford product **4b** (33 mg, 53%) as white solid Melting point: 175-177 ºC. ^{1}H NMR (400 MHz, $CDCl_3$) δ [ppm] 12.88 (s, 1H), 12.00 (s, 1H), 3.39 (d, *J* = 11.2 Hz, 1H), 2.84 (qd, *J* = 12.9, 6.4 Hz, 1H), 2.55 – 2.47 (m, 4H), 2.37 – 2.27 (m, 4H), 1.97 – 1.90 (m, 2H), 1.86 – 1.79 (m, 2H), 0.80 (d, *J* = 6.4 Hz, 6H); ^{13}C{^{1}H} NMR (100 MHz, $CDCl_3$) δ 191.9, 190.8, 117.2, 38.4, 33.5, 32.9, 25.4, 21.8, 20.1. IR (neat): 2958, 2930, 2921, 1577 cm^{-1}. HRMS (ESI-TOF) calculated for $C_{16}H_{22}O_4$ $[M+H]^+$ m/z 279.1595, found 279.1596.

2,2'-(2-methylpropane-1,1-diyl)bis(3-hydroxy-5-methylcyclohex-2-en-1-one) (4c) Prepared according to General Procedure **B**, using 5-methylcyclohexane-1,3-dione (0.4 mmol, 50 mg), triisobutylamine (0.6 mmol, 110 mg) and Eosin-Y (0.02 m mol, 12 mg). The crude reaction mixture was purified by silica gel column chromatography (pet ether/EtOAc = 95:5) to afford product **4c** (34 mg, 56%) as red liquid. ^{1}H NMR (400 MHz, $CDCl_3$) δ [ppm] 11.96 (s, 1H), 3.37 (t, *J* = 11.5 Hz, 1H), 2.85 (dq, *J* = 18.8, 6.3 Hz, 1H), 2.53 – 2.43 (m, 4H), 2.34 – 2.19 (m, 2H), 2.06 – 1.97 (m, 4H), 1.06 (dd, *J* = 12.0, 5.9 Hz, 6H), 0.78 (dd, *J* = 6.4, 2.7 Hz, 6H); ^{13}C{^{1}H} NMR (100 MHz, CDCl3) δ 191.8, 190.7, 117.0, 41.8, 41.2, 38.4, 27.8, 25.3, 22.0, 21.9, 20.6. IR (neat): 2963, 2958, 2944, 1591 cm^{-1}. HRMS (ESI-TOF) calculated for $C_{18}H_{26}O_4$ $[M+H]^+$ m/z 307.1909, found 307.1907.

2,2'-(2-methylpropane-1,1-diyl)bis(3-hydroxy-5-isopropylcyclohex-2-en-1-one) (4d) Prepared according to General Procedure **B**, using 5-isopropylcyclohexane-1,3-dione (0.29 mmol, 50 mg), triisobutylamine (0.43 mmol, 80 mg) and Eosin-Y (0.014 mmol, 9 mg). The crude reaction mixture was purified by silica gel column chromatography (pet ether/EtOAc = 95:5) to afford product **4d** (29 mg, 56%) as viscous red liquid. ^{1}H NMR (400 MHz, $CDCl_3$) δ [ppm] 12.89 (s, 1H), 12.01 (s, 1H), 3.37 (dd, *J* = 11.2, 3.7 Hz, 1H), 2.90 – 2.80 (m, 1H), 2.56 – 2.47 (m, 4H), 2.17 – 2.01 (m, 8H), 1.07 (d, *J* = 6.6 Hz, 12H), 0.92 (d, *J* = 8 Hz, 6H), 0.91 (s, 3H); ^{13}C{^{1}H} NMR (100 MHz, $CDCl_3$) δ 192.1, 191.0, 117.0, 61.4, 38.7, 37.5, 36.9, 31.8, 25.4, 24.3, 21.9, 21.2, 19.6. IR (neat): 2963, 2945, 2903, 1588 cm^{-1}. HRMS (ESI-TOF) calculated for $C_{22}H_{34}O_4$ $[M+H]^+$ m/z 363.2535, found 363.2530.

4,4''-(2-methylpropane-1,1-diyl)bis(5-hydroxy-1,6-dihydro-[1,1'-biphenyl]-3(2H)-one) (4e) Prepared according to General Procedure **B**, using 5-phenylcyclohexane-1,3-dione (0.27 mmol, 50 mg), triisobutylamine (0.4 mmol, 74 mg) and Eosin-Y (0.013 mmol, 9 mg). The crude reaction mixture was purified by silica gel column chromatography (pet ether/EtOAc = 95:5) to afford product **4e** (34 mg, 60%) as white solid. Melting point: 196-198 ºC. ^{1}H NMR (400 MHz, CDCl3) δ

[ppm] 12.96 (s, 1H), 12.10 (s, 1H), 7.38 – 7.29 (m, 5H), 7.26 – 7.19 (m, 5H), 3.49 – 3.45 (m, 1H), 3.27 – 3.23 (m, 1H), 3.00 – 2.78 (m, 4H), 2.76 – 2.62 (m, 4H), 2.59 – 2.54 (m, 2H), 0.92 – 0.85 (m, 6H); $^{13}C\{^{1}H\}$ NMR (100 MHz, $CDCl_3$) δ 191.1, 189.9, 142.1, 128.9, 128.7, 127.2, 126.7, 117.0, 40.7, 40.2, 38.5, 38.2, 25.5, 25.4, 22.0. IR (neat): 2964, 2958, 2944, 1583 cm^{-1}. HRMS (ESI-TOF) calculated for $C_{28}H_{30}O_4$ $[M+H]^+$ m/z 431.2222, found 431.2220. **Crystal preparation**: The crystal was grown by simple recrystallization method. The pure compound isolated after column chromatography was dissolved in dichloromethane inside a glass sample vial and layered with hexane. Then the vial was covered with parafilm and few holes were made using a needle and kept for 2 days at room temperature to get pure crystal. **Crystal data**: The single-crystal X-ray diffraction data for compound **4e** revealed a tetragonal crystal system with the space group $P4_12_12$. The unit cell parameters were determined to be a = b = 8.1138(4) Å, c = 34.075(3) Å, with angles α = β = γ = 90°, and a unit cell volume of 2243.3(3) Å³, containing Z = 4 formula units. The empirical formula is $C_{24}H_{30}O_4$, with a formula mass of 430.2144 g mol^{-1}, and a calculated density (D_{calc}) of 1.298 g cm^{-3}. The crystal appeared as a white needle and data were collected at 150 K using Mo Kα radiation (λ = 0.71073 Å). A total of 62,324 reflections were measured, from which 1,732 were independent with I > 2σ(I). The structure refinement yielded R_1 = 0.0796, wR_2 = 0.2340, and a goodness-of-fit (GoF) of 1.894. The absorption coefficient μ was 0.086 mm^{-1}, and F (000) was 928.0. Data collection was carried out up to a θ value of 25.008°.

2,2'-(propane-1,1-diyl)bis(3-hydroxycyclohex-2-en-1-one) (4f) Prepared according to General Procedure **B**, using cyclohexane-1,3-dione (0.45 mmol, 50 mg), tripropylamine (0.67 mmol, 96 mg) and Eosin-Y (0.02 mmol, 14 mg). The crude reaction mixture was purified by silica gel column chromatography (pet ether/EtOAc = 90:10) to afford product **4f** (27 mg, 46%) as white solid Melting point: 75-77 °C. ^{1}H NMR (400 MHz, $CDCl_3$) δ [ppm] 12.87 (s, 1H), 12.03 (s, 1H), 3.76 (t, *J* = 8.0 Hz, 1H), 2.54 – 2.47 (m, 4H), 2.35 – 2.26 (m, 4H), 2.04 –1.98 (m, 2H), 1.96 –1.77 (m, 4H), 0.79 (t, *J* = 7.3 Hz, 3H); $^{13}C\{^{1}H\}$ NMR (100 MHz, $CDCl_3$) δ 191.8, 191.0, 117.6, 33.5, 32.8, 32.1, 22.4, 20.1, 13.4. IR (neat): 2955, 2947, 2933, 1591 cm^{-1}. HRMS (ESI-TOF) calculated for $C_{15}H_{20}O_4$ $[M+H]^+$ m/z 265.1440, found 265.1436.

2,2'-(butane-1,1-diyl)bis(3-hydroxycyclohex-2-en-1-one) (4g) Prepared according to General Procedure **B**, using cyclohexane-1,3-dione (0.45 mmol, 50 mg), tributylamine (0.67 mmol, 124 mg) and Eosin-Y (0.02 mmol, 14 mg). The crude reaction mixture was purified by silica gel column chromatography (pet ether/EtOAc = 90:10) to afford product **4g** (25 mg, 40%) as yellow solid Melting point: 88-90 °C. ^{1}H NMR (400 MHz, $CDCl_3$) δ [ppm] 12.89 (s, 1H), 12.06 (s, 1H), 3.88 (t, *J* = 7.9 Hz, 1H), 2.53–2.46 (m, 4H), 2.35–2.26 (m, 4H), 1.98 – 1.90 (m, 4H), 1.86 – 1.78 (m, 2H), 1.22 – 1.12 (m,

2H), 0.86 (t, *J* = Hz, 3H) ; ^{13}C {^{1}H} NMR (100 MHz, $CDCl_3$) δ 191.7, 191.1, 117.8, 53.8, 33.6, 32.8, 31.4, 29.9, 29.0, 22.1, 20.9, 20.1, 14.2, 13.9 . IR (neat): 2955, 2945, 2929, 1583 cm^{-1}. HRMS (ESI-TOF) calculated for $C_{16}H_{22}O_4$ $[M+H]^+$ m/z 279.1596, found 279.1585.

2,2'-(hexane-1,1-diyl)bis(3-hydroxycyclohex-2-en-1-one) (4h) Prepared according to General Procedure **B**, using cyclohexane-1,3-dione (0.45 mmol, 50 mg), trihexylamine (0.67 mmol, 180 mg) and Eosin-Y (0.02 mmol, 14 mg). The crude reaction mixture was purified by silica gel column chromatography (petroleum ether/EtOAc = 95:5) to afford product **4h** (27 mg, 40%) as brown liquid. ^{1}H NMR (400 MHz, $CDCl_3$) δ [ppm] 12.90 (s, 1H), 12.03 (s, 1H), 3.85 (t, *J* = 7.9 Hz, 1H), 2.52 – 2.45 (m, 4H), 2.34 – 2.25 (m, 4H), 1.97 – 1.88(m, 4H), 1.33 – 1.23 (m, 6H), 0.90 – 0.81 (m, 5H); $^{13}C\{^{1}H\}$ NMR (100 MHz, $CDCl_3$) δ 190.0, 189.6, 116.6, 47.0, 46.2, 31.8, 31.1, 29.9, 29.2, 29.1, 26.5, 22.6, 14.1. IR (neat): 2957, 2937, 2906, 1594 cm^{-1}. HRMS (ESI-TOF) calculated for $C_{18}H_{26}O_4$ $[M+H]^+$ m/z 307.1909, found 307.1906.

3,4',4',6,6-pentamethyl-3,5,6,7-tetrahydro-4H-spiro[benzofuran-2,1'-cyclohexane]-2',4,6'-trione (5a) 2,2'-(ethane-1,1-diyl)bis(3-hydroxy-5,5-dimethylcyclohex-2-en-1-one) (50 mg, 0.163 mmol) (3f), I2 (42 mg, 0.326 mmol) and K_2CO_3 (46 mg, 0.33 mmol) were stirred at room temperature in acetonitrile solvent to afford product **5a** (38 mg, 77%) as white solid. Melting point: 193-195 ^{o}C. 1H NMR (400 MHz, $CDCl_3$) δ [ppm] 3.46 (q, *J* = 6.8 Hz, 1H), 2.95 (d, *J* = 14.6 Hz, 1H), 2.72 – 2.60 (m, 2H), 2.51– 2.44 (m, 3H), 2.24 – 2.14 (m, 2H), 1.23 (s, 3H), 1.17 (d, *J* = 6.8 Hz, 3H), 1.10 (d, *J* = 7.0 Hz, 6H), 0.89 (s, 3H) ; $^{13}C\{^{1}H\}$ NMR (100 MHz, $CDCl_3$) δ 199.7, 199.7, 194.1, 176.3, 114.1, 102.5, 54.4, 51.2, 50.1, 43.3, 37.2, 34.3, 30.7, 30.4, 28.7, 26.0, 15.3. HRMS (ESI-TOF) calculated for $C_{18}H_{24}O_4$ $[M+H]^+$ m/z 305.1753, found 305.1748.

3,3,6,6,9-pentamethyl-3,4,5,6,7,9-hexahydro-1H-xanthene-1,8(2H)-dione (6a) 2,2'-(ethane-1,1-diyl)bis(3-hydroxy-5,5-dimethylcyclohex-2-en-1-one) (40 mg, 0.13 mmol) and 40 mg amberlyst-15 were stirred overnight at room temperature in acetonitrile solvent to afford product **6a** (33 mg, 88%) as white solid. Melting point: 175-177 ^{o}C. ^{1}H NMR (400 MHz, $CDCl_3$) δ [ppm] 3.64 (q, *J* = 6.4 Hz, 1H), 2.35 (s, 4H), 2.27 (s, 4H), 1.62 (s, 3H), 1.09 (d, *J* = 2.2 Hz, 12H); $^{13}C\{^{1}H\}$ NMR (100 MHz, $CDCl_3$) δ 197.1, 162.7, 116.8, 51.0, 40.9, 32.1, 29.3, 27.2, 21.8, 20.9. HRMS (ESI-TOF) calculated for $C_{18}H_{24}O_3$ $[M+H]^+$ m/z 289.1803, found 289.1806.

3.7. Appendix II: Copies of ^{1}H and ^{13}C NMR spectra of representative compounds of NMR spectra

Entry	Figure No.	Data	Page No.
3a	3.6-3.7	^{1}H and ^{13}C	99
3b	3.8-3.9	^{1}H and ^{13}C	100
3e	3.10-3.11	^{1}H and ^{13}C	101
3f	3.12-3.13	^{1}H and ^{13}C	102
3g	3.14-3.15	^{1}H and ^{13}C	103
3j	3.16-3.17	^{1}H and ^{13}C	104
3p	3.18-3.19	^{1}H and ^{13}C	105
4e	3.20-3.21	^{1}H and ^{13}C	106
5a	3.22-3.23	^{1}H and ^{13}C	107
6a	3.24-3.25	^{1}H and ^{13}C	108

3.7.1. Representative examples of NMR spectra

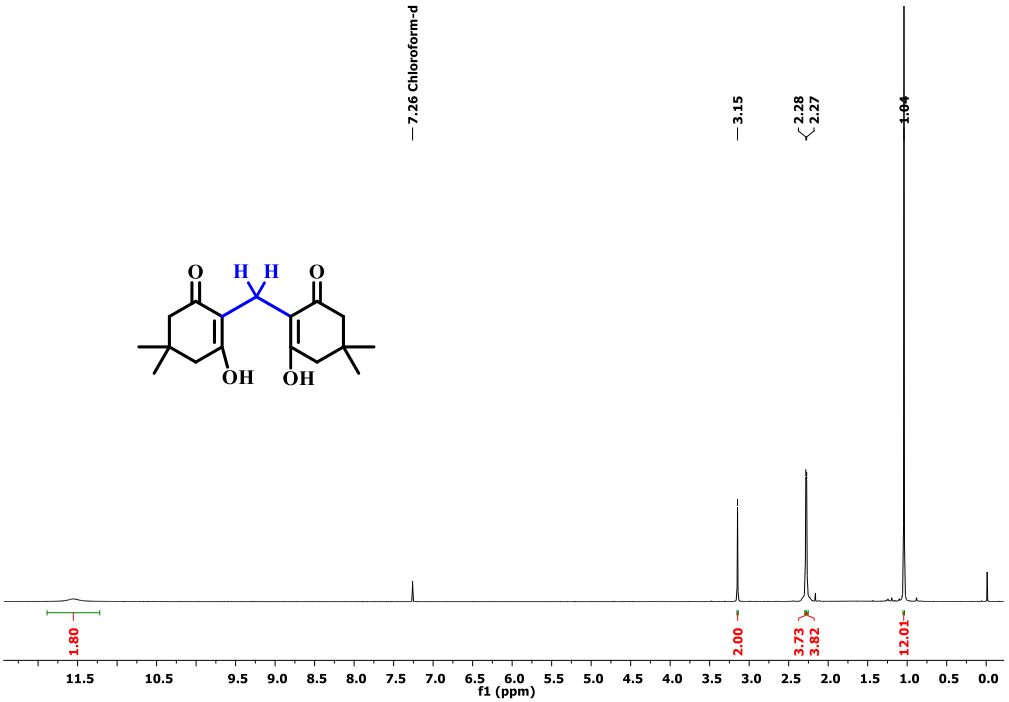


Figure 3.6: ^{1}H NMR of **3a**, 400 MHz, $CDCl_3$

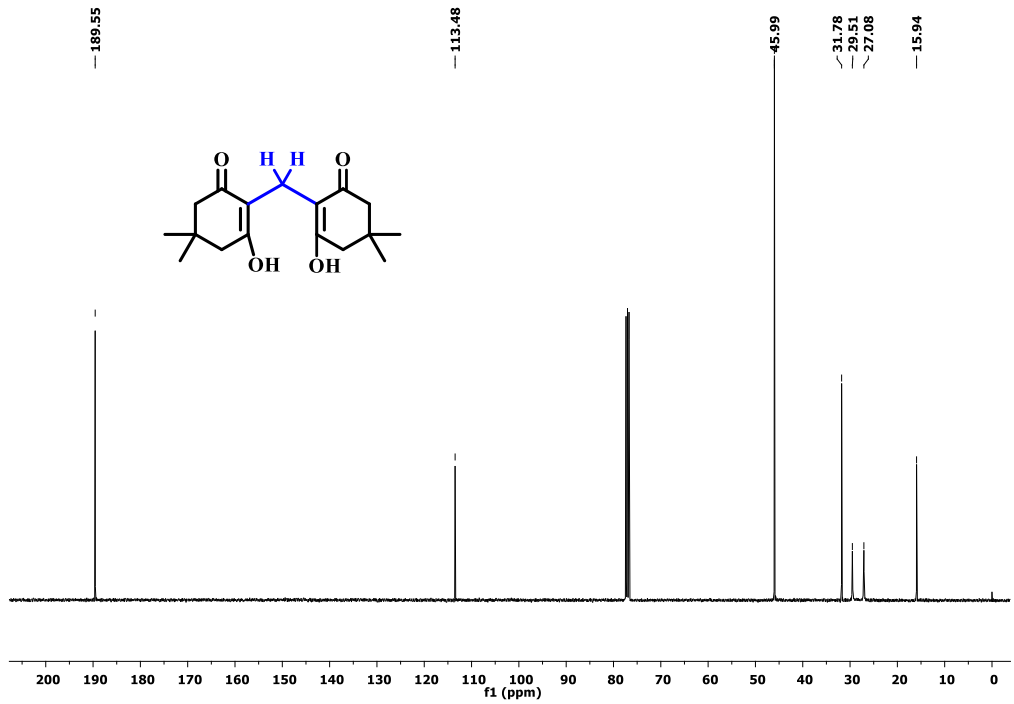


Figure 3.7: ^{13}C $\{^{1}H\}$ NMR of **3a**, 100 MHz, $CDCl_3$

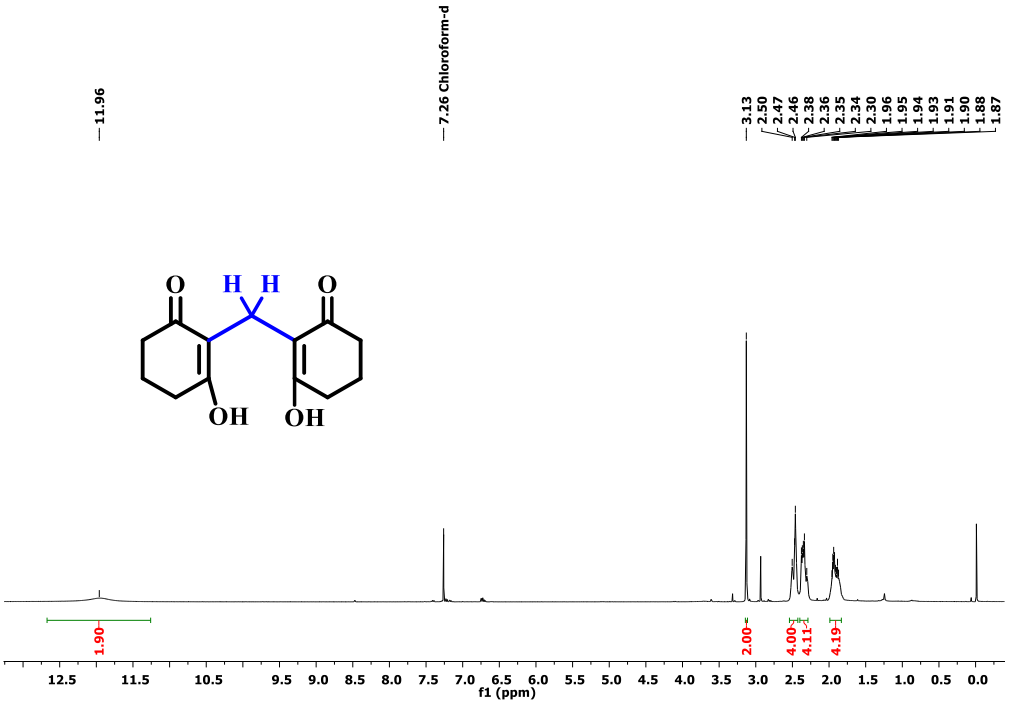


Figure 3.8: ^{1}H NMR of **3b**, 400 MHz, $CDCl_3$

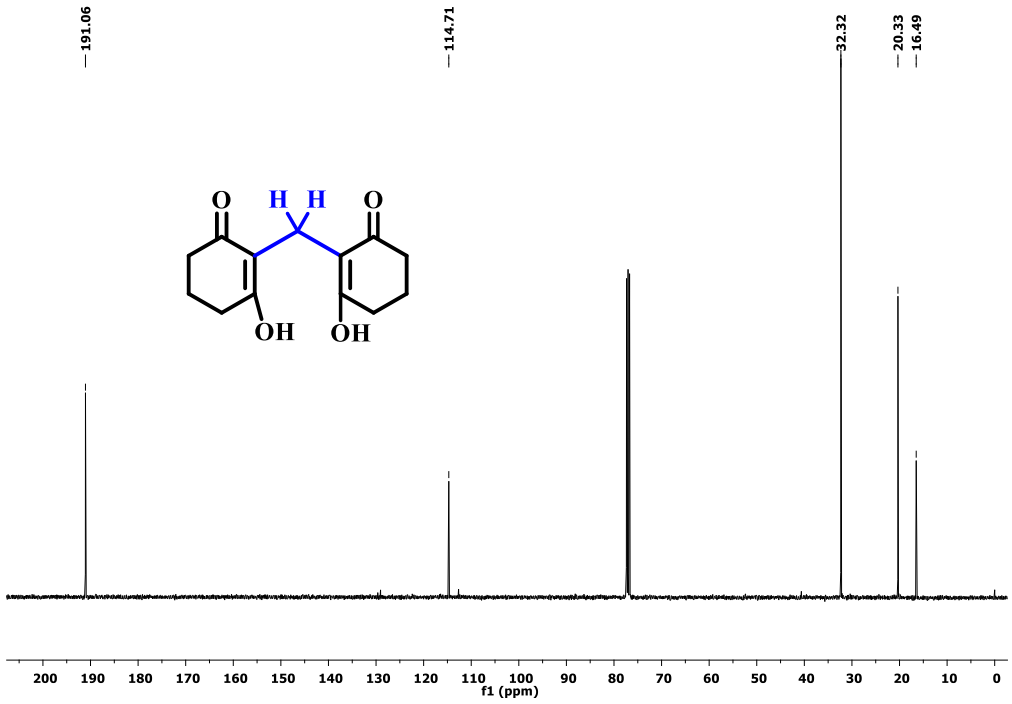


Figure 3.9: ^{13}C {^{1}H} NMR of **3b**, 100 MHz, $CDCl_3$

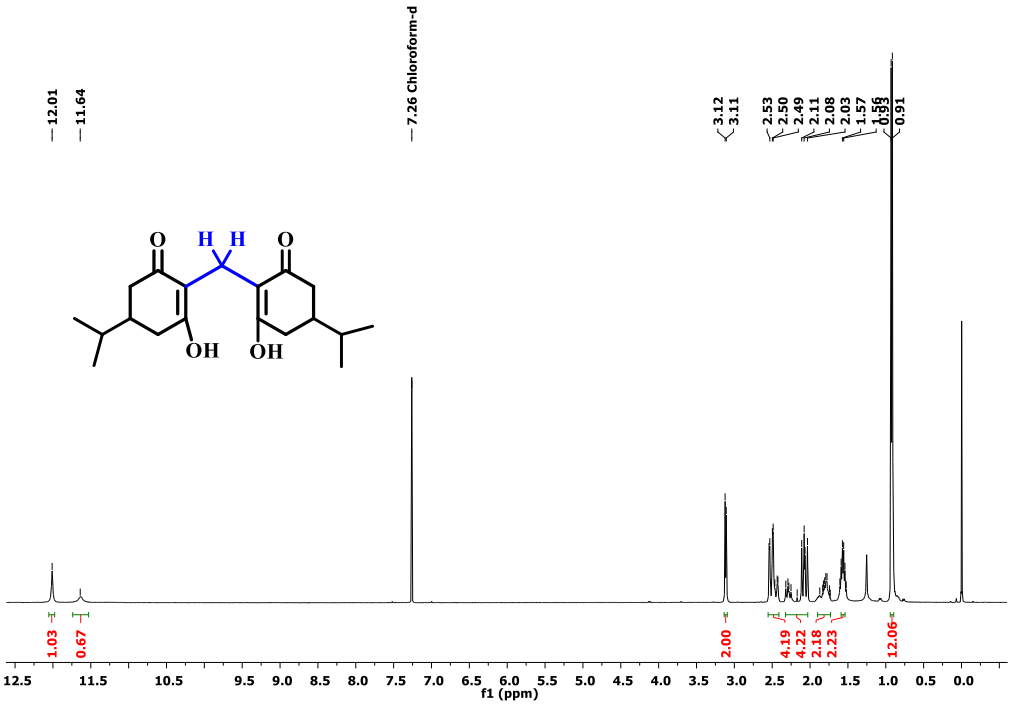


Figure 3.10: ^{1}H NMR of **3e**, 400 MHz, $CDCl_3$

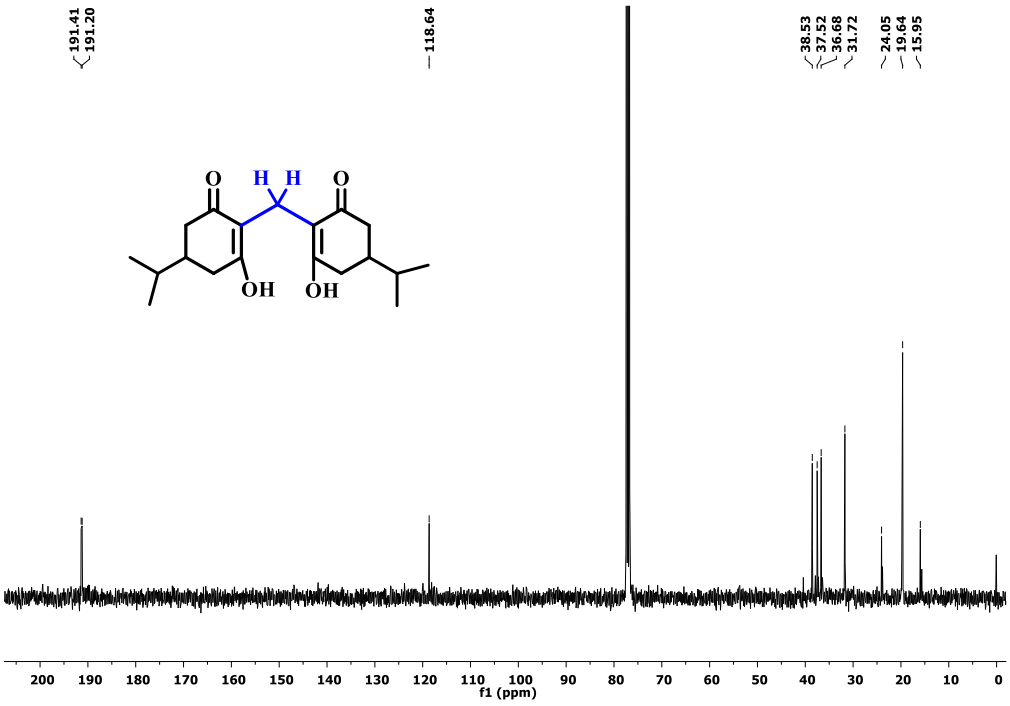


Figure 3.11: ^{13}C $\{^{1}H\}$ NMR of **3e**, 100 MHz, $CDCl_3$

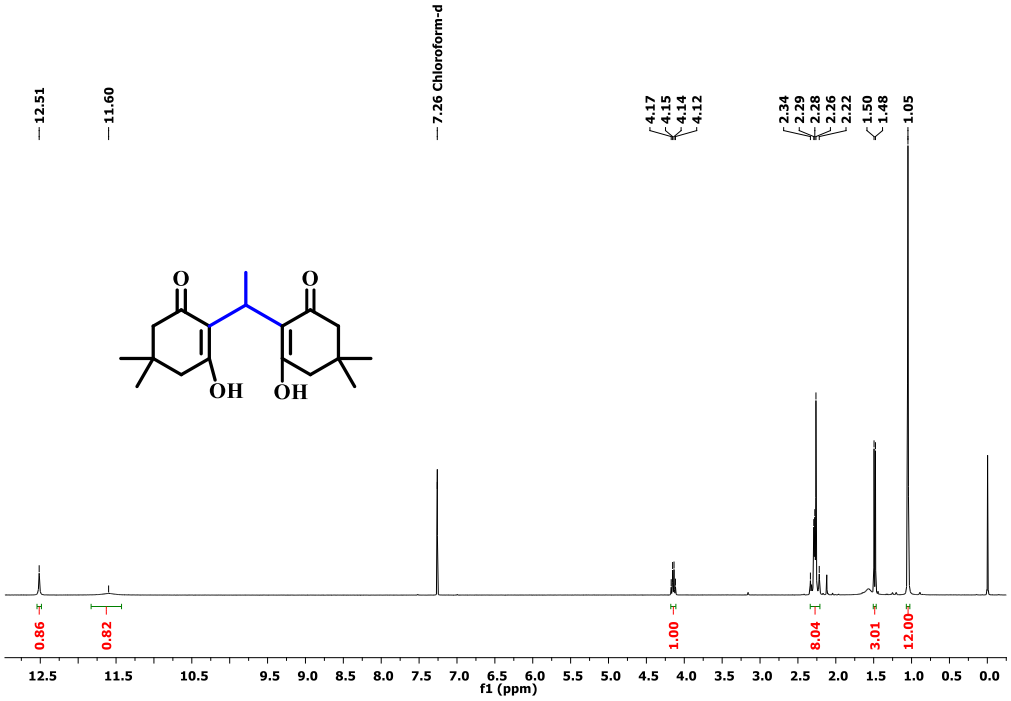


Figure 3.12: ^{1}H NMR of **3f**, 400 MHz, $CDCl_3$

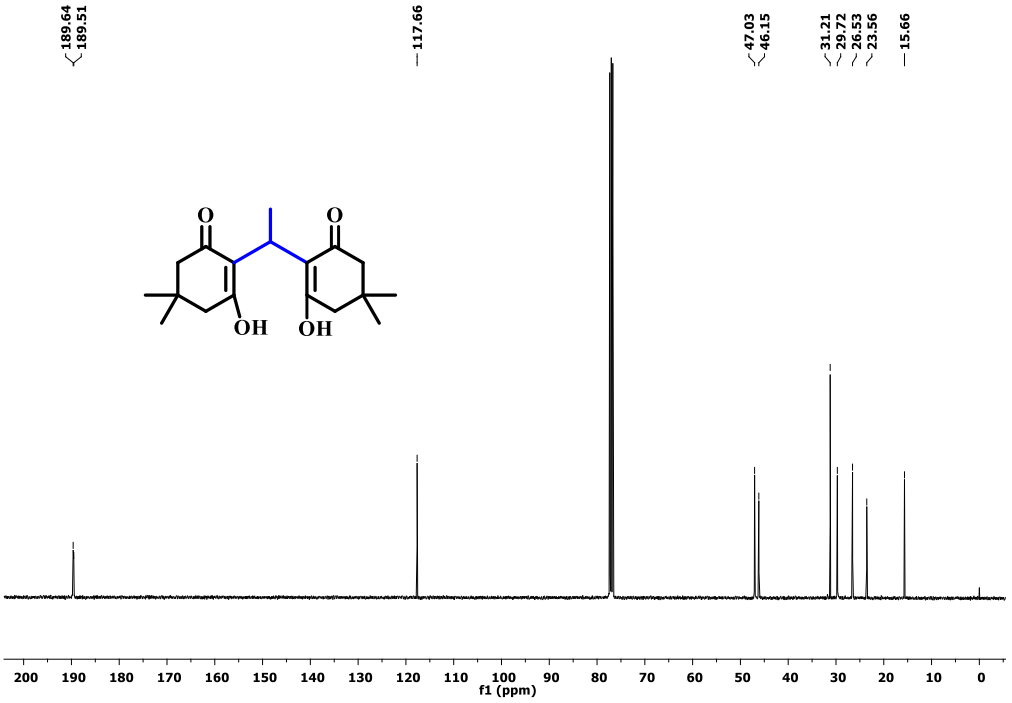


Figure 3.13: ^{13}C {^{1}H} NMR of **3f**, 100 MHz, $CDCl_3$

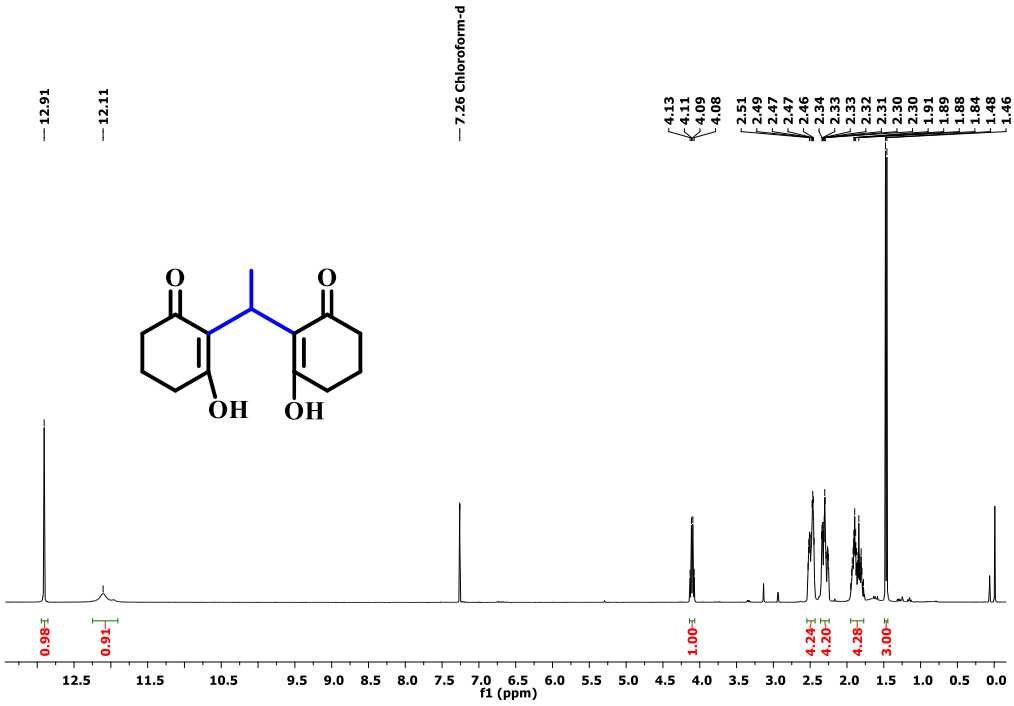


Figure 3.14: ^{1}H NMR of **3g**, 400 MHz, $CDCl_3$

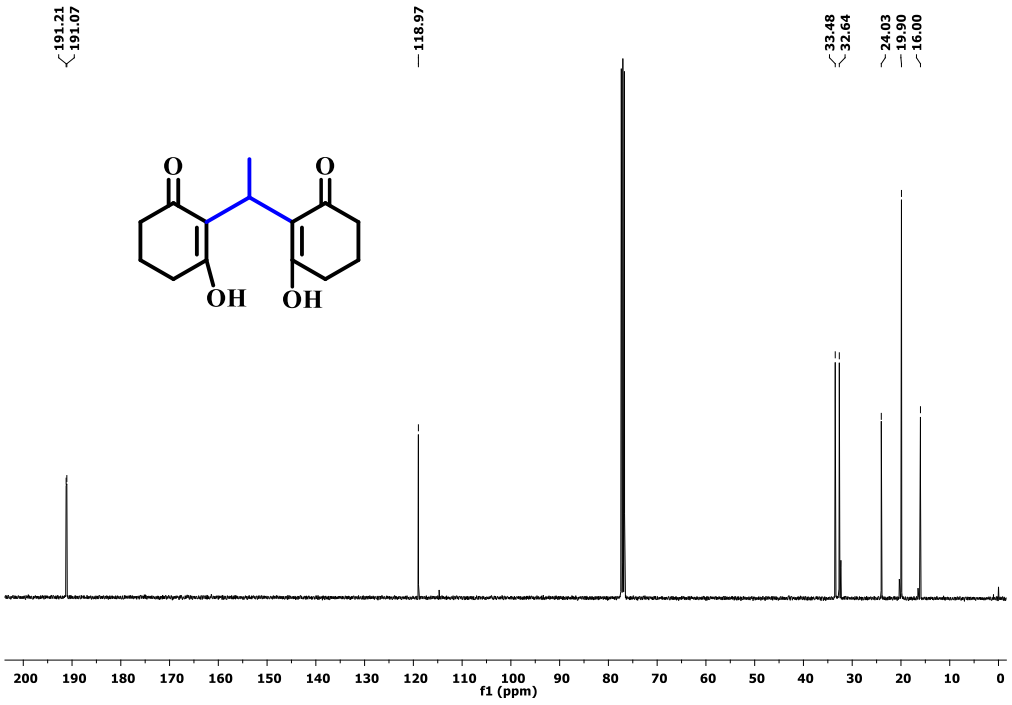


Figure 3.15: ^{13}C {^{1}H} NMR of **3g**, 100 MHz, $CDCl_3$

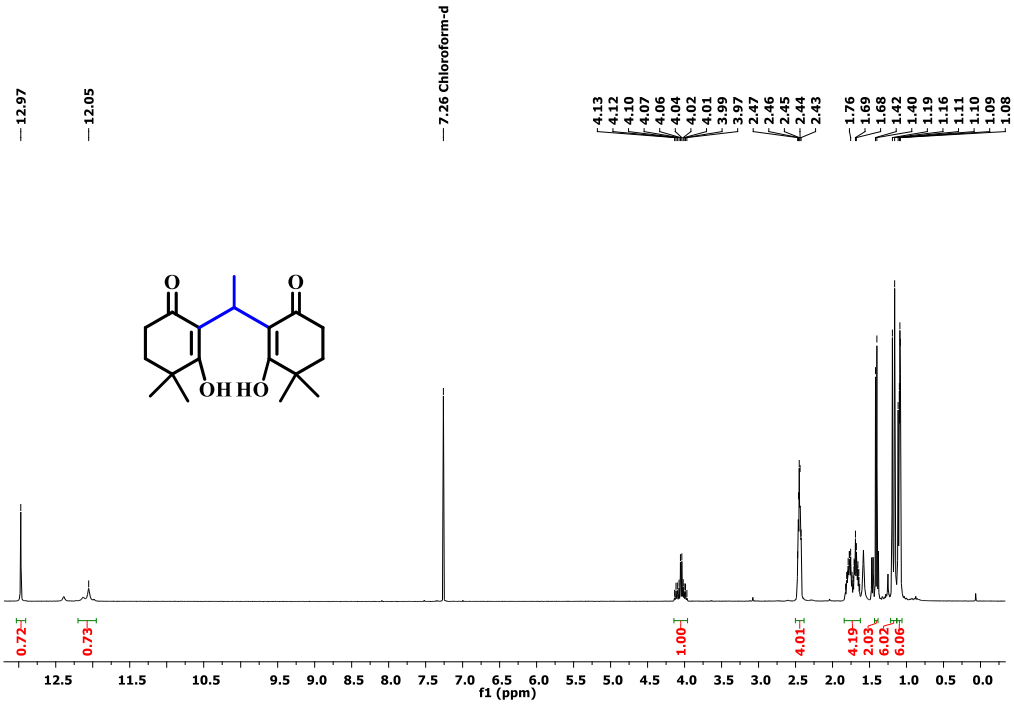


Figure 3.16: ^{1}H NMR of **3j**, 400 MHz, $CDCl_3$

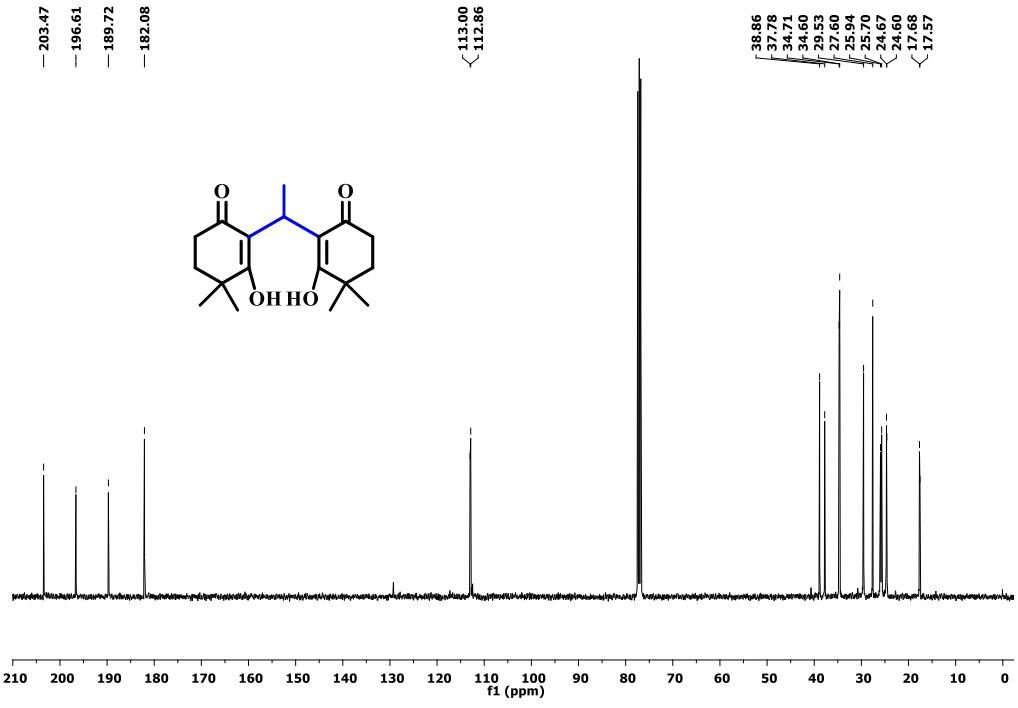


Figure 3.17: ^{13}C $\{^{1}H\}$ NMR of **3j**, 100 MHz, $CDCl_3$

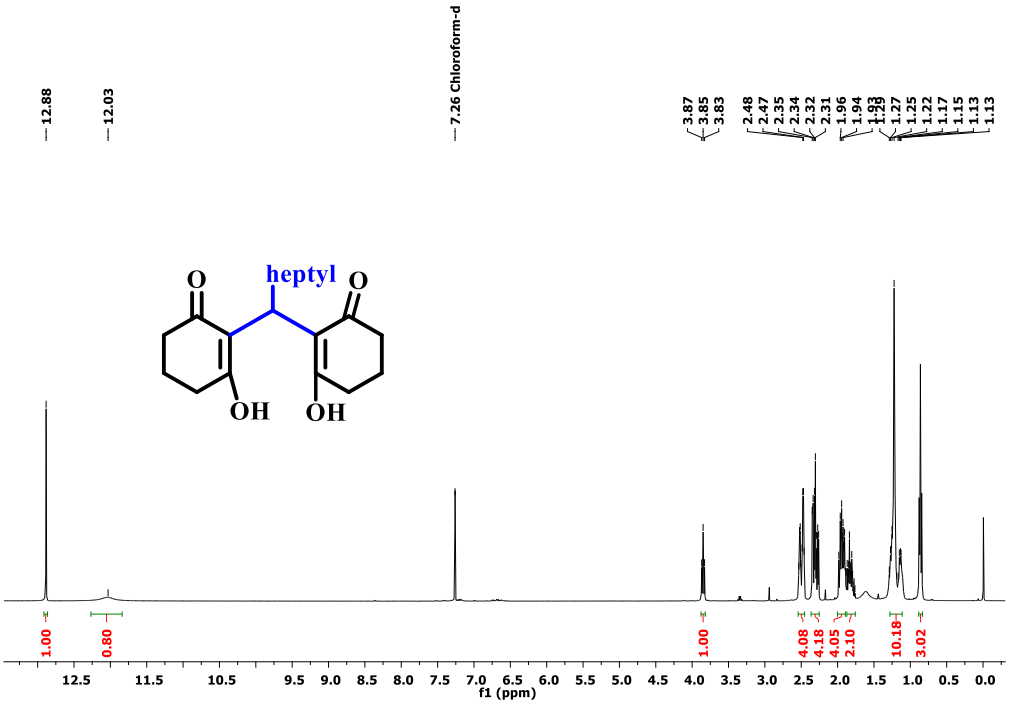


Figure 3.18: ^{1}H NMR of **3p**, 400 MHz, $CDCl_3$

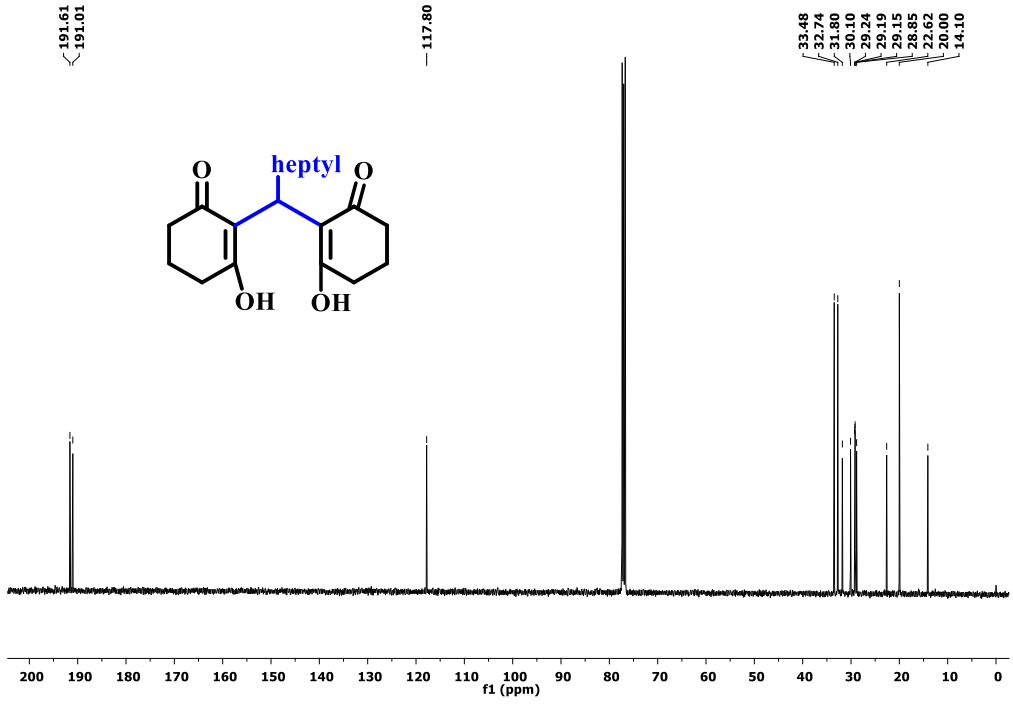


Figure 3.19: ^{13}C $\{^{1}H\}$ NMR of **3p**, 100 MHz, $CDCl_3$

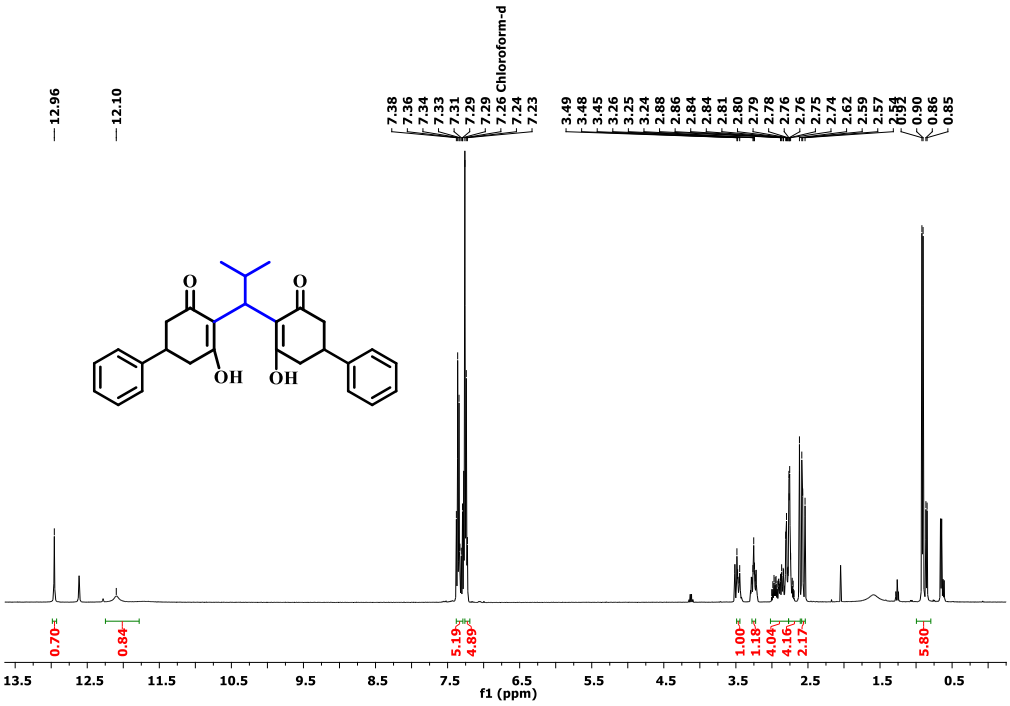


Figure 3.20: ^{1}H NMR of **4e**, 400 MHz, $CDCl_3$

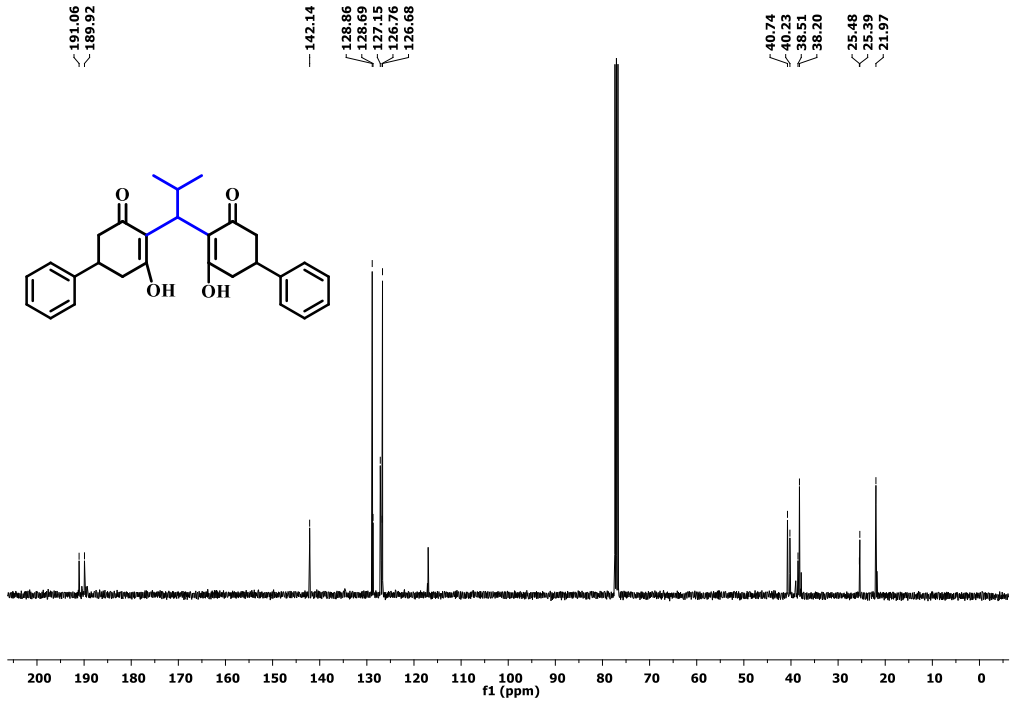


Figure 3.21: ^{13}C $\{^{1}H\}$ NMR of **4e**, 100 MHz, $CDCl_3$

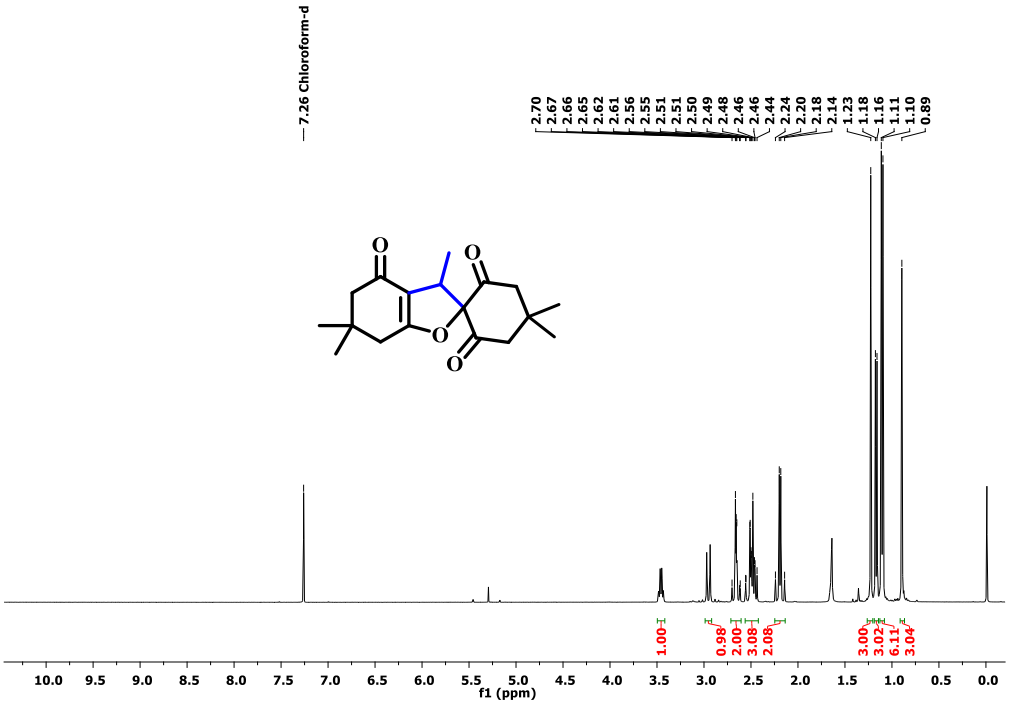


Figure 3.22: ^{1}H NMR of **5a**, 400 MHz, $CDCl_3$

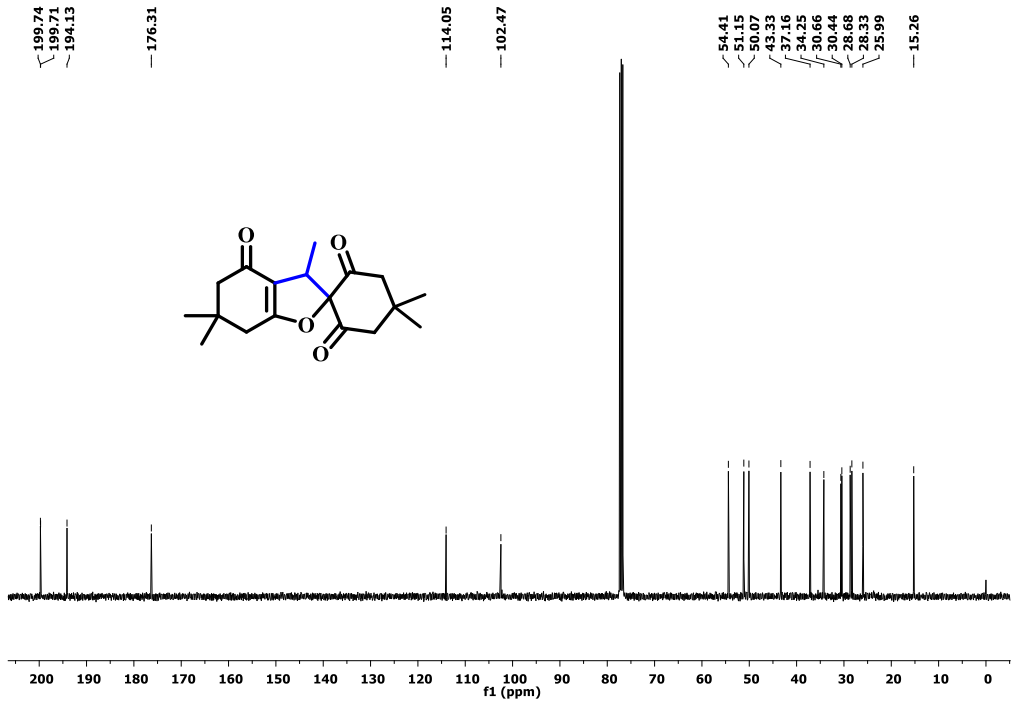


Figure 3.23: ^{13}C {^{1}H} NMR of **5a**, 100 MHz, $CDCl_3$

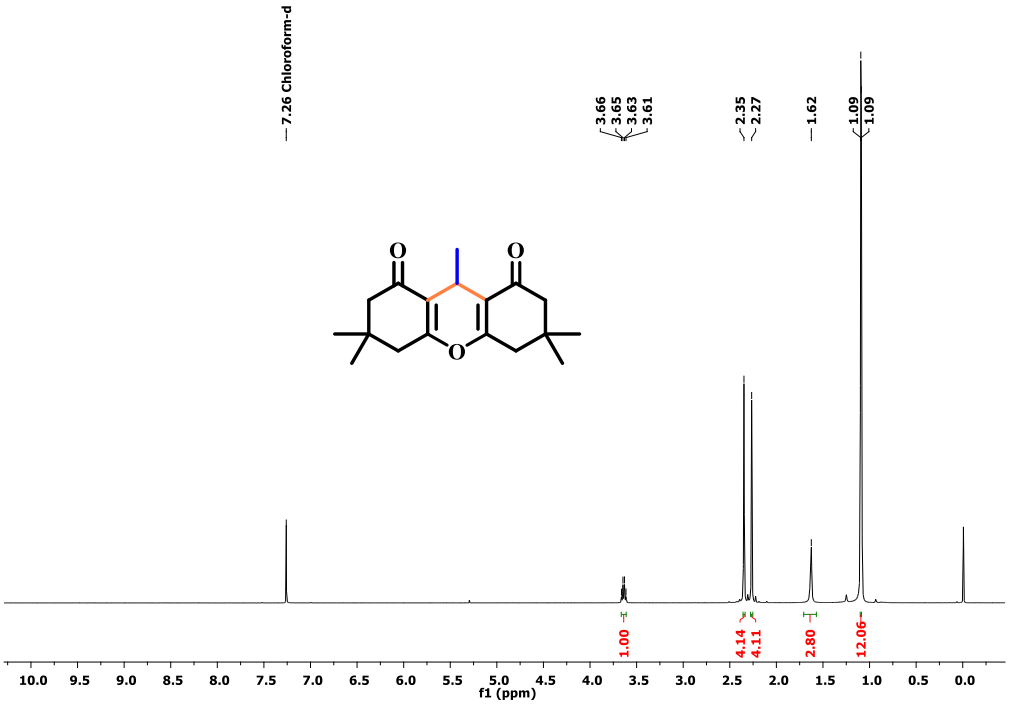


Figure 3.24: ^{1}H NMR of **6a**, 400 MHz, $CDCl_3$

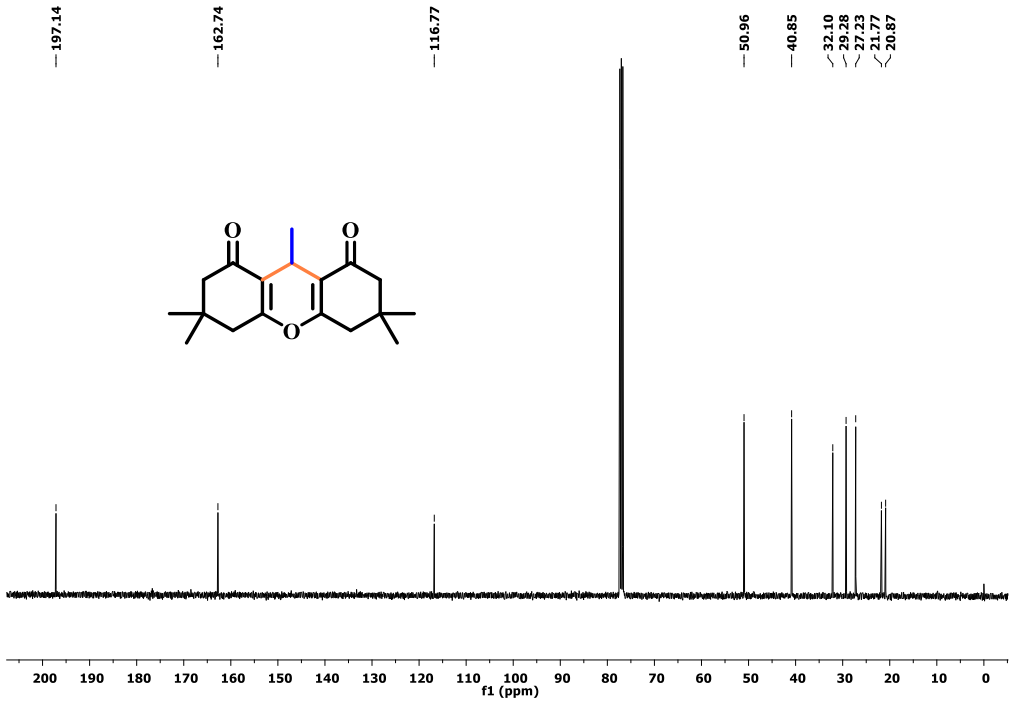


Figure 3.25: ^{13}C $\{^{1}H\}$ NMR of **6a**, 100 MHz, $CDCl_3$

3.7.2 GCMS Analysis

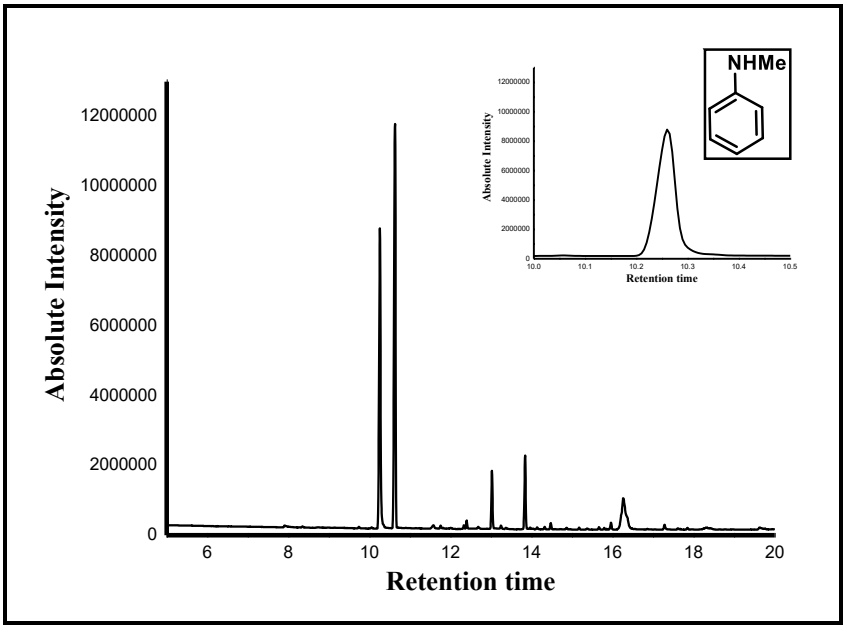


Figure 3.26 GC-MS data of reaction mixture

3.7.3. SCXRD Data

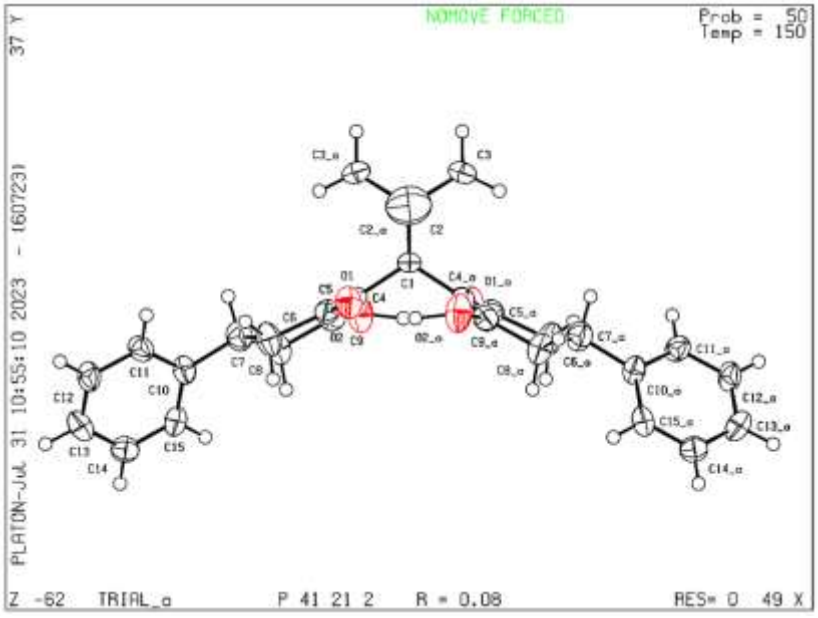


Figure 3.27: ORTEP image of **3p** at 50% probability level

3.8. References:

(1) Crisenza, G. E. M.; Melchiorre, P. *Nat. Commun*. **2020**, *11*, 803.

(2) Xuan, J.; Xiao, W.-J. Visible-Light Photoredox Catalysis. *Angew. Chem., Int. Ed.* **2012**, *51*, 6828–6838.

(3) Douglas, J. J.; Sevrin, M. J.; Stephenson, C. R. J. *Org. Process Res. Dev.* **2016**, *20*, 7, 1134–1147.

(4) Nicholls, T. P.; Leonori, D.; Bissember, A. C. *Nat. Prod. Rep*. **2016**, *33*, 1248–1254.

(5) Kärkäs, M. D.; Porco, J. A., Jr.; Stephenson, C. R. J. *Chem. Rev.* **2016**, *116*, 9683–9747.

(6) Steinhilber, D. *Curr Med Chem.***1999**, *6*, 71 – 85.

(7) Khan, K. M.; Maharvi, G. M.; Khan, M. T. H.; Shaikh, A.J.; Perveen, S.; Begum, S.; Choudhary, M. I. *Bioorg. Med. Chem*. **2006**, *14*, 344-351.

(8) Steinhilber, D. *Curr Med Chem.***1999**, *6*, 71 – 85.

(9) Nie, D.; Honn, K.V. *Cell Mol Life Sci.* **2002**, *59*, 799 – 807.

(10) Schneider, I.; Bucar, F. *Phytother Res.* **2005**,*19*, 81-102.

(11) Maharvi, G.M.; Ali, S.; Riaz, N.; Afza, N.; Malik, A.; Ashraf, M.; Iqbal, L.; Lateef. M. *J. Enzyme Inhib. Med. Chem*. **2008**, *23*, 62 - 69.

(12) Patel, M.S.; Parekh, J. N.; Chudasama, D. D.; Patel, H. C.; Dalwadi, P.; Kunjadiya, A.; Bhatt, V.; Ram, K. R. *ACS Omega.* **2022**, *7*, 34, 30420 – 30439.

(13) Kantevari, S.; Bantu, R.; Nagarapu, L. *J. Mol. Catal. A Chem.* **2007**, *269*, 53–57.

(14) Saha, M.; Pal, A. K.; Nandi, S. *RSC Adv.* **2012**, *2*, 6397–6400.

(15) Maleki, B.; Raei, M.; Alinezhad, H.; Tayebee, R.; Sedrpoushan, A. *Org. Prep. Proced. Int.* **2018**, *50*, 288–300.

(16) Attar, S. R.; Shinde, B.; Kamble, S. B. *Res Chem Intermed.* **2020**, *6*, 4723–4748.

(17) Anastas, P. T.; Warner, J. C. Green Chemistry: Theory and Practice; *Oxford University Press*: Oxford, 1998.

(18) Rafiee, E.; Rahpeima, N.; Eavani, S. Catalysis in Green Chemistry: Focus on Catalyst Design and Sustainability. *Catal. Rev.* **2021**, *63* (3), 266–324.

(19) Arends, I. W. C. E.; Sheldon, R. A. Modern Oxidation Reactions and Green Chemistry. *Catal. Today* **2002**, *77*, 405–418.

(20) Pawar, H. S.; Wagh, A. S.; Lali, A. M. *New J. Chem*. **2016**, *40*, 4962–4968.

(21) Ghosh, I.; Ghosh, T.; Bardagi, J. I.; König, B. *Science.* **2014**, *346*, 725−728.

(22) Jadhav, S.; Bakshi, D.; Singh. A. *J. Org. Chem*. **2015**, *80*, 10187–10196.

(23) Miyake. Y.; Nakajima. K.; Nishibayashi. Y. *J. Am. Chem.Soc.* **2012**, *134*, 3338−3341.

(24) Zheng, L.; Jiang, Q.; Bao, H.; Zhou, B.; Luo, S. P.; Jin, H.; Wu, H.; Liu, Y. *Org. Lett.* **2020**, *22*, 8888– 8893.

(25) Fang, L.; Ye, Z. P.; Hu, Y. Z.; Gao, J.; Zheng, L.; Chen, K.; Xiang, H. Y.; Chen, X. Q.; Yang, H. *J. Org. Chem.* **2021**, *86*, 11905−11914.
(26) Arumugam, A.; Palani, P.; Anandan, M.; Nutalapati, V.; Senadi, G. C. Metal-Free, *Eur. J. Org. Chem.* **2023**, *2023* (12), e202300100.
(27) Das, P.; Begam, H. M.; Bhunia, S. K.; Jana, R. *Adv. Synth. Catal.* **2019**, *361*, 4048−4054.
(28) Lipilin, D. L.; Frumkin, A. E.; Tyurin, A. Y.; Levin, V. V.; Dilman, A. D. *Molecules.* **2021**, *26*, 3323.
(29) Liu, C.; Chen, H.-N.; Xiao, T.-F.; Hu, X.-Q.; Xu, P.-F.; Xu, G.-Q. *Chem. Commun.* **2023**, *59*, 2003–2006.
(30) Zhang, Y.; Schilling, W.; Riemer, D.; Das, S. *Nat. Protoc.* **2020**, *15* (3), 822–839.
(31) Srivastava, V.; Singh, P. K.; Singh, P. P. *Tetrahedron Lett*. **2018**, *59*, 40–43.
(32) Cohen, I.; Mishra, A. K.; Parvari, G.; Edrei, R.; Dantus, M.; Eichena, Y.; Szpilman, A. M. *Chem. Commun.* **2017**, *53*, 10128–10131.
(33) Liu, H.; Zhao, L.; Yuan, Y.; Xu, Z.; Chen, K.; Qiu, S.; Tan, H. *ACS Catal*. **2016**, *6*, 1732–1736.
(34) McCallum, T.; Barriault, L. *J. Org. Chem*. **2015**, *80*, 2874–2878.
(35) Sheldon, R. A. *Chem. Soc. Rev*. **2012**, *41*, 1437–1451.
(36) Oelgemöller, M. *Chem. Rev*. **2016**, *116* (17), 9664–9682.
(37) Li, X.; Wang, Z.; Zhang, Y.; Liu, H.; Chen, Y.; Yang, S. *ACS Sustainable Chem. Eng.* **2022**, *10*, 12345–12356.
(38) Yi, X.; Lei, S.; Liu, W.; Che, F.; Yu, C.; Liu, X.; Wang, Z.; Zhou, X.; Zhang, Y. *Org. Lett.* **2020**, *22*, 4583−4587.
(39) Beatty, J. W.; Stephenson, C. R. J. *Acc. Chem. Res.* **2015**, *48*, 5, 1474–1484.
(40) Romero, N. A.; Nicewicz, D. A. Organic Photoredox Catalysis. *Chem. Rev*. **2016**, *116* (17), 10075–10166.
(41) Hari, D. P.; König, B. *Chem. Commun*. **2014**, *50* (51), 6688–6699.
(42) Majek, M.; Filace, F.; Jacobi von Wangelin, A. *Beilstein J. Org. Chem*. **2014**, *10*, 981–989.
(43) Hazebroucq, S.; Labat, F.; Lincot, D.; Adamo, C. *J. Phys. Chem. A.* **2008**, *112* (31), 7264–7270.
(44) Mohanta, N.; Nair, K.; Sutar, D. V.; Gnanaprakasam, B. *React. Chem. Eng.* **2020**, *5*, 1501–1508.
(45) Srivastava, S. K.; Chauhan, P. M. S.; Bhaduri, A. P. *Syn. Comm*., **1999**, *29*, 12, 2085-2091.

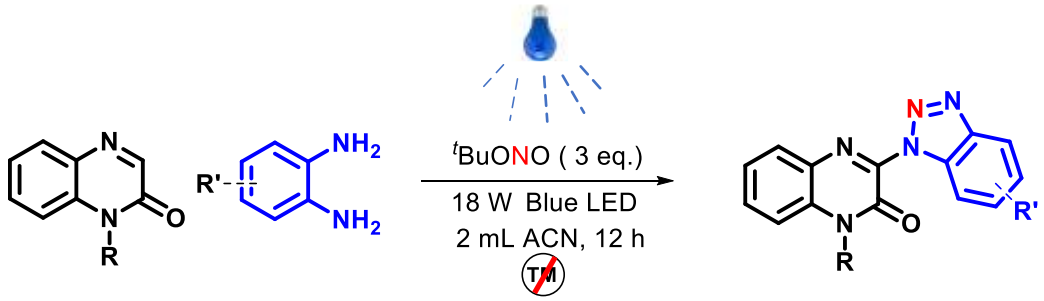
Chapter 4

Visible Light Induced Sequential Nitrogen Insertion and C-H Benzotriazolation of Quinoxaline-2(1*H*)-ones

Visible Light Induced Sequential Nitrogen Insertion and C-H Benzotriazolation of Quinoxaline-2(1*H*)-ones

4.1. Abstract

In this chapter, we have reported a mild and efficient visible light-mediated one-pot sequential reaction that involves the in situ generation of benzotriazole from benzene-1,2-diamine and *tert*-butyl nitrite via nitrogen insertion, followed by cross-coupling at C-3 position of quinoxaline-2(1*H*)-ones through sp^2 C–N bond formation. This metal-free protocol operates under environmentally beinign conditions without using high temperature, transition metal catalyst. The developed protocol demonstrates broad functional group tolerance and has been generalized with 36 examples, achieving yields of up to 80%.



4.2. Introduction

The quinoxaline-2(1*H*)-one moiety is a privileged heterocyclic scaffold with broad applications in medicinal chemistry.[1-3] The C-3 position of quinoxaline-2(1*H*)-ones serves as a reactive center for various functionalization reactions. Substitution at this position with diverse functional groups has been shown to impart a wide range of biological activities, including antifungal, aldose reductase inhibitory, antimicrobial, and histamine-4-receptor antagonistic properties (Figure 4.1).[4-8] The significant biomedical potential of these compounds has driven the development of numerous strategies to synthesize structurally diverse C-3 functionalized quinoxalinones.[9-13] However, most of the existing methods require high temperatures, transition metal catalysts, and harsh reaction conditions. In contrast, photochemical approaches offer a sustainable and energy-efficient alternative to traditional methods.[14] In response to the demand for efficient and atom-economical transformations, several research groups have explored the photochemical functionalization of the C-3 position of quinoxaline-2(1*H*)-ones.[15-19]

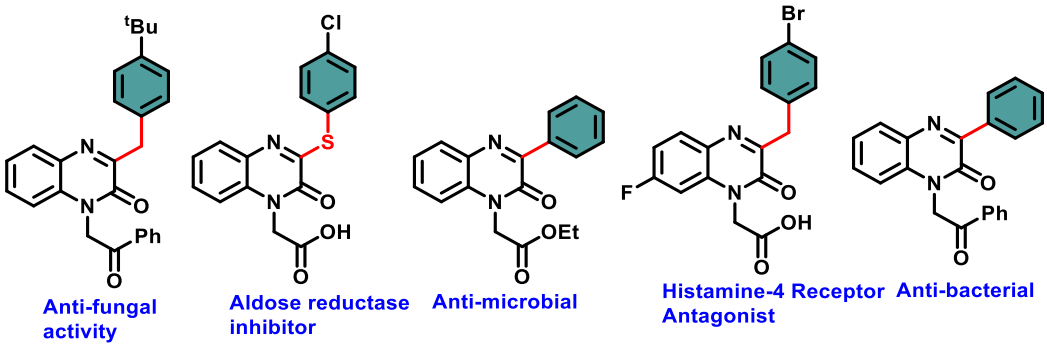
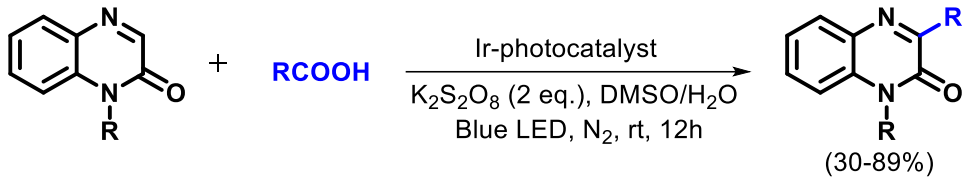


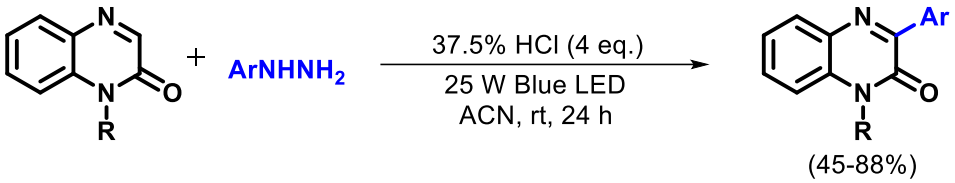
Figure 4.1: Representative examples of bioactive quinoxalinones

Li *et al*. developed an efficient visible-light-mediated C-3 alkylation of quinoxalin-2(1*H*)-ones employing iridium-based photoredox catalysis, where alkyl radicals were generated in situ from readily available carboxylic acids via oxidative decarboxylation (Scheme 4.1).[20]



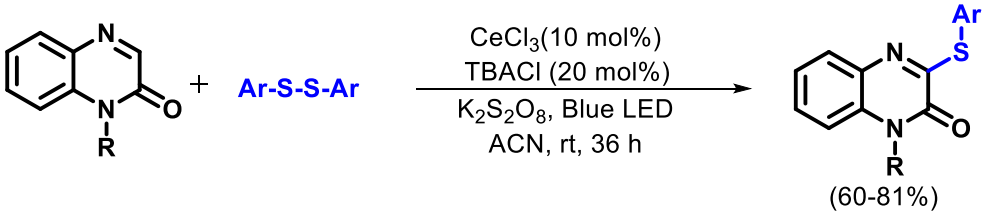
Scheme 4.1: Ir-photocatalyzed C-H alkylation of quinoxalinones

In a mechanistically distinct protocol, Wang *et al.* have developed a HCl photosentized reaction for C-3 arylation of quinioxalinones utilizing aryl hydrazenes as the source of aryl group (Scheme 4.2).[21]



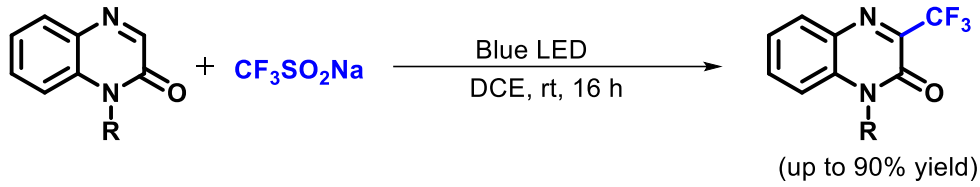
Scheme 4.2: Photochemical C-H arylation of quinoxalinones

Shen *et al.* have established a charge-transfer enabled external-catalyst free and redox-neutral process C-3 thioetherification method for quinoxalinones (Scheme 4.3).[22]



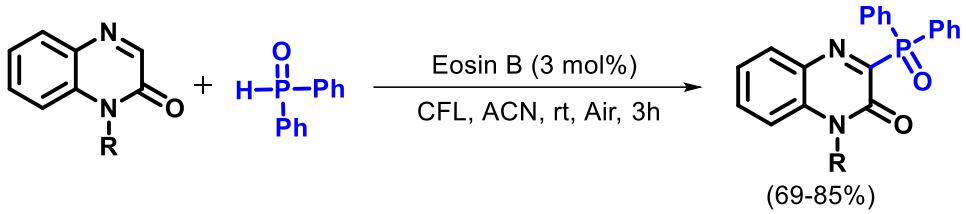
Scheme 4.3: Charge transfer mediated C-H thioetherification of quinoxalinones

In the realm of fluorine-based functional group incorporation, *Jin et al*. have shown catalyst free photochemical trifluoromethylation of quinoxalinones using sodium trifluoromethanesulfinate as the source of trifluoromethyl group (Scheme 4.4).[23]



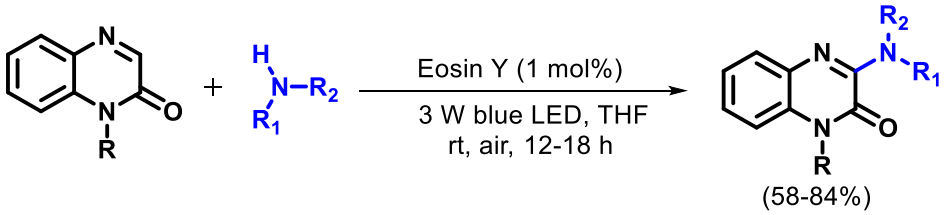
Scheme 4.4: Photochemical C-H trifluoromethylation of quinoxalinones

Kim et. al has established a photoredox catalyzed C-H phosphorylation strategy at C-3 position of quinoxalinones (Scheme 4.5).[24] The methodology employed a phosphorus-based nucleophile and proceeded via radical generation through oxidative quenching of the excited-state photocatalyst.



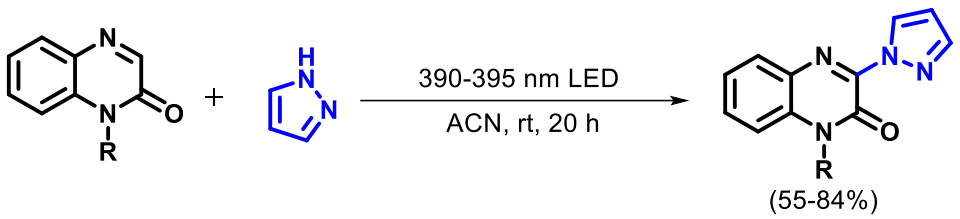
Scheme 4.5: Photocatalyzed C-H phosphorylation of quinoxalinones

However, achieving C–N bond formation at the C-3 position of quinoxaline-2(1*H*)-one remains a significant challenge under conventional reaction conditions. Nonetheless, a few studies have explored visible light-mediated strategies for C–N bond construction through careful selection of coupling partners and reagents. In this connection, Wang *et al.* developed an Eosin Y-catalyzed amination of quinoxalinones using aliphatic amines (Scheme 4.6).[25]



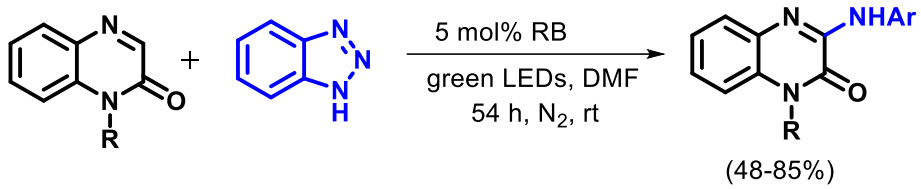
Scheme 4.6: Photocatalyzed C-H phosphorylation of quinoxalinones

In another notable advance, Li *et al*. reported a catalyst-free photochemical azolation of quinoxaline-2(1*H*)-ones via C–N bond formation under green light irradiation (Scheme 4.7).[26]



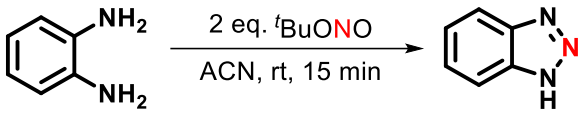
Scheme 4.7: Photocatalyzed C-H azolation of quinoxalinones

More recently, Yi *et al.* demonstrated a photoredox-catalyzed aminoarylation of quinoxalinones through a denitrogenative 1,3-shift mechanism (Scheme 4.8).[27]



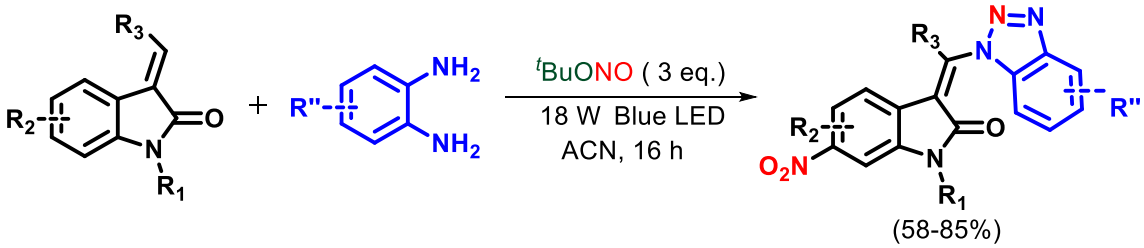
Scheme 4.8: Photocatalyzed denitrogenative amination of quinoxalinones

However, attempts to functionalize the C-3 position of quinoxalinones with benzotriazole were unsuccessful in that study. Recently, Nidhi *et al.* developed an efficient visible light-driven method for the coupling of quinoxalinones with carbazoles and amides.[28] In this regard, we hypothesised to couple quinoxaline and benzotriazole scaffold to obtain benzotriazolated quinoxalinones. From literature survey, we found an interesting report by Kandasamy *et al*. for the nitrogen insertion to form benzotriazoles from *o*-phenylenediamines using *tert*-butyl nitrite (Scheme 4.9).[29]



Scheme 4.9: Nitrogen atom insertion in *o*-phenylenediamine to form benzotriazole

Inspired by this transformation, a photochemical strategy was later developed for the simultaneous benzotriazolation and nitration of arylidene-2-oxindoles under visible light irradiation (Scheme 4.10).[30]



Scheme 4.10: Photoinduced concomitant nitration and benzotriazolation

We hypothesized that if we employ this same protocol with quinoxalinones, we can end up with benzotriazolated quinoxalinone scaffolds which could also show manifold biomedical and

agricultural applications.[31-37] To the best of our knowledge, the photochemical benzotriazolation of quinoxalinones has not yet been explored. In this context, we envisioned generating benzotriazole in situ and couple it across the imine bond of quinoxalinones to achieve the visible light-induced benzotriazolation of quinoxalinones. Thus, we have developed a mild, visible light-mediated protocol for the direct benzotriazolation of quinoxalinones via nitrogen insertion, employing *tert*-butyl nitrite as the N_1 synthon. This method enables selective C–N bond formation at the C-3 position while effectively suppressing side reactions. The key advantages of this approach include step and atom economy, convenient operation under ambient temperature conditions, avoidance of metal catalysts, exclusion of hazardous halogenated solvents and overall sustainability and energy efficiency.

4.3. Result and Discussion

To carry out our investigation, we optimized the light source and reaction conditions in support of our proposed hypothesis (Table 4.1). When *N*-methylquinoxalinone (1 eq.), *o*-phenylenediamine (1 eq.), and *tert*-butyl nitrite (3 eq.) were irradiated under an 18 W blue LED in acetonitrile for 12 h, the desired benzotriazolated product **3a** was obtained in 80% yield. To assess the influence of light intensity, the reaction was repeated using a 9 W blue LED, which resulted in a reduced yield of 64% for product **3a**.

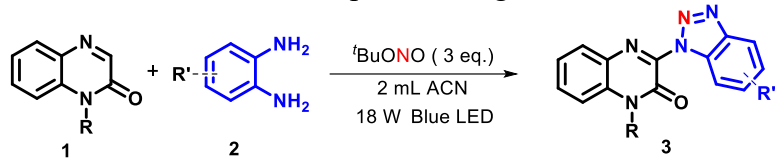
Table 4.1: Optimization of reaction

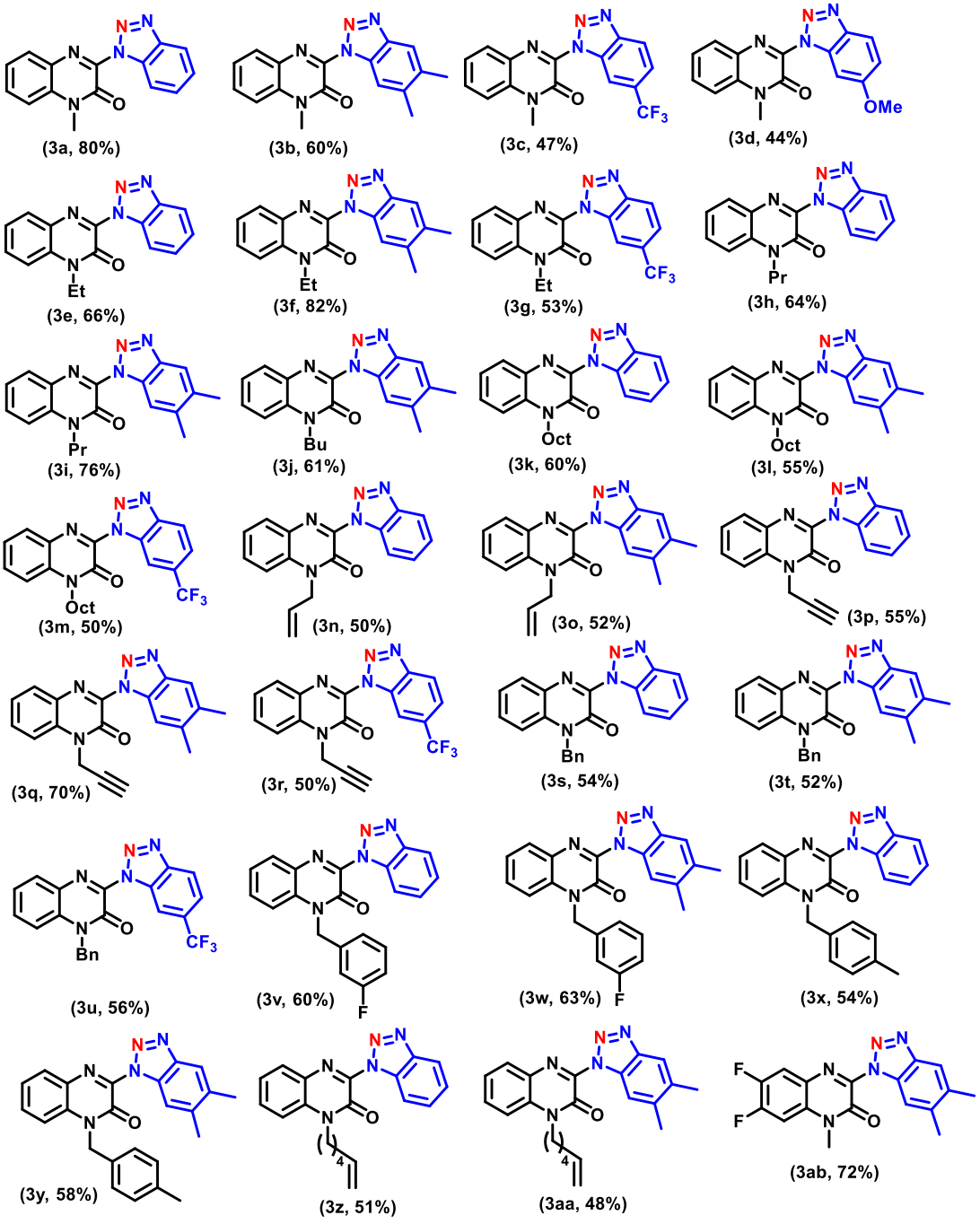


Sr. No.	Deviation From Standard Condition	Yield of 3a (%)
1	9 W instead of 18 W	64
2	30 W instead of 18 W	80
3	DCE instead of ACN	56
4	1,4-dioxane instead of ACN	37
5	*tert*-BuOH instead of ACN	65
6	DMF instead of ACN	35
7	Toluene instead of ACN	22

Reaction conditions: **1a** (0.25 mmol), **2a** (0.25 mmol) and TBN (0.75 mmol) were irradiated for 12 h

No improvement in yield was observed upon increasing the light intensity to a 30 W blue LED. Screening of alternative solvents, including 1,2-dichloroethane (DCE), 1,4-dioxane, *tert*-butanol, DMF, and toluene, resulted in a significant decrease in product yield. Notably, benzotriazole was formed quantitatively in situ from *o*-phenylenediamine when acetonitrile (ACN) was used as the solvent, highlighting its critical role in the transformation. Thus, ACN was identified as the optimal solvent, with 18 W blue LED irradiation as the preferred light source.

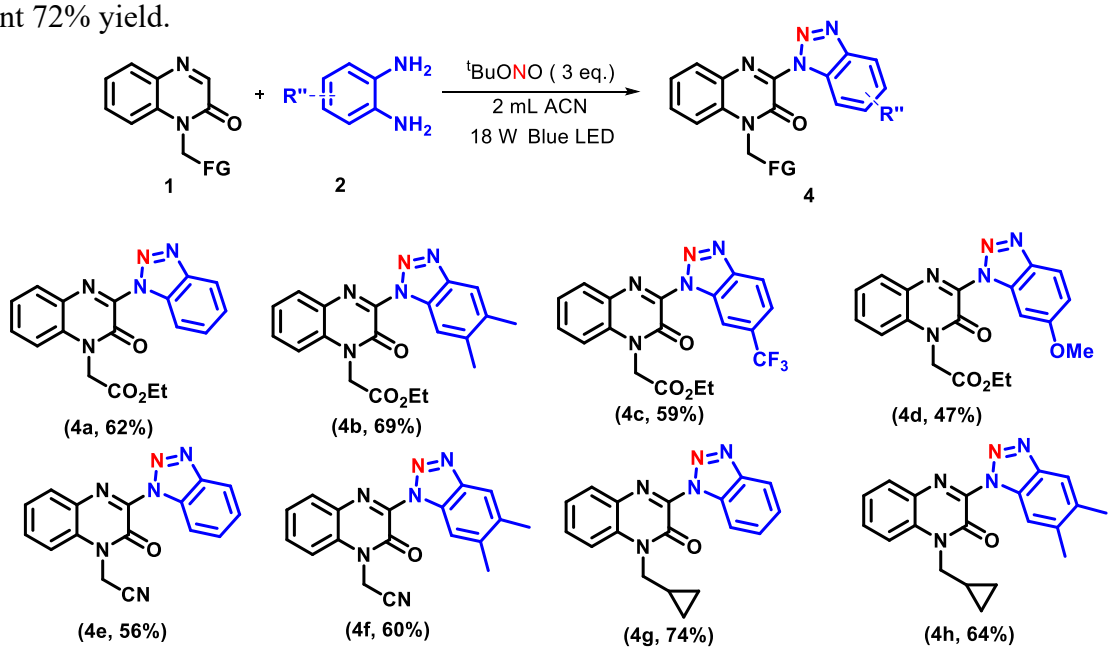




Scheme 4.11: Substrate scope for benzotriazolation of quinoxalinones

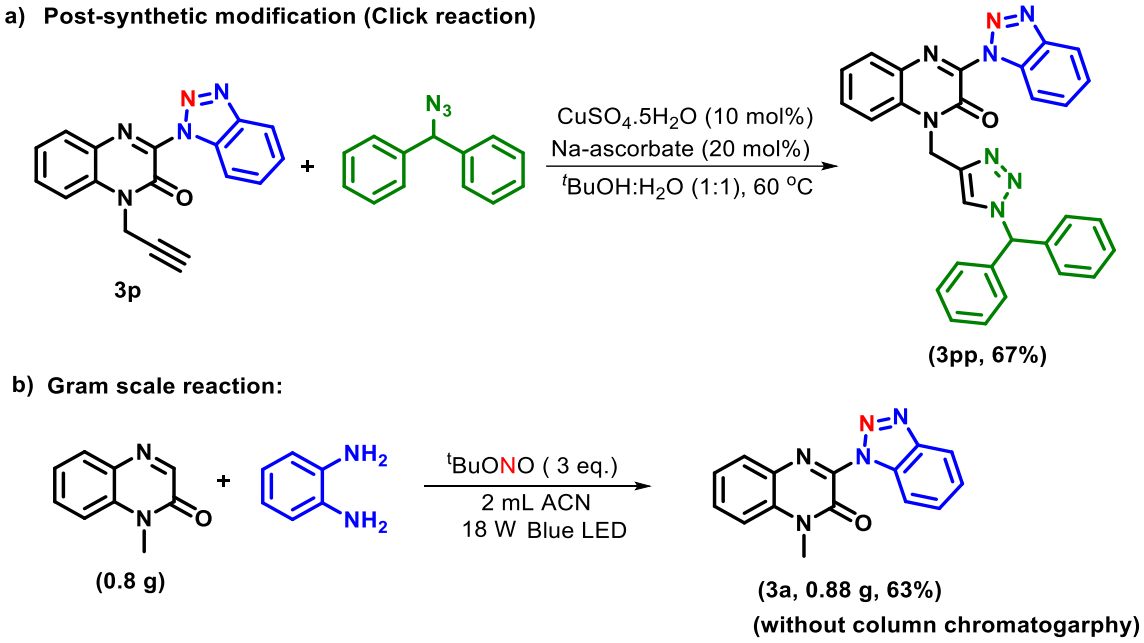
Reaction conditions: **1a** (1 eq.), **2a** (1 eq.) and *tert*-butyl nitrite (3 eq.) in 2 mL ACN were irradiated under 18 W blue LED for 12 h.

With the optimized reaction conditions in hand, we explored the substrate scope to establish the generality of this method by varying the alkyl substituents at the nitrogen atom of quinoxaline-2(1*H*)-one as well as employing different benzene-1,2-diamine derivatives (Scheme 4.12). The use of unsubstituted benzene-1,2-diamine and its 4,5-dimethyl-, 4-trifluoromethyl-, and 4-methoxy-substituted analogues furnished the corresponding products **3a** to **3d** in 80%, 60%, 47% and 44% yields, respectively.Quinoxaline-2(1*H*)-one bearing an ethyl group at the nitrogen atom underwent smooth conversion under the optimized conditions with both unsubstituted and substituted benzene-1,2-diamines, affording products **3e**, **3f**, and **3g** in 66%, 82%, and 53% yields respectively. Remarkably, *N*-propyl- and *N*-butyl-substituted quinoxaline-2(1*H*)-ones also provided the desired products **3h**, **3i**, and **3j** in 64%, 76%, and 61% yields, respectively. Notably, quinoxaline-2(1*H*)-ones bearing a long-chain octyl group at the nitrogen atom afforded the corresponding products **3k**, **3l**, and **3m** in moderate yields of 60%, 55%, and 50%, respectively. Similarly, *N*-allyl and *N*-propargyl substituted quinoxaline-2(1*H*)-ones underwent the reaction smoothly to yield products **3n** to **3r** in 50%, 52%, 55%, 70%, and 50% yields. Subsequently, various benzyl-substituted quinoxaline-2(1*H*)-ones reacted efficiently to furnish products **3s** to **3y** in yields of 54%, 52%, 56%, 60%, 63%, 54%, and 58%. Interestingly, when the R group was modified to a long-chain alkene (hexene), the corresponding products **3z** and **3aa** were obtained in 51% and 48% yields, respectively. Furthermore, the difluoro-substituted quinoxaline-2(1*H*)-one participated well in the reaction, affording product **3ab** in an excellent 72% yield.



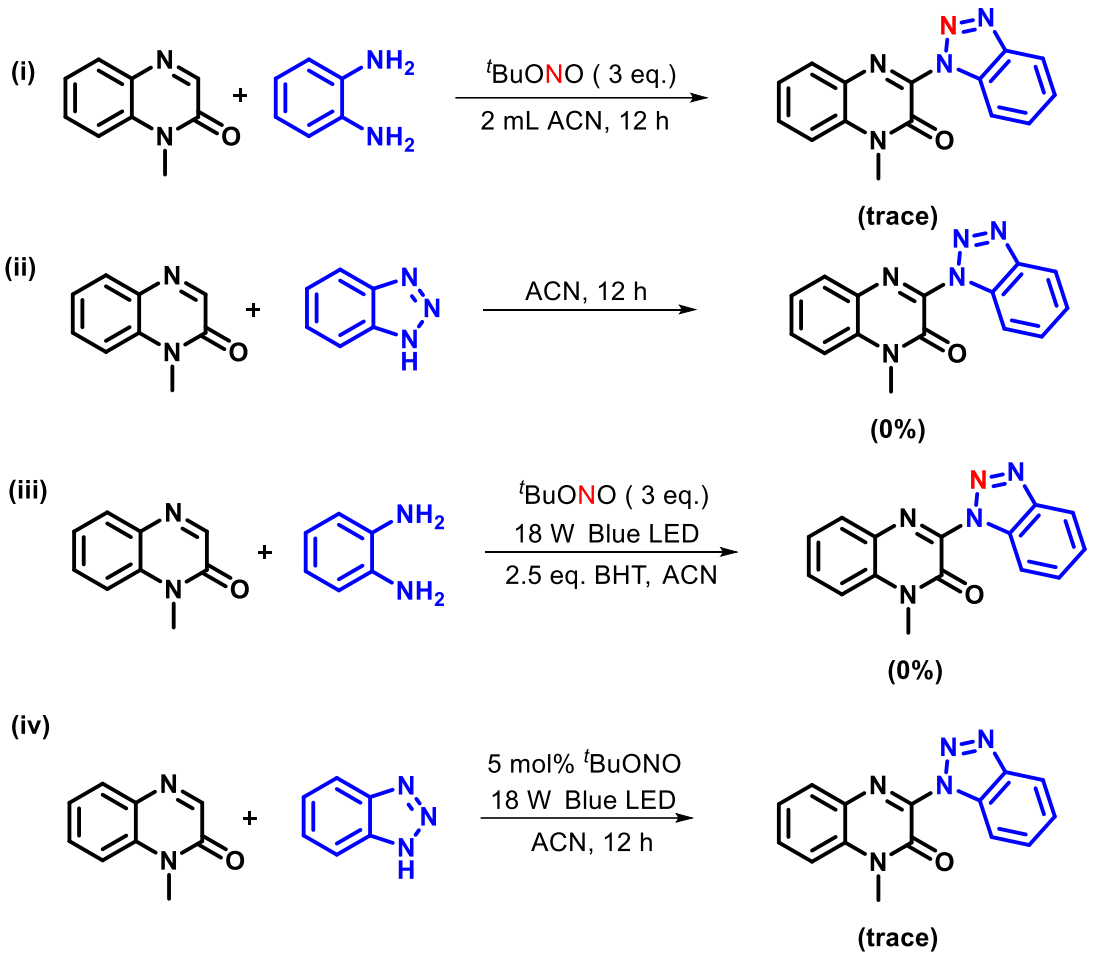
Scheme 4.12: Substrate scope for benzotriazolation of quinoxalinones bearing functional group **Reaction condition**: **1** (0.25), **2** (0.25 mmol) and TBN (3 equiv.) in 18 W blue LED were irradiated in ACN solvent in open atmosphere for 12 h.

The substrate scope was further expanded to include substrates bearing various functional groups and strained ring systems, as depicted in Scheme 4.12. Quinoxaline-2(1*H*)-ones featuring ester functionalities at the nitrogen atom underwent smooth benzotriazolation, delivering products **4a** to **4d** in yields of 62%, 69%, 59%, and 47%, respectively. Similarly, nitrile-substituted quinoxaline-2(1*H*)-ones participated efficiently in the reaction, affording products **4e** and **4f** in 56% and 60% yields, respectively. Moreover, incorporation of a strained cyclopropyl ring on the quinoxaline-2(1*H*)-one scaffold led to the successful formation of products **4g** and **4h** in 74% and 64% yields, respectively (Scheme 4.12).



Scheme 4.13: Post-synthetic modification (Click Reaction) and reaction in 5 mmol scale

Moreover, compound **3p** underwent click reaction with azide to furnish double triazole functionalised derivative **3pp** (Scheme 4.13, entry a). The viability of this method for the gram-scale has been demonstrated in 5 mmol scale (0.8 gm) to yield product **3a** in 63% (Scheme 4.13, entry b).

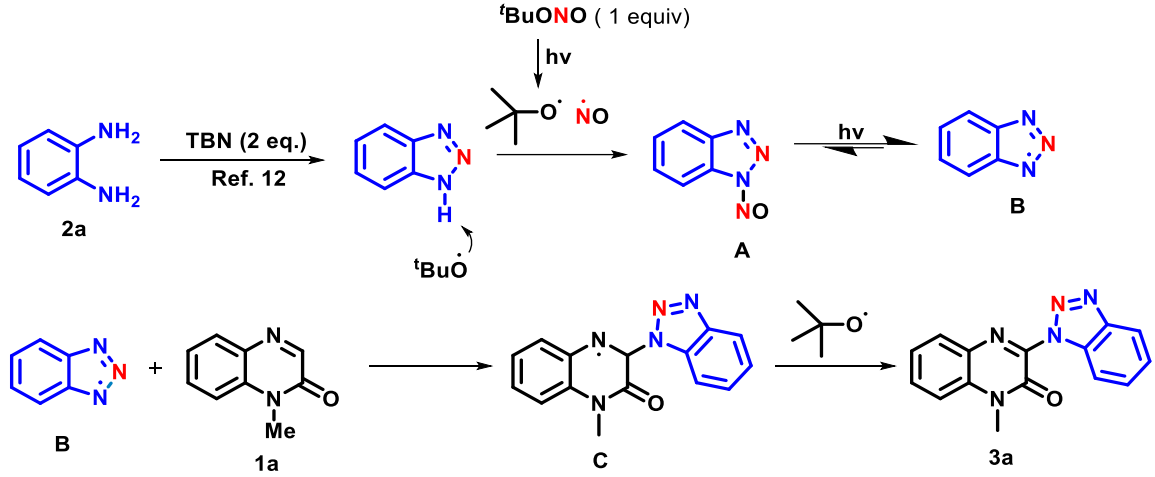


Scheme 4.14: Experimental section and characterization data

To gain insight into the reaction mechanism, a series of control experiments was conducted (Scheme 4.14). In the absence of light, only trace amounts of the desired product were detected (Scheme 4.14, entry i). Moreover, a direct reaction between benzotriazole and quinoxaline-2(1*H*)-one failed to proceed in the dark (Scheme 4.14, entry ii). Additionally, introducing the radical scavenger BHT completely suppressed the reaction (Scheme 4.14, entry iii), strongly supporting the involvement of a radical pathway.

Based on control experiments and literature precedents, a plausible mechanism for the photochemically triggered benzotriazolation of quinoxaline-2(1*H*)-one is proposed in Scheme 4.15.[38-42] Initially, the N–H bond of in situ formed benzotriazole undergoes homolytic cleavage, facilitated by *tert*-butoxy radicals generated from the thermal dissociation of *tert*-butyl nitrite, leading to the formation of a benzotriazole radical. This radical rapidly reacts with a nitric oxide (NO) radical to form adduct **A**. Upon visible light irradiation, adduct **A** undergoes homolytic N–N bond cleavage to generate

a second benzotriazole radical species **B**.[13] This radical then adds across the imine bond of quinoxaline-2(1*H*)-one, forming radical intermediate **C**. Finally, intermediate **C** undergoes hydrogen atom abstraction by a *tert*-butoxy radical, yielding the desired product **3a**.



Scheme 4.15: Plausible Mechanism of benzotriazolation of quinoxalinones

4.4. Conclusions

In summary, we have developed a photoinduced benzotriazolation of quinoxalinones via a sequential nitrogen insertion to generate benzotriazole, followed by C–N bond formation under one-pot conditions. The method does not require transition metals, avoids high temperature and reaction occurs in very simple experimental set up. This protocol features a broad substrate scope with structuraaly diverse quinoxalinones and benzotriazoles and delivers the desired products in good to excellent yields. The scalability of the reaction was demonstrated on the gram scale, and a plausible reaction mechanism was proposed, supported by experimental evidence. Post-synthetic modification of products has been perfomed in the form of Click reaction. The library of substrates opens up new avenue for assessing biomedical applications.

4.5. Experimental section and characterization data

4.5.1. General information & characterization data

All the chemicals were purchased from Sigma-Aldrich and BLD pharma and used without further modification. All solvents were purchased from Rankem and Finar Chemicals. Deuterated solvents were used as received. Column chromatographic separations were performed over 60−120 mesh silica-gel. Visualization was accomplished with UV light. The ^{1}H and $^{13}C\{^{1}H\}$ NMR spectra were recorded on 400 and 100 MHz, respectively, using Bruker spectrometers. Abbreviations used in the NMR follow-up experiments: b, broad; s, singlet; d, doublet; t, triplet; q, quartet. HRMS spectra were obtained with Waters-synapt G2 using electrospray ionization (ESI-TOF). Infrared (ATIR) spectra

were obtained with a Bruker Alpha-E infrared spectrometer. Single-crystal diffraction analysis data were collected at 100K with a BRUKER KAPPA APEX III CCD Duo diffractometer (operated at 1500 W power: 50 kV, 30 mA) using graphite monochromatic Mo-Kα radiation and Cu-Kα radiation. The reaction was performed in a 15 mL borosilicate test tube. The lightsource used was 18 W Lords blue LED. The wavelength of the LEDwas measured with an Ocean Optics USB 400 instrument that detects 200−1100 nm wavelength, and the spectra were recorded in SpectraSuit software. The wavelength of the radiation was 445 nm with fwhm = 18.96 nm.

4.5.2. General procedure for synthesis of 3 & 4:

Benzene-1,2-diamine (1 eq.) was added in a 10 mL teast-tube containing 2 mL ACN. Then 2 eq. *tert*-butyl nitrite was added in to it and the reaction mixture was stirred for 20 min at room temperature. Then quinoxaline-2(1*H*)-one (1 eq.) and 1 eq. tert-butyl nitrite were added into that reaction mixture and the mixture was irradiated under 2 x 9 W blue LED irradiation for 12 h at room temperature. The test tube was kept at a distance of 2.5 cm from each LED. The temperature of the system was measured to be in the range of 30-35 ^{o}C using IR thermometer for 12 h.

4.6. Analytical data of products

3-(1*H*-benzo[d][1,2,3]triazol-1-yl)-1-methylquinoxalin-2(1*H*)-one (3a) Prepared according to the general procedure using 1-methylquinoxalin-2(1*H*)-one (0.25 mmol, 40 mg), *o*-phenylenediamine (0.25 mmol, 27 mg) and *tert*-butyl nitrite (0.75 mmol, 77 mg). The crude reaction mixture was purified by silica gel column chromatography (pet ether/EtOAc = 70:30) to afford product **3a** (55 mg, 80%). Melting point: 208-210 ^{o}C.^{1}H NMR (400 MHz, $CDCl_3$) δ 8.15 (d, J = 8.3 Hz, 1H), 8.00 (d, J = 8.4 Hz, 1H), 7.97 – 7.92 (m, 1H), 7.70 – 7.63 (m, 1H), 7.62 – 7.56 (m, 1H), 7.48 – 7.40 (m, 3H), 3.86 (s, 3H). ^{13}C{^{1}H} NMR (100 MHz, $CDCl_3$) δ 150.8, 145.8, 143.4, 133.6, 132.8, 131.7, 130.9, 130.4, 128.8, 125.0, 124.7, 120.2, 114.1, 113.3, 30.2. IR (neat): 1737, 1664, 1600 cm^{-1}. HRMS (ESI) calculated for $C_{15}H_{12}N_5O$ $[M+H]^+$ m/z 278.1042, found 278.1038.

Large scale synthesis of 3a: *o*-phenylenediamine (540 mg, 5 mmol) was added in a 55 mL borosilicate test-tube containing 6 mL ACN and 2 eq. *tert*-butyl nitrite (1031 mg, 10 mmol) was added into it and the reaction mixture was stirred for 30 min at room temperature. Then 1-methylquinoxaline-2(1*H*)-one (800 mg, 5 mmol) and 1 eq. tert-butyl nitrite (515 mg, 5 mmol) were added into that reaction mixture and the mixture was irradiated under 18 W blue LED for 16 h. After the reaction over, the reaction mixture was kept at room temperature for few hours. It was found that the solid products have precipated out at the bottom of test tube.Then the reaction mixture was collected in a 100 mL RB and

the supernatant solution was thrown out gently. Thereafter, 10 mL MeOH was added to the reaction mixture and it was shaken well. Then again, the supernatant solution was thrown out carefully. This process was repeated 3 more times and the brown-yellow solid was collected after rota evaporation (**3a**, 880 mg, 63%). The product was further confirmed by ^{1}H NMR.

3-(5,6-dimethyl-1*H*-benzo[d][1,2,3]triazol-1-yl)-1-methylquinoxalin-2(1*H*)-one (3b) Prepared according to the general procedure using 1-methylquinoxalin-2(1*H*)-one (0.25 mmol, 40 mg), 4,5-dimethyl-1,2-phenylenediamine (0.25 mmol, 34 mg) and *tert*-butyl nitrite (0.75 mmol, 77 mg). The crude reaction mixture was purified by silica gel column chromatography (pet ether/EtOAc = 70:30) to afford product **3b** (46 mg, 60%). Melting point: 231-233 ºC. ^{1}H NMR (400 MHz, $CDCl_3$) δ 8.02 – 7.96 (m, 1H), 7.89 (s, 1H), 7.77 (s, 1H), 7.68 (td, *J* = 7.8, 1.4 Hz, 1H), 7.46 (t, *J* = 8.2 Hz, 2H), 3.89 (s, 3H), 2.46 (s, 3H), 2.43 (s, 3H). ^{13}C{^{1}H} NMR (100 MHz, $CDCl_3$) δ 150.8, 145.0, 143.8, 139.2, 134.7, 133.5, 131.8, 131.4, 131.1, 130.4, 124.6, 119.3, 114.0, 112.8, 30.2, 21.1, 20.4. IR (neat): 1738, 1666, 1605 cm^{-1}. HRMS (ESI) calculated for $C_{17}H_{16}N_5O$ $[M+H]^+$ m/z 306.1355, found 306.1358.

1-methyl-3-(6-(trifluoromethyl)-1*H*-benzo[d][1,2,3]triazol-1-yl)quinoxalin-2(1*H*)-one(3c)
Prepared according to the general procedure using 1-methylquinoxalin-2(1*H*)-one (0.25 mmol, 40 mg), 4-(trifluoromethyl)-benzene-1,2-diamine (0.25 mmol, 44 mg) and *tert*-butyl nitrite (0.75 mmol, 77 mg). The crude reaction mixture was purified by silica gel column chromatography (pet ether/EtOAc = 70:30) to afford product **3c** (40 mg, 47%). Melting point: 224-226 ºC. ^{1}H NMR (400 MHz, $CDCl_3$) δ 8.48 (s, 1H), 8.11 (d, *J* = 8.7 Hz, 1H), 8.04 – 7.98 (m, 1H), 7.84 (dd, *J* = 8.8, 1.2 Hz, 1H), 7.76 – 7.71 (m, 1H), 7.53 – 7.47 (m, 2H), 3.91 (s, 3H). ^{13}C{^{1}H} NMR (100 MHz, $CDCl_3$) δ 150.7 (s), 145.1 (s), 143.1 (s), 134.3 (s), 133.7 (s), 132.2 (s), 130.9 (s), 130.7 (s), 125.4 (s), 124.9 (s, 122.6 (s), 118.3 (d, *J* = 4.4 Hz), 114.2 (d, *J* = 9.0 Hz), 30.3 (s). ^{19}F{^{1}H} NMR (377 MHz, $CDCl_3$) δ −61.49 (s). IR (neat): 1703, 1665, 1602 cm^{-1}. HRMS (ESI) calculated for $C_{16}H_{11}F_3N_5O$ $[M+H]^+$ m/z 346.0915, found 346.0917.

3-(6-methoxy-1*H*-benzo[d][1,2,3]triazol-1-yl)-1-methylquinoxalin-2(1*H*)-one (3d) Prepared according to the general procedure using using 1-methylquinoxalin-2(1*H*)-one (0.25 mmol, 40 mg), 4-methoxybenzene-1,2-diamine (0.25 mmol, 34.5 mg) and *tert*-butyl nitrite (0.75 mmol, 77 mg). The crude reaction mixture was purified by silica gel column chromatography (pet ether/EtOAc = 70:30) to afford product **3d** (34 mg, 44%). Melting point: 150-152 ºC. ^{1}H NMR (400 MHz, $CDCl_3$) δ 8.03 – 7.95 (m, 2H), 7.72 – 7.67 (m, 1H), 7.53 – 7.42 (m, 3H), 7.39 (d, *J* = 2.2 Hz, 1H), 3.92 (s, 3H), 3.89 (s, 3H).^{13}C{^{1}H} NMR (100 MHz, $CDCl_3$) δ 161.0, 150.8, 141.0, 134.2, 133.6, 131.5, 131.0, 130.3, 124.7,

124.7, 120.7, 116.6, 114.1, 94.4, 55.9, 30.2. IR (neat): 1671, 1604 cm^{-1}. HRMS (ESI) calculated for $C_{16}H_{14}N_5O_2$ $[M+H]^+$ m/z 308.1147, found 308.1152.

3-(1*H*-benzo[d][1,2,3]triazol-1-yl)-1-ethylquinoxalin-2(1*H*)-one (3e) Prepared according to the general procedure 1-ethylquinoxalin-2(1*H*)-one (0.25 mmol, 44 mg), *o*-phenylenediamine (0.25 mmol, 27 mg) and *tert*-butyl nitrite (0.75 mmol, 77 mg). The crude reaction mixture was purified by silica gel column chromatography (pet ether/EtOAc = 70:30) to afford product **3e** (48 mg, 66%). Melting point: 228-230 ºC. ^{1}HNMR (400 MHz, $CDCl_3$) δ 8.35 (d, *J* = 2.2 Hz, 1H), 8.28 (dd, *J* = 8.8, 2.3 Hz, 1H), 8.24 – 8.10 (m, 3H), 7.79 – 7.43 (m, 3H), 4.56 (q, *J* = 7.2 Hz, 2H), 1.55 (t, *J* = 7.2 Hz, 3H).^{13}C{^{1}H} NMR (100 MHz, $CDCl_3$) δ 149.6, 148.5, 145.9, 142.3, 134.9, 132.6, 132.5, 131.4, 129.5, 125.7, 120.6, 118.9, 113.8, 109.7, 39.3, 12.5. IR (neat): 1711, 1672, 1561 cm^{-1}. HRMS (ESI) calculated for $C_{16}H_{14}N_5O$ $[M+H]^+$ m/z 292.1198, found 292.1198.

3-(5,6-dimethyl-1*H*-benzo[d][1,2,3]triazol-1-yl)-1-ethylquinoxalin-2(1*H*)-one (3f) Prepared according to the general procedure using 1-ethylquinoxalin-2(1*H*)-one (0.25 mmol, 44 mg), 4,5-dimethyl-1,2-phenylenediamine (0.25 mmol, 34 mg) and *tert*-butyl nitrite (0.75 mmol, 77 mg). The crude reaction mixture was purified by silica gel column chromatography (pet ether/EtOAc = 75:25) to afford product **3f** (65 mg, 82%). Melting point: 178-180 ºC. ^{1}H NMR (400 MHz, $CDCl_3$) δ 8.00 (dd, J = 8.0, 1.3 Hz, 1H), 7.88 (s, 1H), 7.78 (s, 1H), 7.68 (ddd, *J* = 8.6, 7.3, 1.5 Hz, 1H), 7.50 – 7.42 (m, 2H), 4.50 (q, *J* = 7.2 Hz, 2H), 2.46 (s, 3H), 2.43 (s, 3H), 1.49 (t, *J* = 7.2 Hz, 3H).^{13}C{^{1}H} NMR (100 MHz, $CDCl_3$) δ 150.3, 145.0, 143.8, 139.2, 134.7, 134.5, 131.8, 131.4, 130.7, 124.4, 119.3, 113.8, 112.8, 38.6, 21.1, 20.4, 12.4. IR (neat): 1667,1605, 1591 cm-1. HRMS (ESI) calculated for C18H18N5O [M+H]+ m/z 320.1511, found 320.1513.

1-ethyl-3-(6-(trifluoromethyl)-1*H*-benzo[d][1,2,3]triazol-1-yl)quinoxalin-2(1*H*)-one (3g) Prepared according to the general procedure using 1-ethylquinoxalin-2(1*H*)-one (0.25 mmol, 44 mg), 4-(trifluoromethyl)-benzene-1,2-diamine (0.25 mmol, 44 mg) and *tert*-butyl nitrite (0.75 mmol, 77 mg). The crude reaction mixture was purified by silica gel column chromatography (pet ether/EtOAc = 70:30) to afford product **3g** (48 mg, 53%). Melting point: 187-189 ºC. ^{1}H NMR (400 MHz, $CDCl_3$) δ 8.48 (s, 1H), 8.12 (d, *J* = 8.7 Hz, 1H), 8.05 – 7.99 (m, 1H), 7.83 (dd, *J* = 8.8, 1.1 Hz, 1H), 7.75 – 7.70 (m, 1H), 7.52 – 7.46 (m, 2H), 4.52 (dt, *J* = 11.2, 5.2 Hz, 2H), 1.50 (t, *J* = 7.2 Hz, 3H).^{13}C{^{1}H} NMR (100 MHz, $CDCl_3$) δ 150.2 (s), 145.1 (s), 143.1(s), 132.7 (s), 132.1 (s), 131.2 (s), 130.9 (s), 125.4 (d, *J* = 3.1 Hz), 124.7 (s), 121.2 (s), 118.3 (d, *J* = 4.5 Hz), 114.3 (s), 114.0 (s), 38.7 (s), 12.4 (s).^{19}F{^{1}H} NMR (377 MHz, $CDCl_3$) δ −61.49 (s). IR (neat): 1718, 1677, 1587 cm^{-1}. HRMS (ESI) calculated for $C_{17}H_{13}F_3N_5O$ $[M+H]^+$ m/z 360.1071, found 360.1071.

3-(1*H*-benzo[d][1,2,3]triazol-1-yl)-1-propylquinoxalin-2(1*H*)-one (3h) Prepared according to the general procedure using 1-propylquinoxalin-2(1*H*)-one (0.25 mmol, 47 mg), *o*-phenylenediamine (0.25 mmol, 27 mg) and *tert*-butyl nitrite (0.75 mmol, 77 mg). The crude reaction mixture was purified by silica gel column chromatography (pet ether/EtOAc = 70:30) to afford product **3h** (49 mg, 64%). Melting point: 75-77 ºC. ^{1}H NMR (400 MHz, $CDCl_3$) δ 8.18 (d, *J* = 8.3 Hz, 1H), 8.08 – 7.92 (m, 2H), 7.73 – 7.65 (m, 1H), 7.61 (ddd, *J* = 8.2, 7.0, 1.0 Hz, 1H), 7.51 – 7.41 (m, 3H), 4.46 – 4.36 (m, 2H), 1.99 – 1.84 (m, 2H), 1.12 (t, *J* = 7.4 Hz, 3H).^{13}C{^{1}H} NMR (100 MHz, $CDCl_3$) δ 150.5, 145.9, 143.6, 132.9, 131.5, 131.3, 130.7, 128.8, 124.9, 124.5, 120.2, 114.1, 113.3, 45.0, 20.7, 11.4. IR (neat): 1711, 1670, 1604 cm^{-1}. HRMS (ESI) calculated for $C_{17}H_{16}N_5O$ $[M+H]^+$ m/z 306.1355, found 306.1352.

3-(5,6-dimethyl-1*H*-benzo[d][1,2,3]triazol-1-yl)-1-propylquinoxalin-2(1*H*)-one (3i) Prepared according to the general procedure using 1-propylquinoxalin-2(1*H*)-one (0.25 mmol, 47 mg), 4,5-dimethyl-1,2-phenylenediamine (0.25 mmol, 34 mg) and *tert*-butyl nitrite (0.75 mmol, 77 mg). The crude reaction mixture was purified by silica gel column chromatography (pe ether/EtOAc = 65:25) to afford product **3i** (63 mg, 76%). Melting point: 181-183 ºC. ^{1}H NMR (400 MHz, $CDCl_3$) δ 7.99 (dd, *J* = 8.2, 1.4 Hz, 1H), 7.88 (s, 1H), 7.75 (s, 1H), 7.69 – 7.62 (m, 1H), 7.48 – 7.40 (m, 2H), 4.43 – 4.34 (m, 2H), 2.45 (s, 3H), 2.42 (s, 3H), 1.97 – 1.84 (m, 2H), 1.11 (t, *J* = 7.4 Hz, 3H). ^{13}C{^{1}H} NMR (100 MHz, $CDCl_3$) δ 150.5, 145.0, 143.7, 139.2, 134.7, 132.7, 131.8, 131.3, 130.6, 124.4, 119.3, 114.0, 112.8, 44.9, 21.2, 20.7, 20.4, 11.4. IR (neat): 1710, 1666, 1606 cm^{-1}. HRMS (ESI) calculated for $C_{19}H_{20}N_5O$ $[M+H]^+$ m/z 334.1668, found 334.1666.

3-(1*H*-benzo[d][1,2,3]triazol-1-yl)-1-butylquinoxalin-2(1*H*)-one (3j) Prepared according to the general procedure using 1-butylquinoxalin-2(1H)-one (0.25 mmol, 50.6 mg), *o*-phenylene diamine (0.25 mmol, 27 mg) and *tert*-butyl nitrite (0.75 mmol, 77 mg). The crude reaction mixture was purified by silica gel column chromatography (pet ether/EtOAc = 80:20) to afford product **3j** (53 mg, 61%). Melting point: 205-207 ºC. ^{1}HNMR (400 MHz, $CDCl_3$) δ 8.00 (dd, *J* = 8.3, 1.4 Hz, 1H), 7.89 (s, 1H), 7.76 (s, 1H), 7.73 – 7.63 (m, 1H), 7.58 – 7.39 (m, 2H), 4.49 – 4.37 (m, 2H), 2.46 (s, 3H), 2.44 (s, 3H), 1.86 (ddd, *J* = 12.6, 8.7, 6.7 Hz, 2H), 1.56 (dt, *J* = 15.0, 7.4 Hz, 2H), 1.03 (t, *J* = 7.4 Hz, 3H).^{13}C{^{1}H} NMR (100 MHz, $CDCl_3$) δ 150.5, 145.0, 143.8, 139.2, 134.7, 132.8, 131.8, 131.4, 131.3, 130.6, 124.4, 119.3, 114.0, 112.8, 43.3, 29.3, 21.2, 20.4, 20.3, 13.8. IR (neat): 1704, 1669, 1608 cm^{-1}. HRMS (ESI) calculated for $C_{20}H_{22}N_5O$ $[M+H]^+$ m/z 348.1824, found 348.1820.

3-(1*H*-benzo[d][1,2,3]triazol-1-yl)-1-octylquinoxalin-2(1*H*)-one (3k) Prepared according to the general procedure using 1-octylquinoxalin-2(1*H*)-one (0.25 mmol, 64.6 mg), *o*-phenylenediamine (0.25 mmol, 27 mg) and *tert*-butyl nitrite (0.75 mmol, 77 mg). The crude reaction mixture was purified

by silica gel column chromatography (pet ether/EtOAc = 75:25) to afford product **3k** (56 mg, 60%). Melting point: 62-64 ºC .^{1}H NMR (400 MHz, $CDCl_3$) δ 8.15 (d, *J* = 8.3 Hz, 1H), 8.08 – 7.91 (m, 2H), 7.71 – 7.63 (m, 1H), 7.62 – 7.53 (m, 1H), 7.49 – 7.39 (m, 3H), 4.44 – 4.35 (m, 2H), 1.92 – 1.80 (m, 2H), 1.56 – 1.45 (m, 2H), 1.41 – 1.25 (m, 8H), 0.87 (t, *J* = 6.8 Hz, 3H).^{13}C{^{1}H} NMR (100 MHz, $CDCl_3$) δ 150.5, 145.8, 143.5, 132.8, 132.8, 131.5, 131.3, 130.7, 128.8, 124.9, 124.5, 120.2, 114.1, 113.3, 43.6, 31.8, 29.2, 29.2, 27.3, 27.0, 22.6, 14.1. IR (neat): 1711, 1668, 1605 cm^{-1}. HRMS (ESI) calculated for $C_{22}H_{26}N_5O$ $[M+H]^+$ m/z 376.2137, found 376.2142.

3-(5,6-dimethyl-1*H*-benzo[d][1,2,3]triazol-1-yl)-1-octylquinoxalin-2(1*H*)-one (3l) Prepared according to the general procedure using 1-octylquinoxalin-2(1*H*)-one (0.25 mmol, 64.6 mg), 4,5-dimethyl-1,2-phenylenediamine (0.25 mmol, 34 mg) and tert-butyl nitrite (0.75 mmol, 77 mg). The crude reaction mixture was purified by silica gel column chromatography (pet ether/EtOAc = 80:20) to afford product **3l** (55 mg, 55%). Melting point: 80-82 ºC.^{1}H NMR (400 MHz, $CDCl_3$) δ 7.97 (dd, *J* = 8.2, 1.4 Hz, 1H), 7.86 (s, 1H), 7.74 (s, 1H), 7.68 – 7.62 (m, 1H), 7.46 – 7.38 (m, 2H), 4.43 – 4.35 (m, 2H), 2.44 (s, 3H), 2.41 (s, 3H), 1.87 – 1.81 (m, 2H), 1.54 – 1.45 (m, 2H), 1.40 – 1.24 (m, 8H), 0.86 (t, *J* = 6.8 Hz, 3H).^{13}C{^{1}H} NMR (100 MHz, $CDCl_3$) δ 150.5, 145.0, 143.7, 139.2, 134.6, 132.7, 131.8, 131.3, 130.6, 124.4, 119.3, 114.0, 112.8, 43.5, 31.8, 29.3, 29.2, 27.3, 27.0, 22.6, 21.1, 20.4, 14.1. IR (neat): 1710, 1666, 1606 cm^{-1}. HRMS (ESI) calculated for $C_{24}H_{30}N_5O$ $[M+H]^+$ m/z 404.2450, found 404.2454.

1-octyl-3-(6-(trifluoromethyl)-1*H*-benzo[d][1,2,3]triazol-1-yl)quinoxalin-2(1*H*)-one (3m) Prepared according to the general procedure using 1-octylquinoxalin-2(1*H*)-one (0.25 mmol, 64.6 mg), 4-(trifluoromethyl)-benzene-1,2-diamine (0.25 mmol, 44 mg) and *tert*-butyl nitrite (0.75 mmol, 77 mg). The crude reaction mixture was purified by silica gel column chromatography (pet ether/EtOAc = 70:30) to afford product **3m** (55 mg, 50%) as yellow semi-solid.^{1}H NMR (400 MHz, $CDCl_3$) δ 8.40 – 8.25 (m, 1H), 8.23 – 8.08 (m, 1H), 8.06 – 7.99 (m, 1H), 7.92 – 7.79 (m, 1H), 7.73 (t, *J* = 8.2 Hz, 1H), 7.49 (t, *J* = 6.6 Hz, 2H), 4.48 – 4.39 (m, 2H), 1.93 – 1.83 (m, 2H), 1.57 – 1.48 (m, 2H), 1.35 – 1.25 (m, 8H), 0.88 (t, *J* = 6.6 Hz, 3H).^{13}C{^{1}H} NMR (100 MHz, $CDCl_3$) 153.7 (s), 150.4 (s), 145.1 (s), 133.0 (s), 132.0 (s), 131.0 (s), 125.0 (d, *J* = 66.1 Hz), 124.7 – 124.6 (m), 123.5 (s), 121.1 (s), 114.3 (d, *J* = 15.5 Hz), 113.8 (s), 109.7 (s), 43.7 (s), 31.7 (s), 29.2 (s), 29.2 (s), 27.3(s), 27.0 (s), 22.6 (s), 14.1 (s).^{19}F{^{1}H} NMR (377 MHz, $CDCl_3$) δ −61.50 (s). IR (neat): 1715, 1680,1609 cm^{-1}. HRMS (ESI) calculated for $C_{23}H_{25}F_3N_5O$ $[M+H]^+$ m/z 444.2011, found 444.2008.

1-allyl-3-(1*H*-benzo[d][1,2,3]triazol-1-yl)quinoxalin-2(1*H*)-one (3n) Prepared according to the general procedure using 1-allylquinoxalin-2(1*H*)-one (0.25 mmol, 46.5 mg), *o*-phenylenediamine

(0.25 mmol, 27 mg) and *tert*-butyl nitrite (0.75 mmol, 77 mg). The crude reaction mixture was purified by silica gel column chromatography (pet ether/EtOAc = 70:30) to afford product **3n** (38 mg, 50%) as orange semi-solid.^{1}H NMR (400 MHz, $CDCl_3$) δ 8.18 (d, *J* = 8.3 Hz, 1H), 8.09 – 7.96 (m, 2H), 7.69 – 7.59 (m, 2H), 7.50 – 7.43 (m, 3H), 6.02 (ddt, *J* = 17.1, 10.5, 5.3 Hz, 1H), 5.38 – 5.29 (m, 2H), 5.09 (dt, *J* = 5.3, 1.5 Hz, 2H).^{13}C{^{1}H} NMR (100 MHz, $CDCl_3$) δ 150.4, 145.8, 143.6, 132.8, 132.8, 131.5, 131.2, 130.5, 130.1, 128.9, 125.0, 124.7, 120.2, 119.1, 114.6, 113.2, 45.6. IR (neat): 1711, 1672, 1608 cm^{-1}. HRMS (ESI) calculated for $C_{17}H_{14}N_5O$ $[M+H]^+$ m/z 304.1198, found 304.1201.

1-allyl-3-(5,6-dimethyl-1*H*-benzo[d][1,2,3]triazol-1-yl)quinoxalin-2(1*H*)-one (3o) Prepared according to the general procedure using using 1-allylquinoxalin-2(1*H*)-one (0.25 mmol, 46.5 mg), 4,5-dimethyl-1,2-phenylenediamine (0.25 mmol, 34 mg) and *tert*-butyl nitrite (0.75 mmol, 77 mg). The crude reaction mixture was purified by silica gel column chromatography (pet ether/EtOAc = 70:30) to afford product **3o** (43 mg, 52%). Melting point: 181-183 ºC.^{1}H NMR (400 MHz, $CDCl_3$) δ 7.99 (dd, *J* = 8.2, 1.3 Hz, 1H), 7.88 (s, 1H), 7.78 (s, 1H), 7.68 – 7.60 (m, 1H), 7.44 (dd, *J* = 12.5, 4.8 Hz, 2H), 6.01 (ddt, *J* = 17.1, 10.5, 5.3 Hz, 1H), 5.33 (dd, *J* = 19.5, 8.9 Hz, 2H), 5.08 (dt, *J* = 5.2, 1.5 Hz, 2H), 2.46 (s, 3H), 2.43 (s, 3H).^{13}C{^{1}H} NMR (100 MHz, $CDCl_3$) δ 150.4, 145.0, 143.8, 139.3, 134.7, 132.8, 131.8, 131.3, 131.2, 130.5, 130.1, 124.6, 119.3, 119.0, 114.5, 112.9, 45.6, 21.2, 20.4. IR (neat): 1710, 1671, 1605 cm^{-1}. HRMS (ESI) calculated for $C_{19}H_{18}N_5O$ $[M+H]^+$ m/z 332.1511, found 332.1514.

3-(1*H*-benzo[d][1,2,3]triazol-1-yl)-1-(prop-2-yn-1-yl)quinoxalin-2(1*H*)-one (3p) Prepared according to the general procedure using 1-propargylquinoxalin-2(1*H*)-one (0.25 mmol, 46 mg), o-phenylenediamine (0.25 mmol, 27 mg) and *tert*-butyl nitrite (0.75 mmol, 77 mg). The crude reaction mixture was purified by silica gel column chromatography (pet ether/EtOAc = 70:30) to afford product **3p** (41 mg, 55%). Melting point: 202-204 ºC. ^{1}HNMR (400 MHz, $CDCl_3$) δ 8.18 (d, *J* = 8.3 Hz, 1H), 8.05 (d, *J* = 8.4 Hz, 1H), 8.00 (dd, *J* = 8.0, 1.3 Hz, 1H), 7.73 (ddd, *J* = 8.6, 7.3, 1.4 Hz, 1H), 7.63 (dd, *J* = 10.6, 4.6 Hz, 2H), 7.49 (ddd, *J* = 7.9, 7.1, 1.0 Hz, 2H), 5.24 (d, *J* = 2.5 Hz, 2H), 2.37 (t, *J* = 2.5 Hz, 1H).^{13}C{^{1}H} NMR (100 MHz, $CDCl_3$) δ 149.9, 145.8, 143.4, 132.7, 132.1, 131.7, 132.2, 130.5, 128.9, 125.1, 125.1, 120.3, 114.6, 113.3, 76.2, 74.0, 32.5. IR (neat): 1722, 1670,1607 cm^{-1}. HRMS (ESI) calculated for $C_{17}H_{12}N_5O$ [M+H]+ m/z 302.1042, found 302.1042. **Crystal preperation**: The crystal is grown by simple recrystallization method. The pure compound **3p** isolated after column chromatography was dissolved in MeOH and layered with hexane and kept at room temperature for 3 days to get pure crystal. **Crystal data**: Compound **3p** has the empirical formula $C_{17}H_{11}N_5O$ with a formula mass of 301.310 g mol^{-1}. The crystal was obtained as yellow needles and crystallizes in the monoclinic system with space group $P2_1/c$. The unit cell parameters are: a = 9.4424(6) Å, b =

15.3162(12) Å, c = 10.2702(8) Å, with α = 90°, β = 103.911(2)°, and γ = 90°, giving a unit cell volume of 1441.73(18) Å³ and Z = 4. The calculated density (D_{calcd}) is 1.388 g cm⁻³. Data were collected at 150 K using Mo Kα radiation (λ = 0.71073 Å). The maximum diffraction angle (θ) for complete data was 56.68°. A total of 31,836 reflections were collected, of which 3,585 were independent and significant [I > 2σ(I)]. The absorption coefficient (μ) is 0.092 mm⁻¹, and F (000) is 624.4. The refinement gave final R1 = 0.0453 and wR2 = 0.1246 for observed data, with a goodness-of-fit (GoF) of 1.079.

3-(5,6-dimethyl-1*H*-benzo[d][1,2,3]triazol-1-yl)-1-(prop-2-yn-1-yl)quinoxalin-2(1*H*)-one (3q) Prepared according to the general procedure using 1-propargylquinoxalin-2(1*H*)-one (0.25 mmol, 46 mg), 4,5-dimethyl-1,2-phenylenediamine (0.25 mmol, 34 mg) and *tert*-butyl nitrite (0.75 mmol, 77 mg). The crude reaction mixture was purified by silica gel column chromatography (pet ether/EtOAc = 70:30) to afford product **3q** (58 mg, 70%). Melting point: 232-234 ºC.^{1}H NMR (400 MHz, $CDCl_3$) δ 7.99 (dd, *J* = 8.0, 1.3 Hz, 1H), 7.88 (s, 1H), 7.79 (s, 1H), 7.70 (ddd, *J* = 8.6, 7.3, 1.5 Hz, 1H), 7.59 (dd, *J* = 8.4, 0.9 Hz, 1H), 7.51 – 7.44 (m, 1H), 5.22 (d, *J* = 2.5 Hz, 2H), 2.46 (s, 3H), 2.43 (s, 3H), 2.36 (t, *J* = 2.5 Hz, 1H).^{13}C{^{1}H} NMR (100 MHz, $CDCl_3$) δ 149.9, 145.0, 143.6, 139.4, 134.9, 132.0, 131.7, 131.4, 131.2, 130.5, 124.9, 119.4, 114.6, 112.9, 76.3, 73.9, 32.5, 21.1, 20.4. IR (neat): 1727, 1667, 1604 cm^{-1}. HRMS (ESI) calculated for $C_{19}H_{16}N_5O$ [M+H]+ m/z 330.1355, found 330.1360.

1-(prop-2-yn-1-yl)-3-(6-(trifluoromethyl)-1*H*-benzo[d][1,2,3]triazol-1-yl)quinoxalin-2(1*H*)-one (3r) Prepared according to the general procedure using 1-popargylquinoxalin-2(1*H*)-one (0.25 mmol, 46 mg), 4-(trifluoromethyl)-benzene-1,2-diamine (0.25 mmol, 44 mg) and *tert*-butyl nitrite (0.75 mmol, 77 mg). The crude reaction mixture was purified by silica gel column chromatography (pet ether/EtOAc = 70:30) to afford product **3r** (46 mg, 50%). Melting point: 80-82 ºC.^{1}H NMR (400 MHz, $CDCl_3$) δ 8.49 (s, 1H), 8.19 (d, *J* = 8.7 Hz, 1H), 8.06 – 8.02 (m, 1H), 7.86 (dd, *J* = 8.8, 1.3 Hz, 1H), 7.80 – 7.75 (m, 1H), 7.65 (d, *J* = 8.5 Hz, 1H), 7.57 – 7.51 (m, 1H), 5.26 (d, *J* = 2.6 Hz, 2H), 2.38 (t, *J* = 2.5 Hz, 1H).^{13}C{^{1}H} NMR (100 MHz, $CDCl_3$) δ 150.0 (s), 145.0 (s), 132.2 (d, *J* = 12.1 Hz), 131.0 (d, J = 5.4 Hz), 130.7 (s), 125.7 (d, J = 3.0 Hz), 125.4 (s), 121.2 (s), 118.4 (d, J = 4.4 Hz), 114.8 (s), 114.4 (s), 111.8 (s), 76.0 (s), 74.2 (s), 32.7 (s).^{19}F{^{1}H} NMR (377 MHz, $CDCl_3$) δ −61.53 (s). IR (neat): 1740, 1684, 1609 cm^{-1}. HRMS (ESI) calculated for $C_{18}H_{11}F_3N_5O$ $[M+H]^+$ m/z 370.0915, found 370.0920.

3-(1*H*-benzo[d][1,2,3]triazol-1-yl)-1-benzylquinoxalin-2(1*H*)-one (3s) Prepared according to the general procedure using 1-propargylquinoxalin-2(1*H*)-one (0.25 mmol, 59 mg), *o*-phenylenediamine (0.25 mmol, 27 mg) and *tert*-butyl nitrite (0.75 mmol, 77 mg). The crude reaction mixture was purified

by silica gel column chromatography (pet ether/EtOAc = 70:30) to affo rd product **3s** (48 mg, 54%). Melting point: 174-176 ºC.^{1}H NMR (400 MHz, $CDCl_3$) δ 8.19 (d, *J* = 8.3 Hz, 1H), 8.06 (d, *J* = 8.4 Hz, 1H), 7.99 (dd, *J* = 7.9, 1.0 Hz, 1H), 7.65 – 7.59 (m, 1H), 7.59 – 7.52 (m, 1H), 7.51 – 7.46 (m, 1H), 7.45 – 7.40 (m, 2H), 7.38 – 7.27 (m, 5H), 5.68 (s, 2H). ^{13}C{^{1}H} NMR (100 MHz, $CDCl_3$) δ 151.0, 145.9, 143.7, 134.7, 133.0, 132.8, 131.6, 131.3, 130.6, 129.1, 128.9, 128.1, 121.2, 125.0, 124.7, 120.3, 114.8, 113.4, 47.0. IR (neat): 1703, 1671, 1605 cm^{-1}. HRMS (ESI) calculated for $C_{21}H_{16}N_5O$ $[M+H]^+$ m/z 354.1355, found 354.1353.

1-benzyl-3-(5,6-dimethyl-1*H*-benzo[d][1,2,3]triazol-1-yl)quinoxalin-2(1*H*)-one (3t) Prepared according to the general procedure using procedure using 1-propargylquinoxalin-2(1*H*)-one (0.25 mmol, 59 mg), 4,5-dimethyl-1,2-phenylenediamine (0.25 mmol, 27 mg) and *tert*- butyl nitrite (0.75 mmol, 77 mg). The crude reaction mixture was purified by silica gel column chromatography (pet ether/EtOAc = 70:30) to afford product **3t** (49.5 mg, 52%). Melting point: 208-210 ºC.^{1}HNMR (400 MHz, $CDCl_3$) δ 8.00 (dd, *J* = 8.3, 1.5 Hz, 1H), 7.91 (s, 1H), 7.81 (s, 1H), 7.60 – 7.52 (m, 1H), 7.44 – 7.39 (m, 2H), 7.37 – 7.28 (m, 5H), 5.68 (s, 2H), 2.47 (s, 3H), 2.45 (s, 3H).^{13}C{^{1}H} NMR (100 MHz, $CDCl_3$) δ 151.0, 145.0, 143.9, 139.3, 134.8, 134.7, 132.9, 131.8, 131.3, 131.3, 130.5, 129.1, 128.0, 127.2, 124.6, 119.4, 114.8, 112.9, 47.0, 21.2, 20.5. IR (neat): 1737, 1711, 1673 cm^{-1}. HRMS (ESI) calculated for $C_{23}H_{20}N_5O$ $[M+H]^+$ m/z 382.1668, found 382.1664.

1-benzyl-3-(6-(trifluoromethyl)-1*H*-benzo[d][1,2,3]triazol-1-yl)quinoxalin-2(1*H*)-one (3u) Prepared according to the general procedure using 1-propargylquinoxalin-2(1H)-one (0.25 mmol, 59 mg), 4-(trifluoromethyl)-benzene-1,2-diamine (0.25 mmol, 44 mg) and *tert*-butyl nitrite (0.75 mmol, 77 mg). The crude reaction mixture was purified by silica gel column chromatography (pet ether/EtOAc = 70:30) to afford product **3u** (59 mg, 56%). Melting point: 203-205 ºC. ^{1}H NMR (400 MHz, $CDCl_3$) δ 8.50 (s, 1H), 8.15 (d, *J* = 8.7 Hz, 1H), 8.01 (dd, *J* = 7.9, 1.3 Hz, 1H), 7.85 (dd, *J* = 8.8, 1.3 Hz, 1H), 7.62 (ddd, *J* = 8.6, 7.2, 1.5 Hz, 1H), 7.49 – 7.43 (m, 2H), 7.37 – 7.29 (m, 5H), 5.68 (s, 2H).^{13}C{^{1}H} NMR (100 MHz, $CDCl_3$) δ 152.7 (s), 149.3 (s), 133.4 (s), 131.1 (s), 129.9 (d, *J* = 11.5 Hz), 129.6 (s), 128.1 (t, *J* = 16.7 Hz), 127.4 (s), 127.0 (d, *J* = 38.0 Hz), 126.2 (s), 126.0 (d, *J* = 33.0 Hz), 122.8 (s), 117.2 (s), 113.9 (s), 113.3 (s), 46.1 (s).^{19}F{^{1}H} NMR (377 MHz, $CDCl_3$) δ −61.50 (s). IR (neat): 1738, 1666, 1605 cm^{-1}. HRMS (ESI) calculated for $C_{22}H_{15}F_3N_5O$ $[M+H]^+$ m/z 422.1228, found 422.1231.

3-(1*H*-benzo[d][1,2,3]triazol-1-yl)-1-(3-fluorobenzyl)quinoxalin-2(1*H*)-one (3v) Prepared according to the general procedure using using 1-(3-fluorobenzyl)quinoxalin-2(1*H*)-one (0.25 mmol, 63.5 mg), *o*-phenylenediamine (0.25 mmol, 27 mg) and *tert*-butyl nitrite (0.75 mmol, 77 mg). The

crude reaction mixture was purified by silica gel column chromatography (pet ether/EtOAc = 70:30) to afford product **3v** (55.5 mg, 60%). Melting point: 161-163 °C. ^{1}H NMR (400 MHz, $CDCl_3$) δ 8.19 (d, *J* = 8.3 Hz, 1H), 8.08 (d, *J* = 8.4 Hz, 1H), 8.00 (dd, *J* = 8.0, 1.4 Hz, 1H), 7.69 – 7.56 (m, 2H), 7.51 – 7.42 (m, 2H), 7.39 – 7.29 (m, 2H), 7.14 (dd, *J* = 7.7, 0.6 Hz, 1H), 7.00 (ddd, *J* = 13.5, 10.5, 5.8 Hz, 2H), 5.65 (s, 2H).^{13}C{^{1}H} NMR (100 MHz, CDCl) δ 164.4 (s), 161.9 (s), 150.9 (s), 145.8 (s), 143.6 (s), 137.1 (d, *J* = 7.2 Hz),132.8 (d, *J* = 2.1 Hz), 131.7 (s), 131.2 (s), 130.9 – 130.5 (m), 129.0 (s), 125.0 (d, *J* = 18.6 Hz), 122.8 (d, *J* = 2.9 Hz), 120.3 (s), 115.3 (s), 115.1 (s), 114.6 (s), 114.4 (s), 114.1 (s), 113.4 (s), 46.5 (s). ^{19}F{^{1}H} NMR (377 MHz, $CDCl_3$) δ −111.66 (s).IR (neat): 1703, 1608, 1593 cm^{-1}. HRMS (ESI) calculated for $C_{21}H_{15}FN_5O$ $[M+H]^+$ m/z 372.1260, found 372.1263.

3-(5,6-dimethyl-1H-benzo[d][1,2,3]triazol-1-yl)-1-(3-fluorobenzyl)quinoxalin-2(1H)-one (3w) Prepared according to the general procedure using 1-(3-fluorobenzyl)quinoxalin-2(1*H*)-one (0.25 mmol, 63.5 mg), 4,5-dimethyl-1,2-phenylenediamine (0.25 mmol, 34 mg) and *tert*-butyl nitrite (0.75 mmol, 77 mg). The crude reaction mixture was purified by silica gel column chromatography (pet ether/EtOAc = 70:30) to afford product **3w** (63 mg, 63%). Melting point: 193-195 °C. ^{1}HNMR (400 MHz, $CDCl_3$) δ 8.01 (dd, *J* = 8.0, 1.4 Hz, 1H), 7.90 (s, 1H), 7.83 (s, 1H), 7.57 (ddd, *J* = 8.6, 7.4, 1.5 Hz, 1H), 7.47 – 7.40 (m, 1H), 7.33 (ddd, *J* = 13.8, 10.2, 7.2 Hz, 2H), 7.14 (d, *J* = 7.8 Hz, 1H), 7.00 (ddd, *J* = 13.8, 10.5, 5.8 Hz, 2H), 5.65 (s, 2H), 2.47 (s, 3H), 2.44 (s, 3H). ^{13}C{^{1}H} NMR (100 MHz, $CDCl_3$) δ 164.4 (s), 161.9 (s), 150.9 (s), 145.0 (s), 143.8 (s), 139.4 (s), 137.2 (d, *J* = 7.1 Hz), 134.9 (s), 132.7 (s), 131.7 (s), 131.4 (d, *J* = 12.6 Hz), 130.87 – 130.47 (m), 124.8 (s), 122.8 (d, *J* = 3.0 Hz), 119.4 (s), 115.2 (s), 115.0 (s), 114.5 (d, *J* = 18.7 Hz), 114.1 (s), 112.9 (s), 46.5 (s), 21.2 (s), 20.5 (s). ^{19}F{^{1}H} NMR (377 MHz, $CDCl_3$) δ −111.75 (s). IR (neat): 1737, 1713, 1627 cm^{-1}. HRMS (ESI) calculated for $C_{23}H_{19}FN_5O$ $[M+H]^+$ m/z 400.1573, found 400.1580.

3-(1*H*-benzo[d][1,2,3]triazol-1-yl)-1-(4-methylbenzyl)quinoxalin-2(1*H*)-one (3x) Prepared according to the general procedure using 1-(4-methylbenzyl)quinoxalin-2(1H)-one (0.25 mmol, 62.5 mg), *o*-phenylenediamine (0.25 mmol, 27 mg) and *tert*-butyl nitrite (0.75 mmol, 77 mg). The crude reaction mixture was purified by silica gel column chromatography (pet ether/EtOAc = 70:30) to afford product **3x** (50 mg, 54%). Melting point: 158-160 °C. ^{1}H NMR (400 MHz, $CDCl_3$) δ 8.19 (d, *J* = 8.3 Hz, 1H), 8.06 (d, *J* = 8.4 Hz, 1H), 7.99 (dd, *J* = 8.0, 1.3 Hz, 1H), 7.65 – 7.55 (m, 2H), 7.50 – 7.40 (m, 3H), 7.28 (s, 1H), 7.26 – 7.24 (m, 1H), 7.15 (d, *J* = 7.9 Hz, 2H), 5.64 (s, 2H), 2.32 (s, 3H).^{13}C{^{1}H} NMR (100 MHz, $CDCl_3$) δ 151.0, 145.9, 143.7, 137.9, 133.0, 132.8, 131.7, 131.6, 131.3, 130.6, 129.8, 128.9, 127.2, 125.0, 124.7, 120.3, 114.9, 113.4, 46.8, 21.1. IR (neat): 1738, 1704, 1668 cm^{-1}. HRMS (ESI) calculated for $C_{22}H_{18}N_5O$ $[M+H]^+$ m/z 368.1511, found 368.1508.

3-(5,6-dimethyl-1*H*-benzo[d][1,2,3]triazol-1-yl)-1-(4-methylbenzyl)quinoxalin-2(1*H*)-one (3y) Prepared according to the general procedure using using 1-(4-methylbenzyl)quinoxalin-2(1*H*)-one (0.25 mmol, 62.5 mg), 4,5-dimethyl-1,2-phenylenediamine (0.25 mmol, 27 mg) and *tert*-butyl nitrite (0.75 mmol, 77 mg). The crude reaction mixture was purified by silica gel column chromatography (pet ether/EtOAc = 70:30) to afford product **3y** (57 mg, 58 %). Melting point: 98-100 ºC. ^{1}H NMR (400 MHz, $CDCl_3$) δ 7.99 (dd, *J* = 8.0, 1.2 Hz, 1H), 7.90 (s, 1H), 7.80 (s, 1H), 7.59 – 7.51 (m, 1H), 7.41 (dd, *J* = 17.2, 8.1 Hz, 2H), 7.27 (s, 1H), 7.25 (s, 1H), 7.14 (d, *J* = 8.0 Hz, 2H), 5.63 (s, 2H), 2.47 (s, 3H), 2.44 (s, 3H), 2.31 (s, 3H). ^{13}C{^{1}H} NMR (100 MHz, $CDCl_3$) δ 151.0, 145.0, 143.9, 139.2, 137.8, 134.7, 132.9, 131.8, 131.7, 131.3, 131.3, 130.5, 129.7, 127.2, 124.6, 119.4, 114.8, 112.9, 46.7, 21.2, 21.1, 20.4. IR (neat): 1738, 1712, 1663 cm^{-1}. HRMS (ESI) calculated for $C_{24}H_{22}N_5O$ $[M+H]^+$ m/z 396.1824, found 396.1825.

3-(1*H*-benzo[d][1,2,3]triazol-1-yl)-1-(hex-5-en-1-yl)quinoxalin-2(1*H*)-one (3z) Prepared according to the general procedure using using 1-(hex-5-en-1-yl)quinoxalin-2(1*H*)-one (0.25 mmol, 57 mg), o-phenylenediamine (0.25 mmol, 27 mg) and *tert*-butyl nitrite (0.75 mmol, 77 mg). The crude reaction mixture was purified by silica gel column chromatography (pet ether/EtOAc = 80:20) to afford product **3z** (39 mg, 51%). Melting point: 104-106 ºC.^{1}H NMR (400 MHz, $CDCl_3$) δ 8.18 (d, *J* = 8.3 Hz, 1H), 7.95 (ddd, *J* = 22.6, 13.7, 6.9 Hz, 2H), 7.73 – 7.66 (m, 1H), 7.61 (t, *J* = 7.7 Hz, 1H), 7.50 – 7.42 (m, 3H), 5.82 (ddt, *J* = 17.0, 10.1, 6.7 Hz, 1H), 5.09 – 4.96 (m, 2H), 4.51 – 4.38 (m, 2H), 2.18 (dd, *J* = 14.3, 7.1 Hz, 2H), 1.90 (dt, *J* = 12.5, 7.8 Hz, 2H), 1.71 – 1.62 (m, 2H).^{13}C{^{1}H} NMR (100 MHz, $CDCl_3$) δ 150.5, 145.8, 143.6, 128.0, 132.8, 131.6, 131.3, 130.7, 128.8, 124.9, 124.5, 120.2, 115.3, 114.0. 113.3, 43.4, 33.3, 26.7, 26.2. IR (neat): 1734, 1660, 1604 cm^{-1}. HRMS (ESI) calculated for $C_{20}H_{20}N_5O$ $[M+H]^+$ m/z 346.1668, found 346.1679.

1-allyl-3-(5,6-dimethyl-1*H*-benzo[d][1,2,3]triazol-1-yl)quinoxalin-2(1*H*)-one (3aa) Prepared according to the general procedure using using 1-(hex-5-en-1-yl)quinoxalin-2(1*H*)-one (0.25 mmol, 57 mg), 4,5-dimethyl-1,2-phenylenediamine (0.25 mmol, 34 mg) and tert-butyl nitrite (0.75 mmol, 77 mg). The crude reaction mixture was purified by silica gel column chromatography (petroleum ether/EtOAc = 80:20) to afford product **3aa** (41 mg, 48%) as yellow semi-solid.^{1}H NMR (400 MHz, $CDCl_3$) δ 8.02 – 7.98 (m, 1H), 7.89 (s, 1H), 7.69 – 7.57 (m, 2H), 7.49 – 7.41 (m, 2H), 5.87 – 5.77 (m, 1H), 5.12 – 4.95 (m, 2H), 4.50 – 4.37 (m, 2H), 2.46 (s, 3H), 2.44 (s, 3H), 2.41 (s, 2H), 2.20 – 2.15 (m, 2H), 1.93 – 1.85 (m, 2H). ^{13}C{^{1}H} NMR (100 MHz, $CDCl_3$) δ 150.5, 145.0, 139.2, 138.0, 134,7, 132.7, 131.8, 131.3, 130.7, 124.4, 119.4, 115.3, 114.0, 112.8, 43.3, 33.3, 26.7, 26.2, 21.2, 20.4. IR (neat): 1667, 1605, 1590 cm^{-1}. HRMS (ESI) calculated for $C_{22}H_{24}N_5O$ $[M+H]^+$ m/z 374.1981, found 374.1974.

3-(5,6-dimethyl-1*H*-benzo[d][1,2,3]triazol-1-yl)-6,7-difluoro-1-methylquinoxalin-2(1*H*)-one (3ab) Prepared according to the general procedure using 6,7-difluoro-1-methylquinoxalin-2(1*H*)-one (0.25 mmol, 49 mg), 4,5-dimethyl-1,2-phenylenediamine (0.25 mmol, 34 mg) and tert-butyl nitrite (0.75 mmol, 77 mg). The crude reaction mixture was evaporated in rotary evaporator and 3 mL MeOH was added and supernatant solution was thrown away. This process was repeated 2 times and the traces of solvent was evaporated in rotary evaporator to afford product **3ab** (61 mg, 72%).^{1}H NMR (400 MHz, $CDCl_3$) δ 7.91 – 7.67 (m, 3H), 7.24 – 6.87 (m, 1H), 3.83 (s, 3H), 2.46 (s, 3H), 2.44 (s, 3H). $^{13}C\{^{1}H\}$ NMR (100 MHz, $CDCl_3$) δ 150.3 (s), 144.9 (s), 143.38 – 143.18 (m), 139.5 (s), 135.0 (s), 131.5 (s), 119.5 (s), 118.0 (s), 117.9 (s), 117.8 (s), 112.9 (s), 105.3 (s), 102.9 (s) (s), 102.7 (s), 30.8 (s), 21.3 (s), 20.5 (s). $^{19}F\{^{1}H\}$ NMR (377 MHz, $CDCl_3$) δ −127.89 (s), −139.80 (s). IR (neat): 1708, 1672, 1607 cm^{-1}. HRMS (ESI) calculated for $C_{17}H_{14}F_2N_5O$ $[M+H]^+$ m/z 342.1166, found 342.1165.

Ethyl 2-(3-(1*H*-benzo[d][1,2,3]triazol-1-yl)-2-oxoquinoxalin-1(2*H*)-yl)acetate (4a) Prepared according to the general procedure using ethyl 2-(2-oxoquinoxalin-1(2H)-yl)acetate (0.25 mmol, 58 mg), *o*-phenylenediamine (0.25 mmol, 27 mg) and *tert*-butyl nitrite (0.75 mmol, 77 mg). The crude reaction mixture was purified by silica gel column chromatography (pet ether/EtOAc = 70:30) to afford product **4a** (54 mg, 62%). Melting point: 124-126 ºC.^{1}H NMR (400 MHz, $CDCl_3$) δ 8.15 (d, J = 8.3 Hz, 1H), 8.05 (d, *J* = 8.4 Hz, 1H), 7.98 (d, *J* = 8.0 Hz, 1H), 7.62 (ddd, *J* = 12.7, 10.6, 7.8 Hz, 2H), 7.50 – 7.42 (m, 2H), 7.21 (d, *J* = 8.4 Hz, 1H), 5.19 (s, 2H), 4.27 (q, J = 7.1 Hz, 2H), 1.29 (t, J = 7.1 Hz, 3H).$^{13}C\{^{1}H\}$ NMR (100 MHz, $CDCl_3$) δ 166.6, 150.5, 145.7, 143.3, 132.7, 131.8. 130.7, 129.0, 125.1, 125.0, 120.2, 113.6, 113.5, 62.4, 44.4, 14.1. IR (neat): 1737, 1707, 1608 cm^{-1}. HRMS (ESI) calculated for $C_{18}H_{16}N_5O_3$ $[M+H]^+$ m/z 350.1253, found 350.1255.

Ethyl 2-(3-(5,6-dimethyl-1*H*-benzo[d][1,2,3]triazol-1-yl)-2-oxoquinoxalin-1(2*H*)-yl)acetate (4b) Prepared according to the general procedure using ethyl 2-(2-oxoquinoxalin-1(2*H*)-yl)acetate (0.25 mmol, 58 mg), 4,5-dimethyl-1,2-phenylenediamine (0.25 mmol, 34 mg) and *tert*-butyl nitrite (0.75 mmol, 77 mg). The crude reaction mixture was purified by silica gel column chromatography (pet ether/EtOAc = 70:30) to afford product **4b** (65 mg, 69%). Melting point: 174-176 ºC. ^{1}H NMR (400 MHz, $CDCl_3$) δ 8.02 (dd, *J* = 8.0, 1.2 Hz, 1H), 7.89 (s, 1H), 7.81 (s, 1H), 7.67 – 7.61 (m, 1H), 7.51 – 7.43 (m, 1H), 7.21 (d, *J* = 8.2 Hz, 1H), 5.19 (s, 2H), 4.29 (q, *J* = 7.1 Hz, 2H), 2.46 (s, 3H), 2.44 (s, 3H), 1.30 (t, *J* = 7.1 Hz, 3H). $^{13}C\{^{1}H\}$ NMR (100 MHz, $CDCl_3$) δ 166.7, 150.5, 145.0, 143.6, 139.4, 134.9, 132.7, 131.7, 131.5, 131.2, 130.6, 124.9, 119.4, 113.5, 113.0, 62.4, 44.4, 21.1, 20.4, 14.1. IR (neat): 1737, 1705, 1606 cm^{-1}. HRMS (ESI) calculated for $C_{20}H_{20}N_5O3$ $[M+H]^+$ m/z 378.1566, found 378.1566.

Ethyl 2-(2-oxo-3-(6-(trifluoromethyl)-1*H*-benzo[d][1,2,3]triazol-1-yl)quinoxalin-1(2*H*)yl)acetate (4c) Prepared according to the general procedure using ethyl 2-(2-oxoquinoxalin-1(2*H*)-yl)acetate (0.25 mmol, 58 mg), 4-(trifluoromethyl)-benzene-1,2-diamine (0.25 mmol, 44 mg) and *tert*-butyl nitrite (0.75 mmol, 77 mg). The crude reaction mixture was purified by silica gel column chromatography (petroleum ether/EtOAc = 70:30) to afford product **4c** (61.5 mg, 59%). Melting point: 139-141 ºC. ^{1}H NMR (400 MHz, $CDCl_3$) δ 8.49 (s, 1H), 8.15 (d, *J* = 8.7 Hz, 1H), 8.06 – 8.02 (m, 1H), 7.85 (dd, *J* = 8.8, 1.3 Hz, 1H), 7.72 – 7.68 (m, 1H), 7.52 – 7.48 (m, 1H), 7.24 (s, 1H), 5.21 (s, 2H), 4.34 – 4.27 (m, 2H), 1.34 – 1.29 (m, 3H). ^{13}C{^{1}H} NMR (100 MHz, $CDCl_3$) δ 166.5 (s), 150.4 (s), 145.1 (s), 143.0 (s), 132.9 (s), 132.2 (s), 130.9 (s), 125.5 (d, *J* = 3.1 Hz), 125.2 (d, *J* = 7.2 Hz), 118.3 (d, *J* = 4.4 Hz), 114.4 (s), 113.6 (s), 62.5 (s), 44.4 (s), 14.1 (s). ^{19}F{^{1}H} NMR (377 MHz, $CDCl_3$) δ −61.51 (s). IR (neat): 1747, 1679, 1606 cm^{-1}. HRMS (ESI) calculated for $C_{19}H_{15}F_3N_5O_3$ $[M+H]^+$ m/z 418.1127, found 418.1133.

Ethyl 2-(3-(6-methoxy-1*H*-benzo[d][1,2,3]triazol-1-yl)-2-oxoquinoxalin-1(2*H*)-yl)acetate (4d) Prepared according to the general procedure using ethyl 2-(2-oxoquinoxalin-1(2*H*)-yl)acetate (0.25 mmol, 58 mg), 4-methoxybenzene-1,2-diamine (0.25 mmol, 34.5 mg) and *tert*-butyl nitrite (0.75 mmol, 77 mg). The crude reaction mixture was purified by silica gel column chromatography (petroleum ether/EtOAc = 70:30) to afford product **4d** (44.5 mg, 47%). Melting point: 183-185 ºC. 1HNMR (400 MHz, $CDCl_3$) δ 8.05 – 7.95 (m, 2H), 7.68 – 7.62 (m, 1H), 7.52 – 7.43 (m, 2H), 7.22 (d, *J* = 8.1 Hz, 1H), 7.10 (dd, *J* = 9.1, 2.3 Hz, 1H), 5.20 (s, 2H), 4.29 (q, *J* = 7.1 Hz, 2H), 3.92 (s, 3H), 1.30 (t, *J* = 7.1 Hz, 3H). ^{13}C{^{1}H} NMR (100 MHz, CDCl3) δ 166.6, 161.1, 150.5, 143.6, 140.9, 134.1, 132.7, 131.6, 131.1, 130.6, 130.6, 124.9, 121.1, 120.8, 116.7, 114.2, 113.5, 99.4, 94.6, 62.4, 55.9, 44.4, 14.1. IR (neat): 1736, 1704, 1644 cm-1. HRMS (ESI) calculated for $C_{19}H_{18}N_5O_4$ $[M+H]^+$ m/z 380.1359, found 380.1357.

2-(3-(1*H*-benzo[d][1,2,3]triazol-1-yl)-2-oxoquinoxalin-1(2*H*)-yl)acetonitrile (4e) Prepared according to the general procedure using using 2-(2-oxoquinoxalin-1(2*H*)-yl)acetonitrile (0.25 mmol, 46 mg), *o*-phenylenediamine (0.25 mmol, 27 mg) and *tert*-butyl nitrite (0.75 mmol, 77 mg).The crude reaction mixture was purified by silica gel column chromatography (pet ether/EtOAc = 70:30) to afford product **4e** (42 mg, 56%). Melting point: 202-204 ºC. ^{1}H NMR (400 MHz, $CDCl_3$) δ 8.20 (d, *J* = 7.8 Hz, 1H), 8.13 (d, *J* = 8.3 Hz, 1H), 8.05 (d, *J* = 8.0 Hz, 1H), 7.79 (t, *J* = 7.9 Hz, 1H), 7.71 – 7.64 (m, 1H), 7.59 – 7.47 (m, 3H), 5.39 (s, 2H). ^{13}C{^{1}H} NMR (100 MHz, $CDCl_3$) δ 150.0, 145.7, 132.5, 132.2, 131.2, 131.1, 131.0, 129.3, 125.9, 125.5, 120.4, 113.4, 113.4, 113.1, 30.3. HRMS (ESI) calculated for $C_{16}H_{11}N_6O$ $[M+H]^+$ m/z 303.0994, found 303.0992.

2-(3-(5,6-dimethyl-1*H*-benzo[d][1,2,3]triazol-1-yl)-2-oxoquinoxalin-1(2*H*)-yl)acetonitrile (4f) Prepared according to the general procedure using using 2-(2-oxoquinoxalin-1(2*H*)-yl)acetonitrile (0.25 mmol, 46 mg), 4,5-dimethyl-1,2-phenylenediamine (0.25 mmol, 34 mg) and *tert*-butyl nitrite (0.75 mmol, 77 mg). The crude reaction mixture was purified by silica gel column chromatography (petroleum ether/EtOAc = 70:30) to afford product **4f** (49 mg, 60 %). Melting point: 244-246 ºC. ^{1}H NMR (400 MHz, $CDCl_3$) δ 8.07 – 8.02 (m, 1H), 7.87 (d, *J* = 10.5 Hz, 2H), 7.80 – 7.73 (m, 1H), 7.58 – 7.52 (m, 1H), 7.52 – 7.46 (m, 1H), 5.38 (s, 2H), 2.48 (s, 3H), 2.44 (s, 3H). ^{13}C{^{1}H} NMR (100 MHz, $CDCl_3$) δ 150.0, 144.8, 143.1, 140.0, 135.3, 132.0, 131.4, 131.1, 131.1, 131.0, 125.8, 119.5, 113.4, 113.2, 112.9, 30.3, 21.2, 20.5. HRMS (ESI) calculated for $C_{18}H_{15}N_6O$ $[M+H]^+$ m/z 331.1307, found 331.1314.

3-(1*H*-benzo[d][1,2,3]triazol-1-yl)-1-(cyclopropylmethyl)quinoxalin-2(1*H*)-one (4g) Prepared according to the general procedure using using 1-(cyclopropylmethyl)quinoxalin-2(1*H*)-one (0.25 mmol, 50 mg), *o*-phenylenediamine (0.25 mmol, 27 mg) and *tert*-butyl nitrite (0.75 mmol, 77 mg). The crude reaction mixture was purified by silica gel column chromatography (pet ether/EtOAc = 70:30) to afford product **4g** (58 mg, 74 %). Melting point: 148-150 ºC.^{1}HNMR (400 MHz, $CDCl_3$) δ 8.16 (d, *J* = 8.3 Hz, 1H), 7.99 (d, *J* = 8.2 Hz, 2H), 7.74 – 7.65 (m, 1H), 7.64 – 7.54 (m, 2H), 7.50 – 7.40 (m, 2H), 4.37 (d, *J* = 7.1 Hz, 2H), 1.46 – 1.29 (m, 1H), 0.69 – 0.56 (m, 4H). ^{13}C{^{1}H} NMR (100 MHz, $CDCl_3$) δ 150.9, 145.8, 143.7, 133.0, 132.8, 131.5, 131.2, 130.7, 128.8, 124.9, 124.5, 120.2, 114.3, 113.3, 47.4, 9.7, 4.3. IR (neat): 1733, 1664, 1605 cm^{-1}. HRMS (ESI) calculated for $C_{18}H_{16}N_5O$ $[M+H]^+$ m/z 318.1355, found 318.1347.

1-(cyclopropylmethyl)-3-(5,6-dimethyl-1*H*-benzo[d][1,2,3]triazol-1-yl)quinoxalin-2(1*H*)-one (4h) Prepared according to the general procedure using using 1-(cyclopropylmethyl)quinoxalin-2(1*H*)-one (0.25 mmol, 50 mg), 4,5-dimethyl-1,2-phenylenediamine (0.25 mmol, 34 mg) and *tert*-butyl nitrite (0.75 mmol, 77 mg). The crude reaction mixture was purified by silica gel column chromatography (pet ether/EtOAc = 70:30) to afford product **4h** (55 mg, 64 %). Melting point: 168-170 ºC. ^{1}H NMR (400 MHz, $CDCl_3$) δ 8.04 – 7.98 (m, 1H), 7.88 (s, 1H), 7.74 (s, 1H), 7.71 – 7.64 (m, 1H), 7.59 – 7.54 (m, 1H), 7.45 (t, *J* = 7.6 Hz, 1H), 4.37 (d, *J* = 7.1 Hz, 2H), 2.45 (s, 3H), 2.43 (s, 3H), 1.44 – 1.31 (m, 1H), 0.68 – 0.56 (m, 4H). ^{13}C{^{1}H} NMR (100 MHz, $CDCl_3$) δ 150.9, 145.0, 143.9, 139.2, 134.7, 132.9, 131.8, 131.3, 130.6, 124.4, 119.3, 114.3, 112.8, 47.3, 21.2, 20.4, 9.7, 4.3. IR (neat): 1733, 1663, 1605 cm^{-1}. HRMS (ESI) calculated for $C_{20}H_{20}N_5O$ $[M+H]^+$ m/z 346.1668, found 346.1665.

1-((1-benzhydryl-1*H*-1,2,3-triazol-4-yl)methyl)-3-(1*H*-benzo[d][1,2,3]triazol-1-yl)quinoxalin-2(1*H*)-one (3pp) 3-(1*H*-benzo[d][1,2,3]triazol-1-yl)-1-(prop-2-yn-1-yl)quinoxalin-2(1*H*)-one (30 mg,

0.1 mmol), (azidomethylene)dibenzene (63 mg, 0.3 mmol), sodium ascorbate (4 mg, 0.02 mmol) and $CuSO_4.5H_2O$ (2.5 mg, 0.01 mmol) were mixed in a 20 mL resealable glass vial containing 4 mL ^tBuOH-H_2O (1:1) and stirred at 60 ^oC for 4 h. The crude reaction mixture was then purified by column chromatorgraphy (70:30 PE: EA) to afford product **3pp** as yellow solid (34 mg, 67%). ^{1}HNMR (400 MHz, $CDCl_3$) δ 8.17 (dd, J = 8.3, 0.8 Hz, 1H), 8.08 – 7.91 (m, 2H), 7.74 – 7.70 (m, 1H), 7.64 – 7.51 (m, 2H), 7.49 – 7.43 (m, 1H), 7.35 – 7.30 (m, 7H), 7.14 – 6.96 (m, 6H), 5.69 (s, 1H), 5.52 (s, 1H). $^{13}C\{^1H\}$ NMR (100 MHz, $CDCl_3$) δ 154.8, 150.6, 149.8, 145.8, 143.2, 142.0, 141.5, 137.8, 137.7, 133.6, 132.8, 132.7, 132.3, 131.9, 131.4, 131.1, 130.4, 130.2, 129.0, 128.9, 128.7, 128.1, 125.1, 125.0, 124.3, 124.1, 123.7, 120.3, 115.5, 115.1, 113.3, 68.6, 68.5, 39.1, 37.8. HRMS (ESI) calculated for $C_{30}H_{23}N_8O$ $[M+H]^+$ m/z 511.1995, found 511.1997.

4.7. Appendix III: Copies of ^{1}H and ^{13}C NMR spectra of representative compounds of NMR spectra

Entry	Figure No.	Data	Page No.
3a	4.2-4.3	^{1}H and ^{13}C	137
3b	4.4-4.5	^{1}H and ^{13}C	138
3e	4.6-4.7	^{1}H and ^{13}C	139
3f	4.8-4.9	^{1}H and ^{13}C	140
3h	4.10-4.11	^{1}H and ^{13}C	141
3i	4.12-4.13	^{1}H and ^{13}C	142
3l	4.14-4.15	^{1}H and ^{13}C	143
3o	4.16-4.17	^{1}H and ^{13}C	144
3p	4.18-4.19	^{1}H and ^{13}C	145
3q	4.20-4.21	^{1}H and ^{13}C	146
3s	4.22-4.23	^{1}H and ^{13}C	147
3v	4.24-4.25	^{1}H and ^{13}C	148
4a	4.26-4.27	^{1}H and ^{13}C	149
3pp	4.28-4.29	^{1}H and ^{13}C	150

4.7.1. Representative examples of NMR Spectra

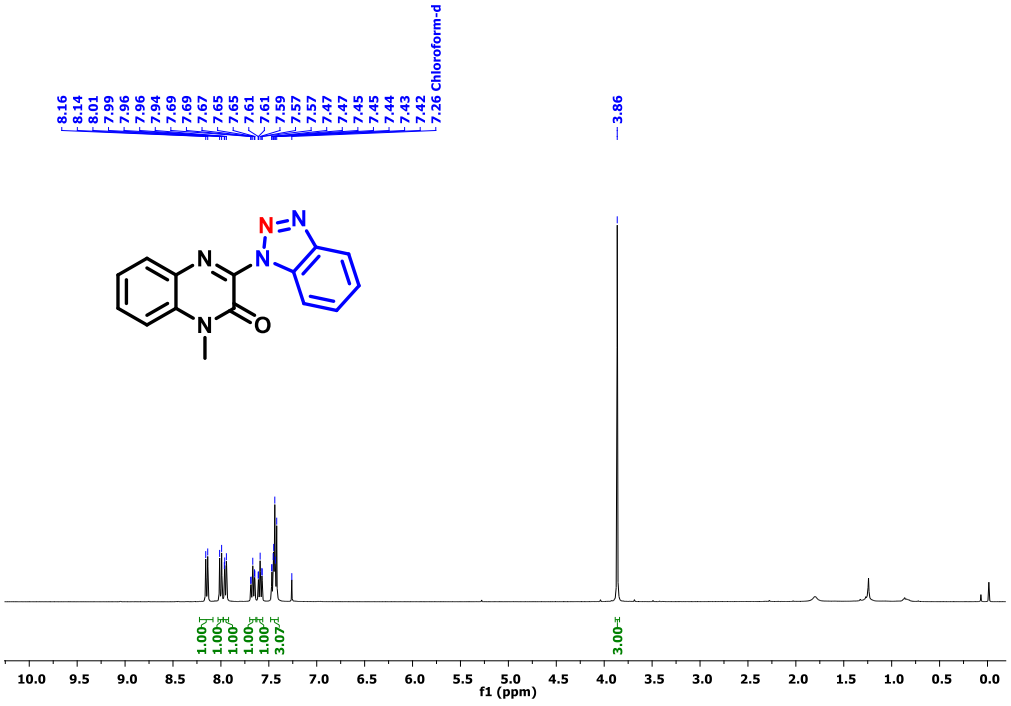


Figure 4.2: ^{1}H NMR of **3a**, 400 MHz, $CDCl_3$

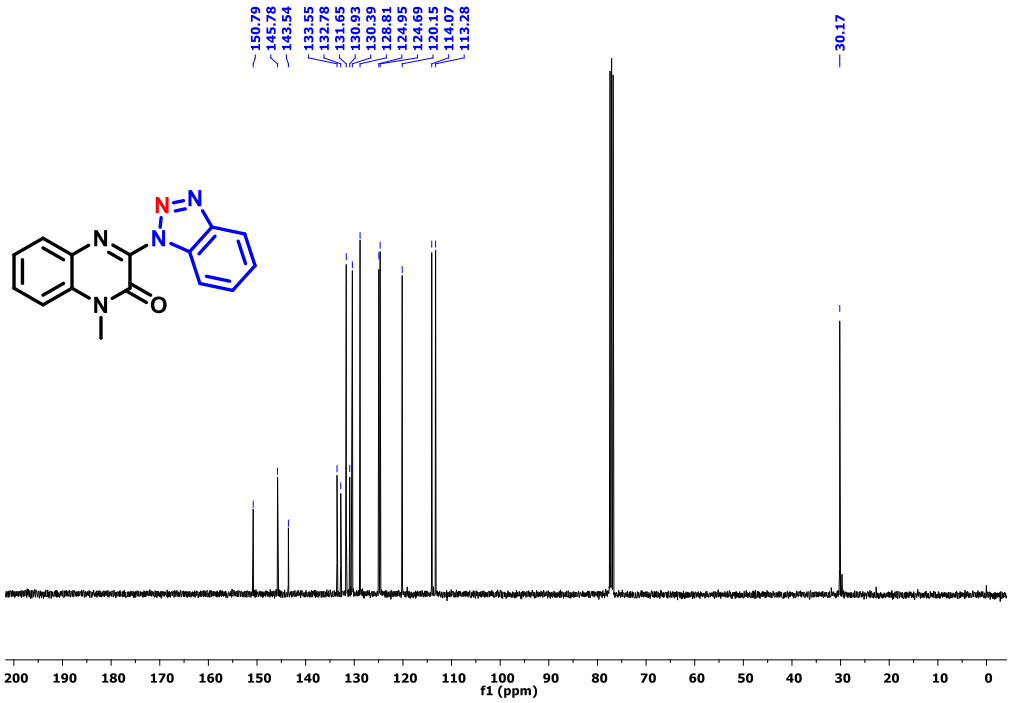


Figure 4.3: ^{13}C {^{1}H} NMR of **3a**, 100 MHz, $CDCl_3$

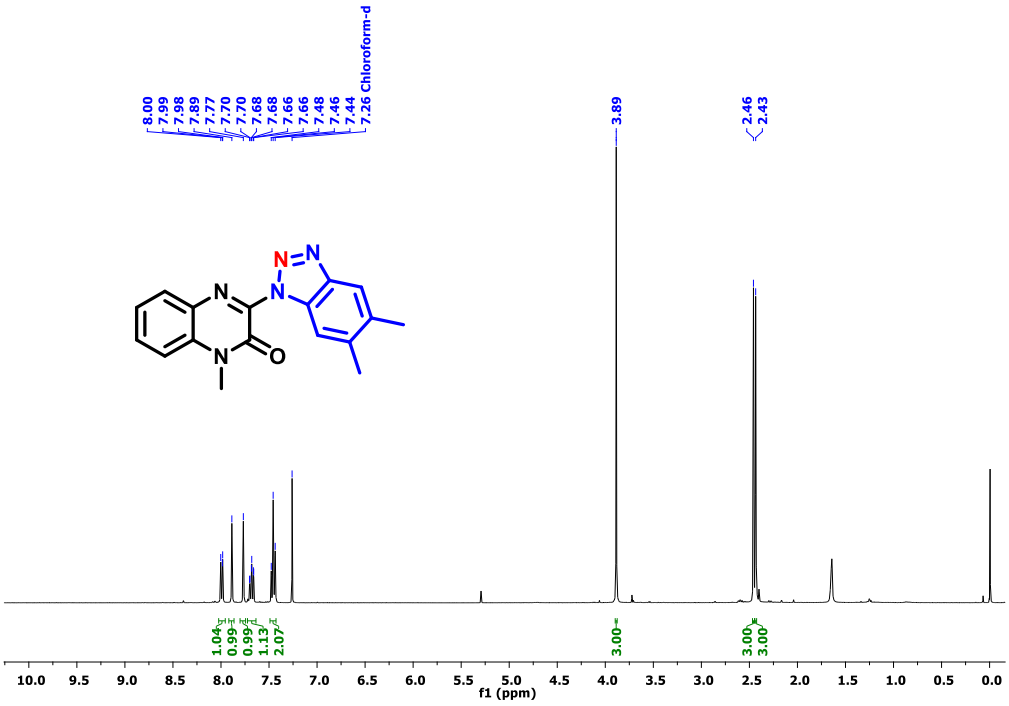


Figure 4.4: ^{1}H NMR of **3b**, 400 MHz, $CDCl_3$

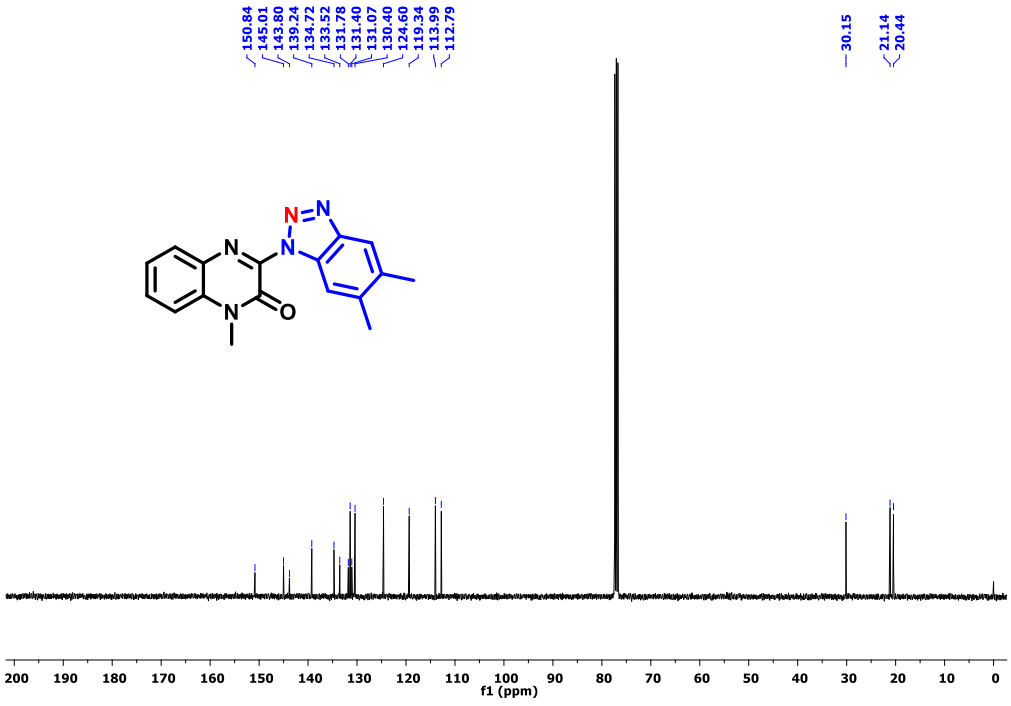


Figure 4.5: ^{13}C $\{^{1}H\}$ NMR of **3b**, 100 MHz, $CDCl_3$

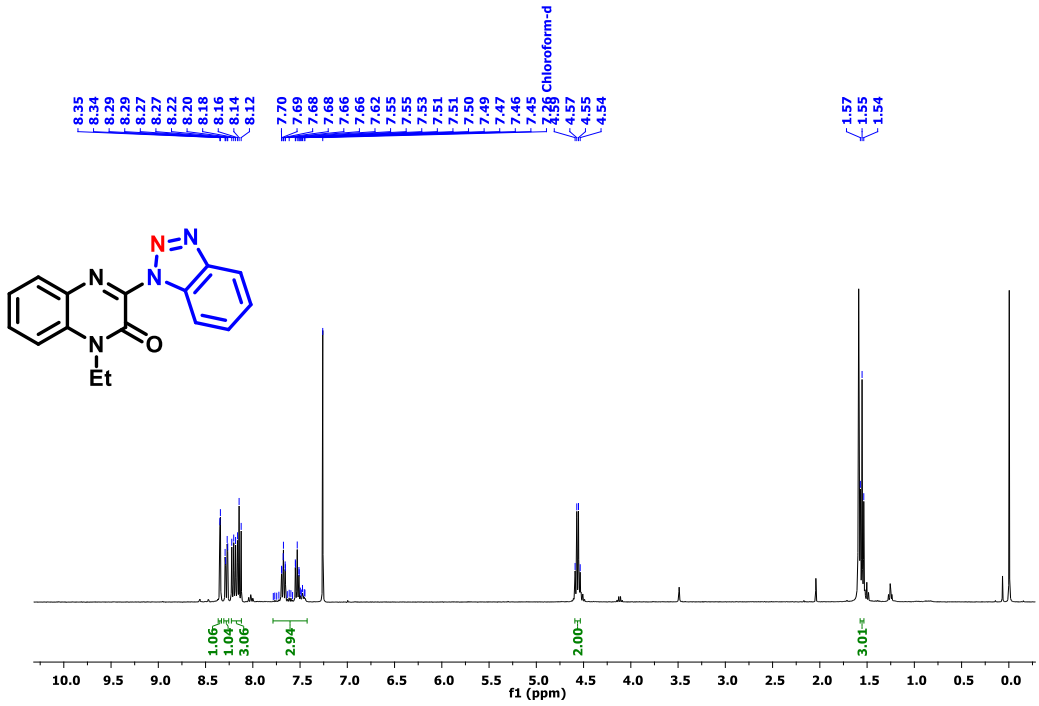


Figure 4.6: ^{1}H NMR of **3e**, 400 MHz, $CDCl_3$

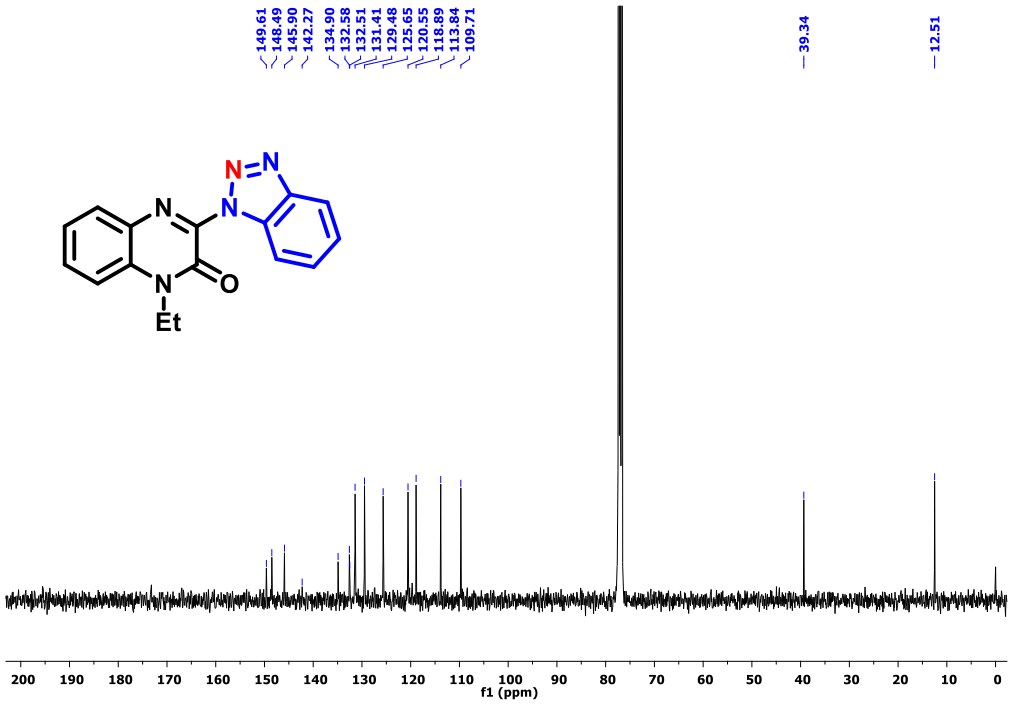


Figure 4.7: ^{13}C $\{^{1}H\}$ NMR of **3e**, 100 MHz, $CDCl_3$

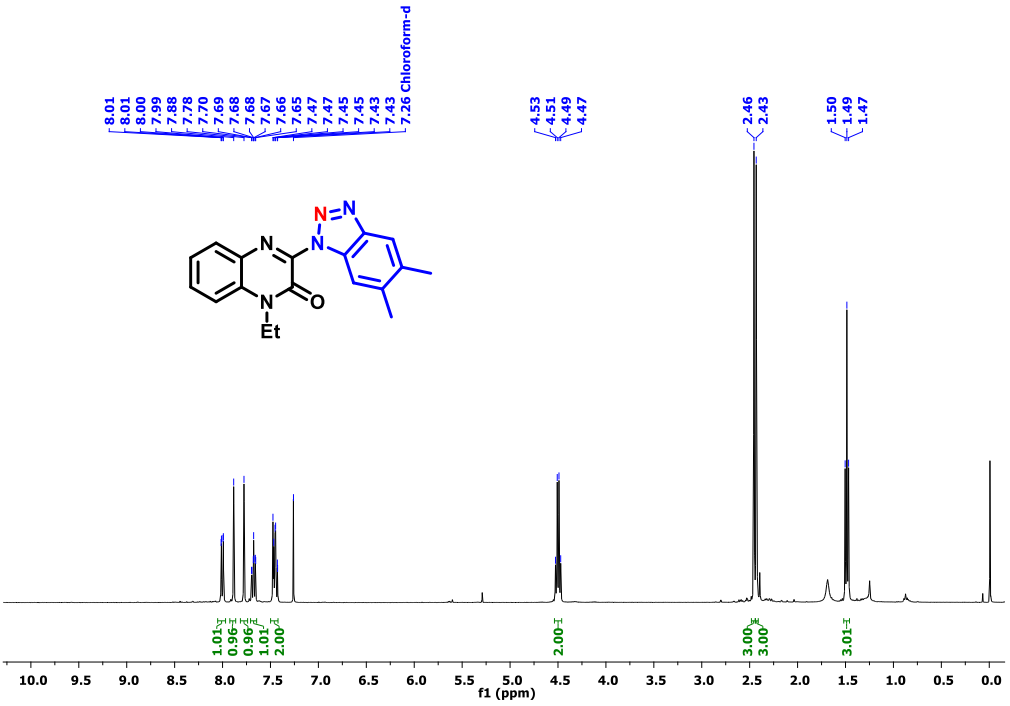


Figure 4.8: ^{1}H NMR of **3f**, 400 MHz, $CDCl_3$

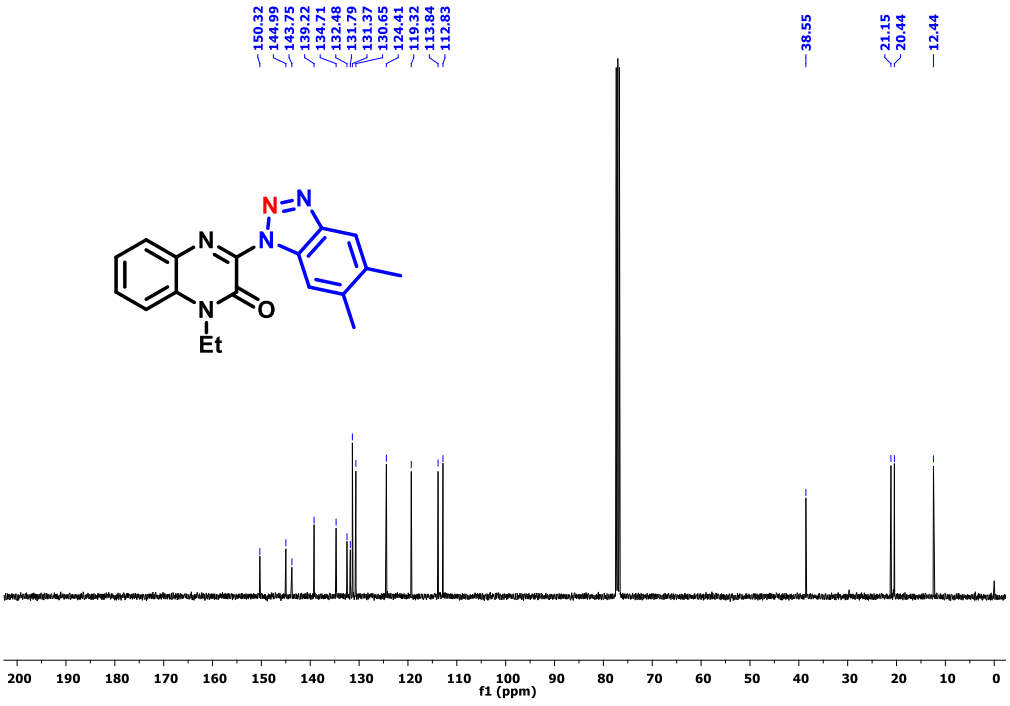


Figure 4.9: ^{13}C $\{^{1}H\}$ NMR of **3f**, 100 MHz, $CDCl_3$

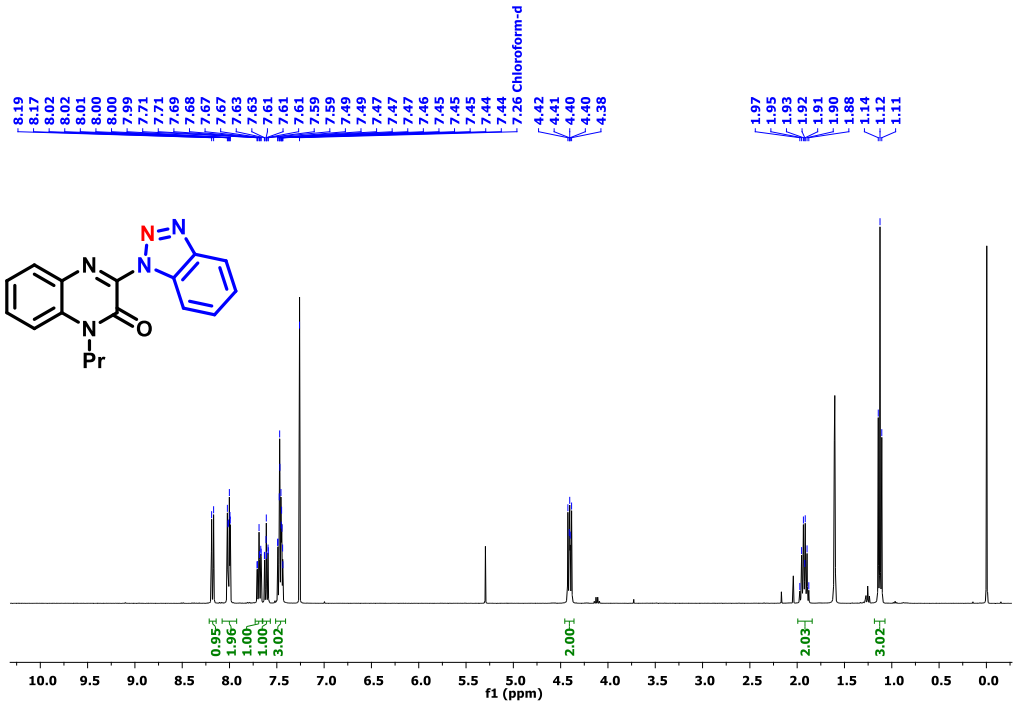


Figure 4.10: ^{1}H NMR of **3h**, 400 MHz, $CDCl_3$

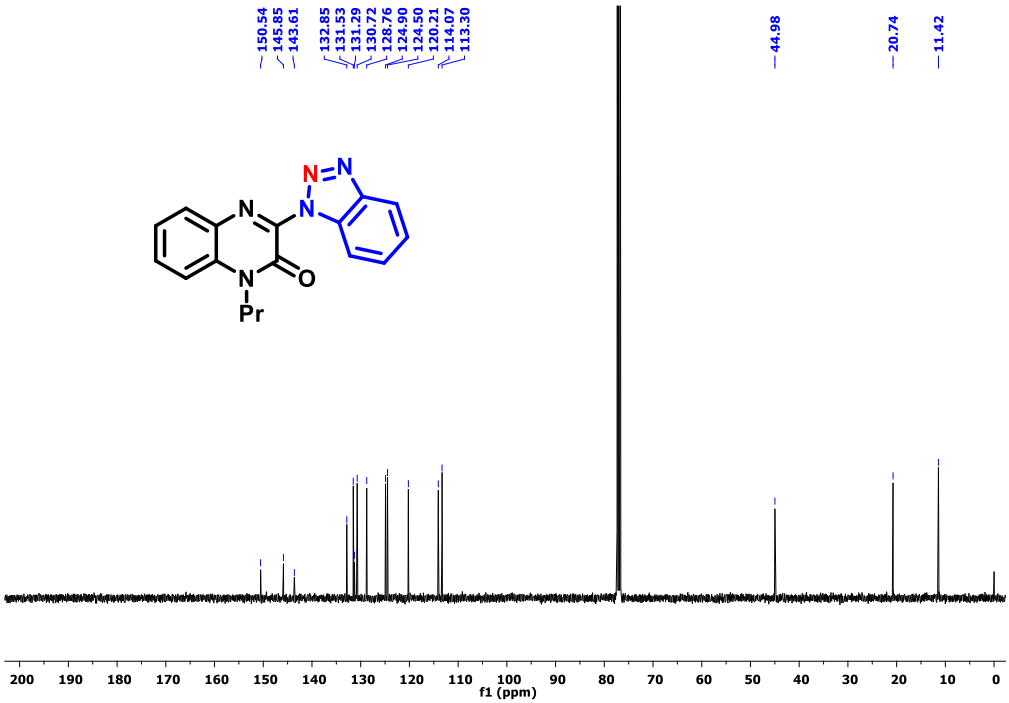


Figure 4.11: ^{13}C {^{1}H} NMR of **3h**, 100 MHz, $CDCl_3$

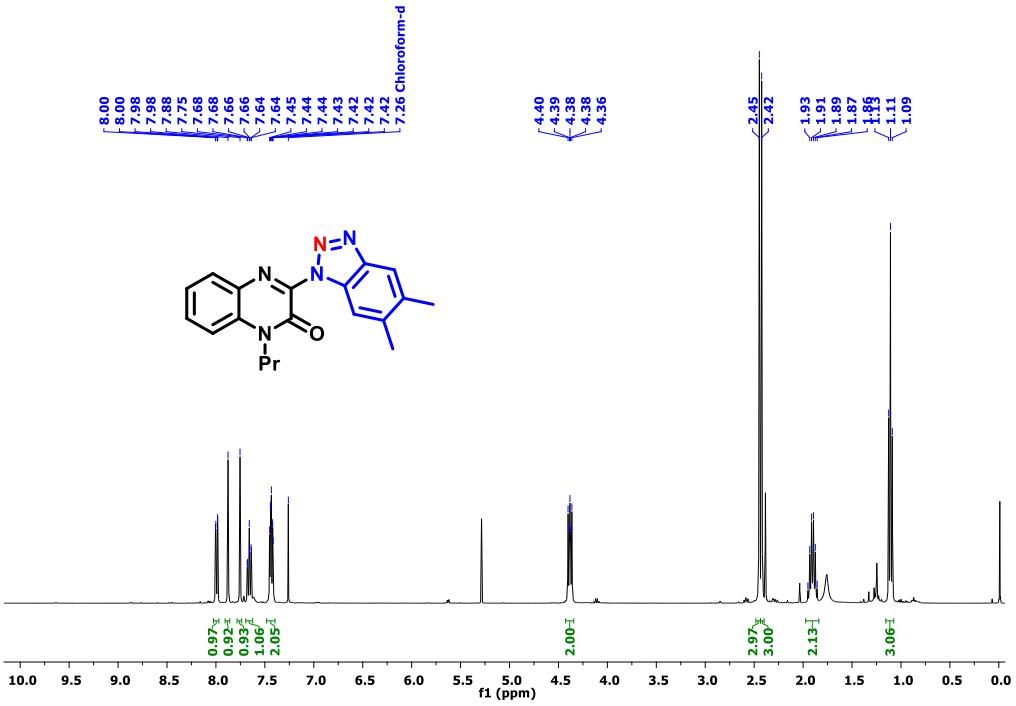


Figure 4.12: ^{1}H NMR of **3i**, 400 MHz, $CDCl_3$

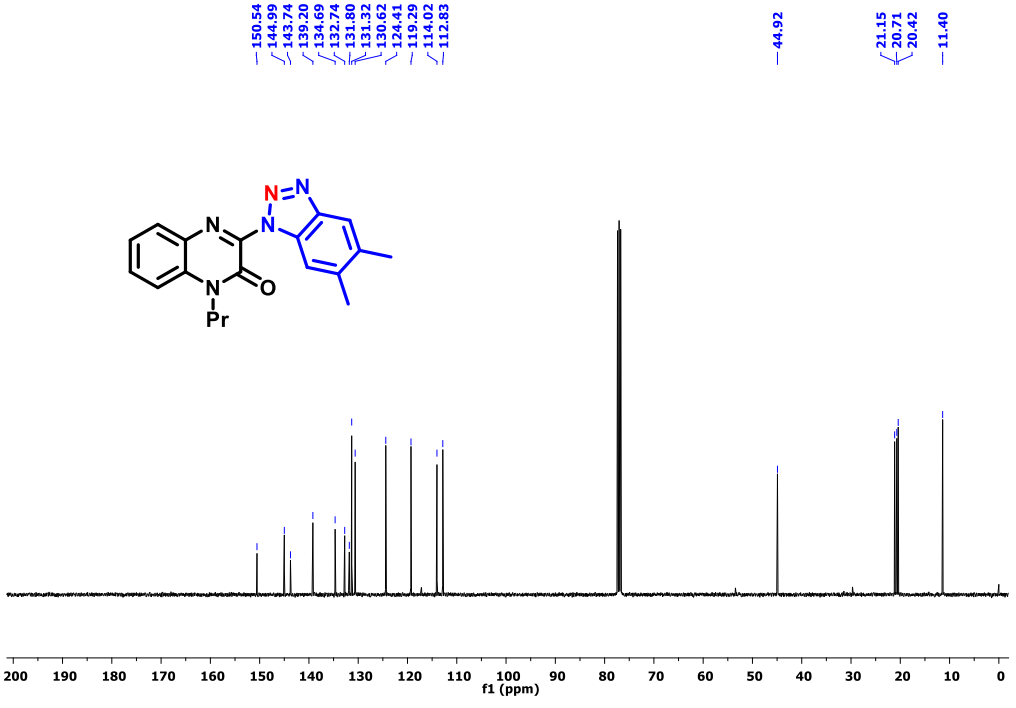


Figure 4.13: ^{13}C $\{^{1}H\}$ NMR of **3i**, 100 MHz, $CDCl_3$

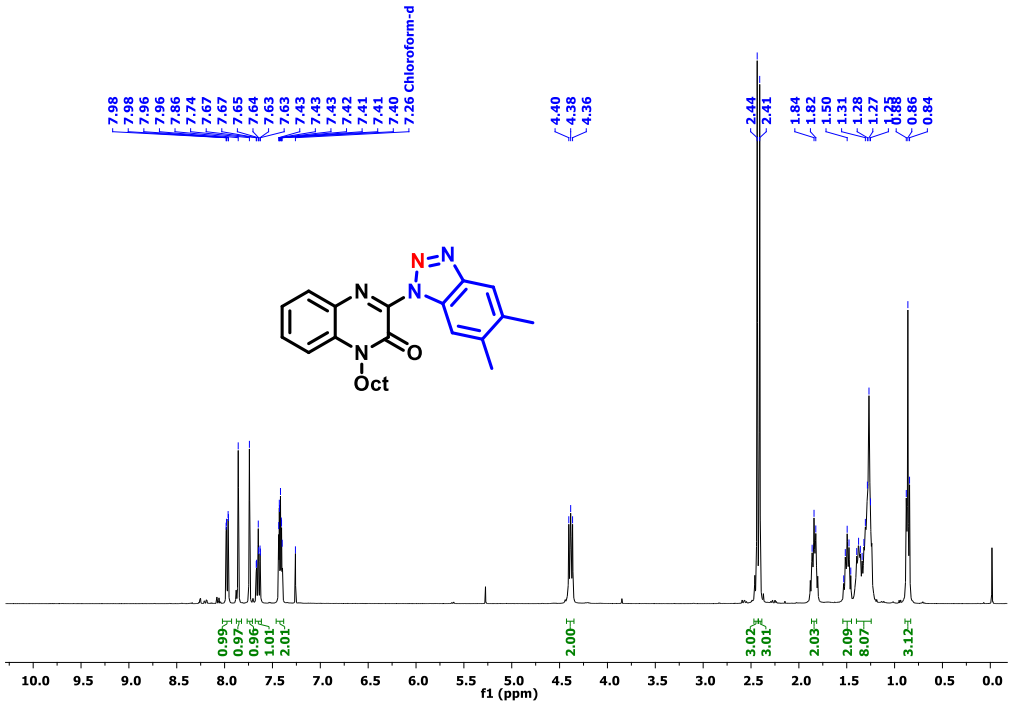


Figure 4.14: ^{1}H NMR of **3l**, 400 MHz, $CDCl_3$

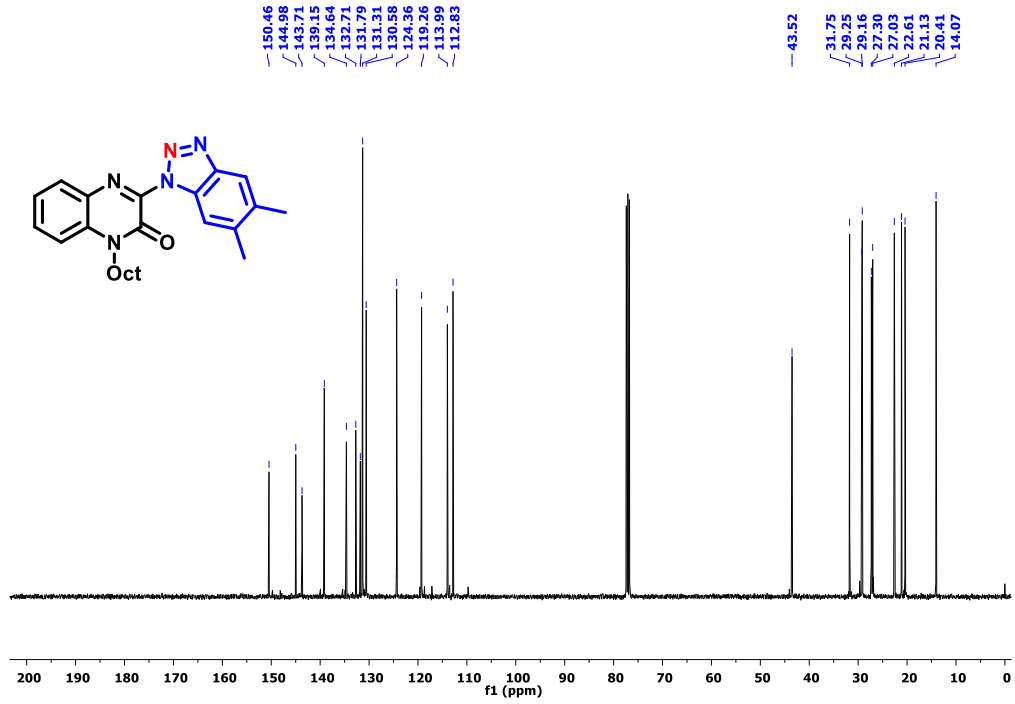


Figure 4.15: ^{13}C {^{1}H} NMR of **3l**, 100 MHz, $CDCl_3$

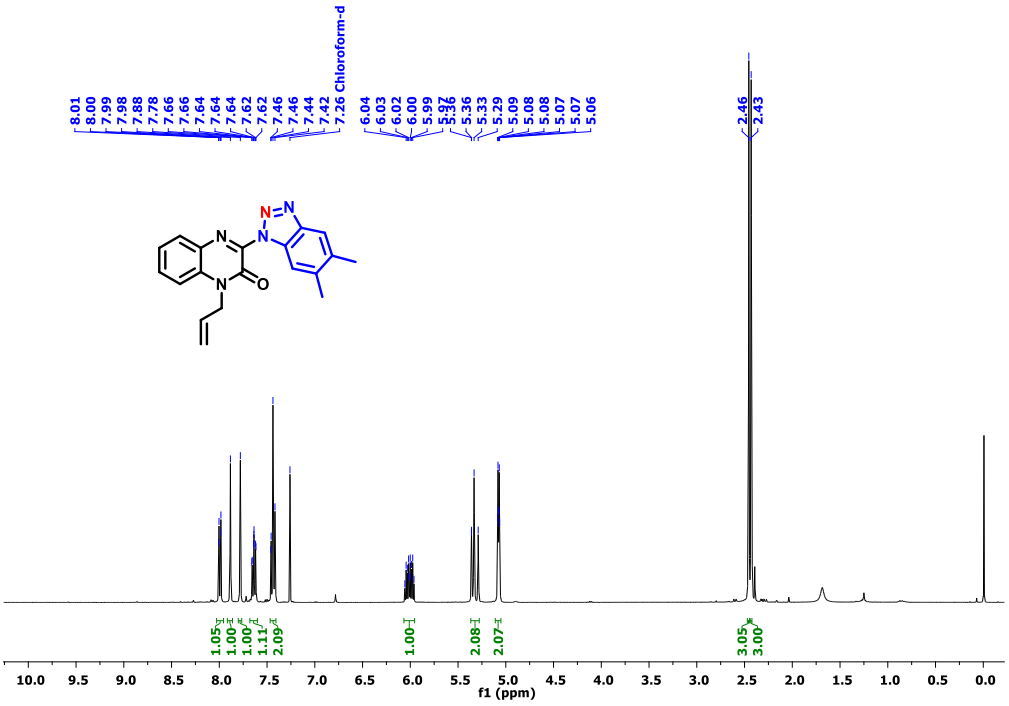


Figure 4.16: ^{1}H NMR of **3o**, 400 MHz, $CDCl_3$

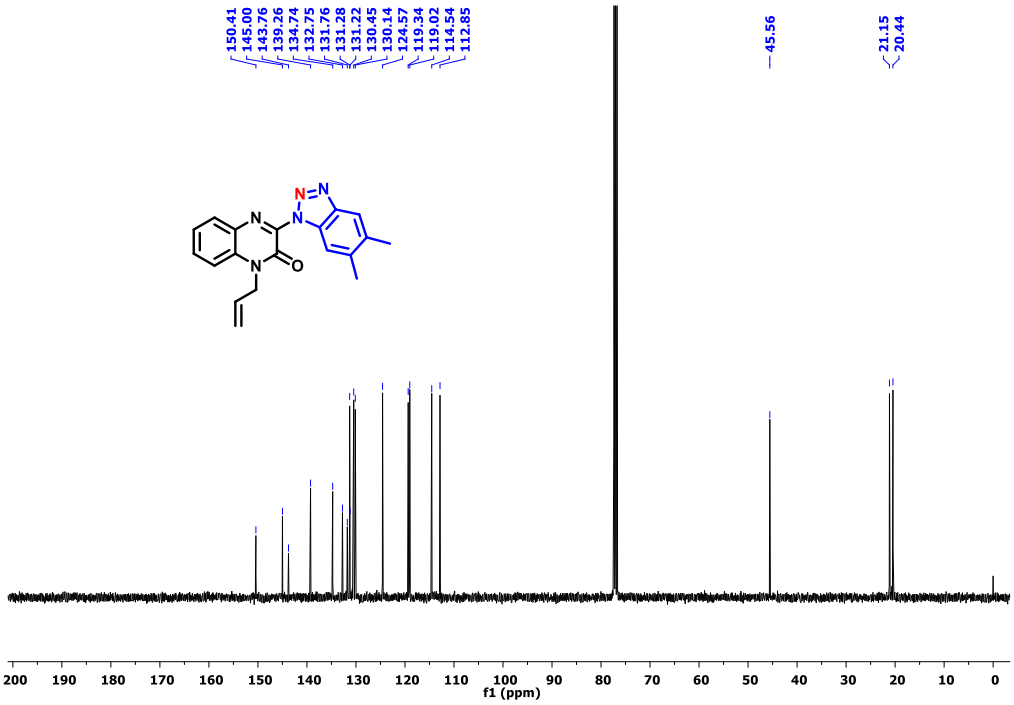


Figure 4.17: ^{13}C $\{^{1}H\}$ NMR of **3o**, 100 MHz, $CDCl_3$

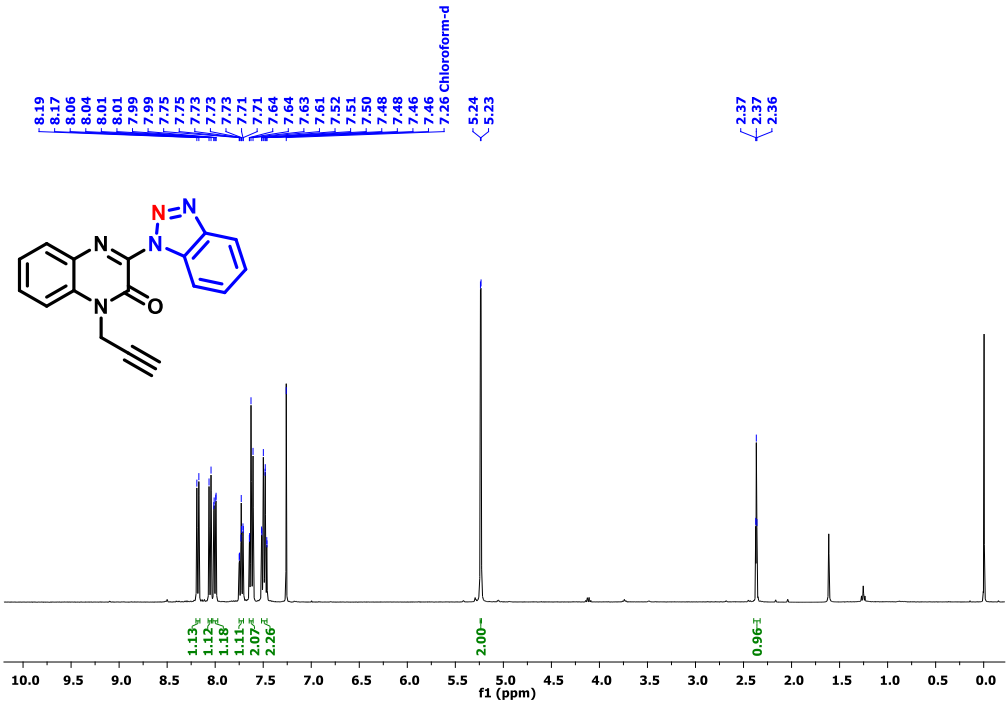


Figure 4.18: ^{1}H NMR of **3p**, 400 MHz, $CDCl_3$

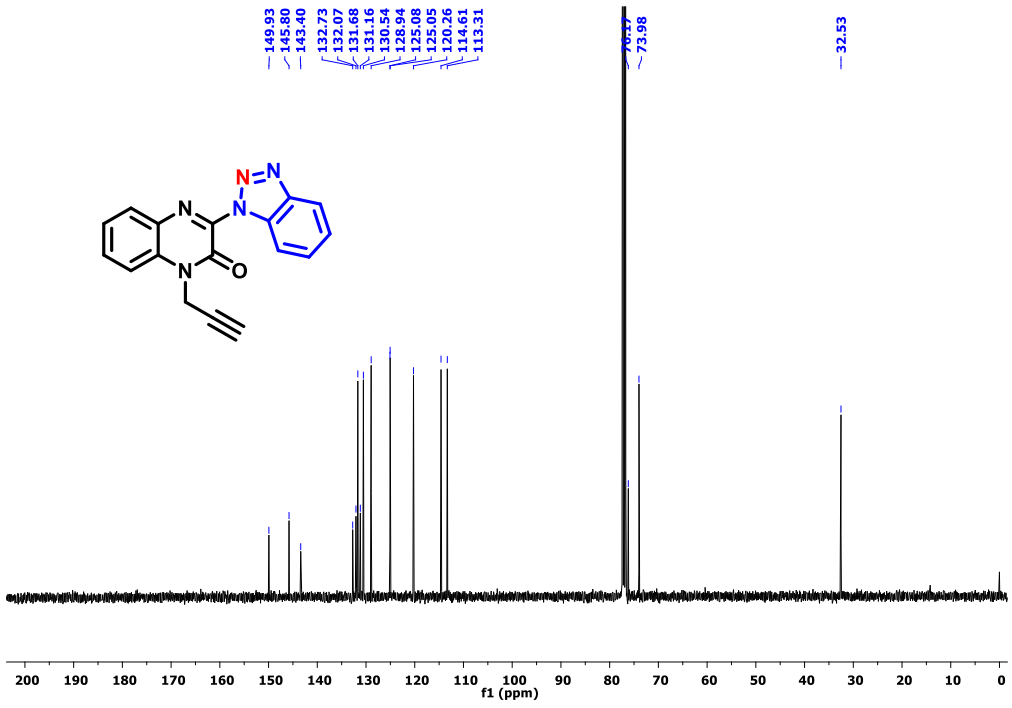


Figure 4.19: ^{13}C $\{^{1}H\}$ NMR of **3p**, 100 MHz, $CDCl_3$

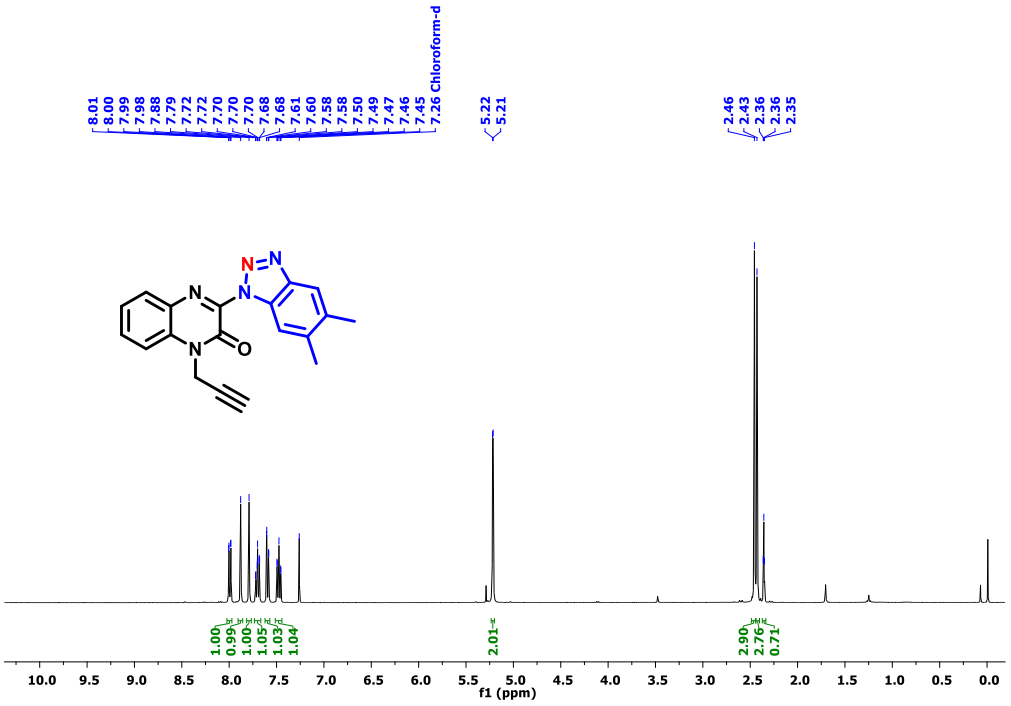


Figure 4.20: ^{1}H NMR of **3q**, 400 MHz, $CDCl_3$

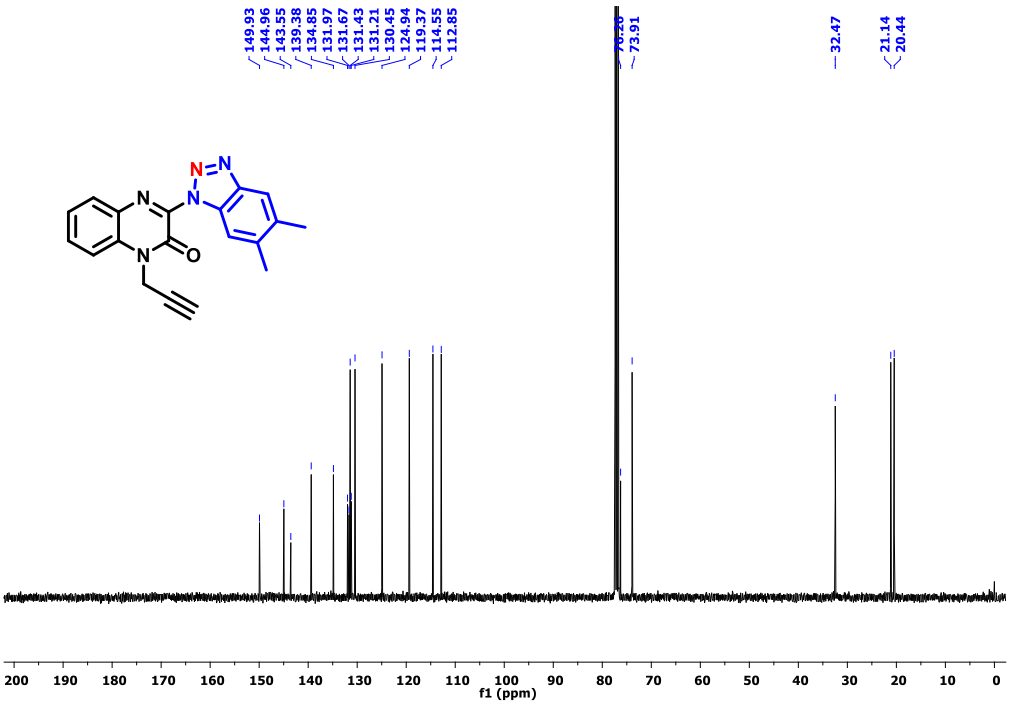


Figure 4.21: ^{13}C {^{1}H} NMR of **3q**, 100 MHz, $CDCl_3$

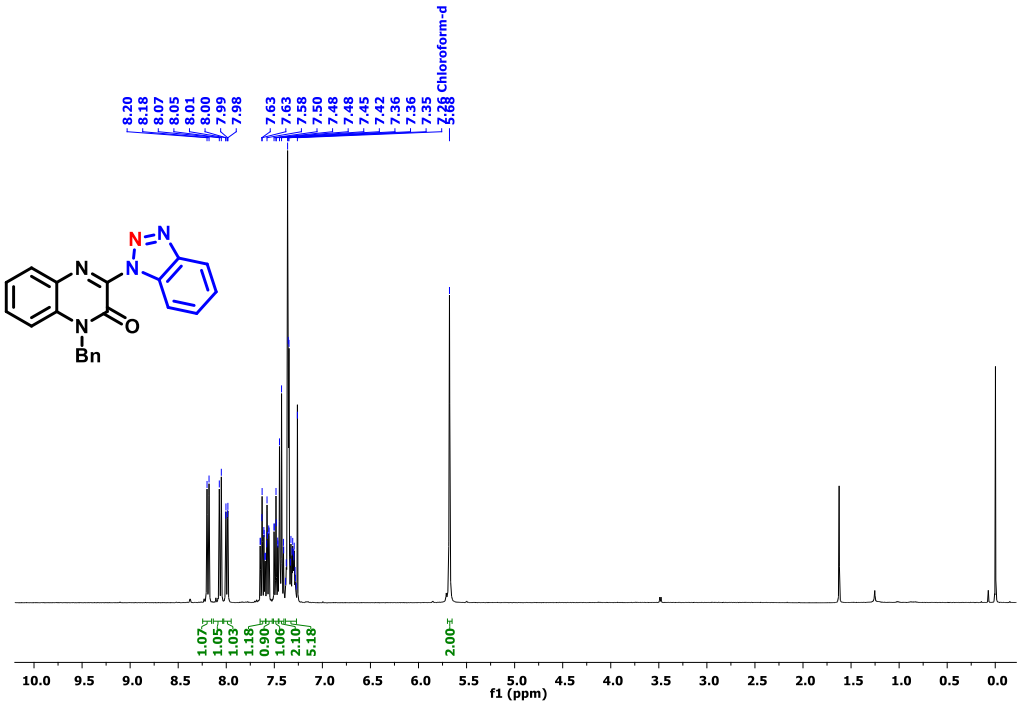


Figure 4.22: ^{1}H NMR of **3s**, 400 MHz, $CDCl_3$

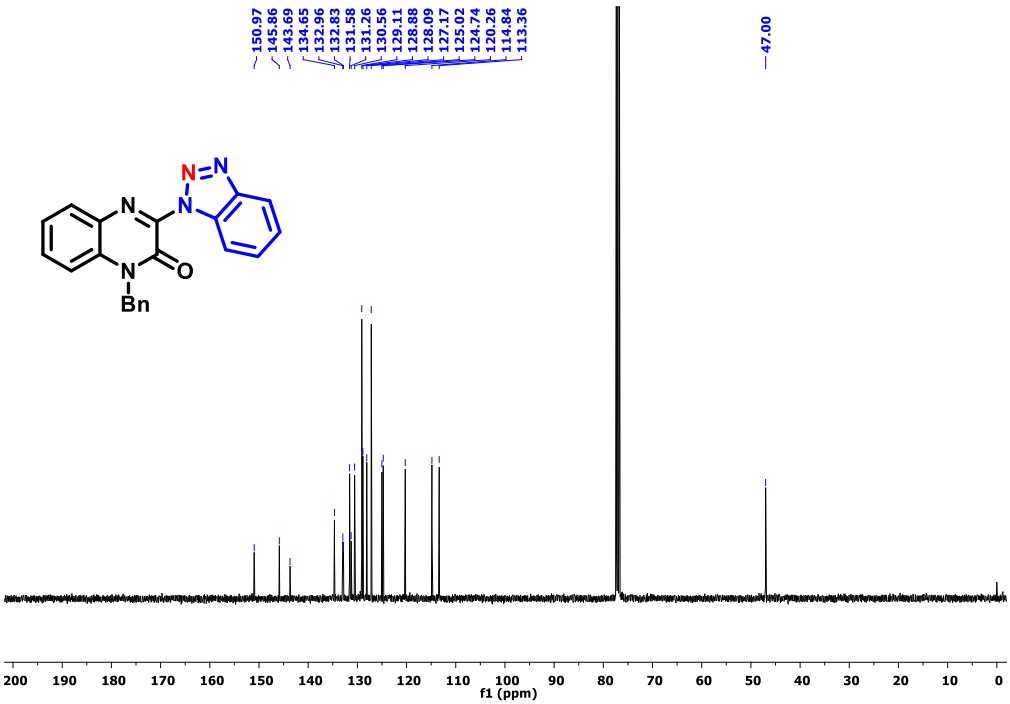


Figure 4.23: ^{13}C {^{1}H} NMR of **3s**, 100 MHz, $CDCl_3$

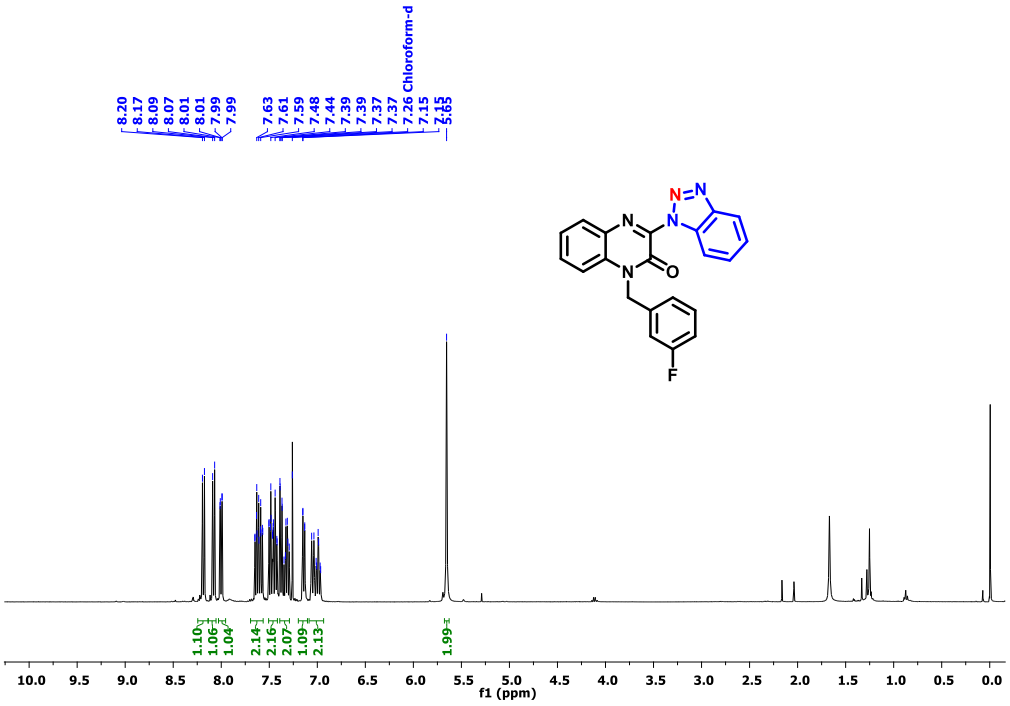


Figure 4.24: ^{1}H NMR of **3v**, 400 MHz, $CDCl_3$

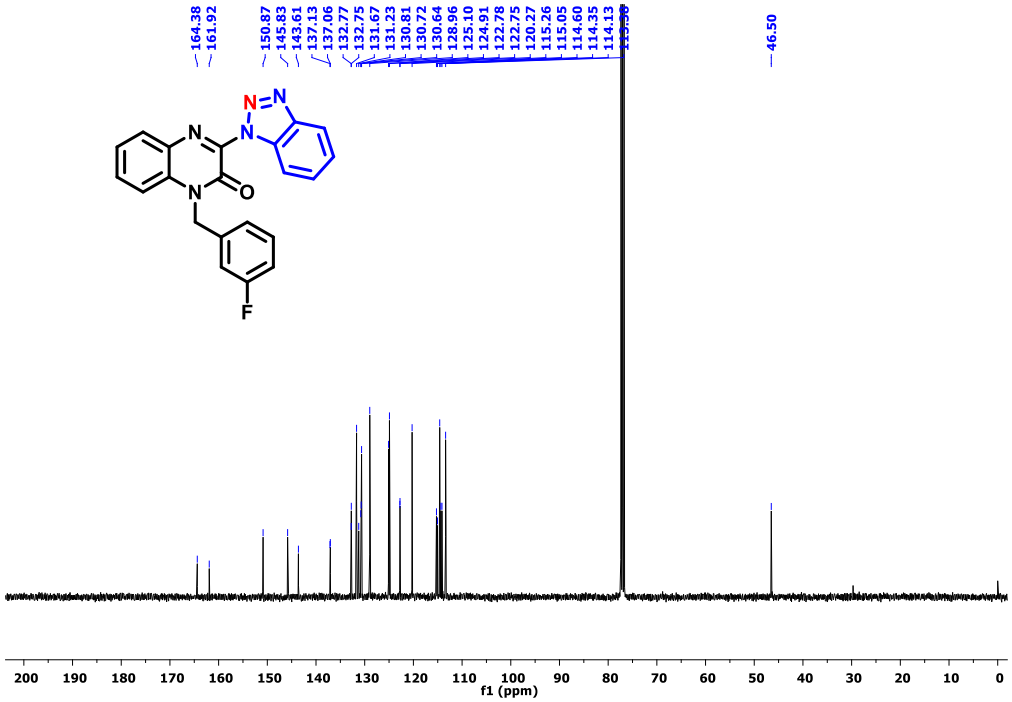


Figure 4.25: ^{13}C $\{^{1}$H$\}$ NMR of **3v**, 100 MHz, $CDCl_3$

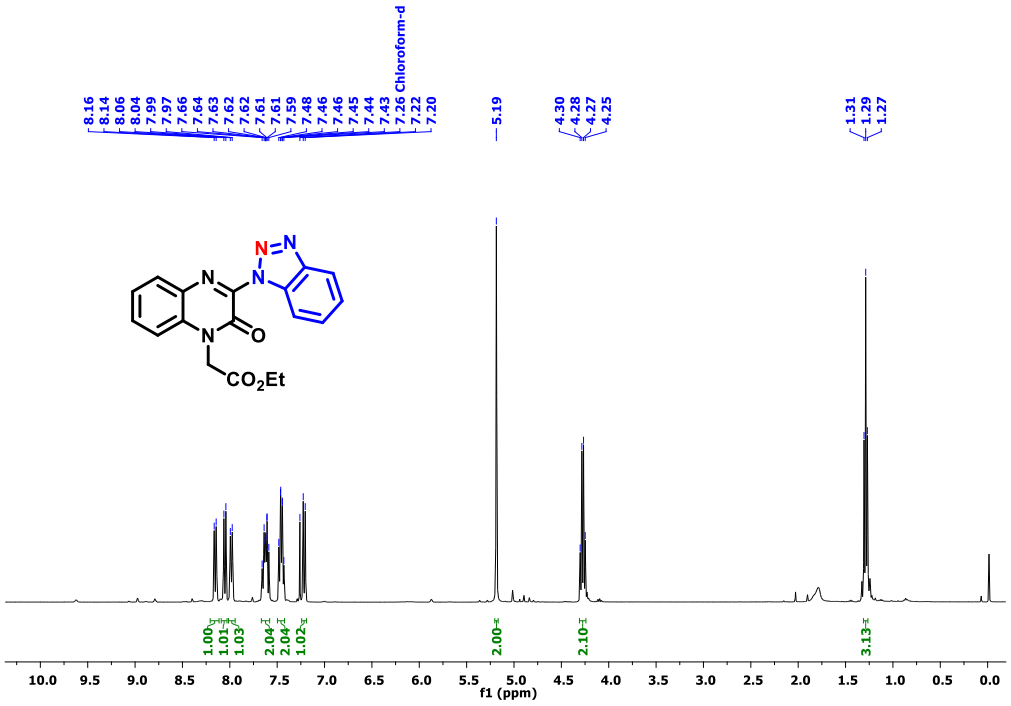


Figure 4.26: ^{1}H NMR of **4a**, 400 MHz, $CDCl_3$

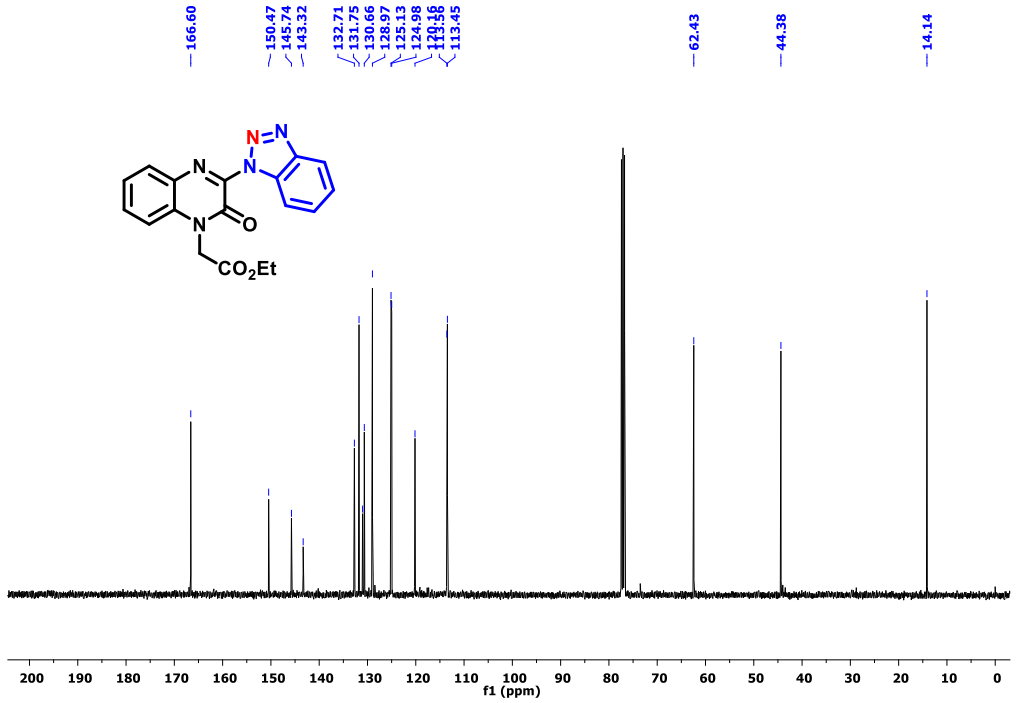


Figure 4.27: ^{13}C {^{1}H} NMR of **4a**, 100 MHz, $CDCl_3$

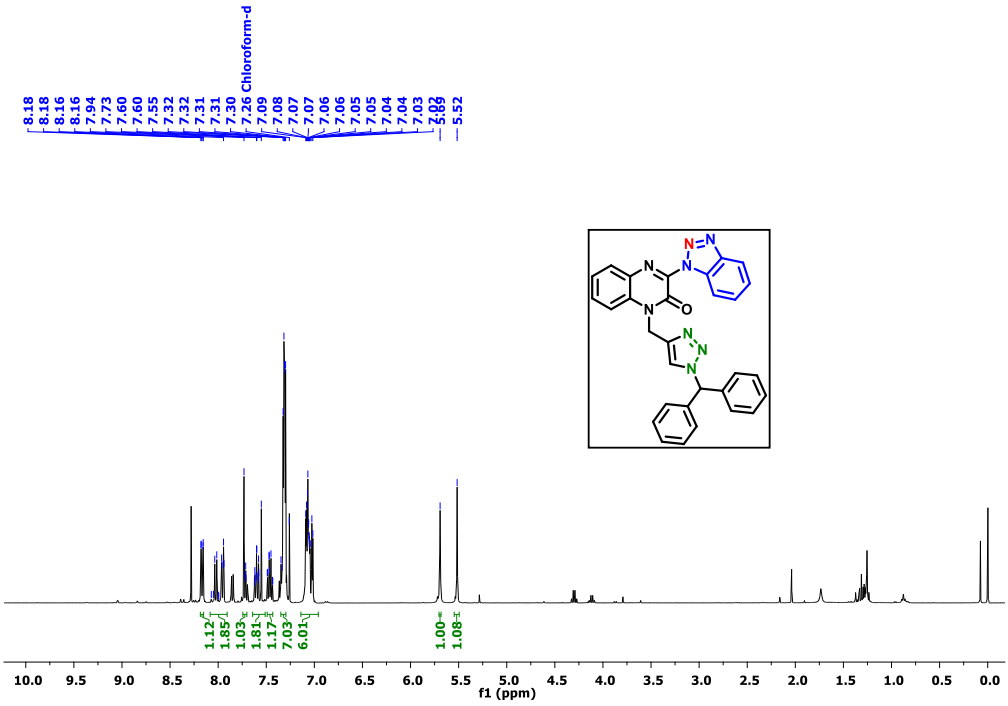


Figure 4.28: ^{1}H NMR of **3pp**, 400 MHz, $CDCl_3$

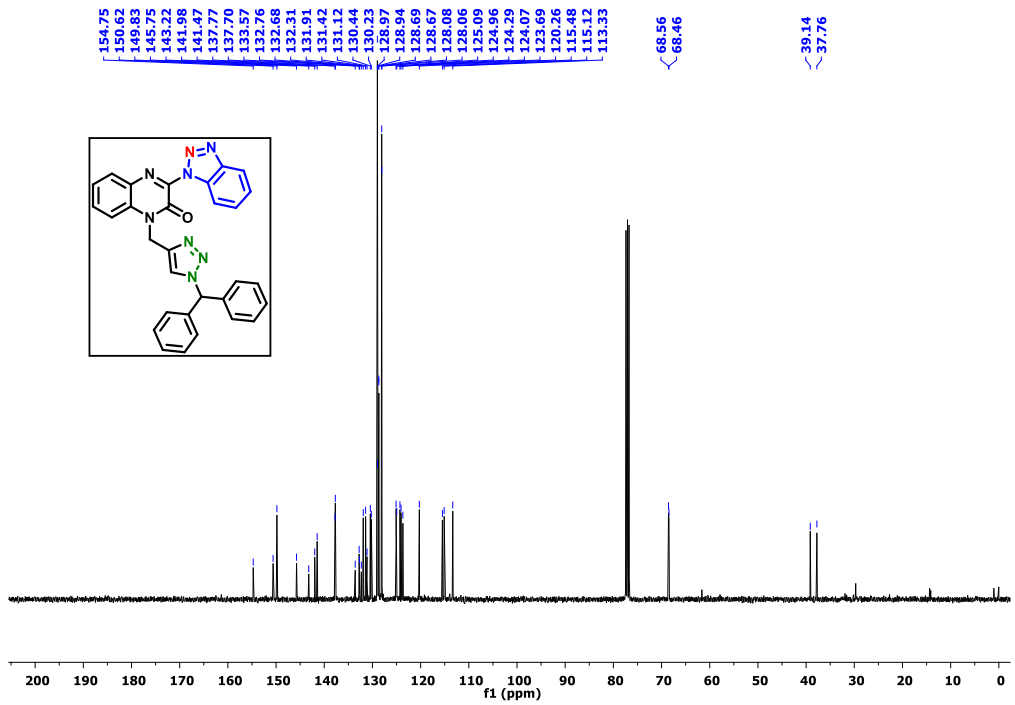


Figure 4.29: ^{13}C {^{1}H} NMR of **3pp**, 100 MHz, $CDCl_3$

4.7.2. SCXRD data

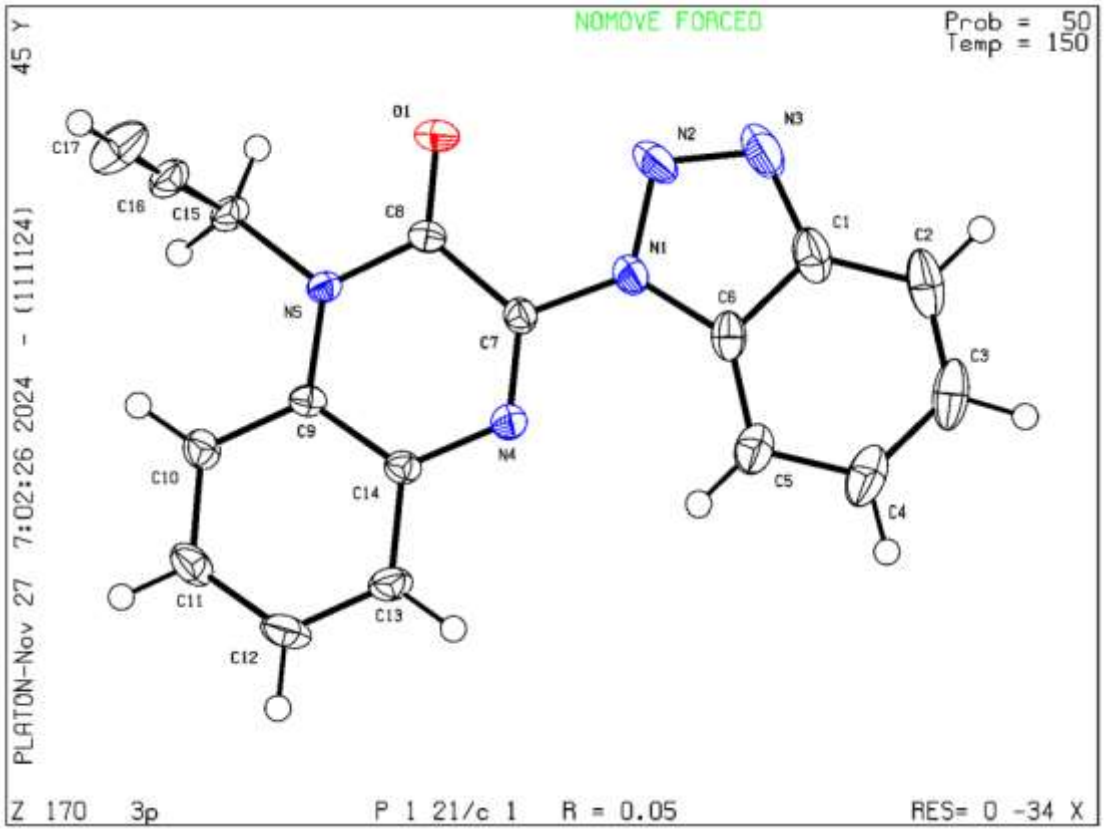


Figure 4.30: ORTEP drawing of **3p** in 50% probability level

4.8. Reference

(1) Jiang, X.; Wu, K.; Bai, R.; Zhang, P.; Zhang, Y. *Eur. J. Med. Chem.* **2022**, *229*, 114085.

(2) Yang, L.; Gao, P.; Duan, X.H.; Gu, Y. R.; Guo, L.N. *Org. Lett*. **2018**, *20*, 1034−1037.

(3) Shi, A.; Sun, K.; Chen, X.; Qu, L.; Zhao, Y.; Yu, B. *Org. Lett*. **2022**, *24*, 299.

(4) Lawrence, D. S.; Copper, J. E.; Smith, C. D. *J. Med. Chem*. **2001**, *44*, 594.

(5) Ramli, Y.; Moussaif,A.; Karrouchi, K.; Essassi, E. M. *J. Chem.,* **2014**, *2014*, 21.

(6) Shao, M.; Liang, H.; Li, Y. L.; Qin, W.; Li, Z. *Asian J. Org. Chem*., **2020**, *9*, 782-787.

(7) Qin, X.; Hao, X.; Han, H.; Zhu, S.; Yang, Y.; Wu, B.; Hussain, S.; Parveen, S.; Jing, C.; Ma, B.; Zhu, C. *J. Med. Chem*., **2015**, *58*, 1254–1267.

(8) Lalji, R. S. K.; Gupta, P. M.; Kumar, S.; Kumar, A.; Singh, B. K. *RSC Adv*., **2023**, *13*, 6191.

(9) Ke, Q.; Yan, G.; Yu, J.; Wu, X. *Org. Biomol. Chem*., **2019**, *17*, 5863–5881.

(10) Li, C. Z.; Lan, X. J.; Li, X.; Fu, Y. X.; Gui, G.; Zhang, X.; Huang, M.; Gan, Z.; Shen, Y. *J. Med. Chem.* **2025**, *68* (2), 1222–1244.

(11) Sun, L.-R.; Zhong, J.-L.; Cui, S.-X.; Fang, Y.-X.; Zhang, Y.-P.; Zhou, Z.-Y.; Cui, H.R. Cells. *Pharmacol. Rep.* **2010**, *62* (2), 333–342.

(12) Wang, H.; Chen, Y.; Zhang, Q.; Liu, J.; Li, M.; Zhang, W.; Ma, Y.; Wang, M.; Zhang, Y. *Bioorg. Med. Chem. Lett.* **2022**, *64*, 128663.

(13) Ginzinger, W.; Mühlgassner, G.; Arion, V. B.; Jakupec, M. A.; Roller, A.; Galanski, M. S.; Reithofer, M.; Berger, W.; Keppler, B. K. *J. Med. Chem.* **2012**, *55* (7), 3398–3413.

(14) Romero, N. A.; Nicewicz, D. A. *Chem. Rev.* **2016**, *116* (17), 10075–10166.

(15) Gao, R.; Wang, F.; Geng, X.; Li,C.; Wang, Lei. *Org. Lett.* **2022**, *24*, 7118−7122.

(16) Liu, D.; Patureau. *Org. Lett.* **2024**, *26*, 6841−6846.

(17) Sau, S.; Takizawa, S.; Kim, H. Y.; Oh, K. *Org. Lett*. **2024**, 2*6*, 8821−8826.

(18) Si, Y.; Chen, X.; Fu, X.; Sun, K.; Song, X.; Qu, L.; Yu, B. *ACS Sustainable Chem*. *Eng*. **2020**, *8*, 10740−10746.

(19) Teng, Q.; Yao, Y.; Wei, W.; Tang, H.; Li, J.; Pan, Y. *Green Chem*., **2019**, *21*, 6241–6245.

(20) Shao, M.; Liang, H.; Liu, Y.; Qin, W.; Li, W. *Asian J. Org. Chem*. **2020**, *9*, 782 – 787.

(21) Wang, K.; Wang, G. *Catalysts*. **2022**, *12*, 6, 633.

(22) Zhang, L.; Shen, C. *Green Synthesis and Catalysis*. **2023**, *4*, 226–230.

(23) J. Wang, B. Sun, L. Zhang, T. Xu, Y. Xie, C. Ji. *Asian J. Org. Chem*. **2019**, *8*, 1942–1948.

(24) Kim, Y.; Kim, D. Y. *Tetrahedron Lett.* **2018**, *59*, 2443–2446.

(25) Wei, W.; Wang, L.; Bao, Pengli.; Shao, Y.; Yue, H.; Yang, D.; Yang, X.; Zhao, X.; Wang, H. *Org. Lett.* **2018**, 20, 7125−7130.

(26) Sun, M.; Wang, L.; Zhao, L.; Wang, Z.; Li, P. *ChemCatChem*, **2020**, *12*, 5261-5268.

(27) Yi, Bing.; Tang, H.; Yi, Z.; Gong, H.; Li, D.; Zhang, W.; Chen, Y.; Tan, J. P.; Xie. Y. *Org. Chem. Front*., **2023**,*10*, 531-539.

(28) Dixit, V.; Pooja.; Jain, N. *Adv. Synth. Catal.*, **2024**, *365*, 4684 – 4691.

(29) Azeez, S.; Chaudhary, P.; Sureshbabu, P.; Sabiah, S.; Kan-dasamy, J. *Org. Biomol. Chem*., **2018**, *16*, 8280-8285.

(30) Sarkar, P.; Rana, S.; Jana, D.; Mandal, S.; Mukhopadhyay, C. *Adv. Synth. Catal.*, **2024**, *366*, 1661 – 1668.

(31) Bollikolla, H. B.; Boddapati, S. N. M.; Thangamani, S.; Mutchu, B. R.; Alam, M. M.; Hussien, M.; Jonnalagadda, S. B. *J. Heterocycl. Chem.* **2023**, *60* (6), 1175–1194.

(32) Suma, B. V.; Natesh, N. N.; Madhavan, V. *J. Chem. Pharm. Res.* **2011**, *3* (6), 375–381.

(33) López-Vallejo, F.; Castillo, R.; Yam-Puc, J. C.; Terrazas, L. I.; Trujillo, J. I.; Medina-Franco, J. L. *J. Med. Chem.* **2011**, *54* (12), 3964–3970.

(34) Caliendo, G.; Di Carlo, R.; Greco, G.; Meli, R.; Novellino, E.; Perissutti, E.; Santagada, V. *Eur. J. Med. Chem*. **1999**, *34* (10), 825–832.

(35) Anjana, V. S.; Kumar, P. M. *Int. J. Res. Rev.* **2021**, *8* (5), 365–378.

(36) Rezaei, Z.; Khabnadideh, S.; Pakshir, K.; Hossaini, Z.; Amiri, F.; Assadpour, E. *Eur. J. Med. Chem*. **2013**, *63*, 487–493.

(37) Kassab, A. E. *Eur. J. Med. Chem.* **2022**, *229*, 114056.

(38) Ploger, S.; Studer, A. *Org. Lett*. **2022**, *24*, 8568−8572.

(39) Sang, J.-W.; Chen, H.; Zhang, Y.; Wang, J.; Zhang, W. D. *Chem. Sci*. **2023**, 14 (7), 1813–1820.

(40) Lan, H.; Su, Y.; Chen, Y.; He, X.; Wang, D. *Org. Chem. Front*. **2024**, *11* (15), 4207–4211.

(41) Rostoll-Berenguer, J.; Blay, G.; Pedro, J. R.; Vila, C. *Eur. J. Org. Chem.* **2020**, 6148–6172.

(42) Qian, C.-W.; Li, X.; Gu, M.-Q. *Chem. Eur. J.* **2024**, *30*, e202402304.

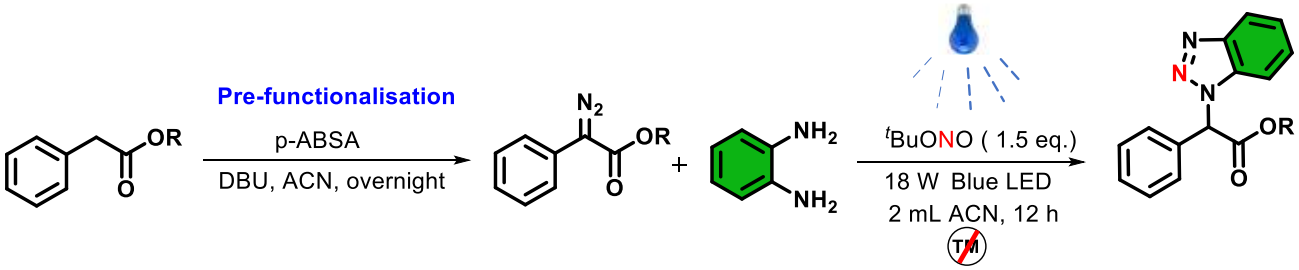
Chapter 5 A

Visible Light-Induced Sequential Nitrogen Insertion and Benzotriazolation of Diazo Esters

Visible Light-Induced Sequential Nitrogen Insertion and Benzotriazolation of Diazo Esters

5.1A. Abstract

In this chapter, we have reported an environmentally benign process for benzotriazolation of α-aryl esters via sp^3 C-N coupling. Following chapter IV, we have utilized o-phenylenediamine as the source of benzotriazole unit that has been generated in reaction by nitrogen insertion reaction with tert-butyl nitrite.The α-aryl ester have preactivated by diazo formation. Thus, in-situ generated benzotriazole scaffold has been coupled with the α-diazo ester via photochemical N-H insertion reaction to form benzotriazolated α-aryl esters. The process has been generalized with library of substrates.The reaction is quite simple and straight-forward providing bioactive scaffolds under eco-friendly conditions.



5.2A. Introduction

The direct formation of C–N bonds via N–H insertion reactions has become an increasingly powerful tool in organic synthesis, particularly for constructing nitrogen-containing heterocycles that are prevalent in natural products, pharmaceuticals, and agrochemicals.[1–3] In this context, α-diazo esters act as valuable precursors to carbenes or metal-carbenoids that are highly reactive intermediates. Carbenes can undergo insertion into a variety of X–H bonds (X = N, O, S, C), enabling modular synthesis of complex molecules with excellent functional group tolerance.[4–6]

In particular, N–H insertion of α-diazo esters into heterocycles and amines has gained significant attention as an atom-economical and efficient method to access α-amino esters and related frameworks.[7-8] This transformation can proceed under both metal-catalyzed (e.g., Rh, Cu, Fe) as well as metal-free conditions, often affording high regio- and chemoselectivity. While the use of transition-metal catalysts such as Rh (II) acetate has been well-established, recent advances have shown that carbene generation can also be promoted via photochemical activation offering greener and more

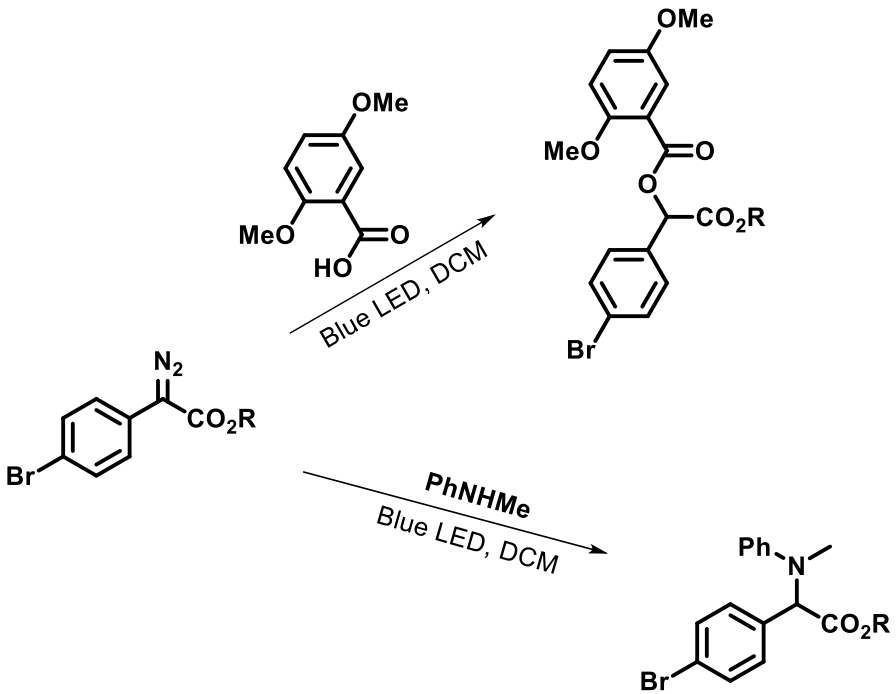
sustainable alternatives.[9-12] Previously, several works has been developed on the reaction of diazo esters that establishes the diazo compounds as useful photolabile reactive group for many diverse synthetic transformations.[13-14]

In a notable study, Jurberg and Davies demonstrated that α-aryl diazoacetates absorb light in the 400–500 nm range, leading to carbene generation. Under photochemical conditions in the presence of styrene, this process yields the corresponding cyclopropanes with high E-diastereoselectivity and good to excellent yields (Scheme 5.1A).[15]



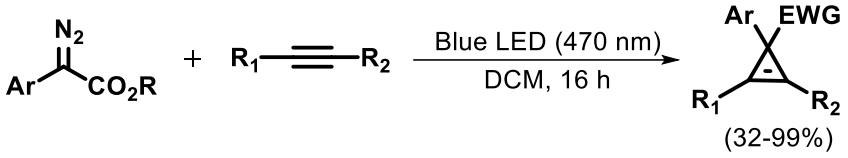
Scheme 5.1A: Cyclopropanation reaction of α-diazoester with olefin

The same paper also reports photo-induced N-H and O-H insertion reaction of α-(4- bromophenyl) diazoacetate (Scheme 5.2A).



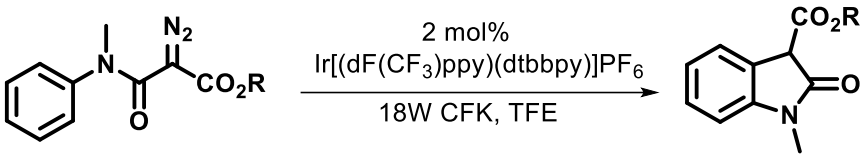
Scheme 5.2A: Photochemical O-H & N-H insertion reaction with α-diazoester

Recently, Koenig *et al.* have explored visible light induced cyclopropenation reaction of alkynes with donor–acceptor diazo compounds (Scheme 5.3A).[16] Diverse cyclopropenes could be obtained by this method in good to excellent yields.



Scheme 5.3A: Cyclopropenation reaction of α-diazoester with alkyne

Xiao *et al.* reported a photocatalytic intramolecular aromatic substitution of disubstituted (EWG–EWG) diazo compounds via a photo-tandem cyclization process. This transformation involves two distinct catalytic cycles: the first, an energy transfer (ET) step facilitated by iridium-catalyzed photocatalysis leading to carbene formation, and the second, a single electron transfer (SET) step (Scheme 5.4A).[17]



Scheme 5.4A: Photocatalyzed oxindole formation from diazo ester

Benzotriazoles are a class of nitrogen-rich heterocycles that have found wide applications in organic synthesis, medicinal chemistry and materials science due to their favorable electronic properties, thermal stability and biological activity.[18-19] Traditionally synthesized via cyclization of *o*-phenylenediamines with nitrosating agents, benzotriazoles possess a reactive N–H unit, which renders them suitable partners for N–H insertion chemistry.[20] The in situ generation of benzotriazoles under mild oxidative or diazotization conditions adds synthetic advantages and better step economy by eliminating the need for its pre-isolation and storage.[21] Despite significant progress in carbene chemistry and N–H insertion reactions, the direct insertion of α-diazo esters into the N–H bond of in situ generated benzotriazoles remains largely underexplored. This transformation presents a unique synthetic opportunity to functionalize benzotriazoles at the *N*-position, leading to the formation of α-substituted triazole derivatives. Such motifs are particularly valuable for the frequent appearance of benzotriazoles in kinase inhibitors, antifungal agents, and corrosion inhibitors. [22–24]

Furthermore, integrating diazo chemistry with in situ heterocycle formation represents a promising avenue toward developing one-pot multicomponent reactions, aligning with principles of green chemistry and operational simplicity.[25] The mechanistic pathway likely involves generation of a free or metal-bound carbene intermediate from the diazo ester, followed by nucleophilic attack of the triazole nitrogen and insertion to form the new C–N bond. [26–28]

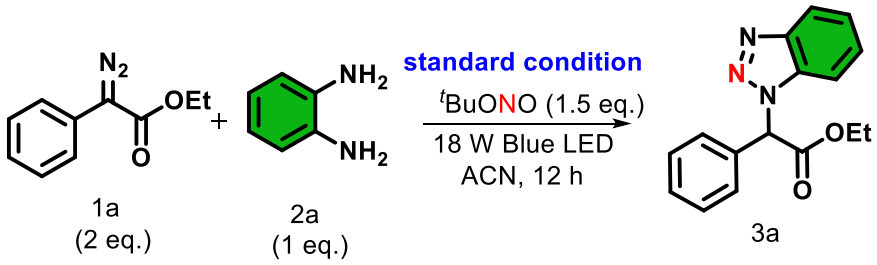
Recent studies have also shown that such N–H insertion processes can proceed with high stereoselectivity, especially when chiral catalysts are employed, opening pathways for enantioselective synthesis of α-functionalized triazoles.[29-30] The combination of diazo compounds, in situ generated heterocycles, and mild activation methods (e.g., photoredox or metal-free thermal conditions) positions this chemistry at the forefront of modern heterocyclic synthesis. Herein, we have developed a photoinduced sustainable methodology for benzotriazolation of α-diazo esters where benzotriazole is generated in situ from *o*-phenylene diamine and *tert*-butyl nitrite and proceeds through generation of carbene intermediates upon light irradiation.

5.3A. Results and discussion

5.3A.1. Optimization studies

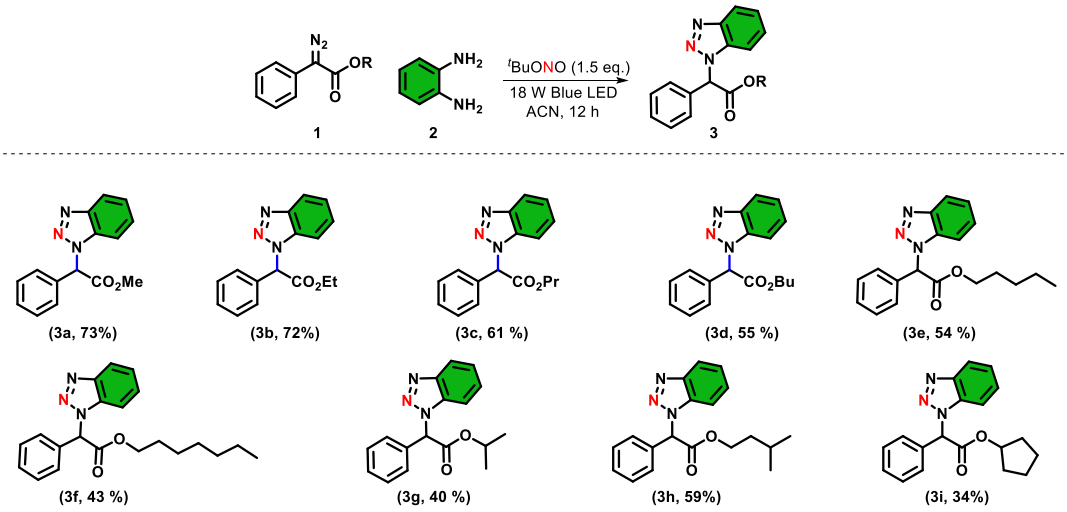
We started optimization for the N-H insertion of in-situ benzotriazole and α-diazo esters taking *o*-phenylene diamine and ethyl diazo ester as model substrates.

Table 5.1A: Optimization table



Entry	Deviation from Standard conditions	Yield (%)
1	none	72
2	1 eq. **1a** and 1 eq. **2a**	30
3	1.3 eq. **1a** and 1 eq. **2a**	40
4	1.8 eq. **1a** and 1 eq. **2a**	60
5	2.5 eq. **1a** and 1 eq. **2a**	72
6	^{t}BuOH instead of ACN	34
7	DCM instead of ACN	36
8	2 eq. ^{t}BuONO	72
9	8 h instead of 12 h	61
10	16 h instead of 12 h	72

To achieve optimal conditions for the N–H insertion of α-diazo esters with in situ generated benzotriazole, several key parameters including the molar ratio of reactants, equivalents of ^{t}BuONO, and reaction time were systematically evaluated. The results are summarized in the table 5.1A. Taking 1:1 ratio of the model substrates a moderate yield of 30% for product **3a** was obtained (Entry 2, Table 5.1A). Next, when 1.3:1 ratio of model substrates was choosen, yield of **3a** had improved to 40% indicating the need for excess of diazo compounds for this transformation (Entry 3, Table 5.1A). So the diazo equivalence was increased gradually. Choosing 1.8 eq. **1a**, we obtained 60% yield of desired product (Entry 4, Table 5.1A). Finally, after taking 2.5 eq. of **1a**, there was no further improvement in yield from standard condition (Entry 5, Table 5.1A). Changing the solvent to ^{t}BuOH there was drastic reduction in yield (Entry 6, Table 5.1A). Further switching the reaction mixture in DCM solvent also gave a reduced yield of 36% (Entry 7, Table 5.1A). We observed that ACN is the best optimum solvent for the reaction. The possible reason could be that in situ generation of benzotriazole is maximum in ACN only. Decrease or increase of reaction time can not improve the yield (Entry 9-10, Table 5.5A)

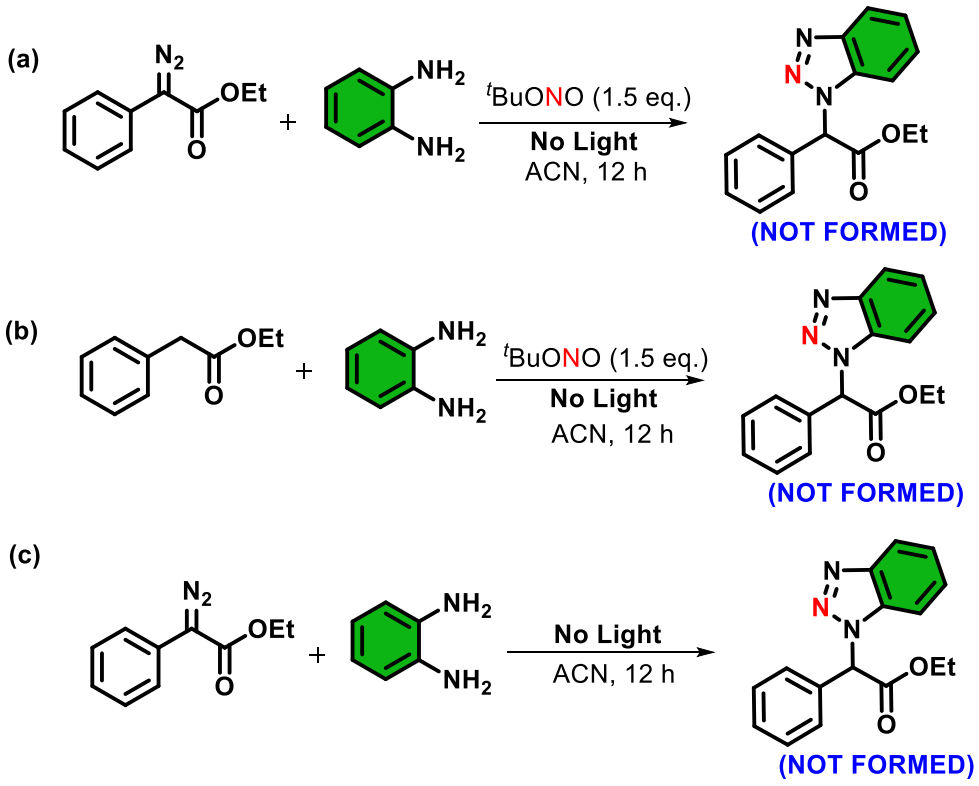


Scheme 5.5A: Substrate scope for benzotriazolation with α-diazoester

Reaction conditions: **1a** (2 eq.), **2a** (1 eq.) and *tert*-butyl nitrite (1.5 eq.) in 2 mL ACN were irradiated under 18 W blue LED for 12 h.

With the optimized reaction conditions in hand (α-diazo ester: 2 eq., ^{t}BuONO: 1.5 eq., 18 W blue LED, ACN, 12 h), the substrate scope of the N–H insertion reaction was evaluated using a range of α-diazo esters to demonstrate the generality and functional group tolerance of the protocol. As illustrated in Scheme 5.5A, the transformation was found to be compatible with various ester substituents on the diazo compound. α-diazo ester derivatives bearing methyl, ethyl, propyl and butyl groups afforded the corresponding *N*-inserted benzotriazole proucts **3a**, **3b**, **3c** and **3d** in

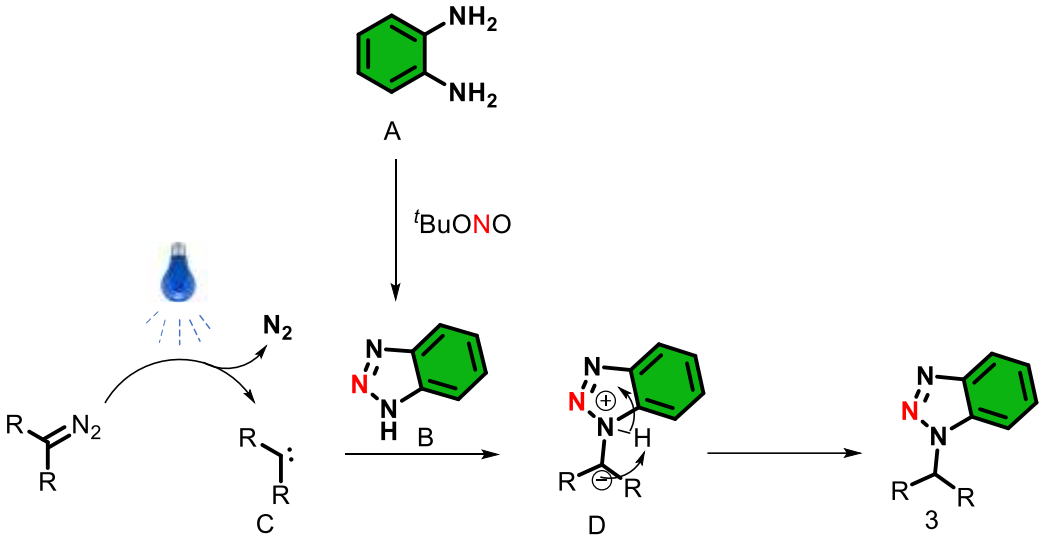
73%, 72%, 61% and 55% yields respectively. The use of relatively bulkier ester groups such as n-pentyl and n-heptyl also proceeded smoothly, albeit with slightly reduced yields affording products **3e** and **3f** in 54% and 43% yields respectively. Notably, substrates incorporating branched alkyl chains such as isopropyl and isopentyl gave corresponding products **3g** and **3h** in 40% and 59% yields respectively. The results indicate that increasing alkyl chain length leads to a gradual decrease in reactivity, likely due to steric and solubility effects. Interestingly, the introduction of cyclic alkyl group like cyclopentyl also proved viable under the reaction conditions giving product **3i** in 34% yield. Overall, the reaction displays good substrate tolerance across a broad range of α-diazo esters. While linear esters generally provided better yields, the method tolerates steric hindrance to some extent, establishing this N–H insertion strategy as synthetically valuable for accessing structurally diverse N-substituted benzotriazoles.



Scheme 5.6A: Control experiments for understanding mechanism

To gain mechanistic insight into the N–H insertion process, a series of control experiments were carried out. When the reaction was performed in absence of light, no product formation was observed under the optimized conditions (Entry a, Scheme 5.6A). This suggests the significance of light in promoting this transformation. Furthermore, when the reaction was carried out with α-aryl ester without diazo formation, we could not detect any product formation (Entry b, Scheme 5.6A). This indicates the importance of diazo formation from its precursor ester. Furthermore, as we have generated the

benzotriazole first from diamine before addition of diazo compound, direct N-H insertion followed by benzotriaole formation is ruled out. So, we can come to conclusion that upon light irradiation the photoactive α-diazoester molecule participates in the reaction. In absence of ^{t}BuONO no products form that further confirms ^{t}BuONO as 'N' atom transferring agent (Entry c, Scheme 5.6A).



Scheme 5.7A: Plausible mechanism of benzotriazolation of α-diazo esters

Based on experimental results and literature precedents, a plausible mechanism for the N–H insertion of α-diazo esters with in situ generated benzotriazoles is outlined in Scheme 5.7A. The reaction initiates with the formation of benzotriazole through a diazotization–cyclization sequence. Specifically, *o*-phenylenediamine **A** undergoes oxidative cyclization in the presence of *tert*-butyl nitrite (^{t}BuONO), acting as a nitrosating agent, to generate benzotriazole intermediate **B** under mild conditions. Concurrently, under visible-light irradiation (18 W blue LED), the α-diazo ester is photolyzed to release molecular nitrogen N_2, generating a reactive singlet carbene intermediate **C**. This free carbene species is highly electrophilic and is capable of inserting into heteroatom–hydrogen (X–H) bonds. In the next step, the N–H group of the benzotriazole undergoes nucleophilic attack by the carbene, likely proceeding through a transition state involving the formation of a transient zwitterionic intermediate **D** stabilized by resonance. This intermediate rapidly collapses to form the desired N–alkylated benzotriazole derivative, which is isolated as the final product.

5.3A.2. Conclusion

Thus, in this chapter, we have reported a photochemical process for synthesis of benzotriazolated α-aryl esters that proceeds through the synergistic combination of in situ heterocycle generation with carbene-mediated N–H insertion, offering a mild, metal-free approach to C–N bond formation. The transformation proceeds via in situ generation of benzotriazole, followed by selective carbene insertion

into the N–H bond, affording the desired N-functionalized triazole products in moderate to good yields. The reaction was carried out under metal-free, photochemical conditions, which eliminates the need for transition-metal catalysts, offering an environmentally benign and cost-effective alternative to traditional methods. The use of mild reaction conditions, visible light as a green energy source, and readily accessible starting materials underscores the practicality and sustainability of the method. Furthermore, the regioselective formation of the C–N bond and the generation of structurally rich benzotriazole scaffolds highlight the synthetic utility of this methodology in the context of medicinal chemistry, heterocyclic synthesis and late-stage functionalization. Overall, this work provides a valuable contribution to the growing field of diazo chemistry and photochemical N–H insertions and it offers a robust platform for the development of novel nitrogen-containing heterocycles with potential applications in drug discovery, materials science, and chemical biology.

5.5A. Experimental section and characterization data

5.5A.1. General information & characterization data

All the chemicals were purchased from Sigma-Aldrich and BLD pharma and used without further modification. All solvents were purchased from Rankem and Finar Chemicals. Deuterated solvents were used as received. Column chromatographic separations were performed over 60−120 mesh silica-gel. Visualization was accomplished with UV light. The ^{1}H and $^{13}C\{^{1}H\}$ NMR spectra were recorded on 400 and 100 MHz, respectively, using Bruker spectrometers. Abbreviations used in the NMR follow-up experiments: b, broad; s, singlet; d, doublet; t, triplet; q, quartet. HRMS spectra were obtained with Waters-synapt G2 using electrospray ionization (ESI-TOF). Infrared (ATIR) spectra were obtained with a Bruker Alpha-E infrared spectrometer. Single-crystal diffraction analysis data were collected at 100K with a BRUKER KAPPA APEX III CCD Duo diffractometer (operated at 1500 W power: 50 kV, 30 mA) using graphite monochromatic Mo Kα radiation and Cu-Kα radiation. The reaction was performed in a 15 mL borosilicate test tube. The lightsource used was 18 W Lords blue LED. The wavelength of the LEDwas measured with an Ocean Optics USB 400 instrument that detects 200−1100 nm wavelength, and the spectra were recorded in SpectraSuit software. The wavelength of the radiation was 445 nm with fwhm = 18.96 nm.

5.5A.2. General procedure for synthesis of 3:

Benzene-1,2-diamine (1 eq.) was added in a 10 mL test tube containing 2 mL ACN. Then 1.5 eq. *tert*-butyl nitrite was added in to it and the reaction mixture was stirred for 30 min at room temperature. Then 2 eq. α-diazo ester was added into the test-tube and the reaction mixture was irradiated under 18

W blue LED for 12 h. The test tube was kept at a distance of 2.5 cm from each LED. The temperature of the system was measured to be in the range of 30-35 ºC using IR thermometer for 12 h.

5.6A. Analytical data of products

Methyl 2-(1*H*-benzo[d][1,2,3]triazol-1-yl)-2-phenylacetate (3a) Prepared according to the general procedure using methyl 2-diazo-2-phenylacetate (1.8 mmol, 325 mg), *o*-phenylenediamine (0.9 mmol, 100 mg) and *tert*-butyl nitrite (0.75 mmol, 77 mg). The crude reaction mixture was purified by silica gel column chromatography (pet ether/EtOAc = 85:15) to afford product **3a** (180 mg, 73%). Melting point: 130-132 ºC.^{1}H NMR (400 MHz, $CDCl_3$) δ 8.06-8.04 (m, 1H), 7.41-7.37 (m, 5H), 7.34 – 7.30 (m, 2H), 7.21 – 7.17 (m, 1H), 6.94 (s, 1H), 3.86 (s, 3H).^{13}C{^{1}H} NMR (100 MHz, $CDCl_3$) δ 168.2, 146.5, 132.6, 132.4, 129.5, 129.2, 128.2, 127.6, 124.0, 120.1, 111.1, 65.7, 53.2. IR (neat): 3067, 2970, 1717, 1410, 1295 cm^{-1}. HRMS (ESI) calculated for $C_{15}H_{13}N_3O_2$ $[M+H]^+$ m/z 268.1086, found 268.1084.

Ethyl 2-(1*H*-benzo[d][1,2,3]triazol-1-yl)-2-phenylacetate (3b) Prepared according to the general procedure using ethyl 2-diazo-2-phenylacetate (1 mmol, 190 mg), *o*-phenylenediamine (0.5 mmol, 54 mg) and *tert*-butyl nitrite (0.75 mmol, 77 mg). The crude reaction mixture was purified by silica gel column chromatography (pet ether/EtOAc = 85:15) to afford product **3b** (101 mg, 72%) as yellow liquid. ^{1}H NMR (400 MHz, $CDCl_3$) δ 8.05-8.03 (m, 1H), 7.41-7.37 (m, 5H), 7.34 – 7.30 (m, 2H), 7.21-7.18 (m, 1H), 6.93 (s, 1H), 4.34 (qd, *J* = 7.1, 4.5 Hz, 2H), 1.28 (t, *J* = 7.1 Hz, 3H).^{13}C{^{1}H} NMR (100 MHz, $CDCl_3$) δ 167.7, 146.6, 132.6, 132.5, 129.4, 129.1, 128.2, 127.5, 124.0, 120.1, 111.3, 65.9, 62.6, 14.1. IR (neat): 3059, 2949, 1710, 1405, 1287 cm^{-1}. HRMS (ESI) calculated for $C_{16}H_{15}N_3O_2$ $[M+H]^+$ m/z 282.1242, found 282.1240.

Propyl 2-(1*H*-benzo[d][1,2,3]triazol-1-yl)-2-phenylacetate (3c) Prepared according to the general procedure using propyl 2-diazo-2-phenylacetate (1 mmol, 204 mg), *o*-phenylenediamine (0.5 mmol, 54 mg) and *tert*-butyl nitrite (0.75 mmol, 77 mg). The crude reaction mixture was purified by silica gel column chromatography (pet ether/EtOAc = 90:10) to afford product **3c** (90 mg, 61%) as yellow semi-solid. ^{1}H NMR (400 MHz, $CDCl_3$) δ 8.04 (dd, *J* = 6.3, 2.3 Hz, 1H), 7.41– 7.39 (m, 5H), 7.34 – 7.30 (m, 2H), 7.21– 7.17 (m, 1H), 6.94 (s, 1H), 4.23 (td, *J* = 6.7, 1.9 Hz, 2H), 1.64 (dt, *J* = 14.3, 7.1 Hz, 2H), 0.84 (t, *J* = 7.4 Hz, 3H).^{13}C{^{1}H} NMR (100 MHz, $CDCl_3$) δ 167.8, 146.6, 132.6, 132.6, 129.4, 129.1, 128.2, 127.5, 124.0, 120.1, 111.3, 68.1, 65.9, 21.8, 10.2. IR (neat): 3045, 2967, 1715, 1405, 1295 cm^{-1}. HRMS (ESI) calculated for $C_{17}H_{17}N_3O_2$ $[M+H]^+$ m/z 296.1399, found 296.1398.

Butyl 2-(1*H*-benzo[d][1,2,3]triazol-1-yl)-2-phenylacetate (3d) Prepared according to the general procedure using using butyl 2-diazo-2-phenylacetate (1 mmol, 218 mg), *o*-phenylenediamine (0.5 mmol, 54 mg) and *tert*-butyl nitrite (0.75 mmol, 77 mg). The crude reaction mixture was purified by silica gel column chromatography (pet ether/EtOAc = 70:30) to afford product **3d** (85 mg, 55%) as yellow semi-solid. ^{1}H NMR (400 MHz, $CDCl_3$) δ 8.07– 8.03 (m, 1H), 7.40 – 7.38 (m, 5H), 7.34 – 7.30 (m, 2H), 7.20 – 7.17 (m, 1H), 6.93 (s, 1H), 4.28 (td, *J* = 6.7, 2.9 Hz, 2H), 1.61 (dd, *J* = 9.9, 5.2 Hz, 2H), 1.30 – 1.24 (m, 2H), 0.86 (t, *J* = 7.4 Hz, 3H).^{13}C{^{1}H} NMR (100 MHz, $CDCl_3$) δ 167.8, 146.6, 132.6, 132.5, 129.4, 129.1, 128.5, 128.2, 127.5, 124.0, 120.1, 111.3, 66.4, 65.9, 30.4, 18.9, 13.5. IR (neat): 3048, 2966, 1710, 1409, 1285 cm^{-1}. HRMS (ESI) calculated for $C_{18}H_{19}N_3O_2$ $[M+H]^+$ m/z 310.1355, found 310.1358.

Pentyl 2-(1*H*-benzo[d][1,2,3]triazol-1-yl)-2-phenylacetate (3e) Prepared according to the general procedure using pentyl 2-diazo-2-phenylacetate (1 mmol, 232 mg), *o*-phenylenediamine (0.5 mmol, 54 mg) and *tert*-butyl nitrite (0.75 mmol, 77 mg). The crude reaction mixture was purified by silica gel column chromatography (pet ether/EtOAc = 90:10) to afford product **3e** (87 mg, 54%) as yellow liquid. ^{1}H NMR (400 MHz, $CDCl_3$) δ 8.06–8.04 (m, 1H), 7.40–7.38 (m, 5H), 7.34 – 7.30 (m, 2H), 7.20 – 7.17 (m, 1H), 6.94 (s, 1H), 4.27 (td, *J* = 6.6, 1.4 Hz, 2H), 1.62 (dt, *J* = 13.7, 6.7 Hz, 2H), 1.26 – 1.19 (m, 4H), 0.83 (t, *J* = 7.0 Hz, 3H).^{13}C{^{1}H} NMR (100 MHz, $CDCl_3$) δ 167.8, 146.6, 132.6, 132.5, 129.4, 129.1, 128.5, 128.2, 127.5, 124.0, 120.1, 111.3, 66.6, 65.9, 28.0, 27.8, 22.1, 13.9. IR (neat): 3056, 2958, 1718, 1410, 1290 cm^{-1}. HRMS (ESI) calculated for $C_{19}H_{21}N_3O_2$ $[M+H]^+$ m/z 324.1712, found 324.1717.

Heptyl 2-(1*H*-benzo[d][1,2,3]triazol-1-yl)-2-phenylacetate (3f) Prepared according to the general procedure heptyl 2-diazo-2-phenylacetate (1 mmol, 260 mg), *o*-phenylenediamine (0.5 mmol, 54 mg) and *tert*-butyl nitrite (0.75 mmol, 77 mg). The crude reaction mixture was purified by silica gel column chromatography (pet ether/EtOAc = 90:10) to afford product **3f** (75 mg, 43%) as yellow liquid. ^{1}H NMR (400 MHz, $CDCl_3$) δ 167.8, 146.6, 132.6, 132.6, 129.4, 129.1, 128.5, 128.2, 127.5, 124.0, 120.1, 111.3, 66.6, 65.9, 31.6, 28.7, 28.4, 25.6, 22.5, 14.0.^{13}C{^{1}H} NMR (100 MHz, $CDCl_3$) δ. IR (neat): 3054, 2969, 1719, 1404, 1297 cm^{-1}. HRMS (ESI) calculated for $C_{21}H_{25}N_3O_2$ $[M+H]^+$ m/z 352.2025, found 352.2020.

Isopropyl 2-(1*H*-benzo[d][1,2,3]triazol-1-yl)-2-phenylacetate (3g) Prepared according to the general procedure using isopropyl 2-diazo-2-phenylacetate (1 mmol, 204 mg), *o*-phenylenediamine (0.5 mmol, 54 mg) and *tert*-butyl nitrite (0.75 mmol, 77 mg). The crude reaction mixture was purified by silica gel column chromatography (pet ether/EtOAc = 90:10) to afford product **3g** (58 mg, 40%).

Melting point: 120-122 ºC. ^{1}HNMR (400 MHz, $CDCl_3$) δ 8.08 – 8.03 (m, 1H), 7.41 – 7.38 (m, 5H), 7.34 – 7.29 (m, 2H), 7.22 – 7.18 (m, 1H), 6.90 (s, 1H), 5.21 (dt, *J* = 12.5, 6.3 Hz, 1H), 1.28 (d, *J* = 2.6 Hz, 3H), 1.27 (d, *J* = 2.6 Hz, 3H).^{13}C{^{1}H} NMR (100 MHz, $CDCl_3$) δ 167.2, 146.5, 132.6, 129.3, 129.1, 128.2, 127.5, 124.0, 120.0, 111.4, 70.8, 66.0, 21.7, 21.0. IR (neat): 3049, 2954, 1715, 1415, 1292 cm^{-1}. HRMS (ESI) calculated for $C_{17}H_{17}N_3O_2$ $[M+H]^+$ m/z 296.1399, found 296.1390.

Isopentyl 2-(1*H*-benzo[d][1,2,3]triazol-1-yl)-2-phenylacetate (3h) Prepared according to the general procedure using isopentyl 2-diazo-2-phenylacetate (1 mmol, 232 mg), *o*-phenylenediamine (0.5 mmol, 54 mg) and *tert*-butyl nitrite (0.75 mmol, 77 mg). The crude reaction mixture was purified by silica gel column chromatography (pet ether/EtOAc = 90:10) to afford product **3h** (94 mg, 59%). Melting point: 231-233 ºC.^{1}HNMR (400 MHz, $CDCl_3$) δ 8.05– 8.03 (m, 1H), 7.40– 7.39 (m, 5H), 7.33 – 7.30 (m, 2H), 7.20 – 7.17 (m, 1H), 6.93 (s, 1H), 4.32– 4.28 (m, 2H), 1.53 – 1.48 (m, 3H), 0.83 (dd, *J* = 6.4, 3.0 Hz, 6H). ^{13}C{^{1}H} NMR (100 MHz, $CDCl_3$) δ 167.8, 146.5, 132.6, 132.5, 129.4, 129.1, 128.2, 127.5, 124.0, 120.1, 111.3, 111.2, 65.9, 65.2, 37.0, 24.9, 22.3. IR (neat): 3053, 2964, 1708, 1407, 1299 cm^{-1}. HRMS (ESI) calculated for $C_{19}H_{21}N_3O_2$ $[M+H]^+$ m/z 324.1712, found 324.1710.

Cyclopentyl-2-(1H-benzo[d][1,2,3]triazol-1-yl)-2-phenylacetate (3i) Prepared according to the general procedure using cyclopentyl 2-diazo-2-phenylacetate (1 mmol, 230 mg), *o*-phenylenediamine (0.5 mmol, 54 mg) and *tert*-butyl nitrite (0.75 mmol, 77 mg). The crude reaction mixture was purified by silica gel column chromatography (petroleum ether/EtOAc = 85:15) to afford product **3i** (54 mg, 34%). Melting point: 105-107 ºC.^{1}H NMR (400 MHz, $CDCl_3$) δ 8.06– 8.04 (m, 1H), 7.41 – 7.37 (m, 5H), 7.34 – 7.30 (m, 2H), 7.20 – 7.15 (m, 1H), 6.89 (s, 1H), 5.37 (tt, *J* = 5.7, 2.7 Hz, 1H), 1.75 – 1.65 (m, 4H), 1.58 – 1.52 (m, 4H).^{13}C{^{1}H} NMR (100 MHz, $CDCl_3$) δ 167.4, 146.5, 132.6, 129.3, 129.1, 128.1, 127.5, 124.0, 120.1, 111.4, 79.9, 66.0, 32.6, 32.5, 23.5, 23.4. IR (neat): 3035, 2944, 1737, 1664, 1600 cm^{-1}. HRMS (ESI) calculated for $C_{19}H_{19}N_3O_2$ $[M+H]^+$ m/z 322.1555, found 322.1555.

5.7A. Appendix IV: Copies of ^{1}H and ^{13}C NMR spectra of representative compounds of NMR spectra

Entry	Figure No.	Data	Page No.
3a	5.1A-5.2A	^{1}H and ^{13}C	166
3c	5.3A-5.4A	^{1}H and ^{13}C	167
3g	5.5A-5.6A	^{1}H and ^{13}C	168
3i	5.7A-5.8A	^{1}H and ^{13}C	169

5.7A.1. Representative examples of NMR spectra

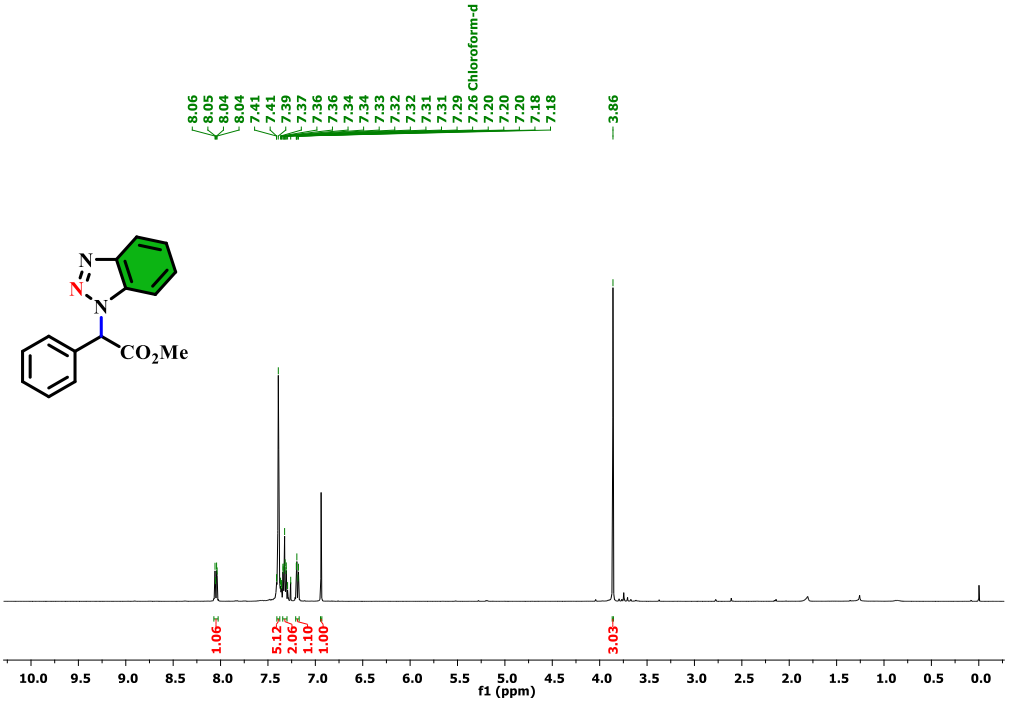


Figure 5.1A: ^{1}H NMR of **3a**, 400 MHz, $CDCl_3$

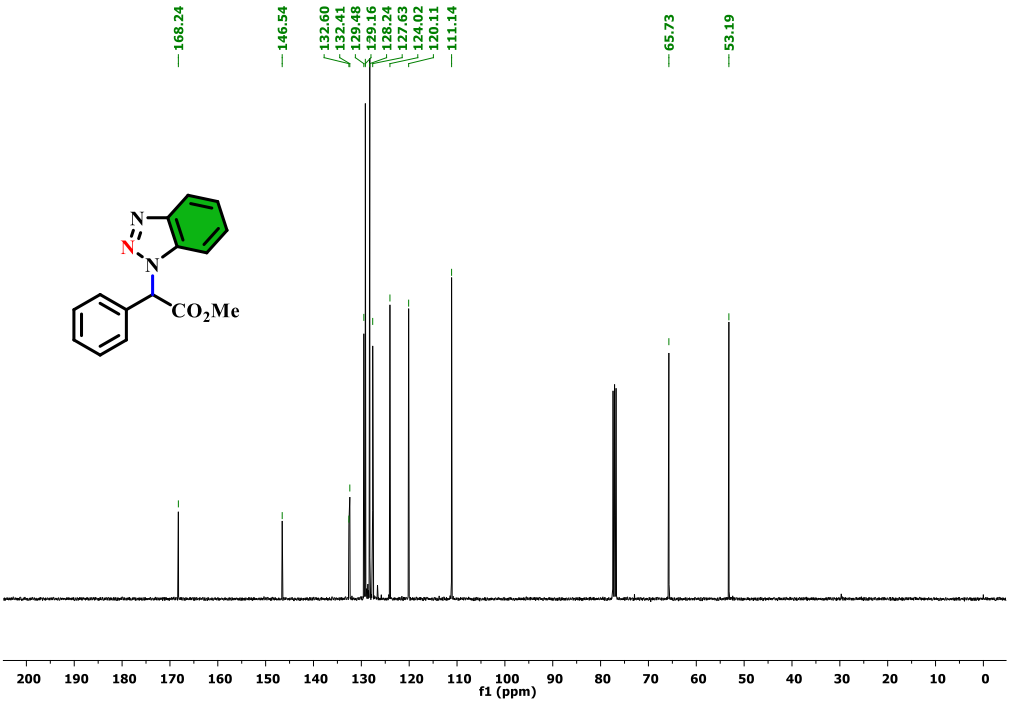


Figure 5.2A: ^{1}H NMR of **3a**, 400 MHz, $CDCl_3$

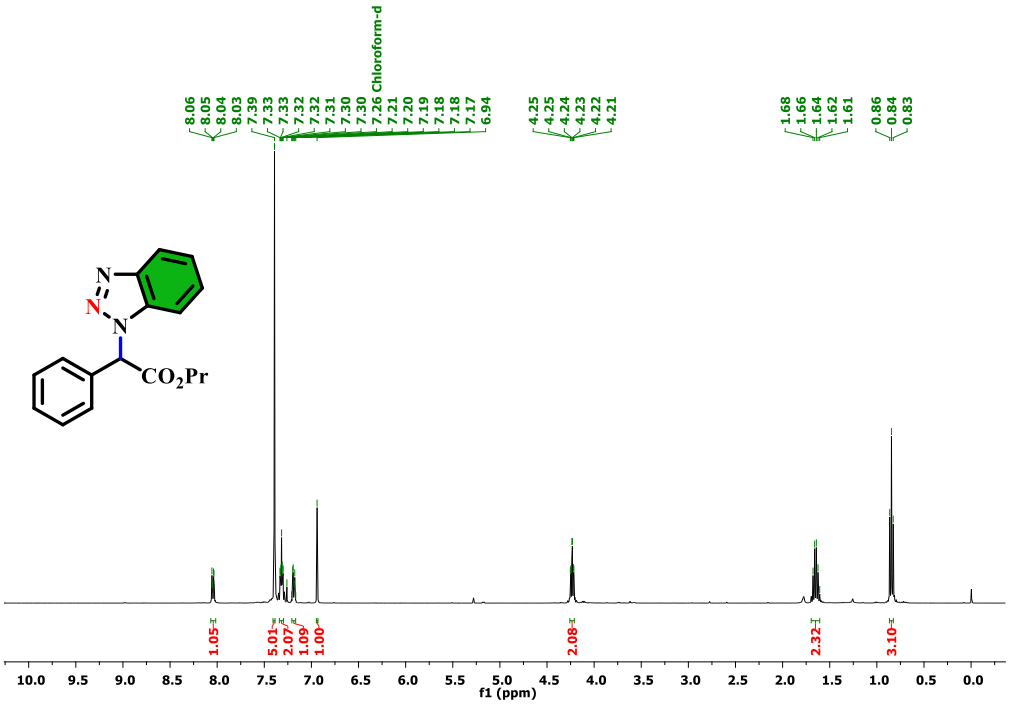


Figure 5.3A: ^{1}H NMR of **3c**, 400 MHz, $CDCl_3$

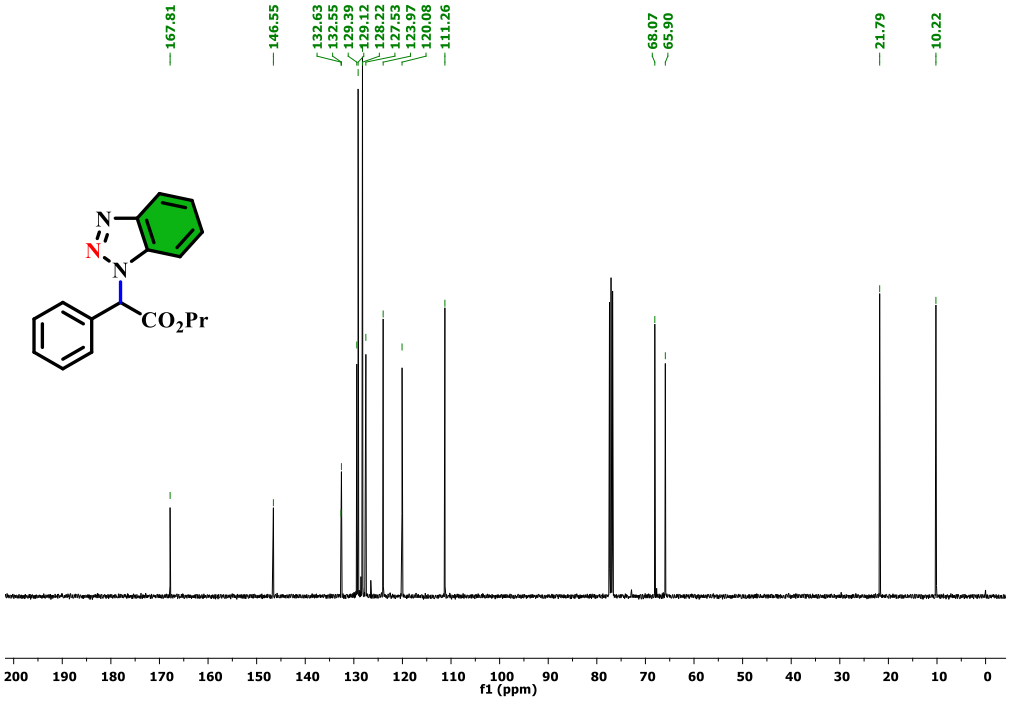


Figure 5.4A: ^{13}C $\{^{1}H\}$ NMR of **3c**, 100 MHz, $CDCl_3$

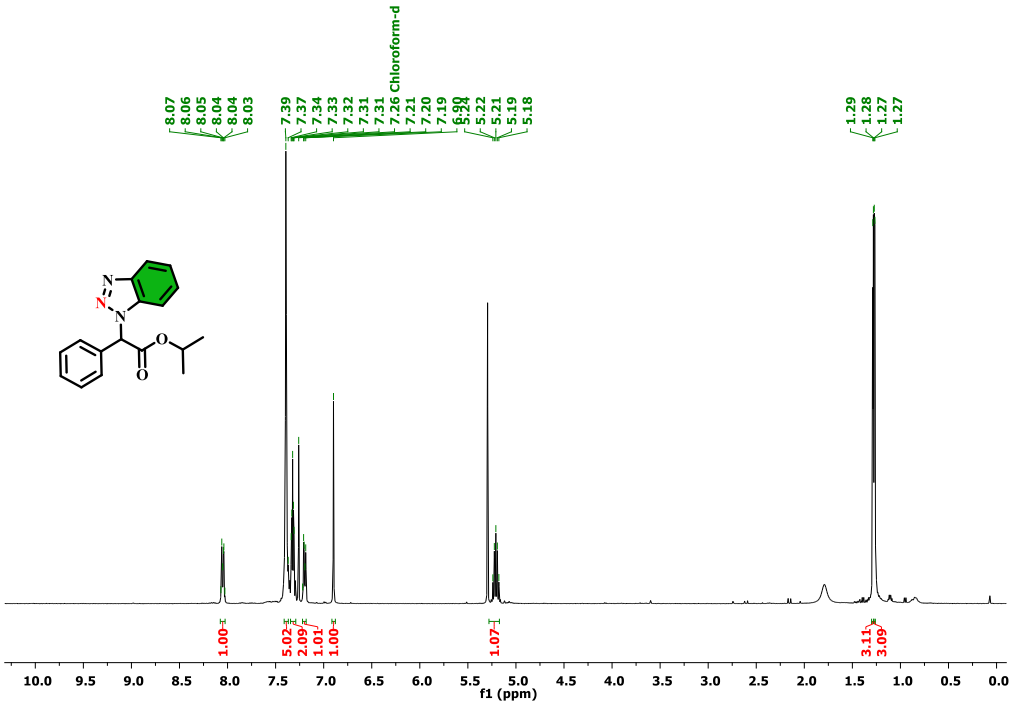


Figure 5.5A: ^{1}H NMR of **3g**, 400 MHz, $CDCl_3$

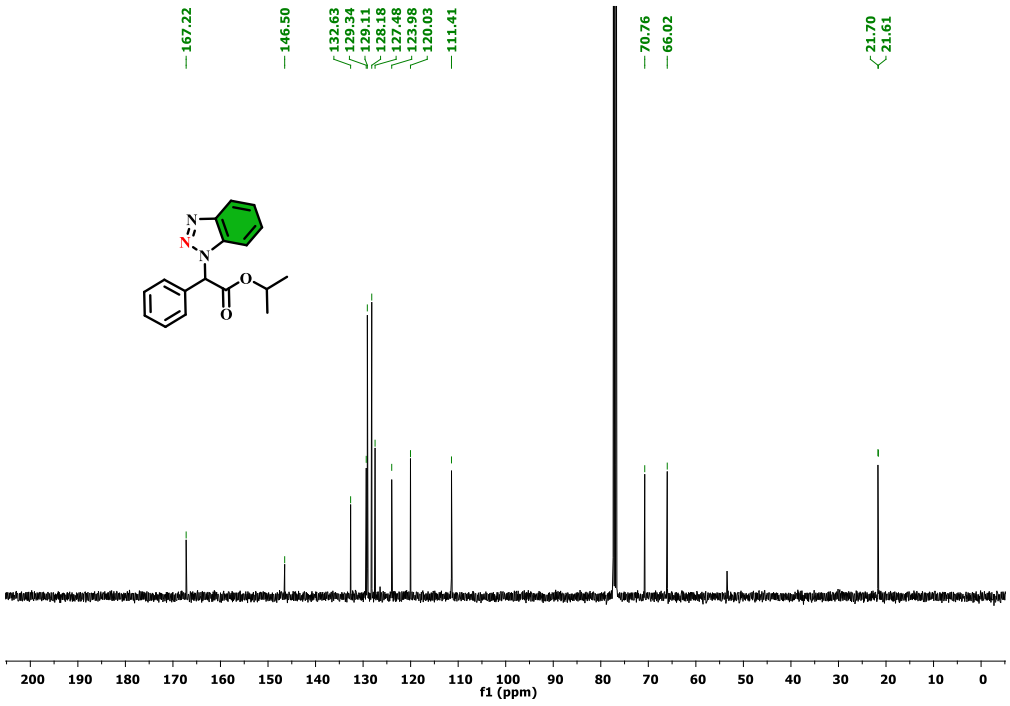


Figure 5.6A: ^{13}C $\{^{1}H\}$ NMR of **3g**, 100 MHz, $CDCl_3$

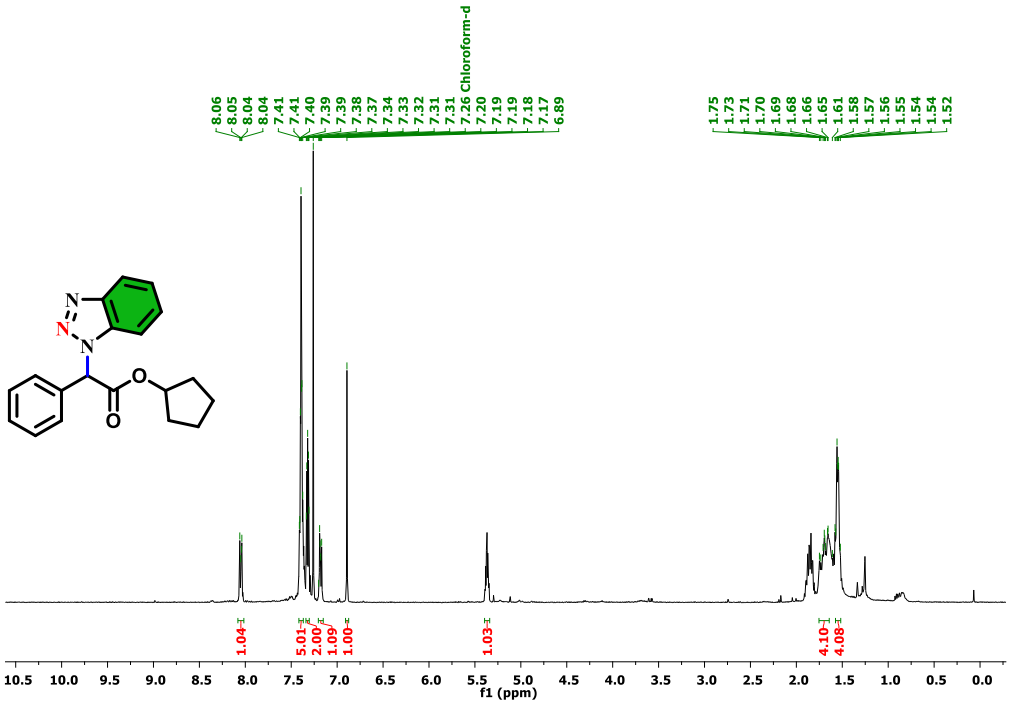


Figure 5.7A: ^{1}H NMR of **3i**, 400 MHz, $CDCl_3$

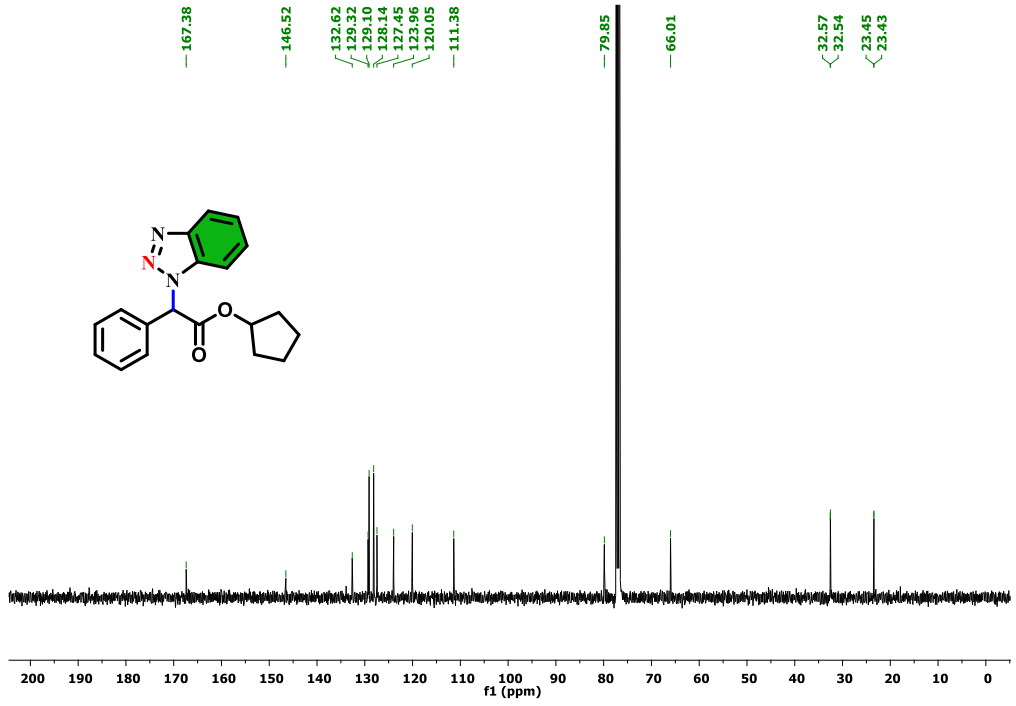


Figure 5.8A: ^{13}C {^{1}H} NMR of **3i**, 100 MHz, $CDCl_3$

5.5A. Reference

1. Müller, P.; Fruit, C. *Chem. Rev.* **2003**, *103* (8), 2905–2920.
2. Zhang, Z.; Wang, J. *Tetrahedron* **2008**, *64* (28), 6577–6605.
3. Davies, H. M. L.; Beckwith, R. E. J. *Chem. Rev.* **2003**, *103* (8), 2861–2903.
4. Doyle, M. P.; McKervey, M. A.; Ye, T. *Modern Catalytic Methods for Organic Synthesis with Diazo Compounds*; Wiley-Interscience: New York, 1998.
5. Ford, A.; Miel, H.; Ring, A.; Slattery, C. N.; Maguire, A. R.; McKervey, M. A. *Chem. Rev.* **2015**, *115* (18), 9981–10080.
6. Zhao, Y.; Zhang, Y. *Chem. Commun.* **2010**, *46* (5), 847–849.
7. Deng, Y.; Wei, X.; Chen, X.; Xu, X. *Org. Lett.* **2020**, *22* (16), 6285–6290.
8. Zhu, S.; Zhou, Q. *Acc. Chem. Res.* **2012**, *45* (9), 1365–1377.
9. Doyle, M. P.; Duffy, R. *Chem. Rev.* **1991**, *91* (5), 225–274.
10. Zhang, Y.; Wang, J. *Tetrahedron* **2011**, *67* (27), 4449–4475.
11. Guo, Y.; Wang, H.; Liu, Y.; Wang, L.; Li, Y. *Adv. Synth. Catal.* **2018**, *360* (9), 1685–1691.
12. Xu, X.; Hu, W. *Chem. Soc. Rev.* **2021**, *50* (3), 1614–1630.
13. Yang, Z.; Stivanin, M. L.; Jurberg, I. D.; Koenigs, R. M. *Chem. Soc. Rev.* **2020**, *49* (19), 6833–6847.
14. Ciszewski, Ł. W.; Rybicka-Jasińska, K.; Gryko, D. *Org. Biomol. Chem.* **2019**, *17*, 432–448.
15. Jurberg, I. D.; Davies, H. M. L. *Chem. Sci.* **2018**, *9*, 5112–5118.
16. Hommelsheim, R.; Guo, Y.; Yang, Z.; Empel, C.; Koenigs, R. M. *Angew. Chem., Int. Ed.* **2019**, *58* (5), 1203–1207.
17. Xia, X. D.; Ren, Y. L.; Chen, J.R.; Yu, X.L.; Lu, L. Q.; Zou, Y.Q.; Wan, J.; Xiao, W. J. *Chem. Asian J.* **2015**, *10*, 124–129.
18. Katritzky, A. R.; Wang, Z.; Slavik, M.; Hall, C. D.; Tsivkovski, R.; Degaonkar, S. V. *Chem. Rev.* **1996**, *96* (1), 93–113.

19. Rasool, F.; Bano, N.; Rashid, N.; Shafi, S.; Shah, A. M.; Khan, R.; Yousuf, S. K.; Ahmed, B. *Eur. J. Med. Chem.* **2021**, *211*, 113090.

20. Sharma, P. K.; Sharma, A. *Tetrahedron* **2005**, *61* (10), 2605–2649.

21. Keum, H.; Lee, S.; Kim, H. *Synthesis* **2016**, *48* (20), 3287–3296.

22. Lindsley, C. W.; Zhao, Z.; Leister, W. H.; Robinson, R. G.; Barnett, S. F.; Defeo-Jones, D.; Jones, R. E.; Hartman, G. D.; Huff, J. R.; Huber, H. E.; Duggan, M. E. *Bioorg. Med. Chem. Lett.* **2004**, *14* (15), 3985–3989.

23. Musa, A. Y.; Kadhum, A. A. H.; Mohamad, A. B.; Takriff, M. S.; Masudi, H. *Corros. Sci.* **2012**, *56*, 129–140.

24. Qian, H.; Xu, B. Benzotriazole Derivatives in Medicinal Chemistry. *Eur. J. Med. Chem.* **2022**, *231*, 114174.

25. Sambiagio, C.; Schönbauer, D.; Blieck, R.; Dao-Huy, T.; Pototschnig, G.; Schaaf, P.; Wiesinger, T.; Zia, M. F.; Wencel-Delord, J.; Besset, T.; Maes, B. U. W.; Schnürch, M. *ACS Catal.* **2020**, *10* (3), 1971–2002.

26. Guo, X.; Liu, Y.; Li, Y.; Wang, J. *Org. Chem. Front.* **2019**, *6* (20), 3403–3410.

27. Zhang, X., & Tang, Y. (2023). Direct C–N bond formation via carbene insertion: Mechanistic insights. *Chemical Science*, **14**, 4650–4663.

28. Zhang, X.; Tang, Y. *Chem. Sci.* **2023**, *14* (15), 4650–4663.

29. Yu, Z.; Mendoza, A.; Bouffard, J.; Kim, D. *J. Am. Chem. Soc.* **2020**, *142* (43), 18223–18230.

30. Zhu, C.; Liu, X.; Wang, M.; Gao, Y.; Yang, L.; Zhang, Y.; Wang, J *Angew. Chem., Int. Ed.* **2021**, *60* (29), 15656–15662.

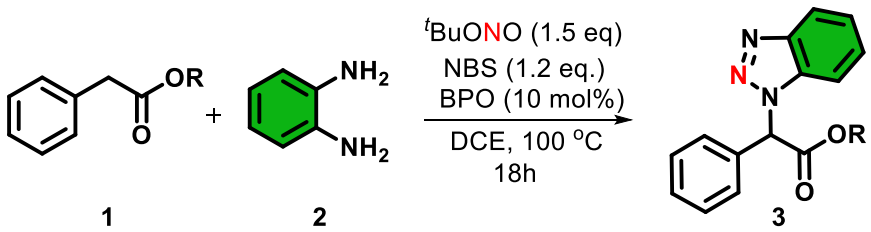
Chapter 5 B

NBS Promoted C-H benzotriazolation of α-aryl esters

NBS Promoted C-H benzotriazolation of α-aryl esters

5.1B. Abstract

In this chapter, a practical and efficient method for the direct benzotriazolation of α-aryl esters has been developed via a one-pot, metal-free approach. The process involves the in-situ formation of benzotriazole from *o*-phenylenediamine and *tert*-butyl nitrite and benzylic C–H bromination using NBS under the catalytic influence of benzoyl peroxide. The resulting benzylic bromide undergoes nucleophilic substitution with the benzotriazole species to afford *N*-substituted benzotriazoles in good to excellent yields. This protocol exhibits broad substrate scope, demonstrated with 30 structurally diverse esters. Mechanistic investigations including radical trapping and control studies support a radical-initiated substitution pathway. The strategy offers a straightforward route to synthetically and biologically relevant benzotriazole derivatives.



1 2 3

5.2B. Introduction

Benzotriazole derivatives have garnered significant attention in recent decades due to their widespread applications in pharmaceuticals, agrochemicals, dyes and corrosion inhibitors (Figure 5.2B.1).[1–8] Their unique bicyclic framework, incorporating three contiguous nitrogen atoms imparts remarkable stability and bioactivity, making them attractive scaffolds for medicinal chemistry and material science.[9-10]As a result, the development of efficient and general strategies for the synthesis of benzotriazole-containing molecules remains a crucial objective in synthetic organic chemistry to explore new classes of bioactive molecules.

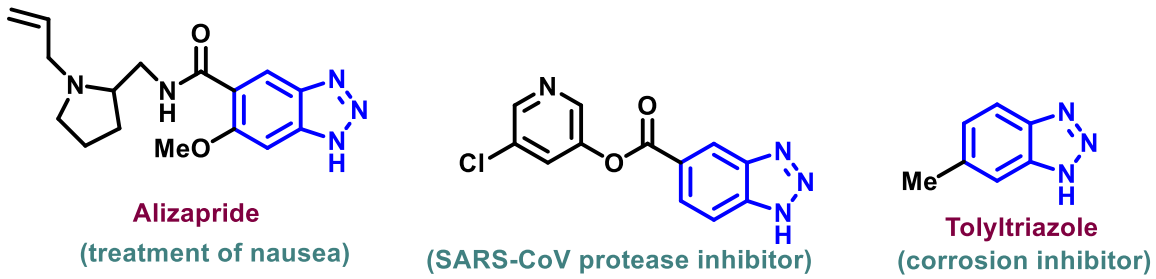
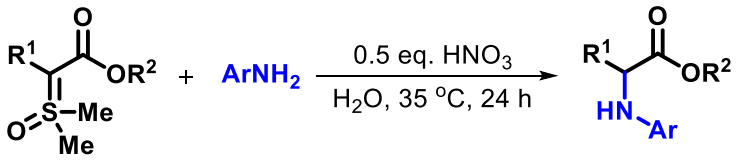


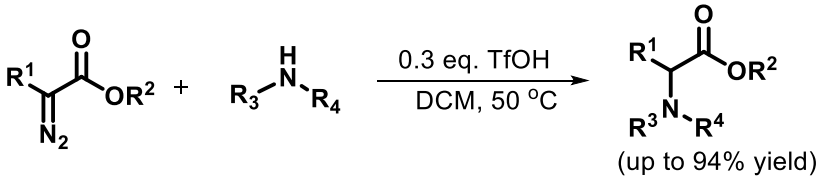
Figure 5.2B.1: Representative examples of bioactive benzotriazoles

Benzotriazolation involves formation of C-N bond. Previously, several strategies have been developed by different research group for efficient C-N bond formation strategies.[11-15] Previously, an acid-mediated intermolecular C–N bond-forming transformation of esters has been developed, wherein sulfoxonium ylides act as stabilized carbene precursors and aromatic amines serve as nucleophilic coupling partners (Scheme 5.2B.1).[16]



Scheme 5.2B.1: C-N bond formation of sulfoxonium ylide with aryl amine

Chen *et al.* have reported TfOH catalyzed direct N-H insertion reaction of diazoesters with secondary amines providing efficient access to α-amino esters through electrophilic carbene intermediates (Scheme 5.2B.2).[17]



Scheme 5.2B.2: C-N bond formation of α-diazo ester with amine

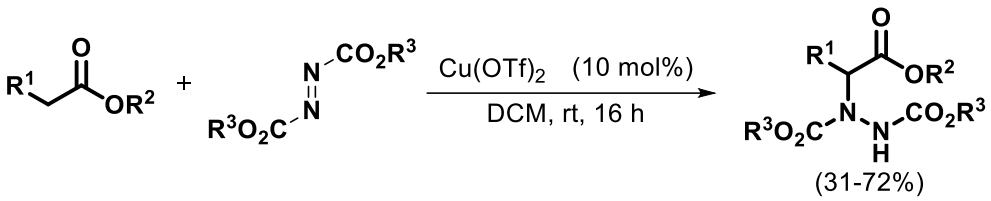
In a notable advancement utilizing photochemical activation, Gaunt *et al.* have established a sustainable visible light induced C-H amination of β-ketoester using amines (Scheme 5.2B.3).[18]



Scheme 5.2B.3: C-N bond formation with α-keto esterss with amines

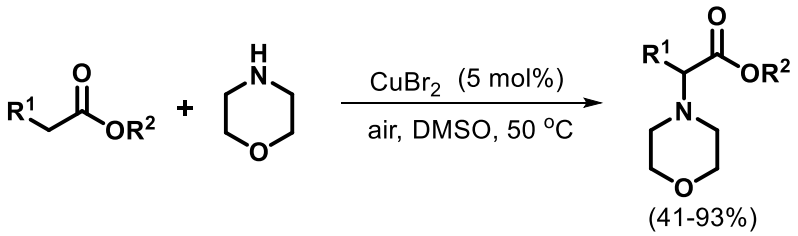
All these methods require pre-activation of α-aryl esters either in the protected form of sulfoxonium ylide or diazo, keto etc. So, to avoid extra step and achieve better step economy, direct C-N bond formation strategies with α-aryl esters have been developed.

Jorgensen *et al.* have disclosed a Cu $(OTf)_2$ catalyzed C-N bond formation methodology at α-position of aromatic ketones and esters using azidocarboxylates (Scheme 5.2B.4) .[19]



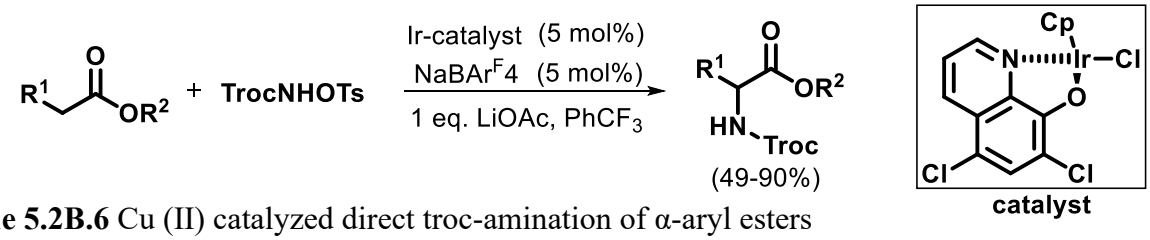
Scheme 5.2B.4: Cu (II) catalyzed direct amination of α-aryl esters

Building on copper catalysis, MacMillan *et al.* demonstrated a $CuBr_2$-mediated oxidative amination of the α-C(sp^3)–H bond in aromatic esters using morpholines as amine sources (Scheme 5.2B.5).[20]



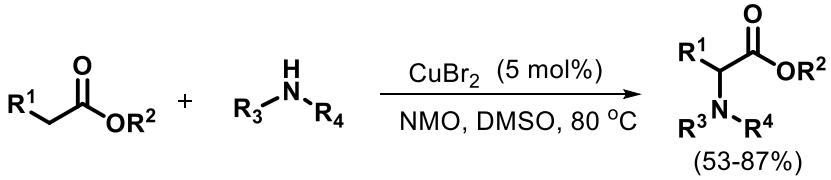
Scheme 5.2B.5: Cu (II) catalyzed direct amination of α-aryl esters with cyclic amine

Chang *et al.* developed a Troc-protected α-amination protocol for α-alkyl esters employing an iridium-based photoredox catalyst. This transformation leverages photoinduced single-electron transfer (SET) to enable formation of α-amino esters under mild and operationally simple conditions (Scheme 5.2B.6).[21]



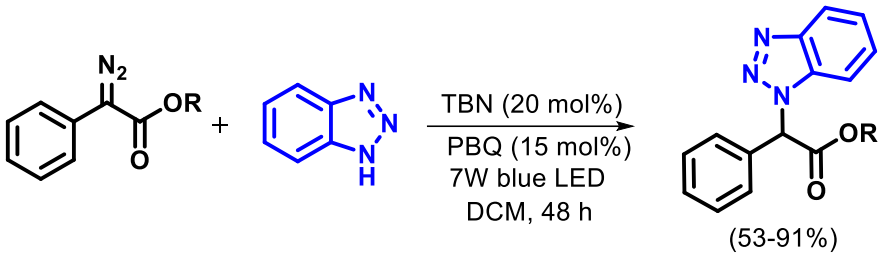
Scheme 5.2B.6 Cu (II) catalyzed direct troc-amination of α-aryl esters

More recently, a sustainable $CuBr_2$-NMO catalyzed direct C-H amination of α-aryl esters has been reported (Scheme 5.2B.7).[22]



Scheme 5.2B.7: Cu (II)-NMO catalyzed direct amination of α-aryl ester

Further literature survey reveals that no methos report the direct C-H benzotriazolation of α-aryl esters. There was one report available on benzotriazolation of α-aryl esters from diazoesters under photoinduced condition (Scheme 5.2B.8).[23]



Scheme 5.2B.8 Photochemical N-H benzotriazolation of α-diazo ester

But this method required preactivation of α-aryl esters and also the diazo compounds are unstable under laboratory condition.[24-25] Traditional methods generally require harsh conditions or metal catalysts, rendering them less appealing for scalability or late-stage functionalization.[26-30] So, we envisioned to get metal-free direct C-H benzotriazolated product from α-aryl esters. Herein, we have disclosed the C-H benzotriazolation reaction of α-aryl esters with the use of ^{t}BuONO, NBS and radical initiator benzoyl peroxide (BPO) in DCE solvent. This method allows the direct assembly of the benzotriazole nucleus from simple precursors. Such mild, metal-free protocols not only streamline the synthetic sequence but also facilitate the preparation of ester-functionalized benzotriazoles, which are highly valuable as fluorescent dyes, therapeutic leads, and synthetic building blocks for subsequent diversification.

5.3B. Rationale of present work

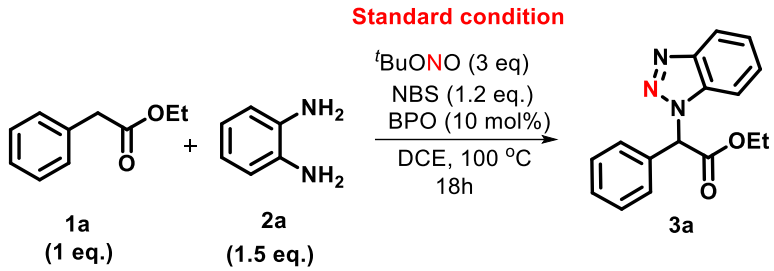
The high biological activities of benzotriazoles have gained substantial attention. In literature, few methods have been reported for the benzotriazolation reaction. However, the reported methods require specially designed starting materials, prolonged duration and needed multistep route. Our previous work in chapter **5A** requires pre-activation of α-aryl esters. Hence, we propose to develop an elegant approach for the synthesis of benzotriazolated α-aryl esters.

5.4B. Result and discussion

In this chapter, we have disclosed a protocol for benzotriazolation of α-aryl esters under metal free conditions using NBS and BPO. The protocol does not need pre-activation of starting material and proceeds under one-pot conditions.

5.4B.1. Optimization

We commenced our initial investigation taking ethyl 2-phenyl acetate (**1a**) and *o*-phenylenediamine (**2b**) as model substrates**.**

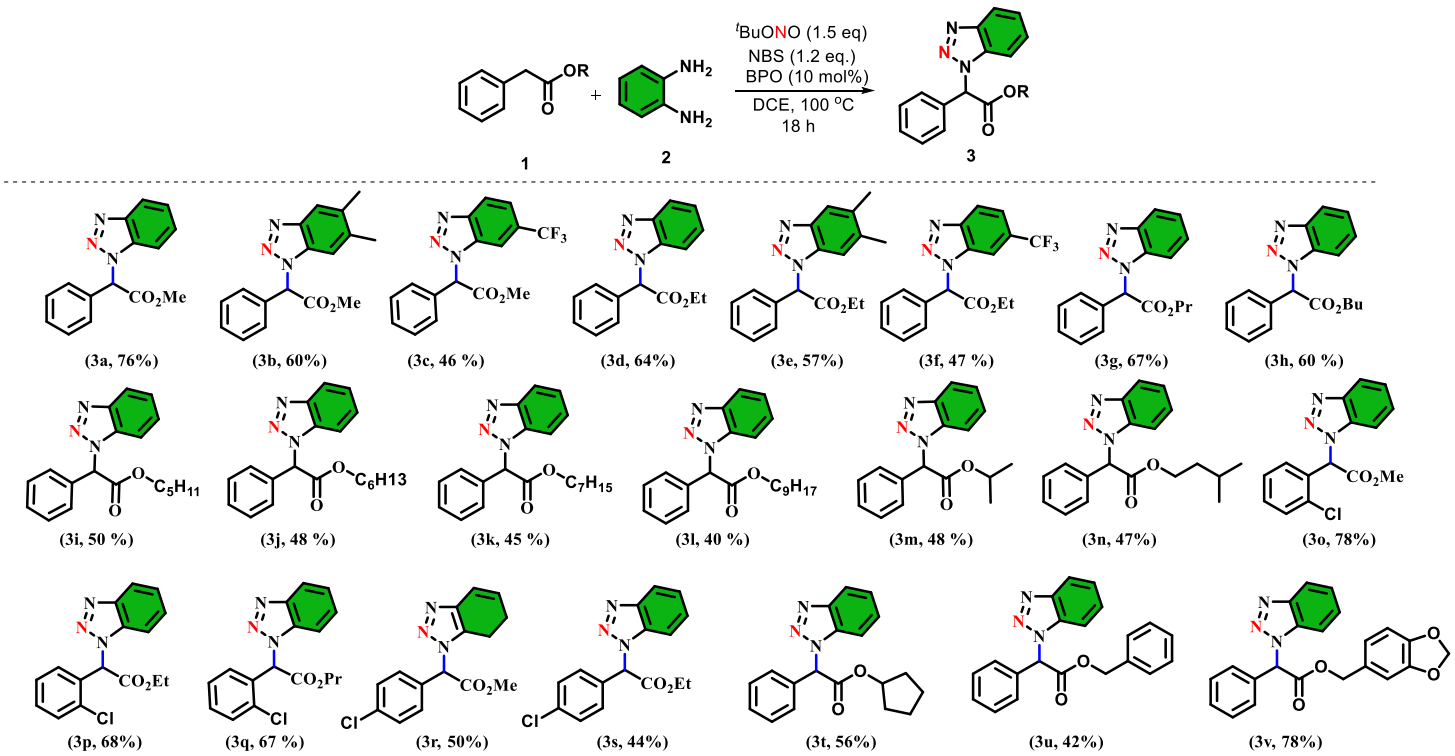


Entry	Deviation from Standard Condition	Yield of 3a (%)
1	none	64
2	5 mol % CuBr in DCE	NR
3	5 mol % CuI in DCE	NR
4	5 mol % CuI + 3 eq. TBHP in ACN	NR
5	1 eq. CAN in DCE/ACN	NR/NR
6	2 eq. Oxone in DCE/DMSO	NR/NR
7	1 eq. DTBP in DMSO/ACN/DCE	NR/NR/NR
8	1 eq. DTBP + 5 mol% $Mn(OAc)_3$ in ACN	NR
9	1 eq. NBS	trace
10	$CHCl_3$ instead of DCE	10
11	ACN instead of DCE	27
12	Chlorobenzene instead of DCE	trace
13	1 eq. 2a	44
14	1 eq. TBN	50

Reaction conditions: 1a (1 equiv.), **2a** (1.5 equiv.), TBN (3 equiv.), NBS (1.2 equiv.), Benzoyl peroxide (10 mol%) and solvent (3 mL) were heated for 18 h at 100 °C.

Then several additives, solvents have been varied to get the desired product **3a**. Employing $CuBr_2$, CuI and CuI along with TBHP as the catalyst, the desired product **3a** was not obtained (Entry 2-4, Table 5.4B.1). Then various oxidants like CAN, oxone, DTBP were screened but that did not afford the desired product (Entry 5-8, Table 5.4B.1). Thereafter using 1 eq. NBS, only traces of product was found (Entry 9, Table 5.4B.1). Changing the solvent to $CHCl_3$, ACN moderate increase in yield was observed (Entry 10-11, Table 5.4B.1). Chlorobenzene as solvent was failed to produce the product

showing only traces (Entry 12, Table 5.4B.1). From the detailed optimisation studies, 1 eq. **1a**, 1.5 eq. **2a**, 1.2 eq. NBS, 10 mol% benzoyl peroxide appears to be optimum reaction conditions for the benzotriazolation of α-aryl esters when heated at 100 °C for 18 h in DCE solvent. Next, to generalise the protocol, substrate scope was extended with the optimized conditions.

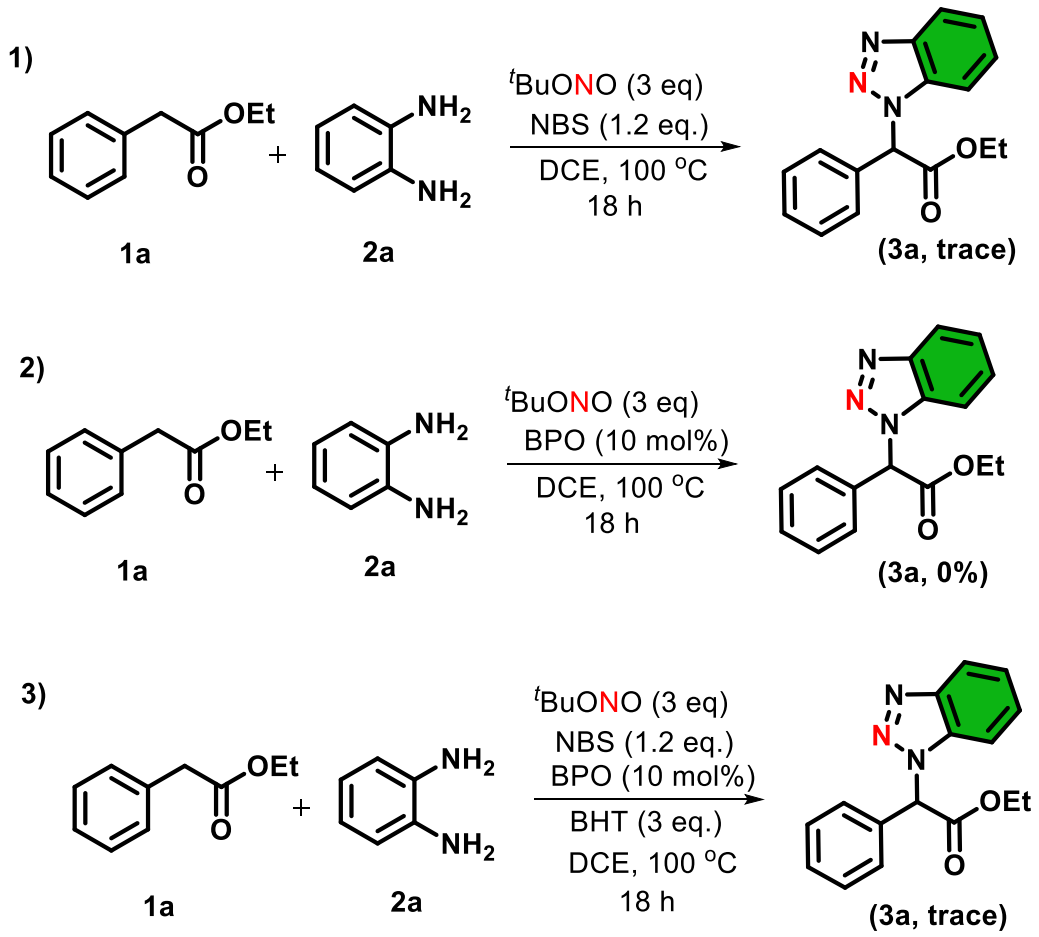


Scheme 5.2B.9: Substrate scope for C-H benzotriazolation of α-aryl esters

[a]**Reaction conditions: 1** (1 eq.), **2** (1.5 eq.), TBN (3 eq.), NBS (1.2 eq.), benzoyl peroxide (10 mol%) and DCE (3 mL) were heated for 18 h at 100 °C.

The reaction was carried out with short to long chain alkyl bearing α-aryl esters and varied the diamine giving the corresponding benzotriazolated α-aryl esters. The corresponding products **3a** to **3l** was obtained in good to excellent yields (76%, 60%, 46%, 64%, 57%, 47%, 67%, 60%, 50%, 48%, 45% and 40% yields respectively) (Scheme 5.2B.9). Interestingly, we observed that α-aryl esters possessing long chain alkyl group demonstrated decreased yield. Further, α-aryl esters containing branched alkyl groups like isopropyl, isopentyl afforded the desired products **3m** and **3n** in 48% and 47% yields respectively (Scheme 5.2B.9). Then, the reaction was performed with α-aryl esters swapped with chloro in 2 and 4 position of phenyl ring giving the desired products **3o** to **3s** in satisfactory yields (78%, 68%, 67%, 50% and 44% respectively) (Scheme 5.4B.9). Afterwards, cyclic alkyl group containing α-aryl esters were choosen. To our delight, alicyclic and aromatic groups like cyclopentyl, benzylic and piperanoyl group containing α-aryl esters were found to react smoothly to afford the desired product. The reactions have furnished the desired products **3t** to **3v** in moderate to good yields

(56%, 42% and 78% yields respectively). This wide substrate scope illustrates the applicability of this developed protocol for C-H benzotriazolation of α-aryl esters.

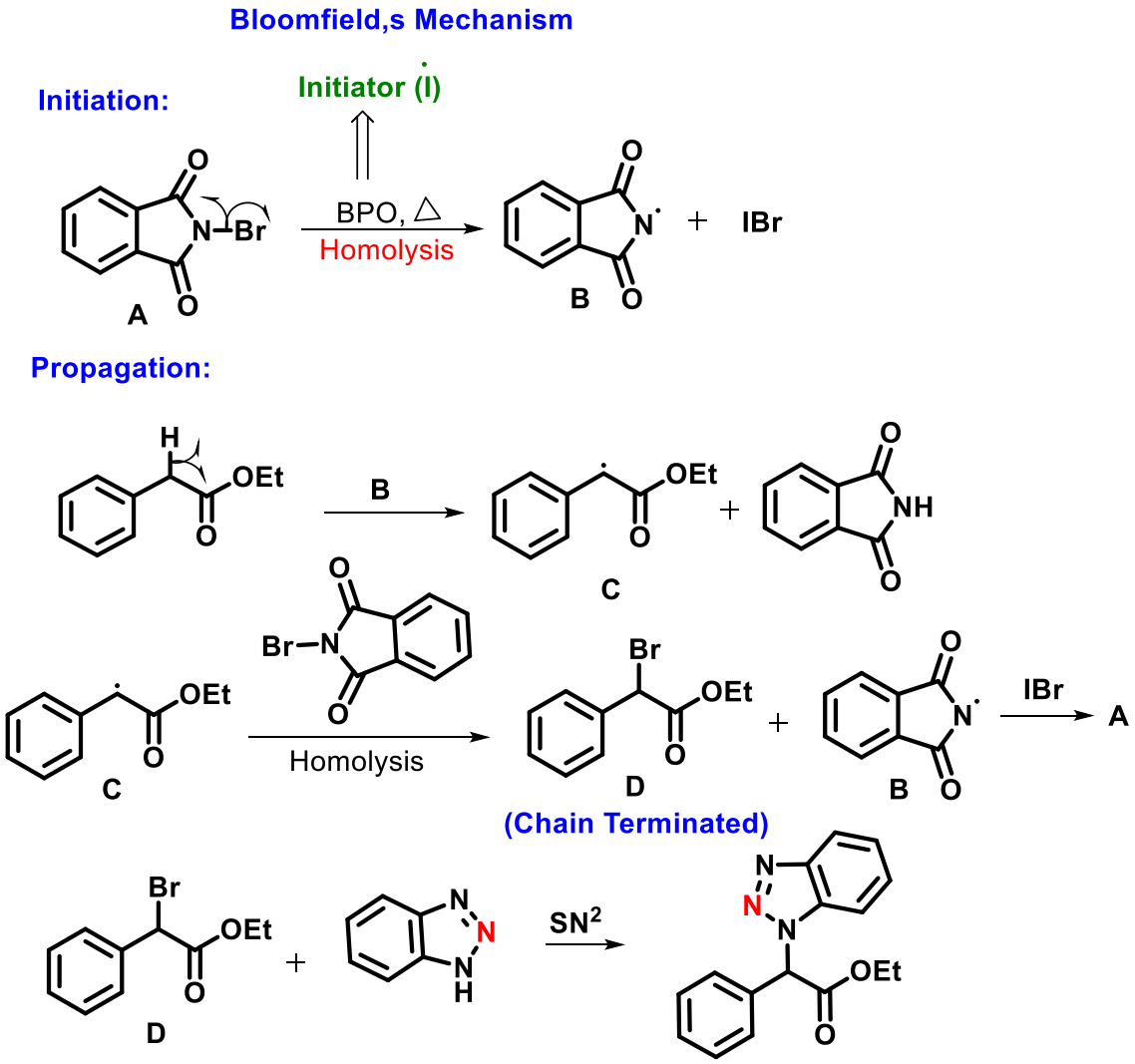


Scheme 5.2B.10: Control experiments to understand the mechanism

Furthermore, to acess the mechanism sets of control studies were carried out. In absence of benzoyl peroxide, only traces of product was obtained (Entry 1, Scheme 5.2B.10). Without addition of NBS, we could not detect any product formation (Entry 2, Scheme 5.2B.10). When the reaction was initiated in the presence of 3 eq. BHT, it was found that the product formation was inhibited (Entry 3, Scheme 5.2B.10) indicating a radical pathway of the initial bromination step.

Therefore, based on control experiments and literature studies, we have sketched a probable radical pathway (Scheme 5.4B.11).[31-34] Under thermal condition, *N*-bromosuccinimide first undergoes homolytic cleavage to produce radical species **B** and Br radical. Radical **B** then abstracts the α hydrogen of α-aryl ester forming ester radical **C** and releases HBr. Radical **C** then reacts with one more molecule of *N*-bromosuccinimide generating α-bromo aryl ester **D** and releases radical **B**. The

bromoaryl ester **D** then undergoes nucleophilic substitution with in situ generated benzotriazole forming the benzotriazolated α-aryl esters.



Scheme 5.2B.11: Plausible Mechanism of direct C-H benzotriazolation

5.5B. Conclusion

Therefore, in summary we have developed an efficient method for benzotriazolation of α-aryl esters. The reaction is induced by stoichiometric NBS and catalytic benzoyl peroxide. Benzoyl peroxide initiates the radical pathway for benzylic bromination. The benzotriazole scaffold has been generated in situ. The reaction has been generalised by using the diverse arrays of α-aryl esters. This method obviates the need for pre-activation of α-aryl ester. So, this one pot process is step economically favourable. The protocol does not use any transition metal based toxic and costly catalyst. Therefore, the protocol is environmentally benign.

5.6B. Experimental section and characterization data

5.6B.1. General information & characterization data

All the chemicals were purchased from Sigma-Aldrich and BLD pharma and used without further modification. All solvents were purchased from Rankem and Finar Chemicals. Deuterated solvents were used as received. Column chromatographic separations were performed over 60−120 mesh silica-gel. Visualization was accomplished with UV light. The ^{1}H and $^{13}C\{1H\}$ NMR spectra were recorded on 400 and 100 MHz, respectively, using Bruker spectrometers. Abbreviations used in the NMR follow-up experiments: b, broad; s, singlet; d, doublet; t, triplet; q, quartet. HRMS spectra were obtained with Waters-synapt G2 using electrospray ionization (ESI-TOF). Infrared (ATIR) spectra were obtained with a Bruker Alpha-E infrared spectrometer. Single-crystal diffraction analysis data were collected at 100K with a BRUKER KAPPA APEX III CCD Duo diffractometer (operated at 1500 W power: 50 kV, 30 mA) using graphite monochromatic Mo-Kα radiation and Cu-Kα radiation. The reaction was performed in a 15 mL borosilicate test tube.

5.6B.2. General procedure for synthesis of 3:

Benzene-1,2-diamine (0.6 mmol) was added in a 10 mL test-tube containing 0.5 mL ACN. Then *tert*-butyl nitrite (124 mg) was added in to it and the reaction mixture was stirred for 30 min at room temperature. After 30 min, the reaction mixture of the test-tube was poured into a sealed tube containing α-aryl ester (0.4 mmol), NBS (0.48 mmol) and benzoyl peroxide (0.04 mmol) in 3 mL DCE solvent. The reaction mixture was then heated at 100 °C for 18 h. After that the solvent was evaporated in rotary evaporator and separated by column chromatography (pet ether: EtOAc = 85:15 to 90: 10).

5.6B.3. Analytical data of products

Methyl 2-(1*H*-benzo[d][1,2,3]triazol-1-yl)-2-phenylacetate (3a) Prepared according to the general procedure using methyl 2-phenylacetate (0.4 mmol, 60 mg), *o*-phenylenediamine (0.6 mmol, 65 mg), *tert*-butyl nitrite (1.2 mmol, 124 mg), NBS (0.48 mmol, 85 mg), and benzoyl peroxide (0.04 mmol, 13 mg). The crude reaction mixture was purified by silica gel column chromatography (pet ether/EtOAc = 85:15) to afford product **3a** (81 mg, 76%). Melting point: 130-132 °C.^{1}H NMR (400 MHz, $CDCl_3$) δ 8.06-8.04 (m, 1H), 7.41-7.37 (m, 5H), 7.34 – 7.30 (m, 2H), 7.21 – 7.17 (m, 1H), 6.94 (s, 1H), 3.86 (s, 3H).$^{13}C\{^{1}H\}$ NMR (100 MHz, $CDCl_3$) δ 168.2, 146.5, 132.6, 132.4, 129.5, 129.2, 128.2, 127.6, 124.0, 120.1, 111.1, 65.7, 53.2. IR (neat): 3067, 2970, 1717, 1410, 1295 cm^{-1}. HRMS (ESI) calculated for $C_{15}H_{13}N_3O_2$ $[M+H]^+$ m/z 268.1086, found 268.1084.

Methyl 2-(5,6-dimethyl-1*H*-benzo[d][1,2,3]triazol-1-yl)-2-phenylacetate (3b) Prepared according to the general procedure using methyl 2-phenylacetate (0.4 mmol, 60 mg), 4,5-dimethylbenzene-1,2-diamine (0.6 mmol, 82 mg), *tert*-butyl nitrite (1.2 mmol, 124 mg), NBS (0.48 mmol, 85 mg), and benzoyl peroxide (0.04 mmol, 13 mg). The crude reaction mixture was purified by silica gel column chromatography (pet ether/EtOAc = 90:10) to afford product **3b** (70 mg, 60%) as yellow semi-solid. ^{1}H NMR (400 MHz, $CDCl_3$) δ 7.78 (s, 1H), 7.41–7.37 (m, 5H), 6.96 (s, 1H), 6.86 (s, 1H), 2.35 (s, 3H), 2.29 (s, 3H), 1.27 (s, 3H). ^{13}C{^{1}H} NMR (100 MHz, $CDCl_3$) δ 167.8, 146.6, 132.6, 131.8, 129.4, 129.0, 128.2, 127.5, 124.1, 120.1, 111.3, 68.1, 65.9, 10.2. IR (neat): 3058, 2937, 1720, 1408, 1300 cm^{-1}. HRMS (ESI) calculated for $C_{17}H_{17}N_3O_2$ $[M+H]^+$ m/z 296.1399, found 296.1400.

Methyl 2-phenyl-2-(6-(trifluoromethyl)-1*H*-benzo[d][1,2,3]triazol-1-yl)acetate (3c) Prepared according to the general procedure using methyl 2-phenylacetate (0.4 mmol, 60 mg), 4-(trifluoromethyl)benzene-1,2-diamine (0.6 mmol, 105 mg), *tert*-butyl nitrite (1.2 mmol, 124 mg), NBS (0.48 mmol, 85 mg), and benzoyl peroxide (0.04 mmol, 13 mg). The crude reaction mixture was purified by silica gel column chromatography (pet ether/EtOAc = 85:15) to afford product **3c** (93 mg, 46%) as yellow liquid. Melting point: 208-210 ºC. ^{1}H NMR (400 MHz, $CDCl_3$) δ 8.41 – 8.39 (m, 1H), 8.37 –8.33 (m, 6H), 7.26 – 7.22 (m, 1H), 6.98 (s, 1H), 3.85 (s, 3H).^{13}C{^{1}H} NMR (100 MHz, $CDCl_3$) δ 168.0 (d, *J* = 2.0 Hz), 145.8, 131.8 (d, *J* = 12.7 Hz), 129.9 (d, *J* = 10.6 Hz), 129.4 (t, *J* = 7.9 Hz), 128., 128.2 (d, *J* = 9.0 Hz), 124.3 (d, *J* = 3.0 Hz), 121.1, 120.8 (d, *J* = 3.2 Hz), 118.3 (d, *J* = 4.4 Hz), 112.4, 109.5 (d, *J* = 4.9 Hz), 77.4, 77.0, 76.7, 66.1 (d, *J* = 6.8 Hz), 53.4 (d, *J* = 4.3 Hz). IR (neat): 3089, 2967, 1715, 1411, 1295 cm^{-1}. HRMS (ESI) calculated for $C_{16}H_{12}F_3N_3O_2$ $[M+H]^+$ m/z 336.0960, found 336.0951.

Ethyl 2-(1*H*-benzo[d][1,2,3]triazol-1-yl)-2-phenylacetate (3d) Prepared according to the general procedure using ethyl 2-phenylacetate (0.4 mmol, 66 mg), *o*-phenylenediamine (0.6 mmol, 65 mg), *tert*-butyl nitrite (1.2 mmol, 77 mg), NBS (0.48 mmol, 85 mg) and benzoyl peroxide (0.04 mmol, 13 mg). The crude reaction mixture was purified by silica gel column chromatography (pet ether/EtOAc = 85:15) to afford product **3d** (72 mg, 64%) as yellow liquid.^{1}H NMR (400 MHz, $CDCl_3$) δ 8.05-8.03 (m, 1H), 7.41-7.37 (m, 5H), 7.34 – 7.30 (m, 2H), 7.21-7.18 (m, 1H), 6.93 (s, 1H), 4.34 (qd, *J* = 7.1, 4.5 Hz, 2H), 1.28 (t, *J* = 7.1 Hz, 3H).^{13}C{^{1}H} NMR (100 MHz, $CDCl_3$) δ 167.7, 146.6, 132.6, 132.5, 129.4, 129.1, 128.2, 127.5, 124.0, 120.1, 111.3, 65.9, 62.6, 14.1. IR (neat): 3059, 2949, 1710, 1405, 1287 cm^{-1}. HRMS (ESI) calculated for $C_{16}H_{15}N_3O_2$ $[M+H]^+$ m/z 282.1242, found 282.1240.

Ethyl 2-(5,6-dimethyl-1*H*-benzo[d][1,2,3]triazol-1-yl)-2-phenylacetate (3e) Prepared according to the general procedure using ethyl 2-phenylacetate (0.4 mmol, 66 mg), 4,5-dimethylbenzene-1,2-

diamine (1.5 mmol, 82 mg), *tert*-butyl nitrite (1.2 mmol, 124 mg), NBS (0.48 mmol, 85 mg), and benzoyl peroxide (0.04 mmol, 13 mg). The crude reaction mixture was purified by silica gel column chromatography (pet ether/EtOAc = 90:10) to afford product **3e** (70 mg, 57%) as yellow oil.^{1}H NMR (400 MHz, $CDCl_3$) δ 7.77 (s, 1H), 7.40–7.36 (m, 5H), 6.96 (s, 1H), 6.86 (s, 1H), 4.38– 4.30 (m, 2H), 2.35 (s, 3H), 2.29 (s, 3H), 1.29 (t, *J* = 7.1 Hz, 3H).^{13}C{^{1}H} NMR (100 MHz, $CDCl_3$) δ 167.9, 145.8, 137.9, 133.8, 132.8, 131.6, 129.2, 129.0, 128.1, 119.1, 110.6, 65.7, 62.5, 21.0, 20.3, 14.1. IR (neat): 3045, 2959, 1715, 1409, 1290 cm^{-1}. HRMS (ESI) calculated for $C_{18}H_{19}N_3O_2$ $[M+H]^+$ m/z 310.1555, found 310.1556.

Ethyl 2-phenyl-2-(6-(trifluoromethyl)-1*H*-benzo[d][1,2,3]triazol-1-yl)acetate (3f) Prepared according to the general procedure using ethyl 2-phenylacetate (0.4 mmol, 66 mg), 4-(trifluoromethyl)benzene-1,2-diamine (0.6 mmol, 106 mg), *tert*-butyl nitrite (1.2 mmol, 124 mg), NBS (0.48 mmol, 85 mg), and benzoyl peroxide (0.04 mmol, 13 mg). The crude reaction mixture was purified by silica gel column chromatography (pet ether/EtOAc = 85:15) to afford product **3f** (65 mg, 47%) yellow liquid.^{1}H NMR (400 MHz, $CDCl_3$) δ 8.36 (s, 1H), 8.56 – 8.53 (m, 1H), 7.97 – 7.92 (m, 1H), 7.44 – 7.36 (m, 6H), 6.98 (s, 1H), 4.41 – 4.33 (m, 2H), 1.33 – 1.29 (m, 3H).^{13}C{^{1}H} NMR (100 MHz, CDCl3) δ 167.5, 167.5, 145.8, 132.0, 131.9, 129.8, 129.7, 129.4, 129.4, 128.2, 128.1, 124.2, 124.1, 121.1, 118.3, 112.5, 66.2, 66.1, 62.8, 14.1, 14.0. IR (neat): 3041, 2998, 1717, 1414, 1290 cm^{-1}. HRMS (ESI) calculated for $C_{17}H_{14}F_3N_3O_2$ $[M+H]^+$ m/z 350.1116, found 350.1112.

Propyl 2-(1*H*-benzo[d][1,2,3]triazol-1-yl)-2-phenylacetate (3g) Prepared according to the general procedure using propyl 2-phenylacetate (0.4 mmol, 60 mg), *o*-phenylenediamine (0.6 mmol, 65 mg), *tert*-butyl nitrite (1.2 mmol, 124 mg), NBS (0.48 mmol, 85 mg) and benzoyl peroxide (0.04 mmol, 10 mg). The crude reaction mixture was purified by silica gel column chromatography (pet ether/EtOAc = 90:10) to afford product **3g** (79 mg, 67%) yellow semi-solid. ^{1}H NMR (400 MHz, $CDCl_3$) δ 8.04 (dd, *J* = 6.3, 2.3 Hz, 1H), 7.41– 7.39 (m, 5H), 7.34 – 7.30 (m, 2H), 7.21– 7.17 (m, 1H), 6.94 (s, 1H), 4.23 (td, *J* = 6.7, 1.9 Hz, 2H), 1.64 (dt, *J* = 14.3, 7.1 Hz, 2H), 0.84 (t, *J* = 7.4 Hz, 3H).^{13}C{^{1}H} NMR (100 MHz, $CDCl_3$) δ 167.8, 146.6, 132.6, 132.6, 129.4, 129.1, 128.2, 127.5, 124.0, 120.1, 111.3, 68.1, 65.9, 21.8, 10.2. IR (neat): 3045, 2967, 1715, 1405, 1295 cm^{-1}. HRMS (ESI) calculated for $C_{17}H_{17}N_3O_2$ $[M+H]^+$ m/z 296.1399, found 296.1398.

Butyl 2-(1*H*-benzo[d][1,2,3]triazol-1-yl)-2-phenylacetate (3h) Prepared according to the general procedure using butyl 2-phenylacetate (0.4 mmol, 77 mg), o-phenylenediamine (0.6 mmol, 65 mg), tert-butyl nitrite (1.2 mmol, 124 mg), NBS (0.48 mmol, 85 mg) and benzoyl peroxide (0.04 mmol, 13 mg). The crude reaction mixture was purified by silica gel column chromatography (pe ether/EtOAc

= 90:10) to afford product **3h** (74 mg, 60%) as yellow semi-solid.^{1}H NMR (400 MHz, $CDCl_3$) δ 8.07–8.03 (m, 1H), 7.40 – 7.38 (m, 5H), 7.34 – 7.30 (m, 2H), 7.20 – 7.17 (m, 1H), 6.93 (s, 1H), 4.28 (td, *J* = 6.7, 2.9 Hz, 2H), 1.61 (dd, *J* = 9.9, 5.2 Hz, 2H), 1.30 – 1.24 (m, 2H), 0.86 (t, *J* = 7.4 Hz, 3H).^{13}C{^{1}H} NMR (100 MHz, $CDCl_3$) δ 167.8, 146.6, 132.6, 132.5, 129.4, 129.1, 128.5, 128.2, 127.5, 124.0, 120.1, 111.3, 66.4, 65.9, 30.4, 18.9, 13.5. IR (neat): 3048, 2966, 1710, 1409, 1285 cm^{-1}. HRMS (ESI) calculated for $C_{18}H_{19}N_3O_2$ $[M+H]^+$ m/z 310.1355, found 310.1358.

Pentyl 2-(1*H*-benzo[d][1,2,3]triazol-1-yl)-2-phenylacetate (3i) Prepared according to the general procedure using pentyl 2-phenylacetate (0.4 mmol, 83 mg), *o*-phenylenediamine (0.6 mmol, 65 mg), *tert*-butyl nitrite (1.2 mmol, 124 mg), NBS (0.48 mmol, 85 mg) and benzoyl peroxide (0.04 mmol, 10 mg). The crude reaction mixture was purified by silica gel column chromatography (pet ether/EtOAc = 90:10) to afford product **3i** (64 mg, 50%) as yellow liquid.^{1}H NMR (400 MHz, $CDCl_3$) δ 8.06–8.04 (m, 1H), 7.40–7.38 (m, 5H), 7.34 – 7.30 (m, 2H), 7.20 – 7.17 (m, 1H), 6.94 (s, 1H), 4.27 (td, *J* = 6.6, 1.4 Hz, 2H), 1.62 (dt, *J* = 13.7, 6.7 Hz, 2H), 1.26 – 1.19 (m, 4H), 0.83 (t, *J* = 7.0 Hz, 3H).^{13}C{^{1}H} NMR (100 MHz, $CDCl_3$) δ 167.8, 146.6, 132.6, 132.5, 129.4, 129.1, 128.5, 128.2, 127.5, 124.0, 120.1, 111.3, 66.6, 65.9, 28.0, 27.8, 22.1, 13.9. IR (neat): 3056, 2958, 1718, 1410, 1290 cm^{-1}. HRMS (ESI) calculated for $C_{19}H_{21}N_3O_2$ $[M+H]^+$ m/z 324.1712, found 324.1717.

Hexyl 2-(1*H*-benzo[d][1,2,3]triazol-1-yl)-2-phenylacetate (3j) Prepared according to the general procedure using hexyl 2-phenylacetate (0.4 mmol, 88 mg), *o*-phenylenediamine (0.6 mmol, 65 mg), *tert*-butyl nitrite (1.2 mmol, 124 mg), NBS (0.48 mmol, 85 mg) and benzoyl peroxide (0.04 mmol, 10 mg). The crude reaction mixture was purified by silica gel column chromatography (pet ether/EtOAc = 90:10) to afford product **3j** (64 mg, 48%) as yellow liquid.^{1}H NMR (400 MHz, $CDCl_3$) δ 8.02 (d, *J* = 8.3 Hz, 1H), 7.42 – 7.35 (m, 3H), 7.31–7.28 (dd, *J* = 7.8, 6.1 Hz, 3H), 7.20 (d, *J* = 7.6 Hz, 2H), 7.07 (s, 1H), 4.18 (t, *J* = 6.6 Hz, 2H), 1.74 – 1.62 (m, 3H), 1.53–1.50 (m, 3H), 1.13–1.12 (m, 2H), 0.76 (t, *J* = 7.0 Hz, 3H).^{13}C{^{1}H} NMR (100 MHz, $CDCl_3$) δ 167.1, 134.6, 133.0, 131.0, 129.9, 127.9, 127.3, 124.2, 120.3, 109.8, 66.9, 62.3, 31.2, 29.7, 28.2, 25.3, 22.4, 13.9. IR (neat): 3065, 2958, 1711, 1415, 1298 cm^{-1}. HRMS (ESI) calculated for $C_{20}H_{23}N_3O_2$ $[M+H]^+$ m/z 338.1868, found 338.1865.

Hepyl 2-(1*H*-benzo[d][1,2,3]triazol-1-yl)-2-phenylacetate (3k) Prepared according to the general procedure using heptyl 2-phenylacetate (0.4 mmol, 94 mg), *o*-phenylenediamine (0.6 mmol, 65 mg), *tert*-butyl nitrite (1.2 mmol, 124 mg), NBS (0.48 mmol, 85 mg) and benzoyl peroxide (0.04 mmol, 10 mg). The crude reaction mixture was purified by silica gel column chromatography (pet ether/EtOAc = 90:10) to afford product **3k** (63 mg, 45%) as yellow liquid.^{1}H NMR (400 MHz, $CDCl_3$) δ 167.8, 146.6, 132.6, 132.6, 129.4, 129.1, 128.5, 128.2, 127.5, 124.0, 120.1, 111.3, 66.6, 65.9, 31.6, 28.7, 28.4,

25.6, 22.5, 14.0.$^{13}C\{^{1}H\}$ NMR (100 MHz, $CDCl_3$) δ. IR (neat): 3054, 2969, 1719, 1404, 1297 cm^{-1}. HRMS (ESI) calculated for $C_{21}H_{25}N_3O_2$ $[M+H]^+$ m/z 352.2025, found 352.2020.

Octyl 2-(1*H*-benzo[d][1,2,3]triazol-1-yl)-2-phenylacetate (3l) Prepared according to the general procedure using octyl 2-phenylacetate (0.4 mmol, 99 mg), *o*-phenylenediamine (0.6 mmol, 65 mg), *tert*-butyl nitrite (1.2 mmol, 124 mg), NBS (0.48 mmol, 85 mg) and benzoyl peroxide (0.04 mmol, 10 mg). The crude reaction mixture was purified by silica gel column chromatography (pet ether/EtOAc = 90:10) to afford product **3l** (58 mg, 40%) as yellow liquid.^{1}H NMR (400 MHz, $CDCl_3$) δ 8.09 (d, *J* = 8.2 Hz, 1H), 7.52 – 7.41 (m, 4H), 7.38– 7.33 (m, 4H), 7.14 (s, 1H), 4.25 (t, *J* = 6.6 Hz, 2H), 1.72 – 1.57 (m, 3H), 1.34 – 1.23 (m, 7H), 0.87 (t, *J* = 7.0 Hz, 5H).$^{13}C\{^{1}H\}$ NMR (100 MHz, $CDCl_3$) δ 167.1, 146.0, 131.0, 130.8, 130.1, 129.9, 129.9, 127.8, 127.3, 126.6, 124.1, 120.3, 109.8, 66.9, 62.3, 31.7, 29.1, 29.0, 28.3, 25.6, 22.6, 14.1.IR (neat): 3047, 2949, 1718, 1410, 1295 cm^{-1}. HRMS (ESI) calculated for $C_{22}H_{27}N_3O_2$ $[M+H]^+$ m/z 366.2181, found 366.2171.

Isopropyl 2-(1*H*-benzo[d][1,2,3]triazol-1-yl)-2-phenylacetate (3m) Prepared according to the general procedure using isopropyl 2-phenylacetate (0.4 mmol, 60 mg), *o*-phenylenediamine (0.6 mmol, 65 mg), *tert*-butyl nitrite (1.2 mmol, 124 mg), NBS (0.48 mmol, 85 mg) and benzoyl peroxide (0.04 mmol, 13 mg). The crude reaction mixture was purified by silica gel column chromatography (pet ether/EtOAc = 90:10) to afford product **3m** (56 mg, 48%). Melting point: 120-122 ºC. ^{1}HNMR (400 MHz, $CDCl_3$) δ 8.08 – 8.03 (m, 1H), 7.41 – 7.38 (m, 5H), 7.34 – 7.29 (m, 2H), 7.22 – 7.18 (m, 1H), 6.90 (s, 1H), 5.21 (dt, *J* = 12.5, 6.3 Hz, 1H), 1.28 (d, *J* = 2.6 Hz, 3H), 1.27 (d, *J* = 2.6 Hz, 3H).$^{13}C\{^{1}H\}$ NMR (100 MHz, $CDCl_3$) δ 167.2, 146.5, 132.6, 129.3, 129.1, 128.2, 127.5, 124.0, 120.0, 111.4, 70.8, 66.0, 21.7, 21.0. IR (neat): 3049, 2954, 1715, 1415, 1292 cm^{-1}. HRMS (ESI) calculated for $C_{17}H_{17}N_3O_2$ $[M+H]^+$ m/z 296.1399, found 296.1390.

Isopentyl 2-(1*H*-benzo[d][1,2,3]triazol-1-yl)-2-phenylacetate (3n) Prepared according to the general procedure using isopentyl 2-phenylacetate (0.4 mmol, 83 mg), *o*-phenylenediamine (0.6 mmol, 65 mg), *tert*-butyl nitrite (1.2 mmol, 124 mg), NBS (0.48 mmol, 85 mg) and benzoyl peroxide (0.04 mmol, 13 mg). The crude reaction mixture was purified by silica gel column chromatography (pet ether/EtOAc = 90:10) to afford product **3n** (60 mg, 47%). Melting point: 231-233 ºC.^{1}HNMR (400 MHz, $CDCl_3$) δ 8.05– 8.03 (m, 1H), 7.40– 7.39 (m, 5H), 7.33 – 7.30 (m, 2H), 7.20 – 7.17 (m, 1H), 6.93 (s, 1H), 4.32– 4.28 (m, 2H), 1.53 – 1.48 (m, 3H), 0.83 (dd, *J* = 6.4, 3.0 Hz, 6H). $^{13}C\{^{1}H\}$ NMR (100 MHz, $CDCl_3$) δ 167.8, 146.5, 132.6, 132.5, 129.4, 129.1, 128.2, 127.5, 124.0, 120.1, 111.3, 111.2, 65.9, 65.2, 37.0, 24.9, 22.3. IR (neat): 3053, 2964, 1708, 1407, 1299 cm^{-1}. HRMS (ESI) calculated for $C_{19}H_{21}N_3O_2$ $[M+H]^+$ m/z 324.1712, found 324.1710.

Methyl 2-(1*H*-benzo[d][1,2,3]triazol-1-yl)-2-(2-chlorophenyl)acetate (3o) Prepared according to the general procedure using methyl 2-(2-chlorophenyl) acetate (0.2 mmol, 36 mg), *o*-phenylenediamine (0.3 mmol, 33 mg), *tert*-butyl nitrite (0.6 mmol, 62 mg), NBS (0.24 mmol, 43 mg), and benzoyl peroxide (0.04 mmol, 6.5 mg). The crude reaction mixture was purified by silica gel column chromatography (pet ether/EtOAc = 85:15) to afford product **3o** (47 mg, 78%) as yellow oil.^{1}H NMR (400 MHz, $CDCl_3$) δ 8.09 (d, *J* = 8.2 Hz, 1H), 7.47 – 7.42 (m, 3H), 7.37– 7.35 (m, 3H), 7.16 (s, 1H), 3.85 (s, 3H).^{13}C{^{1}H} NMR (100 MHz, $CDCl_3$) δ 167.6, 145.9, 134.5, 133.0, 130.9, 130.9, 130.1, 130.0, 128.0, 127.4, 124.2, 120.3, 109.7, 62.1, 53.5. IR (neat): 3063, 2961, 1709, 1418, 1290 cm^{-1}. HRMS (ESI) calculated for $C_{15}H_{12}ClN_3O_2$ $[M+H]^+$ m/z 302.0696, found 302.0695.

Ethyl 2-(1*H*-benzo[d][1,2,3]triazol-1-yl)-2-(2-chlorophenyl)acetate (3p) Prepared according to the general procedure using ethyl 2-(2-chlorophenyl)acetate (0.2 mmol, 40 mg), *o*-phenylenediamine (0.3 mmol, 33 mg), *tert*-butyl nitrite (0.6 mmol, 62 mg), NBS (0.24 mmol, 43 mg), and benzoyl peroxide (0.04 mmol, 6.5 mg). The crude reaction mixture was purified by silica gel column chromatography (pet ether/EtOAc = 85:15) to afford product **3p** (43 mg, 68%) as yellow semi-solid. ^{1}H NMR (400 MHz, $CDCl_3$) δ 8.02 (d, *J* = 8.2 Hz, 1H), 7.41 – 7.34 (m, 3H), 7.32 – 7.27 (m, 3H), 7.19 (s, 1H), 7.06 (s, 1H), 4.26 (dt, *J* = 13.8, 6.8 Hz, 2H), 1.20 (d, *J* = 7.1 Hz, 3H). ^{13}C{^{1}H} NMR (100 MHz, $CDCl_3$) δ 167.0, 146.0, 134.6, 133.0, 131.0, 130.8, 130.2, 130.0, 127.9, 127.4, 124.2, 120.3, 109.8, 62.9, 62.3, 14.0. IR (neat): 3032, 2957, 1737, 1664, 1600 cm-1. HRMS (ESI) calculated for $C_{16}H_{14}ClN_3O_2$ [M+H]+ m/z 316.0853, found 316.0846.

Propyl 2-(1*H*-benzo[d][1,2,3]triazol-1-yl)-2-(2-chlorophenyl)acetate (3q) Prepared according to the general procedure using propyl 2-(2-chlorophenyl) acetate (0.2 mmol, 40 mg), *o*-phenylenediamine (0.3 mmol, 33 mg), *tert*-butyl nitrite (0.6 mmol, 62 mg), NBS (0.24 mmol, 43 mg), and benzoyl peroxide (0.04 mmol, 6.5 mg). The crude reaction mixture was purified by silica gel column chromatography (pet ether/EtOAc = 90:10) to afford product **3q** (44 mg, 67%) yellow semi-solid.^{1}H NMR (400 MHz, $CDCl_3$) δ 8.02 (d, J = 8.2 Hz, 1H), 7.40–7.34 (m, 3H), 7.32 – 7.27 (m, 3H), 7.19 (s, 1H), 7.08 (s, 1H), 4.15 (t, *J* = 6.6 Hz, 2H), 1.56 (dd, *J* = 14.2, 6.9 Hz, 2H), 0.75 (t, *J* = 7.4 Hz, 3H).^{13}C{^{1}H} NMR (100 MHz, $CDCl_3$) δ 167.1, 145.9, 134.6, 133.0, 131.0, 130.8, 130.1, 130.0, 127.9, 127.3, 124.2, 120.3, 109.8, 68.4, 62.3, 21.8, 10.2. IR (neat): 3019, 2969, 1711, 1412, 1299 cm^{-1}. HRMS (ESI) calculated for $C_{17}H_{16}ClN_3O_2$ [M+H]+ m/z 330.1009, found 330.1007.

Methyl 2-(1*H*-benzo[d][1,2,3]triazol-1-yl)-2-(4-chlorophenyl)acetate (3r) Prepared according to the general procedure using methyl 2-(4-chlorophenyl) acetate (0.2 mmol, 36 mg), *o*-phenylenediamine (0.3 mmol, 33 mg), *tert*-butyl nitrite (0.6 mmol, 62 mg), NBS (0.24 mmol, 43 mg),

and benzoyl peroxide (0.04 mmol, 10 mg). The crude reaction mixture was purified by silica gel column chromatography (pet ether/EtOAc = 85:15) to afford product **3s** (30 mg, 50%). Melting point: 152-154 ºC. ^{1}H NMR (400 MHz, CDCl3) δ 8.04 – 8.00 (m, 1H), 7.36 – 7.27 (m, 6H), 7.20 (s, 1H), 7.19 – 7.16 (m, 1H), 6.80 (s, 1H), 3.81 (s, 3H).^{13}C{^{1}H} NMR (100 MHz, $CDCl_3$) δ 167.8, 146.2, 135.7, 131.0, 129.6, 129.4, 127.9, 124.2, 120.3, 110.8, 64.9, 53.4. IR (neat): 3066, 2955, 1719, 1410, 1280 cm^{-1}. HRMS (ESI) calculated for $C_{15}H_{13}ClN_3O_2$ $[M+H]^+$ m/z 302.0691, found 302.0696.

Ethyl 2-(1*H*-benzo[d][1,2,3]triazol-1-yl)-2-(4-chlorophenyl)acetate (3s) Prepared according to the general procedure using ethyl 2-(4-chlorophenyl)acetate (0.2 mmol, 40 mg), *o*-phenylenediamine (0.3 mmol, 33 mg), *tert*-butyl nitrite (0.6 mmol, 62 mg), NBS (0.24 mmol, 43 mg), and benzoyl peroxide (0.04 mmol, 6.5 mg). The crude reaction mixture was purified by silica gel column chromatography (pet ether/EtOAc = 85:15) to afford product **3t** (27 mg, 44%) as yellow oil.^{1}H NMR (400 MHz, $CDCl_3$) δ 8.14 – 8.06 (m, 1H), 7.44 – 7.35 (m, 6H), 7.29 – 7.26 (m, 1H), 6.87 (s, 1H), 4.41 – 4.33 (m, 2H), 1.31 (t, *J* = 7.1 Hz, 3H).^{13}C{^{1}H} NMR (100 MHz, $CDCl_3$) δ 167.3, 146.5, 135.6, 132.5, 131.1, 129.6, 129.4, 127.8, 124.2, 120.2, 110.9, 65.1, 62.8, 14.1. IR (neat): 3083, 2944, 1707, 1414, 1288 cm-1. HRMS (ESI) calculated for $C_{16}H_{14}ClN_3O_2$ $[M+H]^+$ m/z 316.0853, found 316.0850.

Cyclopentyl 2-(1*H*-benzo[d][1,2,3]triazol-1-yl)-2-phenylacetate (3t) Prepared according to the general procedure using cyclopentyl 2-phenylacetate (0.4 mmol, 82 mg), *o*-phenylenediamine (0.6 mmol, 65 mg), *tert*-butyl nitrite (1.2 mmol, 124 mg), NBS (0.48 mmol, 85 mg), and benzoyl peroxide (0.04 mmol, 13 mg). The crude reaction mixture was purified by silica gel column chromatography (pet ether/EtOAc = 85:15) to afford product **3t** (72 mg, 56%) as light-yellow solid. Melting point: 105-107 ºC.^{1}H NMR (400 MHz, $CDCl_3$) δ 8.06– 8.04 (m, 1H), 7.41 – 7.37 (m, 5H), 7.34 – 7.30 (m, 2H), 7.20 – 7.15 (m, 1H), 6.89 (s, 1H), 5.37 (tt, *J* = 5.7, 2.7 Hz, 1H), 1.75 – 1.65 (m, 4H), 1.58 – 1.52 (m, 4H).^{13}C{^{1}H} NMR (100 MHz, $CDCl_3$) δ 167.4, 146.5, 132.6, 129.3, 129.1, 128.1, 127.5, 124.0, 120.1, 111.4, 79.9, 66.0, 32.6, 32.5, 23.5, 23.4. IR (neat): 3035, 2944, 1737, 1664, 1600 cm^{-1}. HRMS (ESI) calculated for $C_{19}H_{19}N_3O_2$ $[M+H]^+$ m/z 322.1555, found 322.1555.

Benzyl 2-(1*H*-benzo[d][1,2,3]triazol-1-yl)-2-phenylacetate (3u) Prepared according to the general procedure using benzyl 2-phenylacetate (0.4 mmol, 91 mg), *o*-phenylenediamine (0.6 mmol, 65 mg), *tert*-butyl nitrite (1.2 mmol, 124 mg), NBS (0.48 mmol, 85 mg), and benzoyl peroxide (0.04 mmol, 13 mg). The crude reaction mixture was purified by silica gel column chromatography (pet ether/EtOAc = 85:15) to afford product **3u** (57 mg, 42%). ^{1}H NMR (400 MHz, $CDCl_3$) δ 8.7 – 8.3 (m, 1H), 8.41–8.38 (m, 3H), 8.37 –8.29 (m, 3H), 7.15 – 7.10 (M, 1H), 6.98 (s, 1H), 5.30 (s, 2H). ^{13}C{^{1}H} NMR (100 MHz, $CDCl_3$) δ 167.6, 146.5, 129.4, 129.1, 128.7, 128.7, 128.6, 128.6, 128.2, 124.0, 120.1, 111.2,

68.1, 65.8. IR (neat): 3097, 2968, 1737, 1664, 1600 cm^{-1}. HRMS (ESI) calculated for $C_{21}H_{17}N_3O_2$ $[M+H]^+$ m/z 344.1399, found 344.1397.

Benzo[d][1,3]dioxol-5-ylmethyl 2-(1*H*-benzo[d][1,2,3]triazol-1-yl)-2-phenylacetate (3v) Prepared according to the general procedure using benzo[d][1,3]dioxol-5-ylmethyl 2-phenylacetate (0.4 mmol, 91 mg), o-phenylenediamine (0.6 mmol, 65 mg), tert-butyl nitrite (1.2 mmol, 124 mg), NBS (0.48 mmol, 85 mg) and benzoyl peroxide (0.04 mmol, 13 mg). The crude reaction mixture was purified by silica gel column chromatography (pet ether/EtOAc = 85:15) to afford product **3v** (120 mg, 78%). ^1H NMR (400 MHz, $CDCl_3$) δ 8.01 – 7.95 (m, 1H), 7.54 – 7.51 (m, 1H), 7.43 (s, 1H), 7.39 – 7.36 (m, 2H), 7.34 – 7.23 (m, 8H), 7.08 – 7.02 (m, 1H), 6.90 (s, 1H), 5.27 (s, 2H).$^{13}C\{^1H\}$ NMR (100 MHz, $CDCl_3$) δ 167.5, 146.5, 132.1, 131.6, 129.6, 129.2, 129.2, 128.2, 127.7, 124.1, 120.2, 111.0, 67.1, 65.7. IR (neat): 3057, 2988, 1737, 1664, 1600 cm^{-1}. HRMS (ESI) calculated for $C_{22}H_{17}N_3O_4$ $[M+H]^+$ m/z 388.1297, found 388.1295.

5.8B. Appendix V: Copies of ^1H and ^{13}C NMR spectra of representative compounds of NMR spectra

Entry	Figure No.	Data	Page No.
3a	5.2B.2-5.2B.3	^1H and ^{13}C	189
3e	5.2B.4-5.2B.5	^1H and ^{13}C	190
3g	5.2B.6-5.2B.7	^1H and ^{13}C	191
3h	5.2B.8-5.2B.9	^1H and ^{13}C	192
3i	5.2B.10-5.2B.11	^1H and ^{13}C	193
3m	5.2B.12-5.2B.13	^1H and ^{13}C	194

5.8B.1. Representative examples of NMR spectra

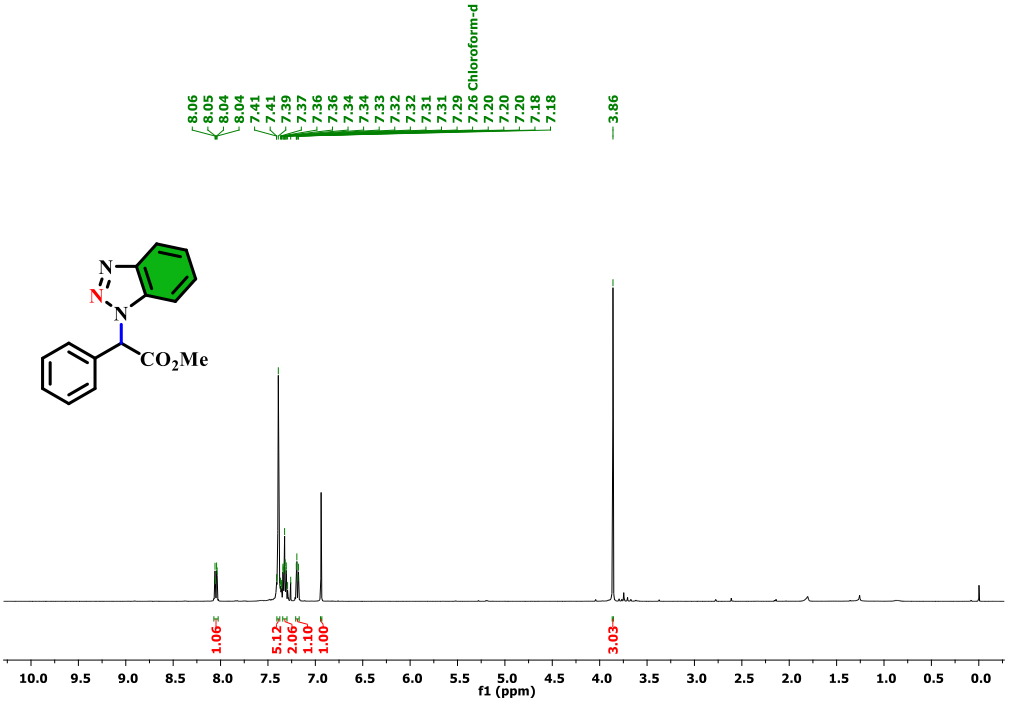


Figure 5.2B.2: ^{1}H NMR of **3a**, 400 MHz, $CDCl_3$

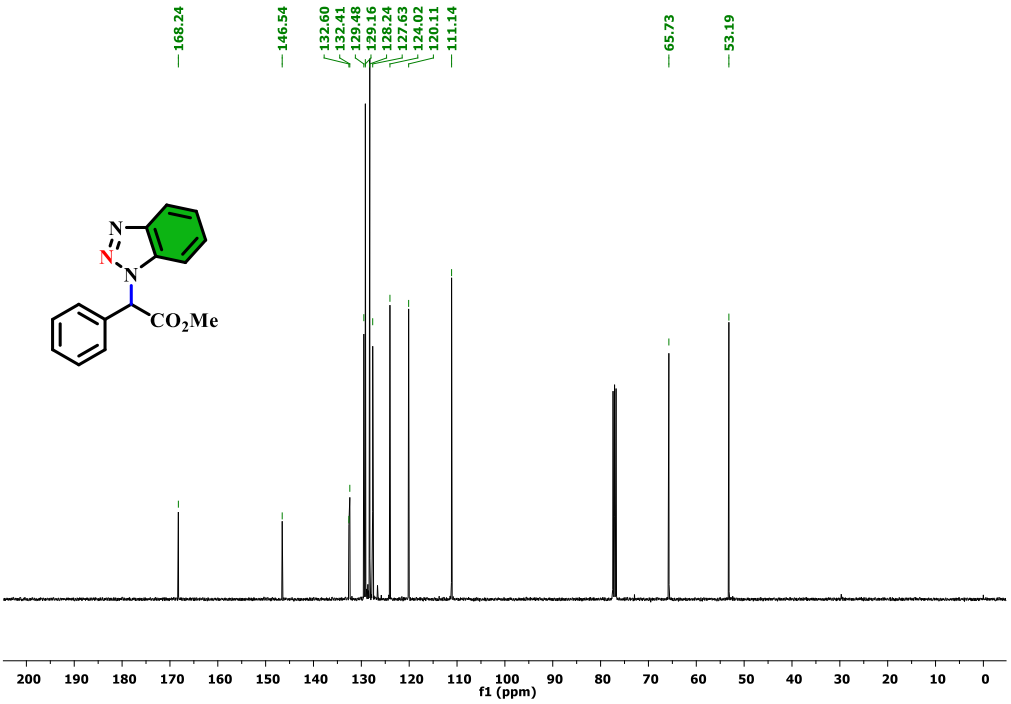


Figure 5.2B.3: ^{13}C $\{^{1}H\}$ NMR of **3a**, 100 MHz, $CDCl_3$

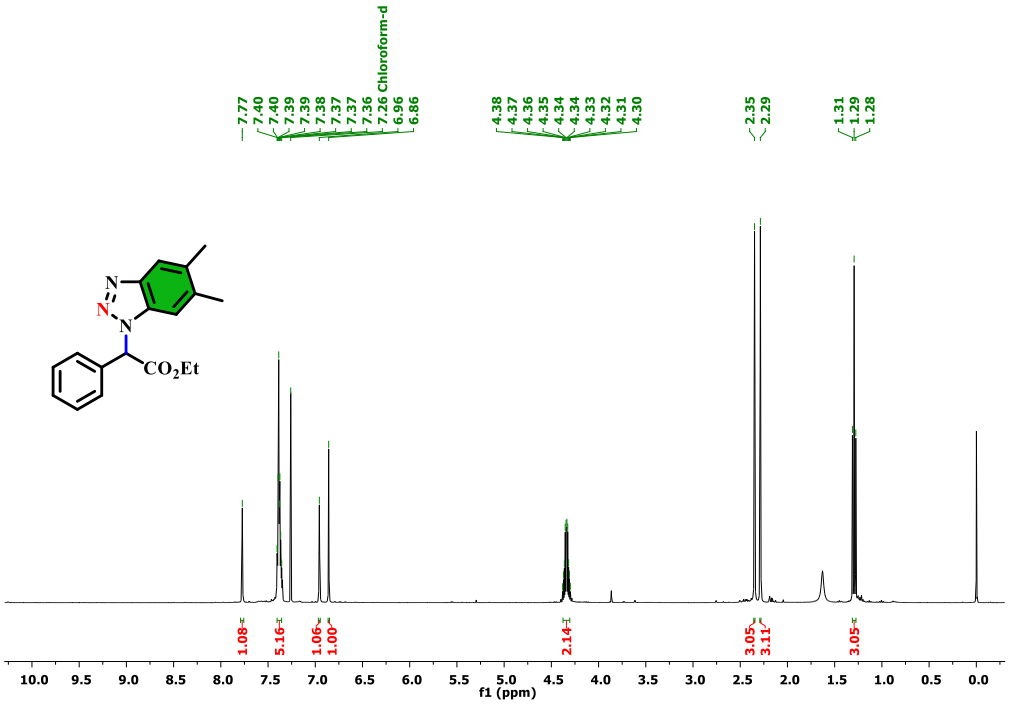


Figure 5.2B.4: ^{1}H NMR of **3e**, 400 MHz, $CDCl_3$

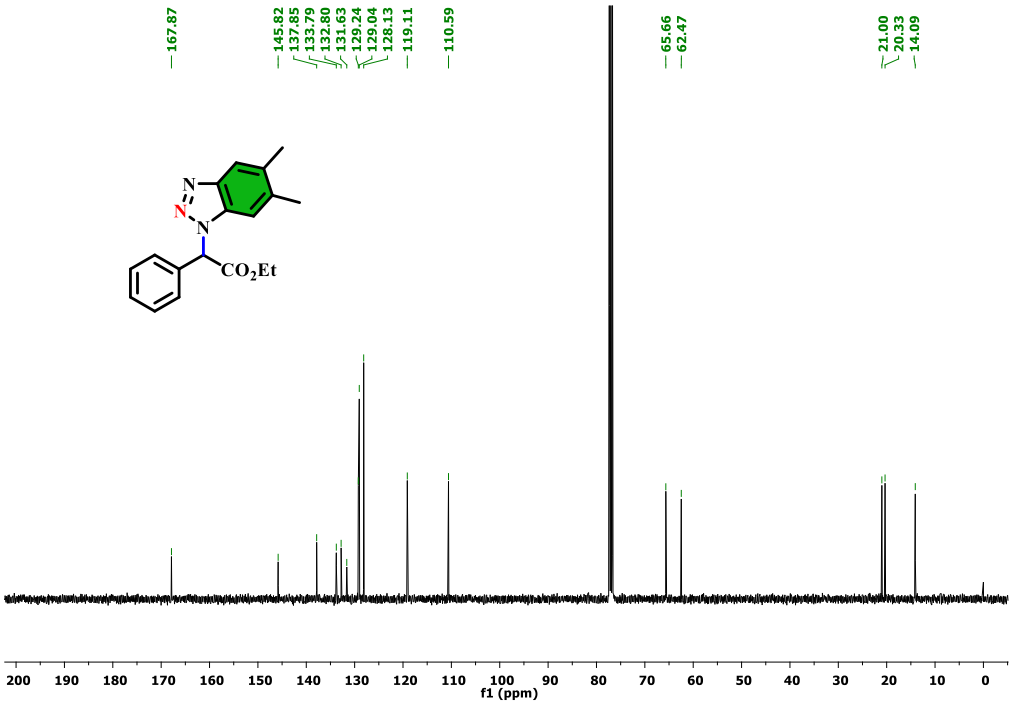


Figure 5.2B.5: ^{13}C $\{^{1}H\}$ NMR of **3e**, 100 MHz, $CDCl_3$

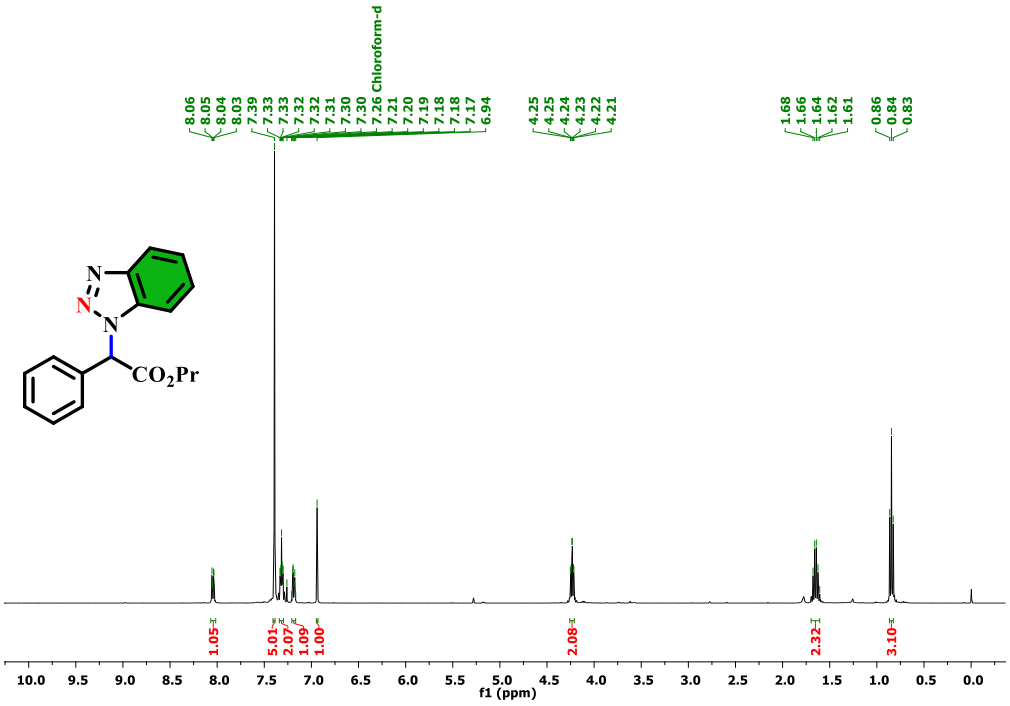


Figure 5.2B.6: ^{1}H NMR of **3g**, 400 MHz, $CDCl_3$

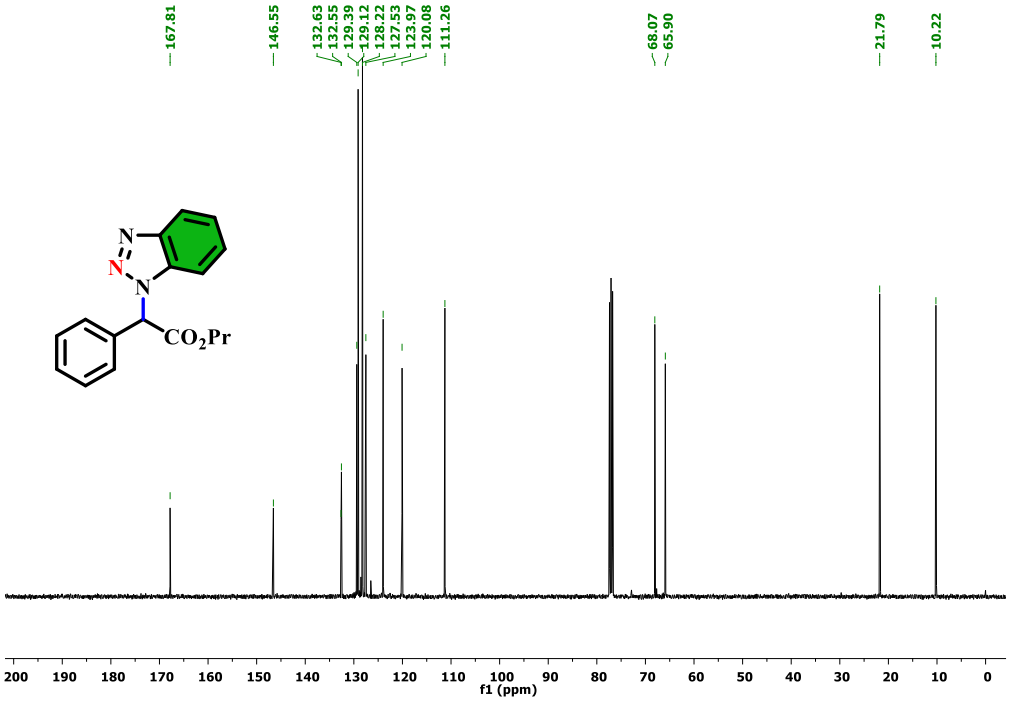


Figure 5.2B.7: ^{13}C $\{^{1}$H$\}$ NMR of **3g**, 100 MHz, $CDCl_3$

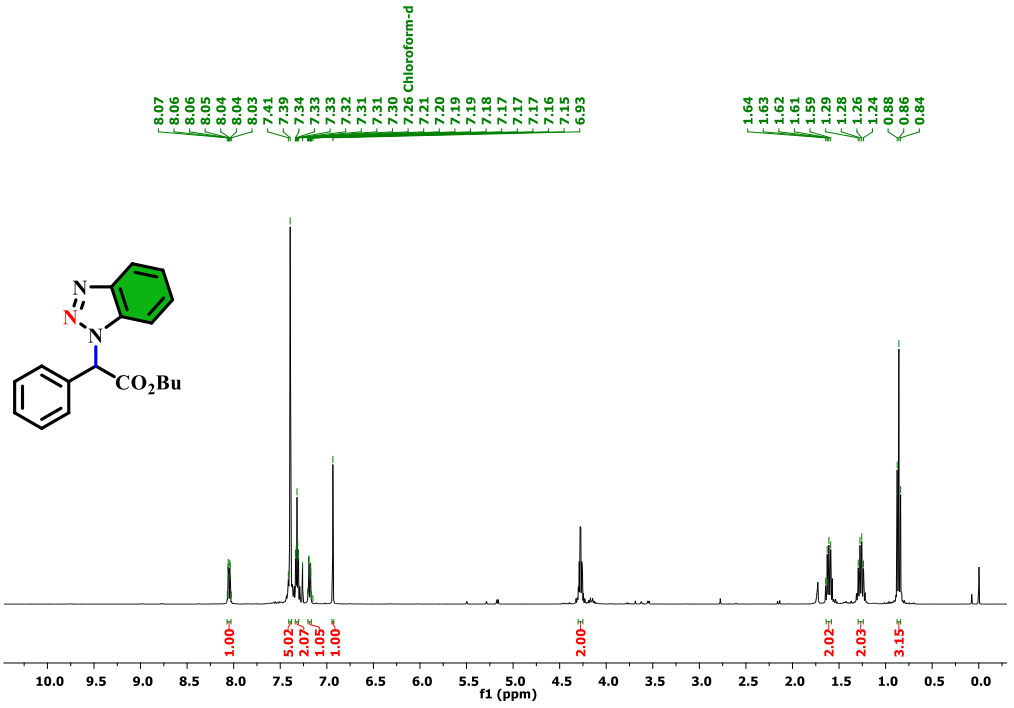


Figure 5.2B.8: ^{1}H NMR of **3h**, 400 MHz, $CDCl_3$

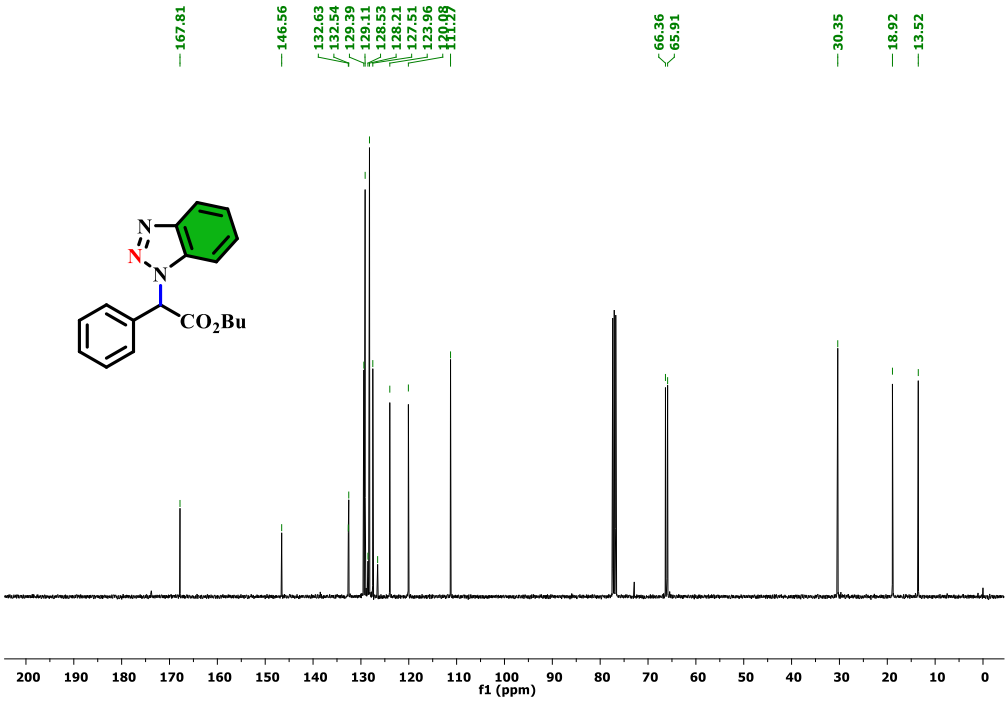


Figure 5.2B.9: ^{13}C {^{1}H} NMR of **3h**, 100 MHz, $CDCl_3$

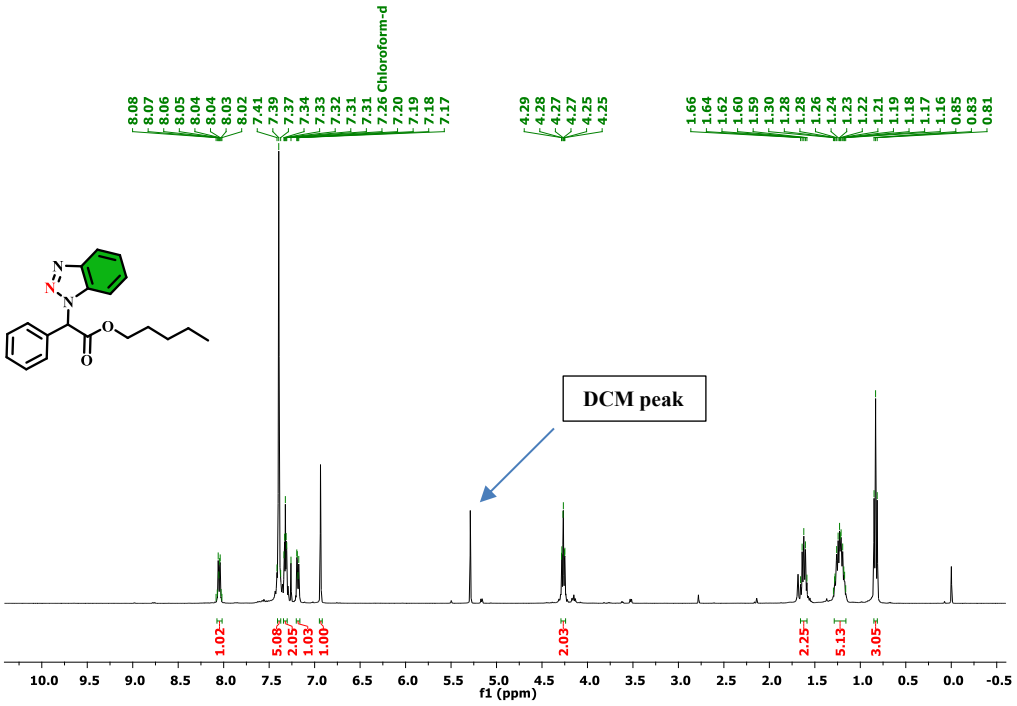


Figure 5.2B.10: ^{1}H NMR of **3i**, 400 MHz, $CDCl_3$

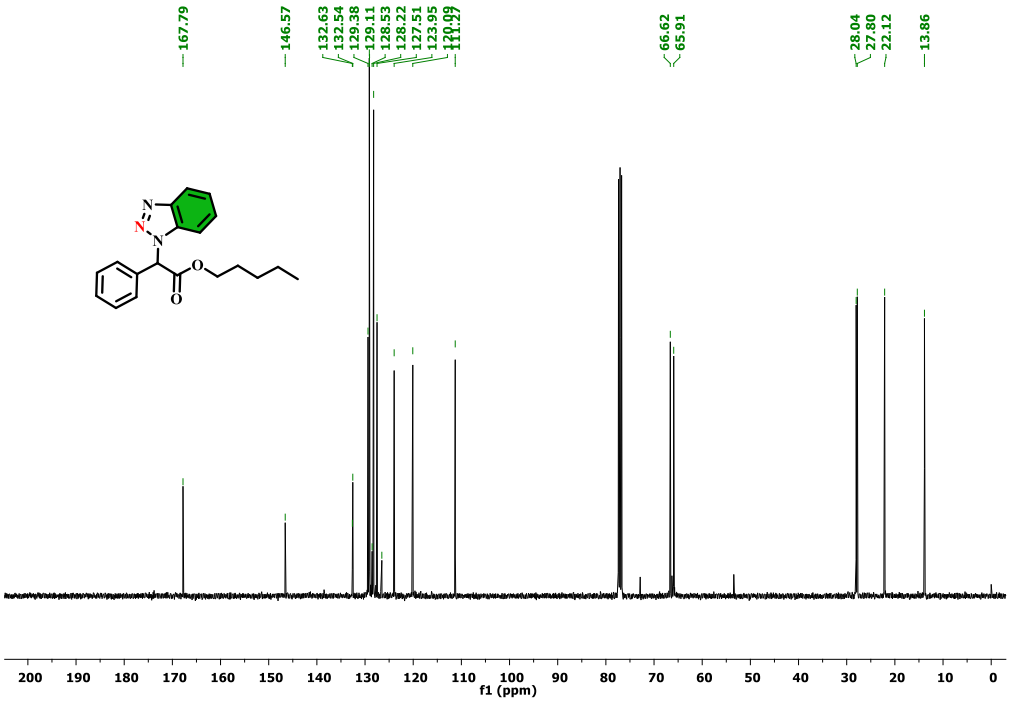


Figure 5.2B.11: ^{13}C {^{1}H} NMR of **3i**, 100 MHz, $CDCl_3$

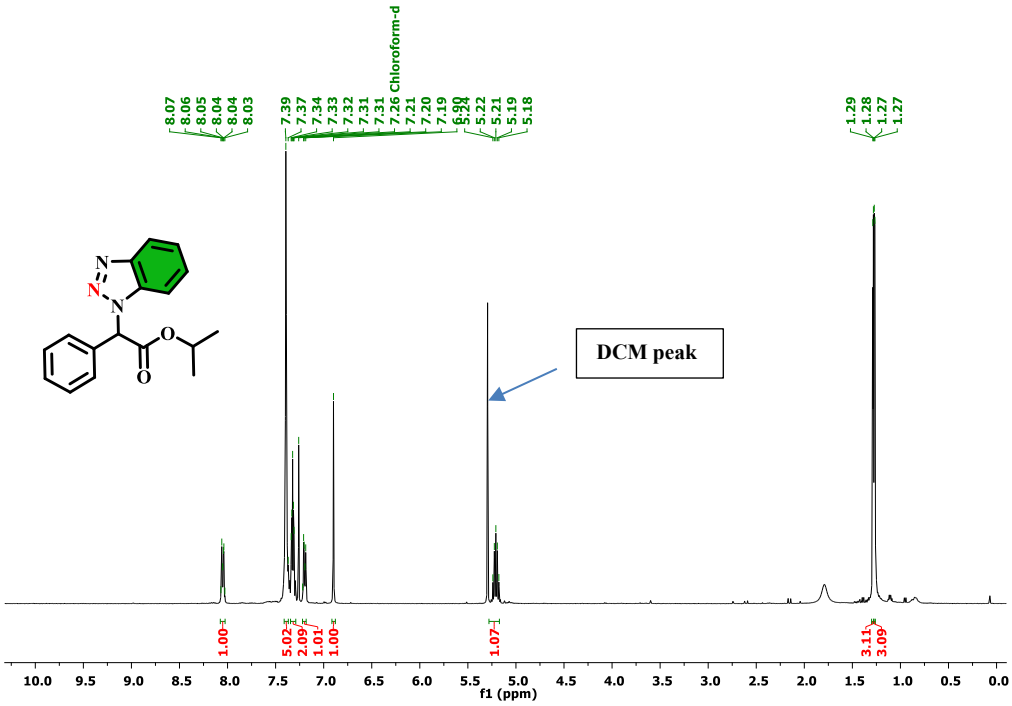


Figure 5.2B.12: ^{1}H NMR of **3m**, 400 MHz, $CDCl_3$

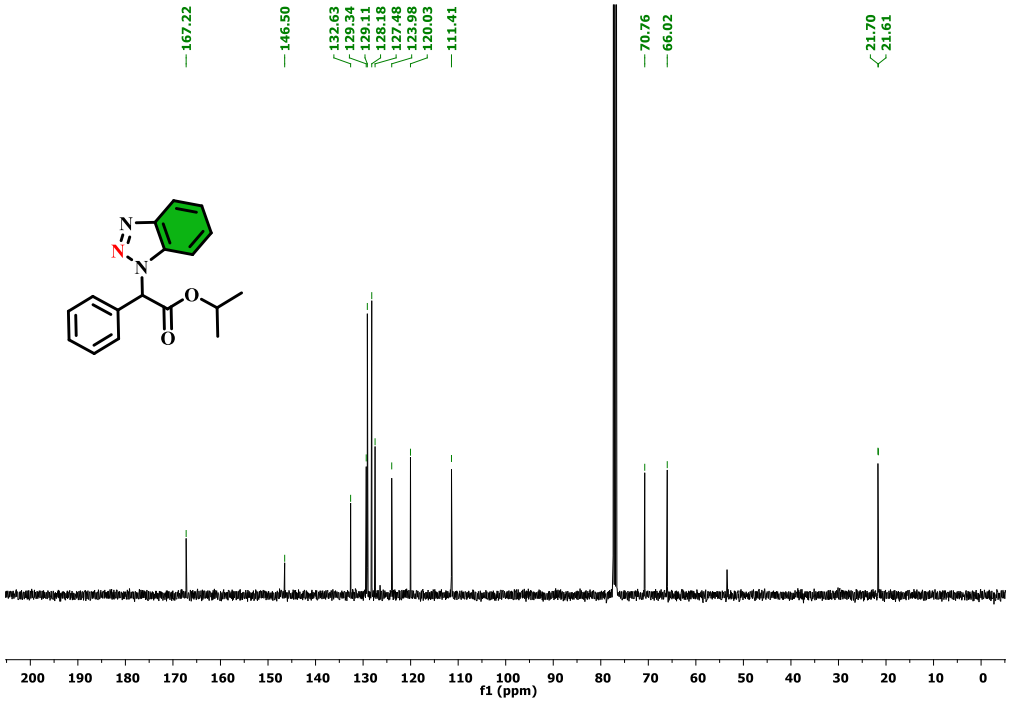


Figure 5.2B.13: ^{13}C {^{1}H} NMR of **3m**, 100 MHz, $CDCl_3$

5.8B.2. SCXRD Structure of 3a

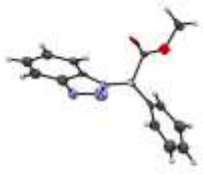


Figure 5.2B.13: SCXRD structure of **3a** (Ball and stick model)

5.9B. Reference

1. Katritzky, A. R.; Rees, C. W.; Scriven, E. F. V. Comprehensive Heterocyclic Chemistry II; Pergamon: Oxford, 1996.

2. Katritzky, A. R.; Pozharskii, A. F. Handbook of Heterocyclic Chemistry, 2nd ed.; Elsevier: Oxford, 2000.

3. Lalezari, I.; Khojasteh, M. A. *J. Heterocycl. Chem*. **2000**, *37*, 1, 183–187.

4. Dwivedi, A. R.; Rawat, S. S.; Kumar, V.; Kumar, N.; Kumar, V.; Yadav, R. P.; Baranwal, S.; Prasad, A.; Kumar, V. *Curr. Drug Targets* **2023**, *23* (4), 278–292.

5. Entezari, M.; Safari, M.; Hekmati, M.; Azin, A. *Med. Chem. Res*. **2014**, *23*, 487–495.

6. Singh, V. K.; Rishishwar, P.; Bhardwaj, P.; Alok, S. *Int. J. Pharm. Sci. Res*. **2017**, *8* (2), 446–456.

7. Yen, Y. S.; Hsu, C. Y.; Chou, H. H.; Chen, Y. C.; Lin, J. T. *Chem. Asian J.* **2013**, *8* (4), 809–816.

8. Liu, J.; Liu, B.; Tang, Y.; Zhang, W.; Wu, W.; Xie, Y.; Zhu, W. H. *J. Mater. Chem. C*. **2015**, *3*, 11069–11077.

9. Demko, Z. P.; Sharpless, K. B. *Angew. Chem., Int. Ed*. **2002**, *41*, 12, 2110–2113.

10.Wang, Z.; Ji, Y.; Zhang, Y.; Wang, J. *Org. Lett.* **2019**, *21*, 2, 450–454.

11. Ganley, J. M.; Murray, P. R. D.; Knowles, R. R. *ACS Catal.* **2020**, *10* (20), 11712–11738.

12. Chan, C. M.; Chow, Y. C.; Yu, W. Y. *Synthesis* **2020**, *52*, 2899–2921.

13. Zhao, Y.; Xia, W. *Chem. Soc. Rev.* **2018**, *47*, 478–496.

14. Chan, A. Y.; Perry, I. B.; Bissonnette, N. B.; Buchwald, S. L.; MacMillan, D. W. C. *Chem. Rev*. **2022**, *122*, 1485–1538.

15. Zhang, J.; Huan, X. D.; Wang, X.; Li, G.-Q.; Xiao, W. J.; Chen, J. R. *Chem. Commun.* **2024**, *60* (10), 10–24.

16. Verma, S.; Jat, J. L. *Synthesis*, **2020**, *52*, 1841-1846.

17. Hu, S.; Chan, F. *J. Org. Chem*., **2021**, *86*, 3223-3231.

18. Blackwell, J.; Kumar, R.; Gaunt, M. *J. Am. Chem. Soc*., **2021**, *143*, 1598-1609.

19. Juhl, K.; Jorgense, K, A. *J. Am. Chem. Soc*., **2002**, *124*, 2420–2421.

20. Evans, R. W.; Macmillan, D. W. *J. Am. Chem. Soc*., **2013**, *135*, 16074–1607.

21. Gwon, Y.; Chang, S. *Org. Lett.,* **2022**, *24*, 1088-1093.

22. Chauhan, Y.; Kumar, K. N.; Ravichandiran, V.; Jethy, S. B.; Mohanta, N.; Swain, *New J. Chem*. **2024**, *48*, 14, 6095–6102.

23. Yang, J.; Duan, J.; Wang, G.; Zhou, H.; Ma, B.; Wu, C.; Xiao, J. *Org. Lett.* **2020**, *22*, 18, 7284–7289.

24. Yamaguchi, J.; Yamaguchi, A. D.; Itami, K. *Angew. Chem. Int. Ed*. 2**012**, *51*, 8960–9009.

25. Ye, T.; McKervey, M. A. *Chem. Rev.* **1994**, *94* (5), 1091–1160.

26. Katritzky, A. R.; Rachwal, S. *Chem. Rev*. **2010**, *110*, 717.

27. Katritzky, A. R.; Rachwal, S. *Chem. Rev.* **2011**, *111*, 747.

28. Pereira, C. M. P.; Stefani, H. A.; Guzen, K. P.; Orfão, A. T. G. *ChemInform*. *2007*, 38, 766.

29. Smiley, R. A. Phenylene- and Toluenediamines. Ullmann's Encyclopedia Ind. Chem. 2002.

30. Katritzky, A. R.; Denisko, O. V.; Lan, X.; Yang, J. Z. *Chem. Rev*. **1998**, *98*, 409-548.

31. Wohl, A. *Ber. Dtsch. Chem. Ges*. **1919**, *52*, 51–63.

32. Ziegler, K.; Schenck, G.; Krockow, E. W.; Siebert, A.; Wenz, A.; Weber, H. *Justus Liebigs Ann. Chem.* **1942**, *551*, 1–79.

33. Incremona, J. H.; Martin, J. C. *J. Am. Chem. Soc*. **1970**, *92* (3), 627–634.

34. Adam, J.; Gosselain, P. A.; Goldfinger, P. *Nature* **1953**, *171* (4355), 704–705.

List of Publication

1. Mondal, S.; Pandey, A. M.; Gnanaprakasam, B. Continuous-flow Fe-zeolite-catalyzed temperature-directed synthesis of bioactive tetraketones and xanthenes using epoxides and cyclic-1, 3-diketones via a Meinwald rearrangement. *React. Chem. Eng.* **2023**, *8*, 855-862.

2. Mondal, S.; Pandey, A. M.; Gnanaprakasam, B. Visible Light Mediated Organophotoredox Catalyzed Synthesis of Tetraketones Using Tertiary Amines as Alkyl Synthons. *J. Org. Chem*. **2024**, *89* (6), 3769–3780.

3. Mondal, S.; Malode, A. N.; Londhe, G. S.; Gnanaprakasam, B. Visible Light-Induced Sequential Nitrogen Insertion and Benzotriazolation of Quinoxaline-2(1*H*)-ones. *Org. Lett.* **2025**, *27* (6), 1465–1469.

4. Mondal, S.; Londhe, G. S.; Gnanaprakasam, B. NBS Promoted C-H Benzotrizolation of α-aryl ester (Manuscript under preparation).

5. Londhe, G. S.; Mondal, S.; Gnanaprakasam, B. Mn (III) Catalyzed One Pot Domino Process for Synthesis of Dihydrocoumarins. *Chem. Commun*., **2025**, *61*, 11617-11620.

6. Pandey, A. M.; Mondal, S.; Andotra, P.; Gnanaprakasam, B. *Asian J. Org. Chem*. **2024**, *13*, e202400459.

7. Mohanta, N.; Samal, P. P.; Pandey, A. M.; Mondal, S.; Krishnamurty, S.; Gnanaprakasam, B. *J. Org. Chem.* **2023**, *88* (14), 9686–9703.

8. Pandey, A. M.; Mondal, S.; Gnanaprakasam, B. *J. Org. Chem*., **2022**, *87* (15), 9926–9939 (Highlighted as useful chemistry in organic chemistry portal).

9. “A Continuous Flow Process for Synthesis of Organic Azides” Indian Patent No. IN440209, dated March 06, 2022.’’

Reprints of Publications

Chapter 2

The content of the Chapter 2 is reproduced from Ref. "*React. Chem. Eng*., **2023**, *8*, 855-862." with permission from the Royal Society of Chemistry**.**

Continuous-flow Fe-zeolite-catalyzed temperature-directed synthesis of bioactive tetraketones and xanthenes using epoxides and cyclic-1,3-diketones *via* a Meinwald rearrangement

S. Mondal, A. M. Pandey and B. Gnanaprakasam, *React. Chem. Eng.*, 2023, **8**, 855 **DOI:** 10.1039/D2RE00452F

To request permission to reproduce material from this article, please go to the Copyright Clearance Center request page.

If you are an author contributing to an RSC publication, you do not need to request permission provided correct acknowledgement is given.

If you are the author of this article, you do not need to request permission to reproduce figures and diagrams provided correct acknowledgement is given. If you want to reproduce the whole article in a third-party publication (excluding your thesis/dissertation for which permission is not required) please go to the Copyright Clearance Center request page.

Chapter 3

The content of the Chapter 3 is reproduced from Ref. "*J. Org. Chem.* **2024***, 89,* 6, 3769–3780" with permission from the American Chemical Society**.**

AMERICAN CHEMICAL SOCIETY LICENSE
TERMS AND CONDITIONS

Aug 07, 2025

This Agreement between Shankhajit Mondal ("You") and American Chemical Society ("American Chemical Society") consists of your license details and the terms and conditions provided by American Chemical Society and Copyright Clearance Center.

License Number	6083610310402
License date	Aug 07, 2025
Licensed Content Publisher	American Chemical Society
Licensed Content Publication	The Journal of Organic Chemistry
Licensed Content Title	Visible Light Mediated Organophotoredox Catalyzed Synthesis of Tetraketones Using Tertiary Amines as Alkyl Synthons
Licensed Content Author	Shankhajit Mondal, Akanksha M. Pandey, Boopathy Gnanaprakasam
Licensed Content Date	Mar 1, 2024
Licensed Content Volume	89
Licensed Content Issue	6
Volume number	89
Issue number	6

Type of Use	Thesis/Dissertation
Requestor type	Author (original work)
Format	Print and Electronic
Portion	Full article
Title of new work	Studies on C-H Functionalization of Cyclic-1,3-diketones, Quinoxalin-2(1H)-ones and α-aryl esters under Thermal, Photochemical and Continuous Flow Conditions
Institution name	IISER Pune
Expected presentation date	Dec 2025
The Requesting Person / Organization to Appear on the License	Shankhajit Mondal
Requestor Location	Mr. Shankhajit Mondal IISER Pune Hostel 2 NCL Colony Pune, Maharashtra 411008 India
Billing Type	Invoice
Billing Address	Mr. Shankhajit Mondal IISER Pune Hostel 2 Dr. Homi Bhaba Jahangir road NCL Colony Pune, India 411008
Total	0.00 USD
Terms and Conditions	

American Chemical Society's Policy on Thesis and Dissertations

If your university requires you to obtain permission, you must use the RightsLink permission system.

See RightsLink instructions at
http://pubs.acs.org/page/copyright/permissions.html.

This is regarding request for permission to include **your** paper(s) or portions of text from **your** paper(s) in your thesis.
Permission is now automatically granted; please pay special attention to the **implications** paragraph below. The Copyright Subcommittee of the Joint Board/Council Committees on Publications approved the following:

> Copyright permission for published and submitted material from thesis and dissertations
> ACS extends blanket permission to students to include in their thesis and dissertations their own articles, or portions thereof, that have been published in ACS journals or submitted to ACS journals for publication, provided that the ACS copyright credit line is noted on the appropriate page(s).
>
> Publishing implications of electronic publication of thesis and dissertation material
> Students and their mentors should be aware that posting of thesis and dissertation material on the Web prior to submission of material from that thesis or dissertation to an ACS journal may affect publication in that journal. Whether Web posting is considered prior publication may be evaluated on a case-by-case basis by the journal's editor. If an ACS journal editor considers Web posting to be "prior publication", the paper will not be accepted for publication in that journal. If you intend to submit your unpublished paper to ACS for publication, check with the appropriate editor prior to posting your manuscript electronically.

Reuse/Republication of the Entire Work in Thesis or Collections: Authors may reuse all or part of the Submitted, Accepted or Published Work in a thesis or dissertation that the author writes and is required to submit to satisfy the criteria of degree-granting institutions. Such reuse is permitted subject to the ACS' "Ethical Guidelines to Publication of Chemical Research" (http://pubs.acs.org/page/policy/ethics/index.htmlb); the author should secure written confirmation (via letter or email) from the respective ACS journal editor(s) to avoid potential conflicts with journal prior publication*/embargo policies. Appropriate citation of the Published Work must be made. If the thesis or dissertation to be published is in electronic format, a direct link to the Published Work must also be included using the ACS Articles on Request author-directed link - see http://pubs.acs.org/page/policy/articlesonrequest/index.html

* Prior publication policies of ACS journals are posted on the ACS website at http://pubs.acs.org/page/policy/prior/index.html

If your paper has not yet been published by ACS, please print the following credit line on the first page of your article: "Reproduced (or 'Reproduced in part') with permission from [JOURNAL NAME], in press (or 'submitted for publication'). Unpublished work copyright [CURRENT YEAR] American Chemical Society." Include appropriate information.

If your paper has already been published by ACS and you want to include the text or portions of the text in your thesis/dissertation, please print the ACS copyright credit line on the first page of your article: "Reproduced (or 'Reproduced in part') with permission from [FULL REFERENCE CITATION.] Copyright [YEAR] American Chemical Society." Include appropriate information.

Submission to a Dissertation Distributor: If you plan to submit your thesis to UMI or to another dissertation distributor, you should not include the unpublished ACS paper in your thesis if the thesis will be disseminated electronically, until ACS has published your paper. After publication of the paper by ACS, you may release the entire thesis (**not the individual ACS article by itself**) for electronic dissemination through the distributor; ACS's copyright credit line should be printed on the first page of the ACS paper.

v1.4

Questions? customercare@copyright.com.

Chapter 4

The content of the Chapter 4 is reproduced from Ref. "*Org. Lett*. **2025**, *27*, 6, 1465–1469" with permission from the American Chemical Society**.**

AMERICAN CHEMICAL SOCIETY LICENSE
TERMS AND CONDITIONS

Aug 07, 2025

This Agreement between Shankhajit Mondal ("You") and American Chemical Society ("American Chemical Society") consists of your license details and the terms and conditions provided by American Chemical Society and Copyright Clearance Center.

License Number	6083611001561
License date	Aug 07, 2025
Licensed Content Publisher	American Chemical Society
Licensed Content Publication	Organic Letters
Licensed Content Title	Visible Light-Induced Sequential Nitrogen Insertion and Benzotriazolation of Quinoxaline-2(1H)-ones
Licensed Content Author	Shankhajit Mondal, Akhilesh Narendra Malode, Gokul S. Londhe, et al
Licensed Content Date	Feb 1, 2025
Licensed Content Volume	27
Licensed Content Issue	6
Volume number	27
Issue number	6
Type of Use	Thesis/Dissertation

Requestor type	Author (original work)
Format	Print and Electronic
Portion	Full article
Title of new work	Studies on C-H Functionalization of Cyclic-1,3-diketones, Quinoxalin-2(1H)-ones and α-aryl esters under Thermal, Photochemical and Continuous Flow Conditions
Institution name	IISER Pune
Expected presentation date	Dec 2025
The Requesting Person / Organization to Appear on the License	Shankhajit Mondal
Requestor Location	Mr. Shankhajit Mondal IISER Pune Hostel 2 Pune, Maharashtra 411008 India
Billing Type	Invoice
Billing Address	Mr. Shankhajit Mondal IISER Pune Hostel 2 Pune, India 411008
Total	0.00 USD
Terms and Conditions	

American Chemical Society's Policy on Thesis and Dissertations

If your university requires you to obtain permission, you must use the RightsLink permission system.

See RightsLink instructions at
http://pubs.acs.org/page/copyright/permissions.html.

This is regarding request for permission to include **your** paper(s) or portions of text from **your** paper(s) in your thesis.
Permission is now automatically granted; please pay special attention to the **implications** paragraph below. The Copyright Subcommittee of the Joint Board/Council Committees on Publications approved the following:

> Copyright permission for published and submitted material from thesis and dissertations
> ACS extends blanket permission to students to include in their thesis and dissertations their own articles, or portions thereof, that have been published in ACS journals or submitted to ACS journals for publication, provided that the ACS copyright credit line is noted on the appropriate page(s).
>
> Publishing implications of electronic publication of thesis and dissertation material
> Students and their mentors should be aware that posting of thesis and dissertation material on the Web prior to submission of material from that thesis or dissertation to an ACS journal may affect publication in that journal. Whether Web posting is considered prior publication may be evaluated on a case-by-case basis by the journal's editor. If an ACS journal editor considers Web posting to be "prior publication", the paper will not be accepted for publication in that journal. If you intend to submit your unpublished paper to ACS for publication, check with the appropriate editor prior to posting your manuscript electronically.

Reuse/Republication of the Entire Work in Thesis or Collections: Authors may reuse all or part of the Submitted, Accepted or Published Work in a thesis or dissertation that the author writes and is required to submit to satisfy the criteria of degree-granting institutions. Such reuse is permitted subject to the ACS' "Ethical Guidelines to Publication of Chemical Research" (http://pubs.acs.org/page/policy/ethics/index.htmlb); the author should secure written confirmation (via letter or email) from the respective ACS journal editor(s) to avoid potential conflicts with journal prior publication*/embargo policies. Appropriate citation of the Published Work must be made. If the thesis or dissertation to be published is in electronic format, a direct link to the Published Work must also be included using the ACS Articles on Request author-directed link - see http://pubs.acs.org/page/policy/articlesonrequest/index.html

* Prior publication policies of ACS journals are posted on the ACS website at http://pubs.acs.org/page/policy/prior/index.html

If your paper has not yet been published by ACS, please print the following credit line on the first page of your article: "Reproduced (or 'Reproduced in part') with permission from [JOURNAL NAME], in press (or 'submitted for publication'). Unpublished work copyright [CURRENT YEAR] American Chemical Society." Include appropriate information.

If your paper has already been published by ACS and you want to include the text or portions of the text in your thesis/dissertation, please print the ACS copyright credit line on the first page of your article: "Reproduced (or 'Reproduced in part') with permission from [FULL REFERENCE CITATION.] Copyright [YEAR] American Chemical Society." Include appropriate information.

Submission to a Dissertation Distributor: If you plan to submit your thesis to UMI or to another dissertation distributor, you should not include the unpublished ACS paper in your

thesis if the thesis will be disseminated electronically, until ACS has published your paper. After publication of the paper by ACS, you may release the entire thesis (**not the individual ACS article by itself**) for electronic dissemination through the distributor; ACS's copyright credit line should be printed on the first page of the ACS paper.

v1.4

Questions? customercare@copyright.com.